Universidade de Aveiro
Ano 2023

HELENA BEATRIZ CINZA SANTOS LEAL FERREIRA DE SOUSA

UMA PERSPECTIVA LIPIDÓMICA DE DOENÇAS AUTOIMUNES PARA A DESCOBERTA DE NOVOS BIOMARCADORES PARA A MEDICINA PERSONALIZADA

A LIPIDOMIC PERSPECTIVE OF AUTOIMMUNE DISEASES FOR THE DISCOVERY OF NEW BIOMARKERS FOR PERSONALIZE MEDICINE

Universidade de Aveiro
Ano 2023

HELENA BEATRIZ CINZA SANTOS LEAL FERREIRA DE SOUSA

UMA PERSPECTIVA LIPIDÓMICA DE DOENÇAS AUTOIMUNES PARA A DESCOBERTA DE NOVOS BIOMARCADORES PARA A MEDICINA PERSONALIZADA

A LIPIDOMIC PERSPECTIVE OF AUTOIMMUNE DISEASES FOR THE DISCOVERY OF NEW BIOMARKERS FOR PERSONALIZE MEDICINE

Tese apresentada à Universidade de Aveiro para cumprimento dos requisitos necessários à obtenção do grau de Doutor em Bioquímica, realizada sob a orientação científica da Professora Doutora Maria do Rosário Gonçalves dos Reis Marques Domingues, Professora Associada com Agregação do Departamento de Química da Universidade de Aveiro, e coorientação do Professor Doutor Artur Augusto Paiva, Coordenador da Unidade Funcional de Citometria de Fluxo e do Biobanco do centro académico clínico de Coimbra (CHUC/UC), e da Doutora Tânia Sofia Rodrigues de Melo, Investigadora do Departamento de Química da Universidade de Aveiro.

Agradecimentos ao CESAM (UIDP/50017/2020+UIDB/50017/2020), LAQV/REQUIMTE (UIDB/50006/2020) e à CA19105 - Pan-European Network in Lipidomics and EpiLipidomics (EpiLipidNET).

Apoio financeiro da FCT e do FSE no âmbito do III Quadro Comunitário de Apoio através da bolsa de Doutoramento atribuída a Helena Ferreira 2020.04611.BD.

“Voando a máquina, todo o céu será música”
José Saramago, *Memorial do Convento*

o júri

presidente

Doutor Vasile Staicu
professor catedrático da Universidade de Aveiro

vogais

Doutora Maria do Rosário Gonçalves dos Reis Marques Domingues
professora associada com agregação da Universidade de Aveiro

Doutor Francisco Manuel Pereira Peixoto
professor associado com agregação da Universidade de Trás-os-Montes e Alto Douro

Doutora Maria Teresa Teixeira da Cruz Rosete
professora associada da Universidade de Coimbra

Doutor Bruno Miguel Rodrigues das Neves
professor auxiliar da Universidade de Coimbra

Doutor Hugo Daniel Carvalho de Azevedo Rocha
especialista em genética do Instituto Nacional de Saúde Doutor Ricardo Jorge

agradecimentos

Agradeço à sempre presente orientadora Professora Rosário Domingues por toda a dedicação, ajuda e conselhos prestados. Foi como uma segunda mãe, estou grata por tudo.

Agradeço aos meus coorientadores, Drª. Tânia Melo e Dr. Artur Paiva, pela simpatia, cooperação, acompanhamento e ajuda prontamente prestada.

Agradeço aos meus colegas do Laboratório de Lipidómica, especialmente à Inês, por toda a ajuda no trabalho experimental.

Um especial reconhecimento aos meus pais que tornaram possível a realização deste objetivo e demonstraram um interesse incansável durante todo o percurso. Obrigada por acreditarem em mim e nunca desistirem de me dar tudo o que creem ser o melhor. Desejo um dia ser o que vocês são para mim.

Ao meu príncipe, que agora tenho a sorte de poder chamar "Marido", por caminhar comigo lado a lado e nunca me deixar desamparada. Obrigada por seres quem és e por tudo o que construímos juntos, hoje e sempre.

Auguro grandes caminhadas bem-sucedidas e, por isso, faz-me feliz saber que posso contar convosco… Um enorme obrigada…

Agradeço também à Universidade de Aveiro e à FCT / MCT pelo apoio financeiro aos projetos UIDB/50006/2020 e UIDP/50006/2020, aos centros de investigação CESAM (UIDB/50017/2020+UIDP/50017/2020+LA/P/0094/2020) e LAQV-REQUIMTE (UIDB/50006/2020), e RNEM, Rede Nacional de Espectrometria de Massa (LISBOA-01-0145-FEDER-402-022125), através de fundos nacionais e, quando aplicável, cofinanciado pelo FEDER, no âmbito do PT2020 e pelo financiamento da minha bolsa de doutoramento (2020.04611.BD).

"Assim que a vida e alma e esperança,
E tudo quanto tenho, tudo é vosso,
E o proveito disso eu só o levo."
Luís de Camões, *Sonetos*

Palavras-chave

Doenças autoimunes; lipidómica; espetrometria de massa; perfil lipídico; peroxidação lipídica; sangue seco em cartão.

Resumo

As doenças autoimunes (DAI) são doenças crónicas com uma elevada taxa de prevalência que afetam cerca de 4% da população mundial e 5% da população portuguesa. Existem várias DAI dentro das quais as mais comuns incluem a esclerose múltipla (do inglês *multiple sclerosis*, MSs), artrite reumatóide (do inglês *rheumatoid arthritis*, RA), lúpus eritematoso sistémico (do inglês *systemic lupus erythematosus*, SLE) e esclerose sistémica (do inglês *systemic sclerosis*, SS) que serão estudadas nesta Tese. As DAI são doenças debilitantes que tornam o paciente incapaz de viver a vida diária normal e têm um grande impacto na economia da sociedade e dos sistemas de saúde. O processo fisiopatológico da maioria das DAI não é totalmente compreendido, e cada DAI parece ter características patológicas específicas que ainda são desconhecidas, o que conduz ao uso de ferramentas de diagnóstico inadequadas e à falta de biomarcadores específicos para cada doença, muitas vezes precedendo situações clínicas incorretamente diagnosticadas. Sentindo a necessidade urgente de uma nova abordagem de diagnóstico (além dos parâmetros imunológicos) e de novos e mais específicos biomarcadores para amenizar o desafio de diagnosticar as DAI, a lipidómica pode ser vista como uma nova ferramenta para enfrentar este desafio, o que é corroborado pelos poucos estudos que abordam alterações do perfil lipídico nas DAI. No entanto, a alteração da homeostase lipídica nas DAI tem sido pouco estudada e a maioria dos estudos relata dados de ensaios enzimáticos/colorimétricos. Muito poucos referem as alterações no lipidoma deste tipo de patologias através da análise lipidómica, o que poderia fornecer novos conhecimentos sobre os distúrbios e adaptações lipídicas nas DAI para elucidar completamente os mecanismos moleculares que regulam a homeostase lipídica nestas patologias. Espera-se que seja possível propor novos biomarcadores, bem como desenhar estratégias terapêuticas inovadoras de acordo com a nova "medicina de precisão".

Assim, o principal objetivo da presente Tese consistiu na identificação do lipidoma de plasma, soro e sangue total das DAI mais prevalentes, nomeadamente MSs, SLE e SS, usando abordagens lipidómicas baseadas em espectrometria de massa (do inglês *mass spectrometry*, MS) acoplada à cromatografia líquida (do inglês *liquid chromatography*, LC). Pretendeu-se identificar uma assinatura lipidómica específica para a descoberta de biomarcadores lipídicos de cada DAI estudada, na esperança de melhorar a medicina personalizada e de precisão. A oxidação de espécies lipídicas, em particular os ésteres de colesterol, também foi objeto de estudo, na tentativa de entender o processo de peroxidação lipídica induzida por condições de stress oxidativo características das DAI. Um objetivo adicional desta Tese foi determinar a viabilidade do sangue seco em cartão (do inglês *dried blood spots*, DBS) como uma abordagem pré-analítica alternativa para a análise lipidómica clínica.

Seguindo o objetivo principal desta Tese, e para obter um conhecimento mais aprofundado sobre as DAI, a análise lipidómica do soro de pacientes com MSs, comparando com controlos saudáveis, mostrou que o perfil lipídico muda com o estado da doença e a espécie lipídica fosfatidilcolina [PC (38:1)] poderia ser um possível biomarcador desta doença. Além disso, estudou-se sangue total e plasma de pacientes diagnosticados com SLE e SS, onde se determinou que a espécie PC(38:1) pode não ser um marcador exclusivo para a MSs, mas sim para as DAI, uma vez que a sua abundância estava alterada em ambas SLE e SS. O conteúdo de esfingomielina e ceramidas no plasma de SS mostrou-se aumentado, podendo ser considerado o seu uso como marcadores específicos desta DAI.

Resumo

A correlação entre inflamação, stress oxidativo e lípidos nas DAI foi avaliada no caso da RA. Foi realizada uma revisão da literatura a respeito da RA, uma das DAI mais prevalentes, e onde já foram reportadas alterações lipídicas relacionadas com o aumento do stress oxidativo. No entanto, o foco das investigações tem sido nas alterações do perfil de ácidos gordos, existindo apenas alguns estudos com aplicação de abordagens lipidómicas. Todavia, há evidências de alteração de algumas espécies de fosfolípidos, como PC e fosfatidilinositóis, e algumas espécies de lípidos oxidados, como os ácidos hidroxieicosatetraenóicos e os ácidos hidroxioctadecadienóicos. Numa tentativa de otimizar as abordagens baseadas em MS para a identificação de lípidos oxidados nas DAI, foram sintetizadas espécies de éster de colesterol oxidado e caracterizadas por LC-MS/MS. Foi determinada a sua fragmentação específica, o que será útil para a identificação destas espécies em doenças relacionadas com stress oxidativo, como é o caso das DAI.

Além disso, os DBS foram avaliados para atender ao propósito do desenvolvimento de um método menos invasivo passível de ser aplicado na análise lipidómica das DAI. Inicialmente, foi realizada uma revisão bibliográfica das aplicações dos DBS na lipidómica onde foram destacados os principais procedimentos e interferências, bem como alguns resultados já descritos sobre este assunto. No entanto, não há consenso sobre este tema e devem ser feitos esforços para harmonizar e padronizar os procedimentos/protocolos utilizados de forma a aplicar este método de colheita de sangue em análises de lipidómica clínica de rotina. Por último, o perfil lipídico de crianças saudáveis foi avaliado usando amostras de DBS, que mostrou variar com a idade. O método utilizado para extrair e analisar os lipídios dos DBS mostrou-se eficiente, o que significa que o uso do método DBS pode ser aplicado no futuro para o estudo das DAI.

Atualmente, são necessárias estratégias que forneçam marcadores da doença e do estado da doença adequados a um diagnóstico preciso, uma intervenção oportuna e uma melhor gestão da doença, especialmente em doenças multifatoriais e de diagnóstico complexo como as DAI. Esta Tese tentou ir ao encontro dos desafios da saúde, criando, por um lado, oportunidades para uma vida mais salutar, repleta de bem-estar e cuidados adequados. Por outro lado, contribui para a evolução do conhecimento sobre as assinaturas lipídicas das DAI e o possível uso dos DBS como substituto das amostras convencionais, todos contribuindo para o inovador método da medicina de precisão. A medicina personalizada/de precisão beneficiaria do diagnóstico precoce personalizado de episódios de recaída, auxiliado pela análise lipidómica, para promover um tratamento mais eficaz para cada paciente com DAI.

Keywords

Autoimmune diseases; lipidomics; mass spectrometry; lipidic profile; lipid peroxidation; dried blood spots.

Abstract

Autoimmune diseases (AID) are chronic diseases with a high prevalence rate that affect approximately 4% of the world population and 5% of Portugal`s population. There are several different AID and the most common include multiple sclerosis (MSs), rheumatoid arthritis (RA), systemic lupus erythematosus (SLE) and systemic sclerosis (SS), which will be studied in this thesis. AID are debilitating diseases that make the patient incapable of living the normal daily life. It highly impacts the economy of both society and health care systems. The pathophysiological process of the majority AID is not fully understood, and each AID seems to have specific pathological features that are still mostly unknown. This leads to impaired proper diagnostic tools and lack of specific biomarkers for each disease, often preceding poorly diagnosed clinical situations. Feeling the urgent need for a new diagnostic approach (besides the immunological factors) as well as new and more specific biomarkers to ease the challenge of diagnosing AID, lipidomics can be seen as a new approach to face this challenge. This is supported by the few studies that have addressed some alterations in lipid profile in AID. Nonetheless, the alteration in lipid homeostasis in AID has been scarcely studied and most of the studies report data from enzymatic/colorimetric experiments. Very few addressed the changes in the lipidome of this type of pathologies through lipidomic analysis, which could give new knowledge on the lipid disturbances and adaptations in AID to fully elucidate the molecular mechanisms regulating lipid homeostasis in these pathologies. Hopefully it will be possible to propose new biomarkers as well as to design innovative therapeutic strategies in agreement with the nowadays so-called precision medicine.

Thus, the main goal of the present Thesis was to fingerprint the plasma, serum, and whole blood lipidome of the most prevalent AID, namely MSs, SLE and SS, by using mass spectrometry (MS) based lipidomic approaches coupled to liquid chromatography (LC). It was intended to identify a specific lipidomic signature for lipid biomarkers discovery of each AID studied, hoping to improve precision and personalized medicine. Oxidation of lipid species, in particular cholesteryl esters, was also explored in an attempt to understand the lipid peroxidation process induced by oxidative stress conditions, which are characteristic of AID. An additional objective of this Thesis was to ascertain dried blood spots (DBS) as an alternative pre-analytical approach for clinical lipidomic analysis.

Following the main goal of this Thesis, and to gain a more in-depth knowledge on AID, lipidomic analysis of serum from MSs patients, comparing with healthy controls, showed that the lipid profile changes with disease status and the lipid species phosphatidylcholine [PC (38:1)] could be a possible biomarker of this disease. In addition, the whole blood and plasma of patients diagnosed with SLE or SS diseases were studied and it was determined that PC(38:1) may not be an exclusive marker for multiple sclerosis but instead for AID, once its abundance was altered in both SLE and SS as well. Sphingomyelin and ceramides content in plasma of SS was shown to be upregulated and could be used as specific markers of this AID.

Abstract

The correlation between inflammation, oxidative stress, and lipids in AID was evaluated in the case of RA. It was performed a review of the literature regarding RA, one of the most prevalent AID, and known to be correlated with lipid alteration and increased oxidative stress. However, the major work was focused on the alterations of the fatty acid profile and only few in lipidomic studies, but giving evidence of alteration of some phospholipid species, such as PC and phosphatidylinositols, and few oxidized lipid species like hydroxyeicosatetraenoic acids and hydroxyoctadecadienoic acids. In an attempt to optimize MS-based approaches for the identification of oxidized lipids in AID, oxidized cholesteryl ester species were synthesised and characterized by LC-MS/MS, and the specific fragmentation fingerprinting was identified, which will be useful for their identification in oxidative stress related diseases such as AID.

Furthermore, DBS were evaluated to meet the purpose of the development of a less invasive method for lipidomic analysis in AID. Initially a bibliographic revision of DBS applications in lipidomics was performed and key procedures and interferences were highlighted, as well as few previous findings on these subjects. There is no consensus on this topic and efforts should be made to harmonize and standardize the procedures/protocols used to apply this blood collection method on routine clinical lipidomic analysis. Lastly, the lipid profile of healthy children was evaluated using DBS samples. The lipid profile was shown to change with age and the method used to extract and analyse the lipids from the DBS was proven efficient, meaning that the use of DBS method can be further exploited to the study of AID.

Nowadays, there is an urgent need for strategies that provide disease and disease-state markers suitable for accurate diagnosis, timely intervention and a better disease management, especially in multifactorial diseases and of complex diagnosis like AID. This Thesis tried to meet health challenges, creating opportunities for good health, well-being, and healthcare, by contributing to the evolution of knowledge concerning AID lipidomic signatures and the possible use of DBS as a substitute of conventional samples, all contributing to the innovative method of precision medicine. Personalized/precision medicine would benefit from the tailored early diagnosis of relapse episodes, aided by lipidomic analysis, to promote a more effective treatment to each AID patient.

Table of Contents

List of Figures

List of Tables

1 CHAPTER 1. INTRODUCTION

1.1 Understanding autoimmune diseases

Autoimmune diseases (AID) are chronic multifactorial diseases that are increasing their prevalence and are responsible for high rates of morbidity and mortality. Worldwide, the population affected by an AID corresponds to approximately 4%[1]. In Portugal, it is estimated that half a million people suffer from an AID, which corresponds to 5% of the country`s population. There are over 80 different AID with different degrees of rarity. The most common AID include type 1 diabetes, multiple sclerosis, rheumatoid arthritis, systemic lupus erythematosus, Crohn's disease, psoriasis and scleroderma[2]. Thus, in this Thesis, efforts were made to broad the knowledge on multiple sclerosis (MSs), rheumatoid arthritis (RA), systemic lupus erythematosus (SLE) and scleroderma, also known as systemic sclerosis (nomenclature used in this work from here forward, SS). AID are associated with debilitating conditions that incapacitate the patients and bring economic burdens not only for the patients and their families but also for the society and health care systems. One of the major difficulties regarding AID is the lack of proper diagnostic tools and specific biomarkers for each disease leading many times to misdiagnosed/undiagnosed situations. Additionally, there is a shortage of qualitative methods that allow the prediction of relapse episodes or the outcome of the treatment. The fact that the pathophysiological process of the majority AID is not fully known, and that each AID seems to have specific pathological features, is a setback for the improvement of clinical tools for a better healthcare.

In AID there is a deregulation of the immune system. This system is the body defence mechanism against disease, aimed to maintain homeostasis. It serves to identify foreign pathogens, commonly known as antigens, and prevent their potentially harmful effects[3]. There are two types of immunity, innate and acquired, and regardless which type, a fully functional immune system has the ability to recognise and distinguish foreign pathogens from “self” molecules, which need to be protected[4]. This protective mechanism is essential to keep homeostasis, but of foremost importance for patients with a compromised immune system`s function. Therefore, when the body starts to look at their own molecules as antigens, the immune response becomes directed to the body itself, leading to the development of an AID[5]. Thus, an impaired and defective immune system is the basis of AID pathogenesis[6].

The pathogenesis of AID is an undeniably complex process. It is influenced by several factors (multifactorial diseases), such as genetic, environmental, life style and hormonal, that work together to disrupt the normal tolerance of the immune system towards self-antigens (Figure 1.1-1)[7].

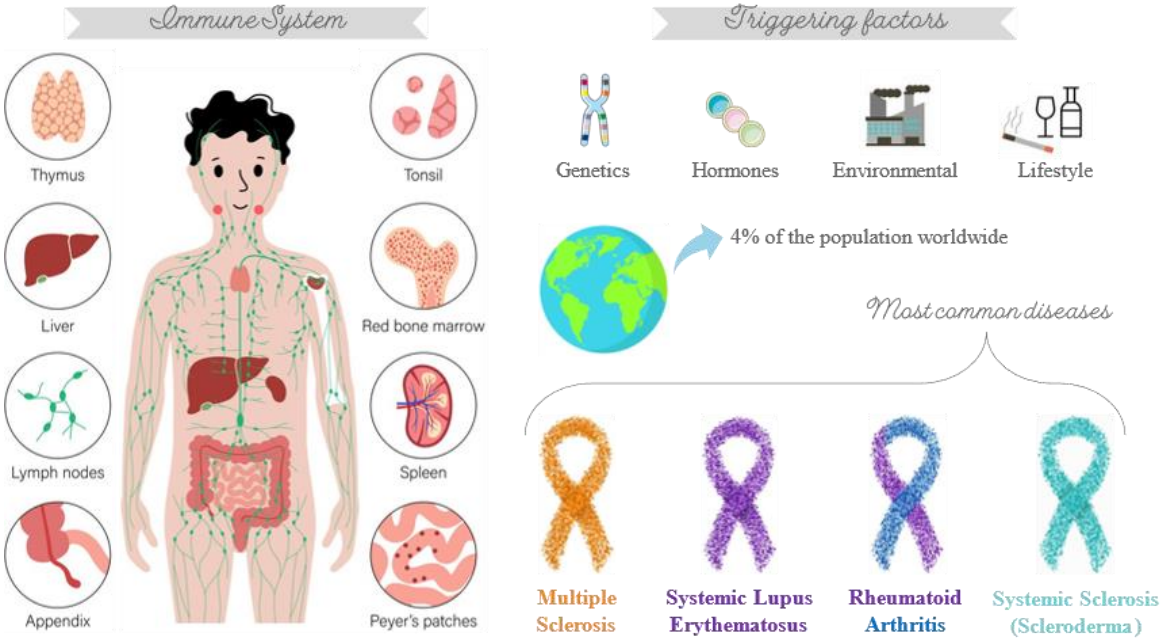

Figure 1.1-1. Autoimmune diseases (AID): risk factors and common examples of AID. These diseases are multifactorial and affect almost 4% of the population in the world. Their development is influenced by different factors such as the patient's lifestyle, the surrounding environment, genetics, and hormonal imbalance. There are plenty of AID, all of them with different pathogenesis and development, but among the most common are multiple sclerosis, systemic lupus erythematosus, rheumatoid arthritis and systemic sclerosis.

There are a large number of AID that are clinically different, and each have an heterogenous development. Some are more prevalent than others and there are AID that are so rare that only affect a very small percentage of the population. For instance, SLE has a prevalence of 43.7 per 100 000 persons[8] while catastrophic antiphospholipid syndrome affects only 5 people per million in the general population[9]. Although the number of diseases is high and their characteristics are different, AID share some physiological processes and symptoms. Autoantigen recognition as non-self, amplification of the immune response, chronic inflammation and tissue destruction are some mechanistic threads that AID have in common[10].

AID can be classified in two different categories (Figure 1.1-2): systemic or organ-specific[11]. Systemic AID are characterized by the immune response being directed against self-antigens scattered throughout the body, leading to a widespread tissue damage and involvement of multiple organs. It is the case of the diseases studied in this Thesis that are all systemic AID. Meanwhile, in organ-specific AID the immune response only attacks self-antigens expressed in specific organs[12]. Type 1 diabetes and Graves disease are two examples of organ-specific AID that particularly affect the beta cells of the endocrine pancreas and the thyroid gland, respectively.

However, the existence of an AID, either systemic or organ-specific, does not prevent the occurrence of another AID in the same patient. In fact, both types of AID can coexist in the same person, either by consequence of each other or all at the same time, supported by the presence of autoantibodies directed against the corresponding autoantigens[13].

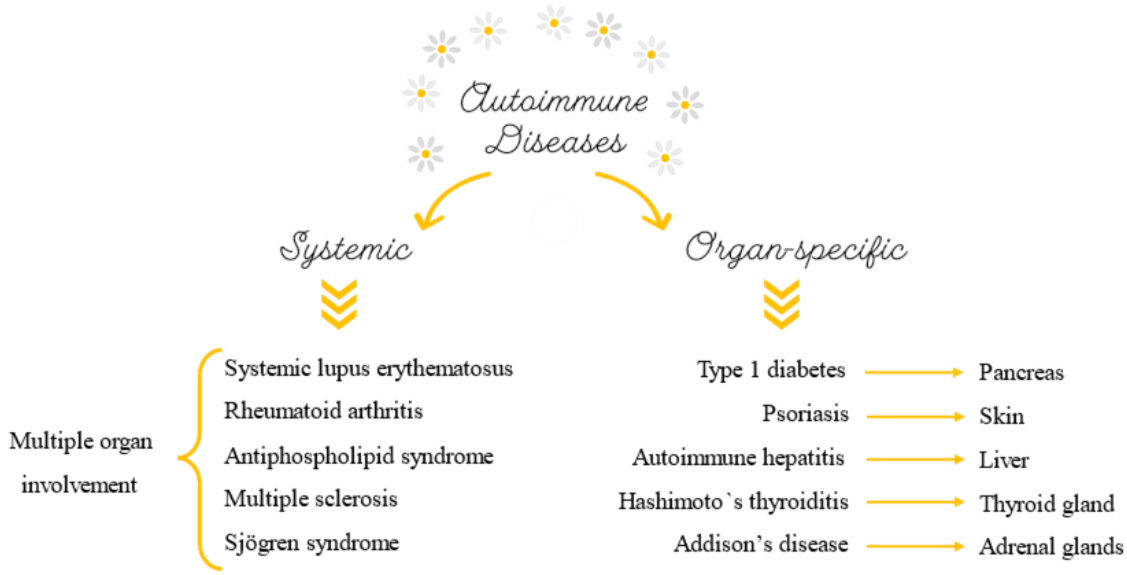

Figure 1.1-2. Autoimmune diseases (AID) are divided in two different categories: systemic and organ-specific. Systemic AID affect multiple organs while in organ-specific AID the immune response is directed to a particular organ. Common AID are shown as an example of each category as well as the organ involved.

Another characteristic shared by AID is that the disease activity changes throughout the patient`s life, meaning that the pathological process is dynamic and oscillates between worsening and improvement[14]. Since the appearance of the symptoms, the patient experiences remission and relapse periods. In remission periods the disease is in an inactive state while in relapse periods there is an exacerbation of disease activity, severity and symptoms[15]. This way, it would be highly beneficial for the patient if there was a possibility to predict relapse episodes and intervene carefully with appropriate therapeutic strategies to prevent the worsening of symptoms. However, there are no specific diagnostic tools or biomarkers that allow the prediction of these periods. To face this drawback and prevent these debilitating periods, new studies are needed to understand the mechanism of disease and to find new biomarkers. Personalized medicine would benefit from the tailored early diagnosis of relapse episodes in order to promote a more effective treatment to each AID patient.

The diagnosis of AID is based on clinical and laboratory data that should be specific for each disease as any other pathology. However, AID have different forms of manifesting and

patients display diverse combinations and overlapping clinical and laboratory features[16]. There are many symptoms and molecular manifestations (laboratory findings) that are common in distinct AID. This way, finding the pathogenesis and achieve a definite diagnosis of AID has been challenging since it is not a straightforward process. Due to scientific, epidemiological and genetic breakthroughs, many classification criteria of AID needed to be updated[17]. The diagnostic criteria provide guidelines that physicians can follow through and in which clinical observations can be tested, therefore reaching a more specific diagnosis. Nonetheless, the establishment of good diagnostic criteria does not imply a less challenging early diagnosis[17].

A hallmark of AID is the production of high-affinity autoantibodies that attack autoantigens[18]. Low titers of autoantibodies are normally produced in the human body, indicating a normal health status. On the contrary, high autoantibody titers may be indicative of an AID[19]. Antinuclear antibodies (ANAs) are autoantibodies that attack self-proteins within cell nucleus structures. A positive test result for ANAs may indicate the presence of a systemic AID, such as SLE, drug-induced lupus, SS, Sjögren syndrome, mixed connective tissue disease, polymyositis /dermatomyositis, RA, oligoarticular juvenile chronic arthritis, polyarteritis nodosum, or an organ-specific AID such as Grave`s disease, Hashimoto thyroiditis or autoimmune hepatitis. ANAs also have been detected in chronic infectious diseases, including viral infections (parvovirus, hepatitis C), tuberculosis, parasitic infections (schistosomiasis), and bacterial endocarditis. Other factors that yield ANA-positive test results include cancers, markers of the future development of AID, certain medications, and having relatives with an AID[19].

Thus, the testing for ANAs is important in the diagnosis of AID, however, the test result for ANAs in itself has no significant meaning if there is no clinical correlation[20]. As ANAs have very low specificity, an individual positive or negative test result gives no information to the patient or clinician, therefore, ANAs test must always be accompanied by the testing of other more specific biomarkers. There are other types of autoantibodies that are tested for AID as well, however, similarly to what happens with ANAs, these autoantibodies can be detected in several AID (Table 1.1-1).

Table 1.1-1. Different types of autoantibodies evaluated in laboratory tests for AID diagnosis.

Autoantibody	Autoantigen	Associated AID
Anti-dsDNA	Double stranded-DNA	Highly specific for SLE Correlated with relapse periods (active, severe disease)
Anti-Extractable Nuclear Antigens:		
• **Anti-Sm**	Smith	
• **Anti-RNP**	Proteins containing U1-RNA	Highly specific for SLE SLE, RA, SS, Sjogren`s syndrome, MCTD
• **Anti-SSA (Ro)**	Ribonucleoproteins	Sjogren`s syndrome, SLE (subacute cutaneous lupus), neonatal SLE
• **Anti-SSB (La)**	Ribonucleoproteins	Sjogren`s syndrome, SLE, neonatal SLE
Anti-centromere	Chromosome (centromere/kinetochore region)	Limited SS, pulmonary hypertension, primary biliary cirrhosis
Anti-Scl 70	DNA topoisomerase I	Diffuse SS
Anti-Jo-1 (anti-synthetase Abs)	Antibody to signal recognition protein	Inflammatory myopathies with poor prognosis
Anti-PM/Scl	Antibody to nucleolar granular component	Polymyositis/SS overlap syndrome
Anti-Mi-2	Antibodies to a nucleolar antigen of unknown function	Dermatomyositis

MCTD: mixed connective tissue disease. Adapted from Castro *et al*[21].

This way, a set of laboratory tests including several different biomarkers is needed to accomplish a better diagnosis. This set of laboratory tests must include parameters like a complete blood count, comprehensive metabolic panel, acute phase reactants (inflammatory markers), immunologic studies, serologies, flow cytometry, cytokine analysis, and HLA typing[21]. Even though some tests may not be specific for a certain disease, like the erythrocyte sedimentation rate analysed in the blood count component, they are very helpful to assess disease activity or even indicate the severity of organ involvement or damage. This way, having a comprehensive set of laboratory tests proves to be useful in the diagnosis, prognosis, and management of patients with AID.

In conclusion, and given the fact that AID are polygenic, genetic markers alone are unlikely to be proven useful for early diagnosis because they have low positive predictive value[17]. This way, it is needed a new approach and new and more specific biomarkers to ease the challenge of

diagnosing AID. In this line of thought, lipidomics can be seen as a new approach to face this challenge.

1.2 Clinical lipidomics as a potential new diagnostic/prognostic approach for AID

Lipids are very important molecules for the regulation of physiological and pathological processes of the organism. They are the building blocks of cell membranes, serve as energy storage, and influence numerous cellular processes by directly participating as both primary and secondary messengers[22]. Phospholipids are the most abundant membrane lipids and are involved in the formation of the characteristic lipid bilayer structure of biological membranes, and are also important signalling molecules[23]. Sphingolipids act as mediators of physiological processes involved in cell proliferation, survival, inflammation, senescence and death[22]. Alterations of lipid metabolism and profile have been frequently associated with disturbances in the homeostasis leading to the development of a pathological state. Thus, lipids have gained substantial clinical relevance for their implications in a large number of human diseases. Many studies reported misbalances in lipid homeostasis in cancers and cardiovascular diseases, and some in neurodegenerative diseases[15]. However, little is known regarding lipids in AID. The majority of the studies report data from enzymatic/colorimetric experiments but very few address the changes in the lipidome of this type of pathologies through lipidomic analysis[15]. Thus, several questions remain unanswered in the field of lipid research in AID. A deeper comprehension of the lipid changes and adaptations is needed to fully elucidate the molecular mechanisms regulating lipid homeostasis in health and loss of homeostasis in AID as well as the specific alterations for each type of AID. This will be of utmost importance for the proposing of biomarkers as well as to design innovative therapeutic strategies in agreement with the nowadays so-called precision medicine.

Lipidomics is an “omic” field of research that studies the alterations of lipids using mass spectrometry-based approaches. Mass spectrometry (MS) is able to reveal and identify, without ambiguity, the full structural details of a molecular lipid species. Due to its high sensitivity, it is possible to perform the identification of several lipid components from a complex mixture simply by analysing the different fragmentation patterns under tandem MS (MS/MS) conditions as well as allowing lipid species quantification[24].

Lipid analysis follows a routine MS workflow (Figure 1.2-1) that starts with a pre-analytical stage, which refers to sample collection and treatment (step one). More and more attention has been given to this step because it highly influences the results of lipidomic analysis. Various pre-analytical parameters have been proven to affect the stability, type and quantity of lipids extracted. The most important pre-analytical parameters to significantly affect the results comprise the

transport and storage conditions, the type of sample (variations in the matrix affect the lipid volume, the extraction efficiency, and the chromatographic results), and the haematocrit[25]. Then, the lipids from the sample (for example plasma, serum, whole blood or cells) are extracted using organic solvents (step two). There are plenty of extraction protocols, which some of them are more suitable for a specific type of sample. The third step is data acquisition by MS based approaches, where the total lipid content can be analysed either by targeted or untargeted analysis, depending on the goal of the research. Targeted lipidomic analysis is used to identify and quantify specific lipids, aiming to profile specific markers or unravel specific pathways. In this case it can be applied a direct infusion MS approach without prior separation of the compounds. On the other hand, lipidomics can be used in an untargeted manner, looking for the identification and quantification of as much lipid species as possible. Untargeted lipidomic analysis is generally used for screening purposes, normally to compare different groups or biological conditions (for instance, an analysis of pathology *vs* health status)[26, 27]. This type of approach is a high throughput lipidomic technique with the application of a chromatographic separation of the lipids, most commonly liquid chromatography coupled with mass spectrometry (LC-MS), in which the lipids are separated according with their different polarities. Regarding the mass spectrometer component, the most used ionization source is Electrospray Ionization and different mass analysers have been used to identify the lipidome of different diseases, such as the Linear Ion Trap, Triple Quadrupole, Time of Flight and Orbitrap, differing between them in several parameters like resolution, mass range, scan rate, detection limits and sensitivity[28]. The final step of the MS workflow is data analysis. The interpretation of the (LC-)MS and MS/MS spectra allows the identification and quantification of the lipid species, either in the positive or in the negative modes, depending on the structural features (polarity) of the polar head group[29]. Several bioinformatic tools can be used for data analysis and treatment, such as MS-DIAL, MZmine, among others[30, 31]. Having said that, the procedures (of each MS workflow step) must be optimized and standardized to increase the consistency and reproducibility of the experimental procedure and allow the comparison of research work data between different labs, for instance in international microsampling cohorts, promoting a harmonization of the lipidomics research field.

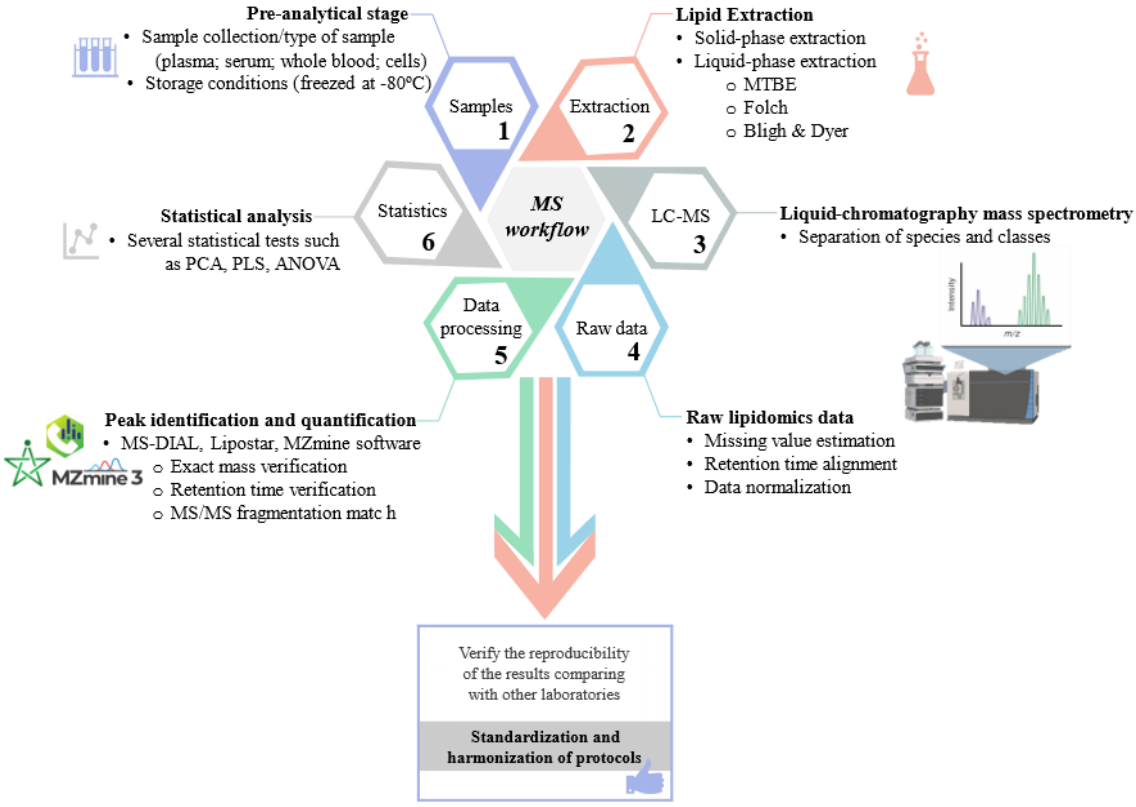

Figure 1.2-1. Mass spectrometry-based lipidomics workflow for the analysis of the lipidome of diseases, such as AID.

The identification of each lipid specie is made based on the retention time (RT), once each lipid class typically displays a characteristic RT range, *m/z* value and exact mass of the ions identified in the MS spectra, along with characteristic fragment ions or neutral losses for each class found in MS/MS spectra. In the positive mode it is possible to detect preferentially phosphatidylcholines (PC), lyso-PC, sphingomyelins and ceramides, due to the formation of the positive ion $[M+H]^+$. Neutral lipids like diacylglycerol, triacylglycerol and cholesteryl esters are also usually identified in the positive mode as $[M+NH_4]^+$ or $[M+Na]^+$ adducts. In the negative mode it is preferentially detected the presence of phosphatidylethanolamine (PE), lyso-PE (although PE class can also be identified in the positive mode), phosphatidylinositol, phosphatidylglycerol, phosphatidic acids and phosphatidylserines with the formation of $[M-H]^-$ ions. The identification of the fatty acyl chain composition and information on the remaining structural features of the molecule is obtained through interpretation of MS/MS spectra of each lipid species. In negative ion mode for instance, it is possible the identification of carboxylate anions, $RCOO^-$ ions, which enables the identification of the fatty acids (FA) present in a specific lipid specie. The interpretation of MS/MS data is crucial on lipidomic research once it enables the identification of the fragment ions characteristic of each lipid class and pinpoints the molecular

structure of polar lipids, including the identification of the polar head group and of FA chains[32]. LC-MS lipidomic approach was employed on the research studies described in the present Thesis for the identification of the lipidome of AID and in the dried blood spots method test. The procedures used for the identification of ions and characteristic fragmentation of each lipid class, along with the strategies for peak integration for quantitative purposes, are clarified in detail throughout the following chapters.

Besides the application of lipidomics for research purposes, the use of this type of analysis is broadening during the recent years to unravel the deregulation of lipid homeostasis in diseases, giving rise to the field that is now called clinical lipidomics. Clinical lipidomics merges the medical sphere with the lipid science in a new and integrative way. It intends to "measure the large scale of lipid species of patient samples, understand disease-specific lipidomic profiles, and fuse with clinical phenomics"[33]. Clinical lipidomics has very defined goals such as to identify disease biomarkers, to comprehend the underlying mechanisms of pathology development and become a standardized, reliable, and reproductible approach to diagnose diseases and monitor therapeutic strategies. More than a mere high throughput measurement of lipids from patient samples, clinical lipidomics aims to connect the patient lipid profile with its clinical phenotypes to achieve a better identification of disease severity, stage, duration and prognosis. Clinical lipidomics works together with precision medicine to provide the best outcome possible concerning treatment and health care to the individual patient and society.

In clinical settings, the pre-analytical stage (sample treatment before any further procedure) is very important and it is presented as a challenge for clinical lipidomics (the first step of the MS workflow) because many times the samples reach the laboratory poorly accommodated or were not stored in the best conditions to prevent lipid degradation. In addition, patients with chronic diseases have to perform routine analysis, which can become a tedious and painful practice by the common venipuncture method. Also, they need to go to medical services quite often for blood collection, which can be inconvenient specially for elderly patients or children. Hence, healthcare agenda aims to smooth the procedure of blood collection, making it a less invasive method that can be performed by the patient himself at home, avoiding specialized handling, storage and transport conditions (to ease the pre-analytical stage), and lowering the costs to the healthcare entities. The feasibility of dried blood spots (DBS) as a new sampling approach in autoimmune patients, as a possible substitute of the traditional methods[25] is a very promising approach.

DBS have been used for a long time in newborn screening programs for the detection of metabolic disorders[34]. The application of DBS in metabolomics[35, 36] and proteomics[37] studies is also well established due to the several advantages that DBS offer. From a single circle of blood, it is possible to analyse thousands of compounds only by using small volumes (μL) of

capillary blood deposited in the DBS paper card[38]. Thus, this microsampling method is very simple and easy to perform, making it possible for the patient to collect the sample at home, instead of having to go to a specialized entity to blood collection. Besides, DBS are a very stable matrix and the samples do not need to be immediately refrigerated facilitating their accommodation and transport[39]. There is evidence that lipids are stable in DBS therefore this type of sample could also be useful in lipidomic analysis (besides being a promising replacement of venipuncture for the routine analysis of AID)[40]. Nevertheless, the analysis of lipids from DBS samples is not yet well established in the lipidomics field and there is a need for more investigation on its applicability on this area. From the few studies that are already published on this matter, one may draw the conclusion that the pre-analytical and analytical methods need to be standardized and harmonized so that different laboratories may have concise results (Figure 1.2-2). Even though, it seems that DBS are as effective as plasma/serum/whole blood samples, reaching high levels of sensitivity and specificity during MS and MS/MS analysis, although scarcely used in lipidomics.

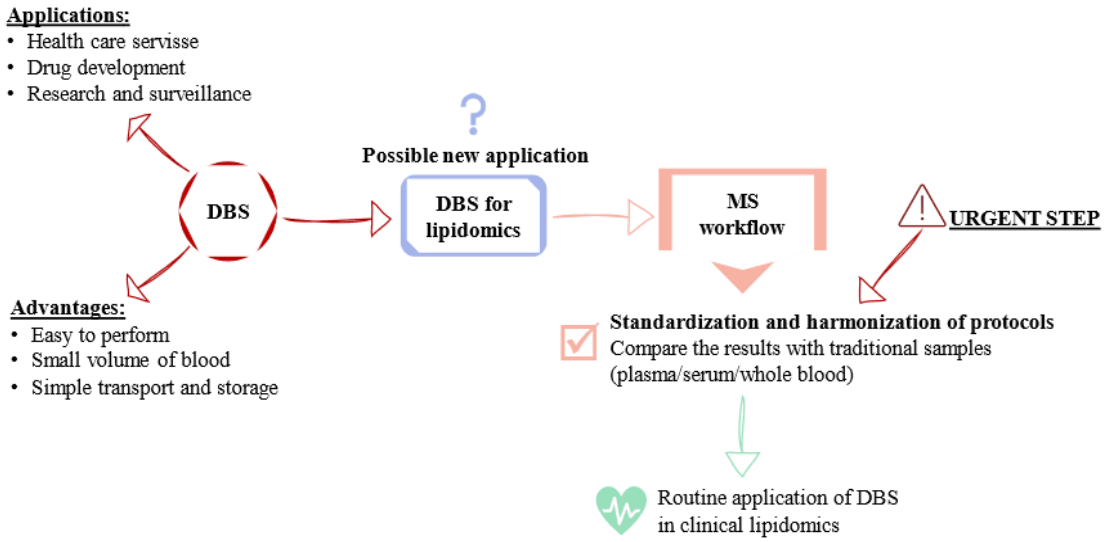

Figure 1.2-2. DBS current applications and advantages. Possible use of DBS method in clinical lipidomics after standardization and checking of protocols.

1.3 Thesis objectives and outline

Lipidomics is an emerging field of research, however its applicability in the investigation of AID is still scarce[15, 41, 42]. In this Thesis it was proposed to fingerprint the plasma, serum, and whole blood lipidome of the most prevalent AID, namely MSs, SLE and SS, and to use lipidomic data as a toolbox to identify specific lipidomic signature for lipid biomarkers discovery of different AID.

Currently, strategies that provide disease and disease-state markers suitable for accurate diagnosis, timely intervention and a better disease management ("precision medicine"), particularly those in scenarios of multifactorial diseases, are highly needed. Universities and hospitals needed to work together to meet social and health challenges, creating opportunities for good health, well-being, and healthcare.

The lack of knowledge regarding plasma/serum/whole blood lipidomics and oxidative lipidomic changes in AID encouraged the proposition of this Thesis with the following main objectives:

(1) fingerprint the lipidomic signature in each AID;

(2) screening of oxidized phospholipids in each AID;

(3) identification, in each AID, of specific markers of disease activity that allow the prediction in a timely manner of the occurrence of relapsing episodes and/or markers to monitor clinical/treatment outcomes and disease progression;

(4) identification of a possible variation of the lipidomic signatures with age and sex of AID patients that can be used as targets for personalized therapies;

(5) development and validation of a non-invasive test for lipid profiling: blood spot test.

These specific goals are addressed in the present Thesis along five Chapters, described below:

Chapter 1. Introduction

A general introduction is provided on the current knowledge of AID. Lipidomic studies on this type of pathologies are found to be scarce and challenging, yet important for the evolution of the understanding of such diseases. The workflow of MS based approaches applied to clinical lipidomics is discussed as well as an innovative non-invasive method of lipid analysis easier to standardize the pre-analytical stage of the lipidomic analysis.

Chapter 2. Lipidomic analysis in autoimmune diseases

This chapter is divided into three subchapters:

- Chapter 2.1 Current knowledge on lipidomics in Multiple Sclerosis provides a systematic review of international peer-reviewed scientific literature on lipidomic studies on MSs to understand the state of the art concerning the relationship between the lipid profile and this pathology. This chapter was published in the journal Multiple Sclerosis and Related Disorders.
- Chapter 2.2 Lipidomic Analysis in Multiple Sclerosis shows the serum phospholipidomic signature of MSs that was determined, revealing promising new putative biomarkers. It was published in the journal Archives of Biochemistry and Biophysics.
- Chapter 2.3 Lipidomics Analysis in Systemic Lupus Erythematosus and Systemic Sclerosis concerns a lipidomic analysis comparing SLE and SS whole blood and plasma samples. Possible future biomarkers were considered. This chapter was submitted to the Journal of Proteome Research.

Chapter 3. Clinical lipidomics, autoimmune diseases and oxidative stress

This chapter is divided into two subchapters:

- Chapter 3.1 Current knowledge on lipidomics and oxidative stress in Rheumatoid Arthritis provides a systematic review of international peer-reviewed scientific literature on lipidomic and oxidative stress studies on RA to understand the state of the art concerning the relationship between the lipid profile, oxidation and the disease. This chapter was published in the journal Antioxidants.
- Chapter 3.2 Oxidation studies on cholesteryl esters reveals the fragmentation patterns of oxidized cholesteryl esters species, important in cardiovascular diseases. This knowledge may now be applied in the lipidomic analysis of AID since cardiac involvement is also a comorbidity of this type of pathologies. It was published in the Journal of the American Society for Mass Spectrometry.

Chapter 4. Novel pre-analytical methods in Clinical lipidomics

This chapter is divided into two subchapters:

- Chapter 4.1 Clinical lipidomics and the use of dried blood spots provides a comprehensive review of international peer-reviewed scientific literature on lipidomic analysis using dried blood spots. Type of paper cards, extraction methods and lipidomic based mass spectrometry approaches were addressed. This chapter was published in the journal Analytical and Bioanalytical Chemistry.
- Chapter 4.2 Lipidomic analysis using dried blood spots discloses that the lipid profile of children varies according with the age. The lipid profile was determined using dried blood

spots and liquid chromatography-mass spectrometry-based approaches. It was published in the journal Molecular Omics.

Chapter 5. Concluding remarks and future perspectives

In this final Chapter, the main findings reported on Chapters 2, 3 & 4 are discussed in an integrated way, with some guidelines being suggested for future research trials.

All the research studies presented in this Thesis are under the scope of clinical lipidomics with the goal to improve the knowledge in this science field regarding AID and contribute to a more refined precision medicine.

References

1. National Stem Cell Foundation (2023) Autoimmune Disease. https://nationalstemcellfoundation.org/glossary/autoimmune-disease/. Accessed 28 Mar 2023
2. Sciences NI of EH (2023) Autoimmune Diseases. In: Heal. Educ. https://www.niehs.nih.gov/health/topics/conditions/autoimmune/index.cfm. Accessed 28 Mar 2023
3. Otto SE (2003) Understanding the Immune System: Overview for Infusion Assessment. J Infus Nurs 26:79–85
4. Foundation ID (2013) Patient & Family Handbook, 5th Editio. Immune Deficiency Foundation, USA
5. Schmitt J (2003) Recombinant autoantigens for diagnosis and therapy of autoimmune diseases. Biomed Pharmacother 57:261–268
6. Lang KS, Burow A, Kurrer M, Lang PA, Recher M (2007) The role of the innate immune response in autoimmune disease. J Autoimmun 29:206–212
7. Osterland CK (1994) Laboratory diagnosis and monitoring in chronic systemic autoimmune diseases. Clin Chem 40:2146–2153
8. Tian J, Zhang D, Yao X, Huang Y, Lu Q (2023) Global epidemiology of systemic lupus erythematosus: a comprehensive systematic analysis and modelling study. Ann Rheum Dis 82:351–356. https://doi.org/10.1136/ard-2022-223035
9. Rodriguez-Pintó I, López-Benjume B, Espinosa G, Cervera R (2021) Catastrophic antiphospholipid syndrome. Rev Colomb Reumatol 28:39–43. https://doi.org/10.1016/j.rcreu.2021.02.004
10. Carter PH, Zhao Q (2010) Clinically validated approaches to the treatment of autoimmune diseases. Expert Opin Investig Drugs 19:195–213
11. Druet P (1992) Diagnosis of autoimmune diseases. J Immunol Methods 150:177–184
12. Raval P (2011) Systemic (Non-Organ Specific) Autoimmune Disorders. In: Enna SJ, Bylund. DB (eds) xPharm: The Comprehensive Pharmacology Reference. Elsevier Inc., pp 1–6
13. Fridkis-Hareli M (2008) Immunogenetic mechanisms for the coexistence of organ-specific and systemic autoimmune diseases. J Autoimmune Dis 5:1. https://doi.org/10.1186/1740-2557-5-1
14. Chandrashekara S (2012) The treatment strategies of autoimmune disease may need a different approach from conventional protocol: A review. Indian J Pharmacol 44:665–671
15. Ferreira HB, Pereira AM, Melo T, Paiva A, Domingues MR (2019) Lipidomics in autoimmune diseases with main focus on systemic lupus erythematosus. J Pharm Biomed Anal 174:386–395
16. Islam A, Kamal MA (2018) Editorial: Current Vision of Systemic Autoimmune Diseases - From Diagnosis to Management Systemic. Endocrine, Metab Immune Disord - Drug Targets 18:96–97
17. Konforte D, Diamandis EP, Van Venrooij WJ, Lories R, Ward MM (2012) Autoimmune diseases: Early diagnosis and new treatment strategies. Clin Chem 58:1510–1514
18. Villalta D, Tozzoli R, Tonutti E, Bizzaro N (2007) The laboratory approach to the diagnosis of autoimmune diseases: Is it time to change? Autoimmun Rev 6:359–365
19. Sur LM, Floca E, Sur DG, Colceriu MC, Samasca G, Sur G (2018) Antinuclear antibodies: Marker of diagnosis and evolution in autoimmune diseases. Lab Med 49:e62–e73
20. Santhosh P, Ajithkumar K (2020) Anti-nuclear antibodies: A practical approach to testing and interpretation. J Ski Sex Transm Dis 3:175. https://doi.org/10.25259/JSSTD_40_2020
21. Castro C, Gourley M (2010) Diagnostic testing and interpretation of tests for autoimmunity. J Allergy Clin Immunol 125:S238–S247. https://doi.org/10.1016/j.jaci.2009.09.041
22. Segatto M, Pallottini V (2020) Facts about fats: New insights into the role of lipids in metabolism, disease and therapy. Int J Mol Sci 21:6651
23. Dorninger F, Brodde A, Braverman NE, Moser AB, Just WW, Forss-Petter S, Brügger B, Berger J (2015) Homeostasis of phospholipids - The level of phosphatidylethanolamine tightly adapts to changes in ethanolamine plasmalogens. Biochim Biophys Acta - Mol Cell Biol Lipids 1851:117–128. https://doi.org/10.1016/j.bbalip.2014.11.005
24. Nelson D, Cox M (2014) Princípios de Bioquímica de Lehninger, 6ª Edição. Artmed, Porto Alegre
25. Ferreira HB, Guerra IMS, Melo T, Rocha H, Moreira ASP, Paiva A, Domingues MR (2022) Dried blood spots in clinical lipidomics: optimization and recent findings. Anal Bioanal Chem 414:7085–7101. https://doi.org/10.1007/s00216-022-04221-1
26. Züllig T, Trötzmüller M, Köfeler HC (2020) Lipidomics from sample preparation to data analysis: a primer. Anal Bioanal Chem 412:2191–2209. https://doi.org/10.1007/s00216-019-02241-y
27. Alves MA, Lamichhane S, Dickens A, McGlinchey A, Ribeiro HC, Sen P, Wei F, Hyötyläinen T, Orešič M (2021) Systems biology approaches to study lipidomes in health and disease. Biochim

Biophys Acta - Mol Cell Biol Lipids 1866:158857. https://doi.org/10.1016/j.bbalip.2020.158857
28. Domingues P, García A, Skrzydlewska E (2018) Advanced Analytical Chemistry for Life Sciences. AACLifeSci
29. Domingues MRM, Reis A, Domingues P (2008) Mass spectrometry analysis of oxidized phospholipids. Chem Phys Lipids 156:1–12
30. Schmid R, Heuckeroth S, Korf A, Smirnov A, Myers O, Dyrlund TS, Bushuiev R, Murray KJ, Hoffmann N, Lu M, Sarvepalli A, Zhang Z, Fleischauer M, Dührkop K, Wesner M, Hoogstra SJ, Rudt E, Mokshyna O, Brungs C, Ponomarov K, Mutabdžija L, Damiani T, Pudney CJ, Earll M, Helmer PO, Fallon TR, Schulze T, Rivas-Ubach A, Bilbao A, Richter H, Nothias L-F, Wang M, Orešič M, Weng J-K, Böcker S, Jeibmann A, Hayen H, Karst U, Dorrestein PC, Petras D, Du X, Pluskal T (2023) Integrative analysis of multimodal mass spectrometry data in MZmine 3. Nat Biotechnol 41:447–449. https://doi.org/10.1038/s41587-023-01690-2
31. Tsugawa H, Ikeda K, Takahashi M, Satoh A, Mori Y, Uchino H, Okahashi N, Yamada Y, Tada I, Bonini P, Higashi Y, Okazaki Y, Zhou Z, Zhu Z-J, Koelmel J, Cajka T, Fiehn O, Saito K, Arita M, Arita M (2020) A lipidome atlas in MS-DIAL 4. Nat Biotechnol 38:1159–1163. https://doi.org/10.1038/s41587-020-0531-2
32. Pulfer M, Murphy RC (2003) Electrospray mass spectrometry of phospholipids. Mass Spectrom Rev 22:332–364
33. Lv J, Zhang L, Yan F, Wang X (2018) Clinical lipidomics: a new way to diagnose human diseases. Clin Transl Med 7:10–12. https://doi.org/10.1186/s40169-018-0190-9
34. Wagner M, Tonoli D, Varesio E, Hopfgartner G (2016) The use of mass spectrometry to analyze dried blood spots. Mass Spectrom Rev 35:361–438. https://doi.org/10.1002/mas.21441
35. Rus C-M, Di Bucchianico S, Cozma C, Zimmermann R, Bauer P (2021) Dried Blood Spot (DBS) Methodology Study for Biomarker Discovery in Lysosomal Storage Disease (LSD). Metabolites 11:382. https://doi.org/10.3390/metabo11060382
36. Li K, Naviaux JC, Monk JM, Wang L, Naviaux RK (2020) Improved Dried Blood Spot-Based Metabolomics: A Targeted, Broad-Spectrum, Single-Injection Method. Metabolites 10:82. https://doi.org/10.3390/metabo10030082
37. Nakajima D, Ohara O, Kawashima Y (2021) Toward proteome-wide exploration of proteins in dried blood spots using liquid chromatography-coupled mass spectrometry. Proteomics 21:2100019. https://doi.org/10.1002/pmic.202100019
38. Konig S, Yildiz O, Hermann N, Steurer A, Singrasa M, Dobelin W (2012) A novel concept for sample collection and sample preparation. Int J Pharm Sci Rev Res 15:90–94
39. Malsagova K, Kopylov A, Stepanov A, Butkova T, Izotov A, Kaysheva A (2020) Dried Blood Spot in Laboratory: Directions and Prospects. Diagnostics 10:248. https://doi.org/10.3390/diagnostics10040248
40. Gao F, McDaniel J, Chen EY, Rockwell HE, Drolet J, Vishnudas VK, Tolstikov V, Sarangarajan R, Narain NR, Kiebish MA (2017) Dynamic and temporal assessment of human dried blood spot MS/MSALL shotgun lipidomics analysis. Nutr Metab (Lond) 14:28. https://doi.org/10.1186/s12986-017-0182-6
41. Ferreira HB, Neves B, Guerra IM, Moreira A, Melo T, Paiva A, Domingues MR (2020) An overview of lipidomic analysis on different human matrices of multiple sclerosis. Mult Scler Relat Disord 44:102189
42. Ferreira HB, Melo T, Paiva A, Domingues MDR (2021) Insights in the role of lipids, oxidative stress and inflammation in rheumatoid arthritis unveiled by new trends in lipidomic investigations. Antioxidants 10:. https://doi.org/10.3390/antiox10010045

2 CHAPTER 2: LIPIDOMIC ANALYSIS IN AUTOIMMUNE DISEASES

2.1 CHAPTER 2.1: CURRENT KNOWLEDGE ON LIPIDOMICS IN MULTIPLE SCLEROSIS

This chapter was integrally published as follows.
Reprinted with permission from:

H.B. Ferreira, B. Neves, I.M. Guerra, A. Moreira, T. Melo, A. Paiva, M.R. Domingues, An overview of lipidomic analysis in different human matrices of multiple sclerosis, *Multiple Sclerosis and Related Disorders* (2020) volume 44, page 102189
http://dx.doi.org/10.1016/j.msard.2020.102189

Abstract

Multiple sclerosis is a chronic inflammatory and neurodegenerative disease of the central nervous system, and it is one of the most common neurological cause of disability in young adults. It is known that several factors contribute to increase the risk of development and pathogenesis of multiple sclerosis, nonetheless, but the true etiology of this pathology remains unknown. Similar to other inflammatory diseases, oxidative stress and lipid peroxidation are also associated to multiple sclerosis. Alterations in the lipid profile seem to be a hallmark of this pathology which can contribute to the dysregulation of lipid homeostasis and lipid metabolism in multiple sclerosis. Lipidomic studies analysed in this review clearly demonstrate the role of lipids in inflammatory processes, in immunity, and in the onset and development of multiple sclerosis. Several investigations reported alterations of some molecular lipid species, in particular, with decrease of fatty acids (FA) 18:2 and 20:4 and total polyunsaturated FA, with compensatory increases of saturated FA with shorter carbon chains. Oxidized phospholipids were reported in few studies as well. Also, it was shown that clinical lipidomics has potential as a tool to aid both in multiple sclerosis diagnosis and therapeutics by allowing a detailed lipidome profiling of the patients suffering with this disease.

Keywords: Multiple sclerosis; lipidomics; mass spectrometry; biomarkers; lipid peroxidation

1. Multiple sclerosis

Multiple sclerosis is a chronic inflammatory and neurodegenerative disease of the central nervous system (CNS), and it is one of the most common neurological (non-traumatic) cause of disability in young adults (Rahmanzadeh et al., 2019; Society, 2020). This disease leads to a progressive accumulation of disability that affects around 2.3 million people worldwide being most prevalent in women (Federation, 2013; Ortiz et al., 2013). Multiple Sclerosis is a demyelinating disease where myelin and oligodendrocytes (myelin producing cells) are destroyed (Love, 2006). Myelin is a lipid bilayer that protects axons from external damage and enhances neural signalling and transmission. Therefore its destruction increases neurological malfunctioning due to impaired axonal tracts and leads to the formation of focal lesions, known as plaques (Love, 2006; Ortiz et al., 2013). Multiple sclerosis is a disease that affects brain, spinal cord and the optic nerves. The main symptoms include fatigue, tremor, motor dysfunction, nystagmus, numbness, loss of coordination or balance, disturbances in speech and vision, cognitive impairment and acute paralysis (Hurwitz, 2009; Ortiz et al., 2013). However, symptoms and signs depend on the location of the multiple sclerosis lesions in the CNS (Hurwitz, 2009). According to the clinical signs, four disease courses have been identified in multiple sclerosis (Hurwitz, 2009; Magalhaes and Salgado, 1983; Society, 2020; Thompson et al., 2018):

i. **Clinically isolated syndrome (CIS):** is the first episode of neurological symptoms in the CNS, caused by inflammation and demyelination, in a patient not known to have multiple sclerosis. Patients with a clinical condition of CIS may or may not progress to develop multiple sclerosis. There are several conditions with similar multiple sclerosis symptoms, thus, to establish an accurate diagnosis, it needs to be considered a differential diagnosis in all patients presenting with CIS.

ii. **Relapsing-remitting multiple sclerosis (RRMS):** is the most common disease course affecting approximately 85% of multiple sclerosis patients. It is characterized by well-defined relapses of new, or already existing neurological symptoms (active disease state), followed

by periods of partial, or complete, remission (inactive disease state). During those periods, the symptoms may disappear, or continue and become permanent. The diagnosis needs to meet the magnetic resonance imaging (MRI) criteria with objective clinical and radiological evidences, proving dissemination in both time and space

iii. Secondary progressive multiple sclerosis (SPMS): is characterized by at least one relapse, after which follows a progressive worsening of neurological function over time. It can initiate as CIS and develop slowly into SPMS. As SPMS progresses, patients become more disabled. This course of multiple sclerosis is responsible for the highest degree of disability of multiple sclerosis patients.

iv. Primary progressive multiple sclerosis (PPMS): is the rarest course of multiple sclerosis, only approximately 15% of multiple sclerosis patients have PPMS. It is characterized by a slowly worsening of the neurological function from the onset of symptoms. This course of multiple sclerosis may be confused with other pathologies therefore the diagnostic criteria should be strictly applied as explained below.

The diagnosis of multiple sclerosis is not a straightforward process, there are several other diseases that resemble multiple sclerosis in terms of symptomatology. The revised McDonald criteria (Thompson et al., 2018) is the most used to reach a consensual and accurate diagnosis of multiple sclerosis. It allows an earlier diagnosis and includes specific guidelines for using MRI and cerebrospinal fluid (CSF) analysis to speed up the diagnostic process (Hurwitz, 2009; Society, 2020; Thompson et al., 2018). The diagnosis requires not only a clear evidence of at least two CNS lesions located in separate areas and formed in different points in time but also, the exclusion of all other possible diagnosis for the CNS lesions (Hurwitz, 2009; Magalhaes and Salgado, 1983; Poser et al., 1983; Society, 2020). Nevertheless, it is necessary to find biochemical parameters, or biomarkers, that help multiple sclerosis diagnosis process and may even predict its relapses.

Multiple sclerosis is a multifactorial disease influenced by both genetic and environmental factors. Modifications of several gene loci increase the risk of developing multiple sclerosis and confirmed evidence points to immune-associated human leukocyte antigen class II locus

(Baranzini, 2011). Epigenetic changes may also be a contributing factor. Similarly, dysregulation of microRNAs in blood and brain of multiple sclerosis patients have been reported (Hassani and Khan, 2019), and they may interrelate with the immune system and viral infections, specially Epstein-Barr virus infection. Nonetheless, the mechanisms of their interaction are still unknown.

Although there is some controversy whether to classify, or not, multiple sclerosis as an autoimmune disease (AID), multiple sclerosis pathogenesis is linked to a deep dysregulation of the immune system (Society, 2020). The classification of multiple sclerosis as an AID is based on the hyperactivity of adaptive immune response, particularly auto-reactive B cells, T cells (CNS antigen specific $CD4^+$ T cells) and antibodies, and accumulation of immune cells at lesion sites (Afshar et al., 2019).

B cells in multiple sclerosis play different roles, acting as both drivers and regulators of the disease. The pathogenic involvement of B cells is proved by the beneficial effect accomplished by B cell depletion therapy. This type of therapy is performed with anti-CD20, such as Rituximab, and promotes the depletion of B cells without affecting plasmocytes directly, leading to the improvement of multiple sclerosis (Rahmanzadeh et al., 2019; Thi Cuc et al., 2019). Normal functioning B cells produce anti-inflammatory interleukin-10 (IL-10) but, in multiple sclerosis patients this function is impaired (Duddy et al., 2007; Knippenberg et al., 2011). Consequently, this pathological defect of incorrect production of IL-10 may enable multiple sclerosis onset and progression (Thi Cuc et al., 2019). However, more studies are needed to understand the mechanism of the defective IL-10 production by B cells from multiple sclerosis patients, in order to adapt new therapeutic strategies and achieve positive outcomes. Multiple animal model and clinical studies have demonstrated up and downregulation of different cytokines in both CSF and brain tissue of multiple sclerosis patients. The imbalance on cytokines levels is extended to a decreased production of other anti-inflammatory cytokines (such as IL-4 and TGF-β by Th2 cells) and an increased generation of pro-inflammatory ones (as IFN-γ and TNF-α by Th1 cells and IL-17, IL-21, IL-22 and IL-26 by Th17 cells), related with an increased immune response (for further information see (Ghasemi et al., 2017; Göbel et al., 2018)).

T cells, mainly $CD4^+$ T cells, are recognised as the primary drivers of multiple sclerosis. Myelin reactive $CD4^+$ T cells, that have escaped from a defective peripheral tolerance, can be primed after encountering molecular mimicry, CNS-sequestered antigens or bystander activation (Rahmanzadeh et al., 2019). Once activated, autoreactive T cells will go through the blood brain barrier, or the blood-CSF barrier, and enter the CNS initiating an inflammatory attack against myelin sheaths. T cell invasion in CNS is associated with the formation of plaques in the brain white matter of multiple sclerosis patients (Kivisakk et al., 2009). However, immune-mediated inflammation do not rely solely on $CD4^+$ T cells; CD8 T cells, B cells and innate immunity are also fundamental players (as reviewed in (Rahmanzadeh et al., 2019)). Another subset of T cells, $CCR5^+$ γδ T_{EMRA} cells, may be a participator in the demyelination process once they are significantly depleted in relapse RRMS patients, which makes this cell subset an attractive peripheral blood biomarker for disease monitoring (Monteiro et al., 2018).

An additional important player of neuroinflammation are platelets, which are overactivated in multiple sclerosis (Dziedzic and Bijak, 2019). In multiple sclerosis pathophysiology, activated platelets are responsible for the formation of new neuroinflammatory lesions in CNS, since they interact with T cells and induce autoreactive T cells infiltration in CNS (Morel et al., 2017). The involvement of platelets in inflammatory and neurodegenerative events is also suggested by the haematological profile of multiple sclerosis patients, in which the number of platelets in circulation is higher than normal (Hon et al., 2012).

Although several factors contribute to increase the risk of development and pathogenesis of multiple sclerosis, the true etiology of this chronic, inflammatory, neurodegenerative and immune-mediated disease remains unknown. Similar to other inflammatory diseases, oxidative stress and lipid peroxidation are associated to multiple sclerosis, detailed in the following chapters.

2. Oxidative stress in multiple sclerosis

Chronic inflammatory pathologies are characterized by increased oxidative stress conditions. Multiple sclerosis neuroinflammation is associated with oxidative stress by at least two

different mechanisms: 1) production of high levels of reactive oxygen species (ROS) by microglia, astrocytes and neutrophils; and 2) arachidonic acid (AA) signalling through the activation of cyclooxygenase and lipoxygenase pathways (Ortiz et al., 2013). Mitochondrial dysfunction is also a key factor in multiple sclerosis progression. It contributes to increase oxidative stress levels by overproduction of ROS leading to many neurodegenerative processes characteristic of multiple sclerosis (Adamczyk et al., 2017). Similarly to mitochondrial dysfunction, platelet overactivation in multiple sclerosis also leads to the production of pro-inflammatory agents (like ROS), which in turn activate other platelets (Dziedzic and Bijak, 2019; Saluk-Juszczak et al., 2000), increasing (neuro)inflammatory, neurodegenerative and oxidative stress conditions in multiple sclerosis patients. Increased oxidative stress contributes develop brain damages and several mechanisms responsible for multiple sclerosis plaques formation (Goes et al., 2001). The neurotransmitter glutamate is responsible for increasing oxidative stress as well (Gilgun-Sherki et al., 2004). It was detected an upregulation of glutamate levels in CSF associated with higher severity and course of multiple sclerosis. This way, overproduction of glutamate by macrophages might induce axonal damage and oligodendrocytes death in multiple sclerosis plaques (Gilgun-Sherki et al., 2004). The human brain is extremely susceptible to oxidative stress due to its high consumption of oxygen, low activity and concentration of antioxidant enzymes, and elevated content of easily peroxidizable fatty acids (FA), such as polyunsaturated fatty acids (PUFA) (Ortiz et al., 2013).

Endogenous antioxidant defences are important players in controlling the oxidative status of the organism and multiple sclerosis have their antioxidant defence line dysregulated in order to face the excessive oxidative conditions that occur in this pathology (Ibitoye et al., 2016; Ortiz et al., 2013). Superoxide dismutase, catalase, heme oxygenase 1 and glutathione peroxidase are antioxidant enzymes that have their levels significantly increased in active demyelinating plaques of multiple sclerosis brain (Horssen et al., 2008). High concentrations of glutathione peroxidase and superoxide dismutase found in serum also suggest a response to minimize oxidative damage to cells (Ibitoye et al., 2016; Ortiz et al., 2013). However, other antioxidant enzymes have either their activity decreased in plasma of multiple sclerosis patients, like paraoxonase, or obtained mixed

results in different studies or tissues (Ibitoye et al., 2016; Langemann et al., 1992). In CSF of multiple sclerosis, superoxide dismutase was decreased and catalase activity had the opposite trend, evidencing its potential as a diagnostic biomarker in multiple sclerosis (Ibitoye et al., 2016). These controversial results reveal the complex and multifactorial aspect of this disease, unveiling the need for more exploratory investigations, in different tissue and fluid samples, to understand the defence line of antioxidant mechanisms of multiple sclerosis.

The use of antioxidants and substances that have an impact on antioxidant pathways affect the disease course, leading to less pronounced neuroinflammation and neurodegeneration, by reducing disease severity and causing faster remissions (Chiurchiù, 2014; Gilgun-Sherki et al., 2004). For instance, melatonin supplementation was confirmed to improve the antioxidant defence line in multiple sclerosis (Emamgholipour et al., 2016). In addition to immunotherapy, antioxidants may represent a possible and highly helpful supplementation to multiple sclerosis therapy, reducing oxidative stress levels.

Oxidative stress is a fundamental factor in multiple sclerosis pathogenesis and disease course. In relapses, oxidative stress processes are intensified, as expected, leading to neurodegeneration over time (Adamczyk and Adamczyk-Sowa, 2016). Several oxidative stress markers are found to be increased even before inflammatory responses in multiple sclerosis patients (Wang et al., 2014), suggesting that the overproduction of ROS and dysregulation of the oxidant/antioxidant system precedes the neuroinflammatory processes in multiple sclerosis. However, more studies are needed to clarify this matter.

3. The role of lipids in multiple sclerosis pathogenesis

Lipids have several important biological functions and are central players in mediating intra and intercellular signalling pathways. Alterations in lipid metabolism and individual lipid molecular species have been suggested to play important roles on multiple sclerosis pathogenesis and contribute to disease severity.

The metabolic pathway of AA is overactivated in the CNS of multiple sclerosis patients

(Palumbo, 2017). AA is released from the phospholipid (PL) bilayer of cellular membranes by phospholipase A_2 enzyme, which is over activated due to the elevated concentrations of ROS and cytokines in multiple sclerosis (Rajda et al., 2017). In turn, released AA, via cyclooxygenases and lipoxygenases, produces pro-inflammatory prostaglandins and leukotrienes, respectively, that are upregulated in this pathology (Palumbo, 2017). These pro-inflammatory derivatives of AA have been suggested to be involved in the pathogenic mechanisms of demyelination, axonal pathology and oligodendrocyte loss, contributing to the development of motor disabilities. Scientific evidence shows that CSF and post-mortem brains of multiple sclerosis patients have increased levels of AA metabolic pathway (Palumbo, 2017). Also, prostaglandins PGD_2, PGE_2 and PGF_2, and leukotrienes LTB_4 and LTC_4, are upregulated in CSF of patients with multiple sclerosis (Dore-Duffy et al., 1991; Neu et al., 2001; Rosnowska et al., 1981).

The activation of platelets (discussed above) is responsible for the overactivation of the AA pathway as well. Peripheral blood platelets of multiple sclerosis patients were found to excessively express cyclooxygenase 2, which contributes to a hyper-induced AA cascade (Morel et al., 2016).

Additionally, changes in plasma FA have been correlated with multiple sclerosis. Most of the epidemiological studies state that diets rich in saturated FA negatively correlate with multiple sclerosis, increasing the prevalence of this pathology. On the other side, diets rich in PUFA seem to decrease the risk of multiple sclerosis development and may even ameliorate multiple sclerosis symptoms (Harbige and Sharief, 2007). Haghikia and co-authors (Haghikia et al., 2015) determined that long chain, especially C14-C18, are able to supress the differentiation potential of regulatory T cells and decrease the anti-inflammatory cytokine IL-10 expression. In contrast, short chain FA with a three to five carbon atom backbone were found to induce regulatory T cells and supress the production of pro-inflammatory Th17 cells, promoting an anti-inflammatory environment (Haase et al., 2018).

Ceramides (Cer) have been suggested as signalling molecules in CSF of multiple sclerosis leading to mitochondrial dysfunction. Cer with short carbon chains in the C2 position of the sphingosine backbone were found to stimulate oxygen species production in hippocampal glial

cells, resulting in oxidative stress reactions and neuronal death (Darios et al., 2003; Falluel-Morel et al., 2004; Halmer et al., 2014). Moreover, imbalanced cytokine production and activity, namely for the TNF-α, together with stress responses, were associated with Cer accumulation (Singh et al., 1998). TNF-α mediated signalling is related with activation of phospholipase A_2 and the release of AA, which in turn leads to the activation of sphingomyelinases that cleave sphingomyelin (SM) to release Cer (Jana and Pahan, 2010; Jayadev et al., 1997). In this way, the imbalance of cytokines modulates PL and sphingolipid metabolism.

As described in the previous chapter, increased oxidative stress is harmful in multiple sclerosis and contributes to the formation of oxidized lipids. Lipid peroxidation is an alarming process in multiple sclerosis pathogenesis since it can stimulate apoptotic events (Ibitoye et al., 2016; Noseworthy et al., 2000). PUFA are prone to be oxidized therefore lipid peroxidation can affect the integrity and functionality of cell membranes and myelin sheaths. Lipid peroxidation products, such as malondialdehyde (MDA); 4-hydroxy-2-nonenal (4-HNE); 4-hydroxy-2-hexenal and isoprostanes, cross-react with proteins and contribute to increase oxidative stress conditions and (neuro)inflammation (Ortiz et al., 2013). The 4-HNE is a well-known reactive carbonyl specie, that was found to be present in elevated concentrations in foamy macrophages and astrocytes in active demyelinating multiple sclerosis lesions (Ortiz et al., 2013). Also, 4-HNE along with ROS are detrimental to cellular viability, CNS and blood-brain barrier integrity and functionality (Horssen et al., 2008; Usatyuk et al., 2006).

Several studies have identified increased levels of lipid peroxidation products and ROS in CSF and plasma of multiple sclerosis patients, which, along with mitochondrial damage, strongly reiterates the importance of oxidative damage in multiple sclerosis progression (Gilgun-Sherki et al., 2004; Haider et al., 2011; Ibitoye et al., 2016; Ortiz et al., 2009; Qin et al., 2007). Increased levels of lipid peroxidation are shown by markedly higher concentrations of isoprostanes and MDA in plasma, serum, brain and CSF (Adamczyk and Adamczyk-Sowa, 2016; Calabrese et al., 2002; Greco et al., 1999; Haider et al., 2011; Ibitoye et al., 2016; Karg et al., 1999; Mattsson et al., 2007). Lipid oxidation is associated with ongoing demyelination and neurodegeneration in active plaques

of multiple sclerosis. Oxidized PL (ox-PL) have been identified by the monoclonal antibody E06 in multiple sclerosis (Haider et al., 2011; Qin et al., 2007). There is an accumulation of ox-PL within active areas of multiple sclerosis lesions which is associated with disease severity (Haider et al., 2011). Oxidized phosphatidylcholine (ox-PC) was significantly higher in multiple sclerosis plaques being considered has a marker for neuroinflammation in multiple sclerosis brain (Qin et al., 2007). The formation of ox-PC may be a result of a defective clearance of apoptotic cells, which also leads to proinflammatory conditions, stimulating multiple sclerosis development (Elliott and Ravichandran, 2010).

Cholesteryl ester hydroperoxides are useful markers of lipid peroxidation of lipoproteins and were found to be significantly increased in plasma of multiple sclerosis patients (Ferretti et al., 2005). Moreover, oxidized low-density lipoproteins (LDL) and lipid peroxidation products were observed in actively demyelinating lesions in multiple sclerosis brains (Newcombe et al., 1994).

In summary, changes in the lipid profile seem to be a hallmark of multiple sclerosis (Figure 1). There are evidences that lipid peroxidation leads to alterations in lipids, which can contribute to the dysregulation of lipid homeostasis and lipid metabolism in multiple sclerosis patients, as will be detailed in the next chapter.

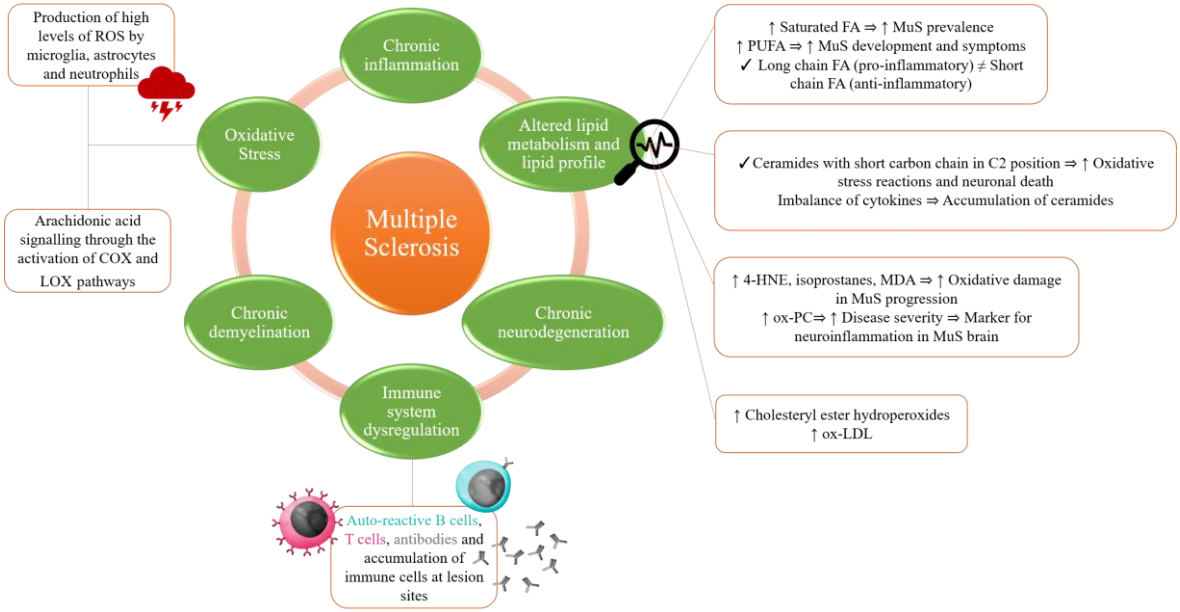

Figure 2.1-1 Overview of the main physio-pathological alterations occurring in multiple sclerosis, including changes related with lipid metabolism and profile.

4. Lipidomics in multiple sclerosis

It is well accepted that changes in lipid metabolism and lipids at molecular level can occur as a consequence of metabolism adaptation in a pathological environment. Thus, lipids can be used as important biomarkers of this disease. High-throughput lipidomics analysis allows the evaluation of the variation of lipids at a molecular level (Figure 2) and has been used with a clinical purpose for the study of several chronic diseases, including diseases of the immune system (Zhao et al., 2014). Clinical lipidomics empowers the understanding of metabolic mechanisms, identification of diagnostic biomarkers and therapeutic targets. Besides that, aims to be a reliable and constant approach to disease diagnostics and therapy monitorization (Lv et al., 2018).

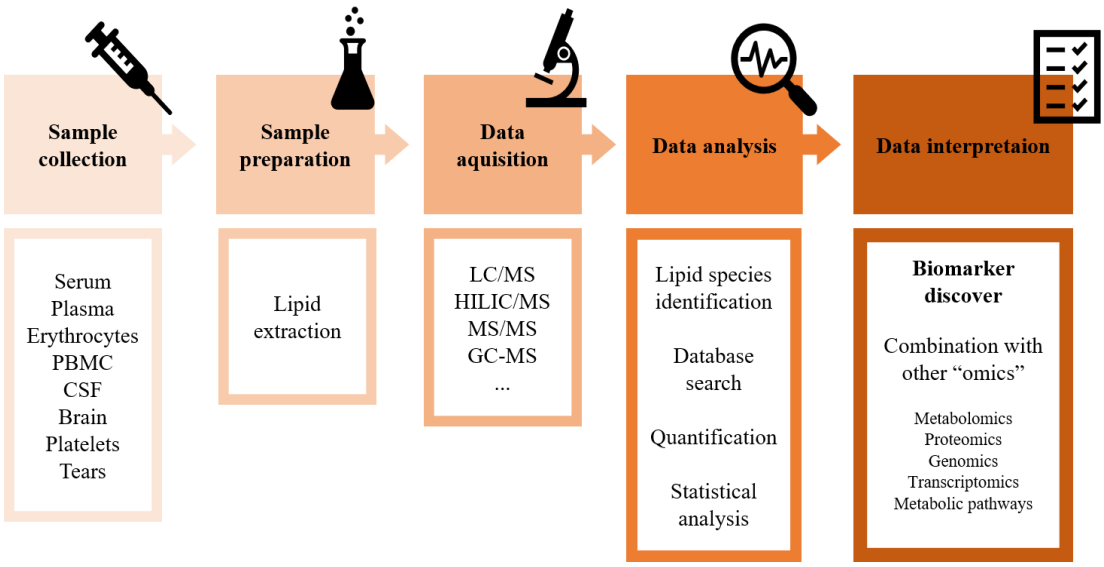

Figure 2.1-2 Lipidomics workflow in multiple sclerosis: from sample collection to biomarker discovery contributing to the understanding of disease pathology.

Studies on the variation of the multiple sclerosis lipid profile at a molecular level using lipidomics were gathered in this review. The research was conducted on PubMed data base with the following keywords: lipid profile, lipidomic(s), phospholipid(s), fatty acid(s), sphingomyelin, sphingolipid(s), ceramide(s) and oxidized, combined with multiple sclerosis. All studies published until 2020 were analysed. The studies that did not use mass spectrometry (MS) techniques were not taken into consideration. To structure this review, the studies were divided according to the type of sample used for the lipidomic approaches and organized in a chronological order.

4.1 Lipidomic analysis of serum/plasma of multiple sclerosis

The analysis of the serum/plasma reveals important information since it is the body fluid that most reflect the metabolic alterations induced by pathologies. Actually, the highest volume of studies focused on lipid analysis has been performed in serum/plasma samples using mainly gas chromatography-mass spectrometry (GC-MS) for profiling of FA.

Through GC-MS, Baker and colleagues (Baker et al., 1964) detected a significant reduction of FA 18:2. This reduction of FA 18:2 was also detected to be more evident in multiple sclerosis patients with increased disease severity, while the concentrations of the other FA analysed remained remarkably constant. The low proportions of plasma FA 18:2 may be due to multiple

sclerosis pathology that changes lipid metabolism, resulting in alterations in the uptake rate of FA 18:2 from the plasma, or in its intake (Baker et al., 1964). In line with these evidences, Love and co-workers (Love et al., 1974) also observed a significant decrease in FA 18:2 levels in multiple sclerosis patients, along with a significant reduction of FA 18:0 and increase of FA 16:0; 16:1 and 18:1. The authors also confirmed the correlation between the decrease of FA 18:2 and the increase of multiple sclerosis severity (Love et al., 1974). According with the previous studies, Neu (Neu, 1983) found significantly diminished concentrations of FA 18:2, as well as of FA 20:4 and total PUFA levels in multiple sclerosis. On the other side, it was determined a significant increase of FA 12:0; 14:0; 16:1; 18:1, as well as total levels of saturated FA (Neu, 1983). Cherayil (Cherayil, 1984) analyzed plasma neutral lipids of multiple sclerosis patients and also observed a significant decrease of FA 18:2 and 20:4, and increase of FA 16:0 and 18:1. Navarro and co-worker (Navarro and Segura, 1988) conducted a detailed study of different plasma lipid fractions in multiple sclerosis and detected a marked reduction of FA 18:0 in free FA and SM fractions; FA 18:1 in triglyceride (TG) fraction; FA 18:2 in SM, cholesterol high density lipoproteins (HDL) and cholesteryl esters (CE) fractions; and FA 20:4 in cholesterol HDL fraction. Additionally, it was determined a significant increase of FA 14:1 in CE fraction; FA 16:0 in cholesterol HDL, LDL + very low-density lipoproteins (VLDL) and CE fractions; FA 16:1 in free FA, CE and TG fractions; FA 18:2 in free FA fraction; and FA 20:0; 20:4 and 24:1 in SM fraction (Navarro and Segura, 1988). The reduction of FA 18:2 was primarily evident in the CE fraction and slightly in the TG and PL fractions (Navarro and Segura, 1988). Another very detailed study on plasma PL, CE and TG was made by Holman and colleagues (Holman et al., 1989), where they identified significant decreases of FA 20:1; 20:2; 20:3; 20:4; 22:0; 22:4; 22:5; 22:6 and 24:1, and in total levels of ω-3 FA, ω-6 FA and PUFA of multiple sclerosis patients. On the other hand, it was determined markedly increased concentrations of FA 14:0; 15:0; 16:0; 16:1 and 18:0, and total levels of saturated FA and branched FA (Holman et al., 1989).

The low levels of total ω-3 FA, ω-6 FA and PUFA in multiple sclerosis indicate that the polyunsaturation process was impaired. Metabolic alterations of multiple sclerosis lipid metabolism

caused a decrease of PUFA that was compensated with an elevation of total saturated FA. The considerable deficiency of unsaturation reduces the fluidity of the membrane`s lipid bilayer. However, the increase of branched FA could partially compensate the decreased fluidity caused by PUFA deficiency (Holman et al., 1989). On the other side, the increase of FA 15:0 in multiple sclerosis patients suggests an increased synthesis of odd-chain FA, which may promote fluidity of membrane PL. This way, high concentrations of shorter chain, saturated, branched and odd-chain FA could have compensatory effects on membranes` fluidity caused by deficiency of PUFA (Holman et al., 1989).

Through MS combined with liquid chromatography (LC), Del Boccio and collaborators (Del Boccio et al., 2011a) found markedly reduced levels of lyso-phosphatidylcholine (LPC) species, LPC(16:0), LPC(18:0) and LPC(18:1), and unequivocally increased concentrations of lyso-phosphatidylethanolamine (LPE) species, LPE(24:1), in multiple sclerosis patients (Del Boccio et al., 2011a). Also, a decrease in LPC/PC ratio was observed highlighting a specific trend in reduced LPC in multiple sclerosis. Kurz and co-workers (Kurz et al., 2018) quantified the level of sphingolipids in plasma of multiple sclerosis and found significantly decreased concentrations of C16:0-lactosylceramide (LacCer) and significantly increased levels of C16:0-Cer; C16:0-glucosylceramide (GlcCer); C18:0-LacCer; C18:0-GlcCer; C24:0-Cer; C24:1-Cer and C24:1-GlcCer (Kurz et al., 2018).

In contrast, (Karlsson et al., 1971), (Shukla and Clausen, 1978) and (Wilkins et al., 2009) did not find statistically significant differences between the plasma lipid profile of multiple sclerosis patients and controls. Further studies are needed to characterize multiple sclerosis lipid profile and metabolism.

To conclude, the studies previously mentioned suggest that there are alterations in multiple sclerosis lipid metabolism that can be evaluated through serum/plasma lipidomic analysis. Overall, plasma FA alterations are manifested as a considerable deficit of FA 18:2 and total PUFA, a less pronounced deficit of FA 20:4 (AA) and an increase of short chain FA.

Table 2.1-1. Main lipid variations observed in serum/plasma of multiple sclerosis patients reported in published lipidomic studies, available in PubMed data base, using MS approaches.

Reference	Analytical method	Lipid extraction method	Results	
			↓ Reduction	↑ Increase
(Baker et al., 1964)	GC-MS	Sperry and Brand method	18:2	-
(Karlsson et al., 1971)	GC-MS	Chloroform/methanol (1:1, v/v)	NSD	NSD
(Love et al., 1974)	GC-MS	INF	18:0; 18:2	16:0; 16:1; 18:1
(Shukla and Clausen, 1978)	GC-MS	INF	NSD	NSD
(Neu, 1983)	GC-MS	Modified Folch	18:2; 20:4; Σ PUFA	12:0; 14:0; 16:1; 18:1; Σ saturated FA
(Cherayil, 1984)	GC-MS	Isopropanol/heptane/NH_2SO_4 (40:10:1, v/v/v)	18:2; 20:4	16:0; 18:1
(Navarro and Segura, 1988)	GC-MS	Isopropanol (1:5, v/v)	In FFA fraction: 18:0 In SM fraction: 18:0; 18:2 In cholesterol HDL fraction: 18:2; 20:4 In CE fraction: 18:2 In TG fraction: 18:1	In FFA fraction: 16:1; 18:2 In SM fraction: 20:0; 20:4; 24:1 In cholesterol HDL and LDL+VLDL fractions: 16:0 In CE fraction: 14:1; 16:0; 16:1 In TG fraction: 16:1
(Holman et al., 1989)	GC-MS	Chloroform/methanol (2:1, v/v)	20:1; 20:2; 20:3; 20:4; 22:0; 22:4; 22:5; 22:6; 24:1; Σ ω-3; Σ ω-6; Σ PUFA	14:0; 15:0; 16:0; 16:1; 18:0; Σ saturated FA; Branched FA
(Wilkins et al., 2009)	GC-MS	INF	NSD	NSD
(Del Boccio et al., 2011b)	LC-MS	Modified Bligh and Dyer	LPC(16:0); LPC(18:0); LPC(18:1) LPC/PC ratio	LPE(24:1)
(Kurz et al., 2018)	LC-MS/MS	Methanol/chloroform/hydrochloric acid (15:83:2, v/v/v)	C16:0-LacCer	C16:0-Cer; C16:0-GlcCer; C18:0-LacCer; C18:0-GlcCer; C24:0-Cer; C24:1-Cer; C24:1-GlcCer

NSD: no significant differences; INF: information not found

4.2 Lipidomic analysis of erythrocytes of multiple sclerosis

Erythrocytes, or red blood cells (RBC), usually have bigger diameters in multiple sclerosis, which is positively correlated with the activity of the disease (Plum and Fog, 1959; Prineas, 1968). Therefore, erythrocytes` fragility, lipid content and possible alterations of the lipid metabolism and profile are higher than non-pathological erythrocytes. Up to date and to the best of our knowledge, GC-MS was the only MS approach used in lipidomic works performed in RBC.

Gul and colleagues (Gul et al., 1970) analysed total PL fraction of RBC and it was verified that multiple sclerosis patients had significantly lower concentrations of FA 18:2. In agreement with these results, Cherayil (Cherayil, 1984) not only determined reduced levels of FA 18:2, but also markedly higher levels of FA 16:0 and 16:1 in RBC of multiple sclerosis. On the other hand, Evans and collaborator (Evans and Dodd, 1989) found FA 18:1 to be considerably reduced and FA 18:2 and 22:6 to be elevated. However, it should be noticed that these results were from multiple sclerosis patients receiving dietary supplements containing PUFA, once the dada obtained for multiple sclerosis patients without supplementation did not statistically differ from healthy controls (Evans and Dodd, 1989). Navarro and co-worker (Navarro and Segura, 1989) separated PL fractions [LPC, PC, SM, phosphatidylethanolamine (PE), phosphatidylserine (PS), phosphatidylinositol (PI) and phosphatidic acid] of RBC by thin-layer chromatography and lipidomic analysis revealed significant reductions of PC molecular species with 18:2 and 20:4; SM molecular species with 23:0 and 24:1; PE molecular species with 18:0; 20:3; 20:4 and 22:4 and remaining PL species with 18:2 and 20:4 (Navarro and Segura, 1989). They also determined significantly increased concentrations of PC molecular species bearing 14:0; 16:0 and 16:1; SM molecular species carrying 14:0; 16:0; 18:0 and 18:1; PE molecular species having 14:0; 16:0 and 18:1 and remaining PL species with 16:0 and 18:0. In PL fractions, there was a decrease of very long chain FA, in particular PUFA, and an increase of short chain FA with lower degree of unsaturations in multiple sclerosis. As explained before, the reduction of PUFA and long chain FA, may induce a reduction in membrane fluidity and resistance that can be compensated by the

increase of saturated FA with shorter carbon chains. Aupperle and partners (Aupperle et al., 2008) studied the FA content of membrane PL of RBC of multiple sclerosis patients and verified that the levels of FA 20:3 ω-6; 20:5 ω-3; 22:6 ω-3; total ω-3; total ω-6 and total PUFA were significantly reduced while FA 14:0; 18:0; 18:1 ω-9; 22:1 ω-9 and total monounsaturated FA (MUFA) had the opposite behaviour, having markedly higher concentrations in multiple sclerosis. The reduction of ω-3 and ω-6 FA may be explained by the increased activity of phospholipase A_2 and higher eicosanoid production that are characteristic of multiple sclerosis, and might deplete certain ω-3 and ω-6 FA from RBC membrane pools (Aupperle et al., 2008; Palumbo, 2017). The authors also studied the relationship between FA levels of multiple sclerosis and depression, no significant correlations between groups were found (Aupperle et al., 2008). Hon`s research group conducted several studies on erythrocytes of multiple sclerosis however only one obtained significant results (G. M. Hon et al., 2009b). It was found markedly reductions of PC molecular species bearing C20:4 ω-6 and PE molecular species carriers of C22:4 ω-6 in multiple sclerosis erythrocyte samples (G. M. Hon et al., 2009b). Moreover, the decrease of PC with C20:4 ω-6 was inversely correlated with disease severity and inflammation. These authors attributed the reduction of C20:4 ω-6 in erythrocytes membrane to an insufficient uptake of this FA due to depleted plasma stores (G. M. Hon et al., 2009b).

Unlike the previously described investigations, (Koch et al., 2006) and (G. M. Hon et al., 2009a; Hon et al., 2011) did not find statistically significant differences between the erythrocytes lipid profile of multiple sclerosis patients and controls, once again revealing the complexity of multiple sclerosis lipid profile.

In summary, RBC are a possible mean to evaluate lipid alterations in multiple sclerosis as well. A deficit in FA 18:2 and 20:4 is also detected in erythrocytes of multiple sclerosis. The depletion of PUFA and long chain FA in RBC of multiple sclerosis patients seems to be compensated by the increase of saturated FA and with shorter carbon chains. This could possibly be an adaptation mechanism of the organism to maintain cellular homeostasis, by trying to maintain cell membranes` fluidity.

Table 2.1-2. Main lipid variations observed in erythrocytes of multiple sclerosis patients reported in published lipidomic studies, available in PubMed data base, using MS approaches.

Reference	Analytical method	Lipid extraction method	Results	
			↓ Reduction	↑ Increase
(Gul et al., 1970)	GC-MS	Folch	18:2	-
(Cherayil, 1984)	GC-MS	Folch	18:2	16:0; 16:1
(Evans and Dodd, 1989)	GC-MS	INF	18:1	18:2; 22:6
(Navarro and Segura, 1989)	GC-MS	Isopropanol	PC(C18:2); PC(C20:4); SM(C23:0); SM(C24:1); PE(C18:0); PE(C20:3); PE(C20:4); PE(C22:4) Remaining PL species with C18:2; C20:4	PC(C14:0); PC(C16:0); PC(C16:1); SM(C14:0); SM(C16:0); SM(C18:0); SM(C18:1); PE(C14:0); PE(C16:0); PE(C18:1) Remaining PL species with C16:0; C18:0
(Koch et al., 2006)	GC-MS	INF	NSD	NSD
(Aupperle et al., 2008)	GC-MS	Methanol/chloroform (1:2, v/v) (Dodge and Phillips 1967), Folch	20:3 ω-6; 20:5 ω-3; 22:6 ω-3 Σ ω-3; Σ ω-6; Σ PUFA	14:0; 18:0; 18:1 ω-9; 22:1 ω-9 Σ MUFA
(G. M. Hon et al., 2009b)	GC-MS	Folch	PC(C20:4 ω-6); PE(C22:4 ω-6)	-
(G. M. Hon et al., 2009a)	GC-MS	Folch	NSD	NSD
(Hon et al., 2011)	GC-MS	Folch	NSD	NSD

NSD: no significant differences; INF: information not found

4.3 Lipidomic analysis of peripheral blood mononuclear cells (PBMC) of multiple sclerosis

Changes in the membrane PL composition have a direct impact on immune cell functions. Some examples of these effects are the changes in physical properties of the membrane, cell signalling pathways, production of lipid mediators and eicosanoid production as part of the inflammation process (Calder, 2007). PBMC are peripheral blood cells that have a round nucleus, which include lymphocytes and monocytes, and are affected by lipid changes. In the lipidomic investigations of PBMC analysed in this review, GC-MS was still the most used technique, but LC-MS approaches are starting to be performed.

Cherayil (Cherayil, 1984) analysed FA methyl esters from lymphocytes of multiple sclerosis patients and saw a significant reductions of FA 18:2, in agreement with the results obtained in the same study for RBC and plasma. Hon and co-workers conducted several investigations on PBMC and reported different results (G. Hon et al., 2009; G. M. Hon et al., 2009a; Hon et al., 2011). Initially, this team analysed PBMC membrane FA composition of PC, PE, PS, PI and SM and found markedly reduced levels of PE bearing 22:4 ω-6; PS with 22:4 ω-6 and total 22:4 ω-6 in multiple sclerosis patients (G. Hon et al., 2009). The authors state that the lower levels of ω-6 PUFA may be due to an increased production of eicosanoids that regulate an elevated number of inflammatory effects (G. Hon et al., 2009). Additionally, they found considerably higher concentrations of PI with 22:0; SM with 14:0; total 14:0 and total SM saturated FA (G. M. Hon et al., 2009a). Lastly, Hon and colleagues found significantly lower concentrations of PE bearing 18:1 ω-7 and total PE MUFA on PBMC of multiple sclerosis patients (Hon et al., 2011). The increase in saturated FA and decrease of MUFA might be associated with an increased risk of developing multiple sclerosis (Harbige and Sharief, 2007). Through MALDI-TOF/TOF and GC-MS lipidomic approaches, and compared with the previous researchers, Vergara and colleagues (Vergara et al., 2015) obtained opposing results to those published in previous studies. Their results revealed markedly reduced levels of total saturated FA and increased levels of

PG(42:0) or PI(36:2); PI(40:5); cardiolipin CL(72:8); CL(74:10); total ω-6; total MUFA and total PUFA on human $CD4^+$ T lymphocytes in multiple sclerosis (Vergara et al., 2015). Using high-performance LC-MS/MS lipidomic approaches, Kurz and partners (Kurz et al., 2018) identified significantly decreased concentrations of C16:0-LacCer; C24:0-Cer and C24:1-Cer. Similarly to the results obtained by this team for plasma lipidomic analysis, Cer levels in white blood cells of multiple sclerosis patients did not correlate with disease severity and drug treatment (Kurz et al., 2018).

To conclude, PBMC are a practical mean to evaluate lipid alterations in multiple sclerosis however, lipidomic analysis revealed inconsistent results. Increase/decrease of PUFA and decrease/increase of saturated FA and short chain FA were reported by different studies. Nonetheless, even with conflicting results, it is possible to verify that multiple sclerosis induced lipid compositional changes preferably occur at the molecular-specie level.

Table 2.1-3. Main lipid variations observed in PBMC of multiple sclerosis patients reported in published lipidomic studies, available in PubMed data base, using MS approaches.

Reference	Analytical method	Lipid extraction method	Results	
			↓ Reduction	↑ Increase
(Cherayil, 1984)	GC-MS	Chloroform/methanol (2:1, v/v)	18:2	-
(G. Hon et al., 2009)	GC-MS	Modified Folch	PE(C22:4 ω-6); PS(C22:4 ω-6) Σ C22:4 ω-6	-
(G. M. Hon et al., 2009a)	GC-MS	Folch	-	PI(C22:0); SM(C14:0) Σ C14:0; Σ SM saturated FA
(Hon et al., 2011)	GC-MS	Folch	PE(C18:1 ω-7) Σ PE MUFA	-
(Vergara et al., 2015)	MALDI-TOF/TOF, GC-MS	Bligh and Dyer	Σ saturated FA	PG(42:0) or PI(36:2); PI(40:5); CL(72:8); CL(74:10); Σ ω-6; Σ MUFA; Σ PUFA
(Kurz et al., 2018)	LC-MS/MS	Methanol/chloroform/hydrochloric acid (15:83:2, v/v/v)	C16:0-LacCer; C24:0-Cer; C24:1-Cer	-

4.4 Lipidomic analysis of cerebrospinal fluid of multiple sclerosis

CSF is in direct contact and accurately reflects changes that may happen in the CNS and so, it is a reliable and great source of information regarding pathological alterations of the CNS. Lipidomic work in CSF was performed using GC-MS and LC-MS/MS approaches.

Neu (Neu, 1983) analysed by GC-MS the FA methyl esters of CSF, of multiple sclerosis patients and found significant decreases of FA 18:2; 20:4 and total PUFA and increases of FA 16:0; 16:1; 18:0 and 18:1. It should be noted that once again it is seen the deficit of FA 18:2, 20:4 and PUFA being compensated with higher levels of saturated FA. Through targeted LC-MS/MS approaches, Vidaurre and colleagues (Vidaurre et al., 2014) identified significantly increased levels of C16:0-Cer; C16:0-monohexosylCer and C24:0-Cer. These findings are in agreement with the results obtained by Kurz and partners (Kurz et al., 2018) for plasma lipidomic analysis of multiple sclerosis. Pieragostino and co-workers (Pieragostino et al., 2018) performed an untargeted lipidomic analysis on CSF of patients with multiple sclerosis that showed marked reductions of PC(28:0); PC(28:1); PC(35:4); PC(36:1); PC(36:8); PC(37:6); LPC(18:1); LPC(20:4); SM[d18:0/16:1(9Z)(OH)]; SM(d18:1/13:0); SM(d18:1/14:0); SM(d18:1/16:0); SM(d18:2/20:0); SM(d18:2/22:1) and SM[d18:1/24:1(15Z)] in multiple sclerosis. On the other side, PC(32:2) and PC(36:3) showed significantly higher levels in multiple sclerosis patients than in controls (Pieragostino et al., 2018). The authors state that the low levels of SM in multiple sclerosis are able to discriminate disease with good statistical performances and suggest SM to serve as potential biomarkers of this disease. Nogueras and collaborators (Nogueras et al., 2019) performed a non-targeted lipidomic approach as well and found that PC(P27:1); PS(40:3); TG(37:2); TG(44:4); TG(44:5); TG(50:1); TG(52:3); TG(55:5); TG(56:6); TG(57:4); TG(57:7); TG(58:1); TG(58:3); TG(59:6); TG(60:10); TG(61:8); TG(61:10); TG(62:8); diglyceride [DG(32:1)]; 22:0 CE; cholest-5-en-3alpha-ol; C20-Sulfatide and Ceramide-Phosphate(d42:2) had significantly reduced concentrations in multiple sclerosis. It was also determined considerably increased concentrations of FA 18:3 ω-3; FA 20:0; PC(25:2); PC(42:6); PE-N-methylethanolamine(O,O-28:0); PE(21:0);

TG(56:4); TG(57:6); TG(59:2); TG(63:8); TG(64:10); DG(18:3); DG(32:2); DG(36:6); DG(38:6); DG(38:7); DG(39:2); DG(42:5); 5-beta-cholestane-3alpha, 7-alpha-diol; 5-beta-dihydrotestosterona; 12-methyl-10-oxo-tridecanoic acid; N-oleoylethanolamine and GlcCer(d42:0) (Nogueras et al., 2019). An up-regulation of DG and down-regulation of TG may be justified by a defect of the acyl-CoA:diacylglycerol acyltransferase enzyme, associated with a worse insulin sensitivity (Penesova et al., 2015). However, a limitation of this study is that the non-multiple sclerosis group was not composed of healthy controls (Nogueras et al., 2019).

In summary, CSF gives important information of alterations on lipid profile and metabolism of multiple sclerosis. A deficit in FA 18:2; 20:4 and PUFA is also detected in CSF of multiple sclerosis. Untargeted lipidomic is a useful tool to understand changes that are broadly distributed at a molecular level of multiple sclerosis lipid profile. SM demonstrate potential to become putative biomarkers of this pathology.

Table 2.1-4. Main lipid variations observed in CSF of multiple sclerosis patients reported in published lipidomic studies, available in PubMed data base, using MS approaches.

Reference	Analytical method	Lipid extraction method	Results	
			↓ Reduction	↑ Increase
(Neu, 1983)	GC-MS	Modified Folch	18:2; 20:4; Σ PUFA	16:0; 16:1; 18:0; 18:1
(Vidaurre et al., 2014)	LC-MS/MS	Modified Bligh and Dyer	-	C16:0-Cer; C16:0-monohexosylCer; C24:0-Cer
(Pieragostino et al., 2018)	LC-MS/MS	Modified Bligh and Dyer	PC(28:0); PC(28:1); PC(35:4); PC(36:1); PC(36:8); PC(37:6); LPC(18:1); LPC(20:4) SM(d18:0/16:1(9Z)(OH)); SM(d18:1/13:0); SM(d18:1/14:0); SM(d18:1/16:0); SM(d18:2/20:0); SM(d18:2/22:1); SM(d18:1/24:1(15Z))	PC(32:2); PC(36:3)
(Nogueras et al., 2019)	LC-MS/MS; GC-MS	MTBE/ultrasonic bath	PC(P27:1); PS(40:3) TG(37:2); TG(44:4); TG(44:5); TG(50:1); TG(52:3); TG(55:5); TG(56:6); TG(57:4); TG(57:7); TG(58:1); TG(58:3); TG(59:6); TG(60:10); TG(61:8); TG(61:10); TG(62:8); DG(32:1); 22:0 CE; cholest-5-en-3alpha-ol; C20-Sulfatide; CerP(d42:2)	18:3 ω-3; 20:0; PC(25:2); PC(42:6); PE-NMe(O,O-28:0); PE(21:0); TG(56:4); TG(57:6); TG(59:2); TG(63:8); TG(64:10) DG(18:3); DG(32:2); DG(36:6); DG(38:6); DG(38:7); DG(39:2); DG(42:5) 5beta-cholestane-3alpha, 7alpha-diol; 5beta-dihydrotestosterona; 12-methyl-10-oxo-tridecanoic acid; N-oleoylethanolamine; GlcCer(d42:0)

4.5 Lipidomic analysis of other types of matrices of multiple sclerosis

Besides serum/plasma, erythrocytes, PBMC and CSF, there are other types of samples that were analysed with lipidomic approaches and revealed interesting results regarding changes in the lipid profile and metabolism of multiple sclerosis.

Platelets, as mentioned before, are important players in multiple sclerosis pathogenesis. Thus, using a GC-MS approach, Gul and co-workers (Gul et al., 1970) analysed the FA composition of PL from platelets and determined significantly lower levels of FA 18:2 in multiple sclerosis patients. Platelets have been described to have increased adhesiveness which might be correlated with platelet FA 18:2 levels (Gul et al., 1970).

The demyelination process in multiple sclerosis involves the breakdown of PL of the myelin sheaths, therefore, the analysis if the lipid profile of multiple sclerosis brain may disclose important alterations of lipids in multiple sclerosis brains. Through GC-MS approaches, Moscatelli and colleague (Moscatelli and Isaacson, 1969) found no significant differences between sphingolipids of multiple sclerosis and controls. The most likely explanation for the non-significant findings is the fact that only one sample of multiple sclerosis tissue was available. In contrast to Moscatelli, Craelius and collaborators (Craelius et al., 1981) analysed FA methyl esters from the brain and found markedly reduced levels of FA 24:4 in multiple sclerosis. Using shotgun lipidomics, Wheeler and partners (Wheeler et al., 2008) identified significantly reduced concentrations of SM(d18:1/16:0); SM(d18:1/20:0); SM(d18:1/22:0); SM(d18:1/24:0); C18:0-Cer; C20:0-Cer; C22:0-Cer; C24:0-Cer; monomeric, dimeric and trimeric cholesterol and total cholesterol. PE(C18:2); PE(C20:2); PE(C22:2); Σ PE; PS(C16:2); PS(C18:2) and lysine and histadine adducts of 4-HNE were determined to be significantly increased. Levels of these lipid molecular species varied with disease activity (Wheeler et al., 2008). Ho and co-workers (Ho et al., 2012) determined significantly lower levels of PS [1-palmitoyl-2-oleoyl-*sn*-glycero-3-(phosphor-L-serine)(POPS)] and ox-PC derivatives [1-hexadecyl-2-azelaoyl-*sn*-glycero-3-phosphocholine (azPC); 1-palmitoyl-2-azelaoyl-*sn*-glycero-3-phosphocholine (azPC ester) and 1-palmitoyl-2-

glutaroyl-*sn*-glycero-3-phosphorylcholine (PGPC)] in multiple sclerosis samples, consistent with the decrease of PC levels. PS and ox-PC derivatives with saturated FA may serve as natural inhibitors of inflammation in the CNS. However, this protective mechanism is compromised in multiple sclerosis due to the attack of the immune system to these lipid species (Ho et al., 2012). Dasgupta and co-worker (Dasgupta and Ray, 2017) quantified Cer, monoGlcCer and sphingosine content of brain samples of multiple sclerosis patients and found a reduction in total monoGlcCer and total Cer levels and an increase in total sphingosine and total psychosine levels in multiple sclerosis brain matter. Concentrations of sphingosine higher than normal lead to oligodendrocyte death, with consequent demyelination.

The eye can be considered an extension of the CNS, reflecting physiopathological alterations caused by diseases. This way, Cicalini and colleagues (Cicalini et al., 2019) conducted a lipidomic analysis on tears of multiple sclerosis patients to obtain information about the lipid profile of this biological fluid and demonstrate its potential as a source of biomarkers. The team verified significantly decreased levels of PC(32:1); PC(32:2); PC(33:0); PC(34:5); PC(35:1); PC(36:5); PC(37:5); PC(38:0); PC(38:1); PC(40:2); PC(40:7); PC(40:8); PC(P32:0); LPC(17:1); LPC(20:2); LPC(20:3); LPC(20:4); LPC(22:6); SM(d18:0/14:0); SM(d18:0/22:0); SM(d18:1/12:0); SM(d18:1/18:0); SM(d18:1/20:0); SM(d18:1/24:0); SM(d18:2/14:0); SM(d18:2/22:1) and SM(d18:1/24:1(15Z)) in multiple sclerosis (Cicalini et al., 2019). On the other side, PC(36:3); PC(36:4) and LPC(18:0) showed the opposite trend in patients with multiple sclerosis (Cicalini et al., 2019).

In summary, different types of matrices present different types of results, nonetheless, they all should be considered as important information to improve our knowledge on multiple sclerosis. A noteworthy aspect that should be considered is the reduction of SM levels in multiple sclerosis tears, in particular SM(d18:1/24:1(15Z)), that is consistent with the results obtain by Pieragostino`s team (Pieragostino et al., 2018) for CSF and is in agreement with the accumulation of neurotoxic ceramides in CSF (Vidaurre et al., 2014).

Table 2.1-5. Main variations in lipid composition observed in other types of matrices (platelets (Gul et al., 1970), brain (Craelius et al., 1981; Dasgupta and Ray, 2017; Ho et al., 2012; Moscatelli and Isaacson, 1969; Wheeler et al., 2008) and tears (Cicalini et al., 2019)) of multiple sclerosis patients reported in published lipidomic studies, in PubMed data base, using MS approaches.

Reference	Analytical method	Lipid extraction method	Results	
			↓ Reduction	↑ Increase
(Gul et al., 1970)	GC-MS	Folch	18:2	-
(Moscatelli and Isaacson, 1969)	GC-MS	Folch	NSD	NSD
(Craelius et al., 1981)	GC-MS	Folch	24:4	-
(Wheeler et al., 2008)	Triple-quadrupole ESI-MS/MS	Modified Bligh and Dyer	SM(d18:1/16:0); SM(d18:1/20:0); SM(d18:1/22:0); SM(d18:1/24:0); C18:0-Cer; C20:0-Cer; C22:0-Cer; C24:0-Cer; Monomeric, Dimeric and Trimeric Cholesterol; Σ Cholesterol	PE(C18:2); PE(C20:2); PE(C22:2); Σ PE; PS(C16:2); PS(C18:2); Lysine and Histadine adducts of 4-HNE
(Ho et al., 2012)	Triple-quadrupole ESI-MS; LC-HRMS	INF	azPC; azPC ester; PGPC; POPS	-
(Dasgupta and Ray, 2017)	GC-MS	Chloroform/methanol/water (2:4:1, v/v/v)	Σ MonoGlcCer; Σ Cer	Σ sphingosine; Σ psychosine
(Cicalini et al., 2019)	LC-ESI-MS/MS	Methanol extraction solution PerkinElmer®	PC(32:1); PC(32:2); PC(33:0); PC(34:5); PC(35:1); PC(36:5); PC(37:5); PC(38:0); PC(38:1); PC(40:2); PC(40:7); PC(40:8); PC(P32:0); LPC(17:1); LPC(20:2); LPC(20:3); LPC(20:4); LPC(22:6); SM(d18:0/14:0); SM(d18:0/22:0); SM(d18:1/12:0); SM(d18:1/18:0); SM(d18:1/20:0); SM(d18:1/24:0); SM(d18:2/14:0); SM(d18:2/22:1); SM(d18:1/24:1(15Z))	PC(36:3); PC(36:4); LPC(18:0)

NSD: no significant differences; INF: information not found

All of these studies clearly demonstrate the role of lipids in inflammatory processes, in immunity, and in the onset and development of multiple sclerosis (Figure 3). Also, clinical lipidomics has potential as a tool to aid both in multiple sclerosis diagnosis and therapeutics by allowing a detailed lipidome profiling of multiple sclerosis patients. This detailed multiple sclerosis lipid profile is the first step for the identification of new lipid biomarkers of disease and targets for (personalized) therapy.

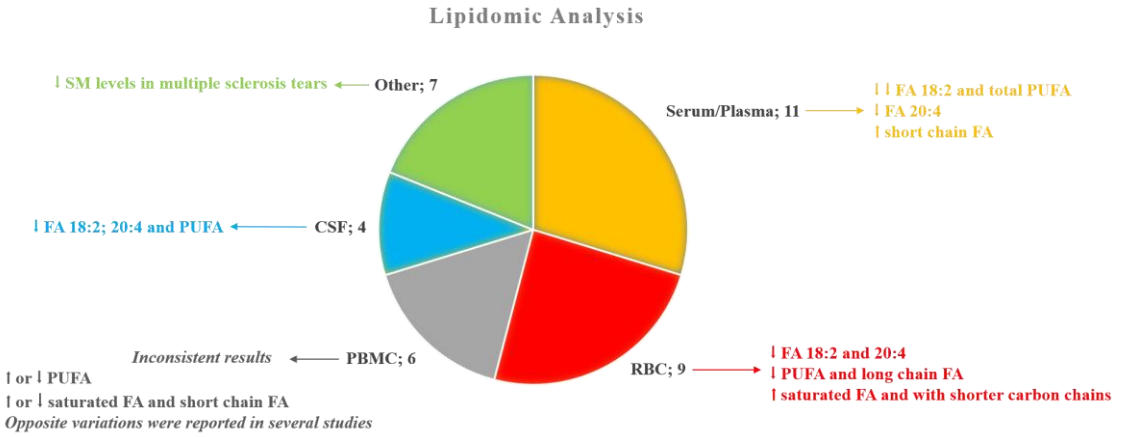

Figure 2.1-3 Summary of main results gathered using lipidomics based on mass spectrometry approaches in the analysis of different human samples reported in published work related to Multiple Sclerosis including type of matrix (platelets, brain, tears; CSF: cerebrospinal fluid; PBMC: peripheral blood mononuclear cells; RBC: red blood cells) and the number of lipidomics studies per matrix.

5. Concluding remarks and future perspectives

Lipids are recognized to have important biological functions, they are fundamental in many signalling pathways that are related with the maintenance of cell and tissue homeostasis. Changes in lipid metabolism, lipid profile and individual lipid molecular species are key parameters of several pathologies, including multiple sclerosis. Alteration in lipids metabolism, in particular AA pathway, are well established and there are evidences of alterations in the lipid profile of multiple sclerosis patients, showing the importance that lipid regulation has in multiple sclerosis pathogenesis. Several studies reported alterations of some lipid entities in particular, deficit of FA 18:2, FA 20:4 and total PUFA, with compensatory increases of saturated FA with shorter carbon chains. Oxidized PL were also reported in few studies.

Alteration in lipids seems to be a common issue in multiple sclerosis that is far from being completely elucidated due to the controversial results obtained for the same matrix type. Therefore, it is of utmost importance to improve the screening methodologies to evaluate the alterations in lipid profile of multiple sclerosis. Clinical lipidomics is nowadays the best methodological approach to understand the modulation of lipid metabolism in multiple sclerosis, advance knowledge on multiple sclerosis pathology and identify potential disease biomarkers. To standardize knowledge of the multiple sclerosis lipid profile, it should be considered an untargeted and targeted lipidomic approach to analyse the entire multiple sclerosis lipidome on the same type of matrix. Thus, clinical lipidomics would contribute to a more precise and early diagnosis, evaluation of disease progression, to predict relapse episodes, and evaluate therapy strategies and outcomes. Utmost, clinical lipidomic approaches could be a promising tool to personalised medicine.

Conflict of interest

The authors declare that there is no conflict of interests regarding the publication of this paper.

Acknowledgments

Thanks are due for the financial support to the University of Aveiro and FCT/MCT for the financial support to QOPNA (FCT UID/QUI/00062/2019), LAQV/REQUIMTE (UIDB/50006/2020), CESAM (UID/AMB/50017/2019), CICECO (UID/CTM/50011/2019) and to RNEM, Portuguese Mass Spectrometry Network (LISBOA-01-0145-FEDER-402-022125) through national founds and, where applicable, co-financed by the FEDER, within the PT2020.

References

Adamczyk, B., Adamczyk-Sowa, M., 2016. New Insights into the Role of Oxidative Stress Mechanisms in the Pathophysiology and Treatment of Multiple Sclerosis. Oxid. Med. Cell. Longev. 1–18.

Adamczyk, B., Niedziela, N., Adamczyk-Sowa, M., 2017. Novel Approaches of Oxidative Stress

Mechanisms in the Multiple Sclerosis Pathophysiology and Therapy, in: Zagon, I., McLaughlin, P. (Eds.), Multiple Sclerosis: Perspectives in Treatment and Pathogenesis. Codon Publications, Brisbane, Australia, pp. 155–171.

Afshar, B., Khalifehzadeh-Esfahani, Z., Seyfizadeh, N., Rezaei Danbaran, G., Hemmatzadeh, M., Mohammadi, H., 2019. The role of immune regulatory molecules in multiple sclerosis. J. Neuroimmunol. 337, 577061.

Aupperle, R.L., Denney, D.R., Lynch, S.G., Carlson, S.E., Sullivan, D.K., 2008. Omega-3 fatty acids and multiple sclerosis: Relationship to depression. J. Behav. Med. 31, 127–135.

Baker, R.W., Thompson, R.H., Zilkha, K.J., 1964. Serum Fatty Acids in Multiple Sclerosis. J. Neurol. Neurosurg. psychiatry 27, 408–414.

Baranzini, S.E., 2011. Revealing the genetic basis of multiple sclerosis: are we there yet? Curr Opin Genet Dev. 21, 317–324.

Calabrese, V., Scapagnini, G., Ravagna, A., 2002. Nitric oxide synthase is present in the cerebrospinal fluid of patients with active multiple sclerosis and is associated with increases in cerebrospinal fluid protein nitrotyrosine and S-nitrosothiols and with changes in glutathione levels. J. Neurosci. Res. 70, 580–587.

Calder, P.C., 2007. Immunomodulation by omega-3 fatty acids. Prostaglandins Leukot Essent Fat. Acids 77, 327–335.

Cherayil, G.D., 1984. Sialic acid and fatty acid concentrations in lymphocytes, red blood cells and plasma from patients with multiple sclerosis. J. Neurol. Sci. 63, 1–10.

Chiurchiù, V., 2014. Novel targets in multiple sclerosis: to oxidative stress and beyond. Curr Top Med Chem 14, 2590–2599.

Cicalini, I., Rossi, C., Pieragostino, D., Agnifili, L., Mastropasqua, L., di Ioia, M., De Luca, G., Onofrj, M., Federici, L., Del Boccio, P., 2019. Integrated Lipidomics and Metabolomics Analysis of Tears in Multiple Sclerosis: An Insight into Diagnostic Potential of Lacrimal Fluid. Int. J. Mol. Sci. 20, 1–16.

Craelius, W., Gurmankin, R.S., Rosenheck, D.M., Schaefer, D.C., 1981. Free fatty acid patterns in normal and multiple sclerosis white matter. Acta Neurol. Scand. 63, 197–203.

Darios, F., Lambeng, N., Troadec, J.-D., Michel, P.P., Ruberg, M., 2003. Ceramide increases mitochondrial free calcium levels via caspase 8 and Bid: role in initiation of cell death. J. Neurochem. 84, 643–654.

Dasgupta, S., Ray, S.K., 2017. Diverse Biological Functions of Sphingolipids in the CNS: Ceramide and Sphingosine Regulate Myelination in Developing Brain but Stimulate Demyelination during Pathogenesis of Multiple Sclerosis. J Neurol Psychol 5, 1–7.

Del Boccio, P., Pieragostino, D., Di Ioia, M., Petrucci, F., Lugaresi, A., De Luca, G., Gambi, D., Onofrj, M., Di Ilio, C., Sacchetta, P., Urbani, A., 2011a. Lipidomic investigations for the characterization of circulating serum lipids in multiple sclerosis. J. Proteomics 74, 2826–2836.

Del Boccio, P., Pieragostino, D., Di Ioia, M., Petrucci, F., Lugaresi, A., De Luca, G., Gambi, D., Onofrj, M., Di Ilio, C., Sacchetta, P., Urbani, A., 2011b. Lipidomic investigations for the characterization of circulating serum lipids in multiple sclerosis. J. Proteomics 74, 2826–2836.

Dore-Duffy, P., Ho, S.Y., Donovan, C., 1991. Cerebrospinal fluid eicosanoid levels: Endogenous PGD2 and LTC4 synthesis by antigen-presenting cells that migrate to the central nervous system. Neurology 41, 322–324.

Duddy, M., Niino, M., Adatia, F., Hebert, S., Freedman, M., Atkins, H., Kim, H., Bar-Or, A., 2007. Distinct effector cytokine profiles of memory and naive human B cell subsets and implication in multiple sclerosis. J Immunol 178, 6092–6099.

Dziedzic, A., Bijak, M., 2019. Interactions between platelets and leukocytes in pathogenesis of multiple sclerosis. Adv. Clin. Exp. Med. 28, 277–285.

Elliott, M.R., Ravichandran, K.S., 2010. Clearance of apoptotic cells: implications in health and disease. J. Cell Biol. 189, 1059–1070.

Emamgholipour, S., Hossein-Nezhad, A., Sahraian, M.A., Askarisadr, F., Ansari, M., 2016. Evidence for possible role of melatonin in reducing oxidative stress in multiple sclerosis through its effect on SIRT1 and antioxidant enzymes. Life Sci. 145, 34–41.

Evans, P., Dodd, G., 1989. Erythrocyte fatty acids in multiple sclerosis. Acta Neurol. Scand. 80, 501–503.
Falluel-Morel, A., Aubert, N., Vaudry, D., 2004. Opposite regulation of the mitochondrial apoptotic pathway by C2-ceramide and PACAP through a MAP-kinase-dependent mechanism in cerebellar granule cells. J. Neurochem. 91, 1231–1243.
Federation, M.S.I., 2013. Atlas of MS [WWW Document]. URL https://www.msif.org/about-us/who-we-are-and-what-we-do/advocacy/atlas/ (accessed 11.26.19).
Ferretti, G., Bacchetti, T., Principi, F., 2005. Increased levels of lipid hydroperoxides in plasma of patients with multiple sclerosis: a relationship with paraoxonase activity. Mult. Scler. 11, 677–682.
Ghasemi, N., Razavi, S., Nikzad, E., 2017. Multiple Sclerosis: Pathogenesis, Symptoms, Diagnoses and Cell-Based Therapy. Cell J. 19, 1–10.
Gilgun-Sherki, Y., Melamed, E., Offen, D., 2004. The role of oxidative stress in the pathogenesis of multiple sclerosis: The need for effective antioxidant therapy. J. Neurol. 251, 261–268.
Göbel, K., Ruck, T., Meuth, S.G., 2018. Cytokine signaling in multiple sclerosis: Lost in translation. Mult. Scler. J. 24, 432–439.
Goes, A. Vander, D. Wouters, DerPol, S.M.V., 2001. Reactive oxygen species enhance the migration ofmonocytes across the blood-brain barrier in vitro. FASEB J. 15, 1852–1854.
Greco, A., Minghetti, L., Sette, G., 1999. Cerebrospinal fluid isoprostane shows oxidative stress in patients with multiple sclerosis. Neurology 53, 1876–1879.
Gul, S., Smith, A.D., Thompson, R.H., Wright, H.P., Zilkha, K.J., 1970. Fatty acid composition of phospholipids from platelets and erythrocytes in multiple sclerosis. J. Neurol. Neurosurg. psychiatry 33, 506–510.
Haase, S., Haghikia, A., Gold, R., Linker, R.A., 2018. Dietary fatty acids and susceptibility to multiple sclerosis. Mult. Scler. 24, 12–16.
Haghikia, A., Jörg, S., Duscha, A., Berg, J., Manzel, A., Waschbisch, A., Hammer, A., Lee, D., May, C., Wilck, N., Balogh, A., Ostermann, A., Schebb, N., Akkad, D., Grohme, D., Kleinewietfeld, M., Kempa, S., Thöne, J., Demir, S., Müller, D., Gold, R., Linker, R., 2015. Dietary fatty acids directly impact central nervous system autoimmunity via the small intestine. Immunity 43, 817–829.
Haider, L., Fischer, M.T., Frischer, J.M., Bauer, J., Höftberger, R., Botond, G., Esterbauer, H., Binder, C.J., Witztum, J.L., Lassmann, H., 2011. Oxidative damage in multiple sclerosis lesions. Brain 134, 1914–1924.
Halmer, R., Walter, S., Faßbender, K., 2014. Sphingolipids: Important players in multiple sclerosis. Cell. Physiol. Biochem. 34, 111–118. https://doi.org/10.1159/000362988
Harbige, L.S., Sharief, M.K., 2007. Polyunsaturated fatty acids in the pathogenesis and treatment of multiple sclerosis. Br. J. Nutr. 98, 46–53.
Hassani, A., Khan, G., 2019. Epstein-Barr virus and miRNAs: Partners in crime in the pathogenesis of multiple sclerosis? Front. Immunol. 10, 1–9.
Ho, P.P., Kanter, J.L., Johnson, A.M., Srinagesh, H.K., Chang, E.J., Purdy, T.M., Van Haren, K., Wikoff, W.R., Kind, T., Khademi, M., Matloff, L.Y., Narayana, S., Hur, E.M., Lindstrom, T.M., He, Z., Fiehn, O., Olsson, T., Han, X., Han, M.H., Steinman, L., Robinson, W.H., 2012. Identification of naturally occurring fatty acids of the myelin sheath that resolve neuroinflammation. Sci. Transl. Med. 4, 1–12.
Holman, R.T., Johnson, S.B., Kokmen, E., 1989. Deficiencies of polyunsaturated fatty acids and replacement by nonessential fatty acids in plasma lipids in multiple sclerosis. Proc. Natl. Acad. Sci. U. S. A. 86, 4720–4724.
Hon, G., Hassan, M., Rensburg, S. van, Erasmus, R., Matsha, T., 2012. The haematological profile of patients with multiple sclerosis. Open J Mod Neurosurg. 2, 36–44.
Hon, G., Hassan, M., Van Rensburg, S.J., Abel, S., Marais, D.W., Van Jaarsveld, P., Smuts, C., Henning, F., Erasmus, R., Matsha, T., 2009. Immune cell membrane fatty acids and inflammatory marker, C-reactive protein, in patients with multiple sclerosis. Br. J. Nutr. 102, 1334–1340.
Hon, G.M., Hassan, M.S., van Rensburg, S.J., Abel, S., Erasmus, R.T., Matsha, T., 2011. Monounsaturated fatty acids in blood cell membranes from patients with multiple sclerosis. Eur. J. Lipid Sci. Technol. 114, 703–709.
Hon, G.M., Hassan, M.S., Van Rensburg, S.J., Abel, S., Erasmus, R.T., Matsha, T., 2009a. Membrane

saturated fatty acids and disease progression in Multiple Sclerosis patients. Metab. Brain Dis. 24, 561–568.
Hon, G.M., Hassan, M.S., van Rensburg, S.J., Abel, S., Marais, D.W., van Jaarsveld, P., Smuts, C.M., Henning, F., Erasmus, R.T., Matsha, T., 2009b. Erythrocyte membrane fatty acids in patients with multiple sclerosis. Mult. Scler. 15, 759–762.
Horssen, J. van, Schreibelt, G., Drexhage, J., 2008. Severe oxidative damage in multiple sclerosis lesions coincides with enhanced antioxidant enzyme expression. Free Radic. Biol. Med. 45, 1729–1737.
Hurwitz, B.J., 2009. The diagnosis of multiple sclerosis and the clinical subtypes. Ann. Indian Acad. Neurol. 12, 226–230.
Ibitoye, R., Kemp, K., Rice, C., Hares, K., Scolding, N., Wilkins, A., 2016. Oxidative stress-related biomarkers in multiple sclerosis: A review. Biomark. Med. 10, 889–902.
Jana, A., Pahan, K., 2010. Sphingolipids in multiple sclerosis. NeuroMolecular Med. 12, 351–361.
Jayadev, S., Hayter, H.L., Andrieu, N., Gamard, C.J., Liu, B., Balu, R., Hayakawa, M., Ito, F., Hannun, Y.A., 1997. Phospholipase A2 Is Necessary for Tumor Necrosis Factor α-induced Ceramide Generation in L929 Cells. J. Biol. Chem. 272, 17196–17203.
Karg, E., Klivenyi, P., Nemeth, R., 1999. Nonenzymatic antioxidants of blood in multiple sclerosis. J Neurol 246, 533–539.
Karlsson, I., Alling, C., Svennerholm, L., 1971. Major plasma lipids and their fatty acid composition in multiple sclerosis and other neurological diseases. Acta Neurol. Scand. 47, 403–412.
Kivisakk, P., Imitola, J., Rasmussen, S., Elyaman, W., Zhu, B., Ransohoff, R.M., Khoury, S.J., 2009. Localizing central nervous system immune surveillance: meningeal antigen-presenting cells activate T cells during experimental autoimmune encephalomyelitis. Ann. Neurol. 65, 457–469.
Knippenberg, S., Peelen, E., Smolders, J., Thewissen, M., Menheere, P., Tervaert, J.C., Hupperts, R., Damoiseaux, J., 2011. Reduction in IL- 10 producing B cells (Breg) in multiple sclerosis is accompanied by a reduced naive/memory Breg ratio during a relapse but not in remission. J Neuroimmunol 239, 80–86.
Koch, M., Ramsaransing, G.S.M., Fokkema, M.R., Heersema, D.J., De Keyser, J., 2006. Erythrocyte membrane fatty acids in benign and progressive forms of multiple sclerosis. J. Neurol. Sci. 244, 123–126.
Kurz, J., Brunkhorst, R., Foerch, C., Blum, L., Henke, M., Gabriel, L., Ulshöfer, T., Ferreirós, N., Parnham, M.J., Geisslinger, G., Schiffmann, S., 2018. The relevance of ceramides and their synthesizing enzymes for multiple sclerosis. Clin. Sci. 132, 1963–1976.
Langemann, H., Kabiersch, A., Newcombe, J., 1992. Measurement of low-molecular-weight antioxidants, uric acid, tyrosine and tryptophan in plaques and white matter from patients with multiple sclerosis. Eur. Neurol. 32, 248–252.
Love, S., 2006. Demyelinating diseases. J Clin Pathol. 59, 1151–1159.
Love, W.C., Cashell, A., Reynolds, M., Callaghan, N., 1974. Linoleate and fatty-acid patterns of serum lipids in multiple sclerosis and other diseases. Br. Med. J. 3, 18–21.
Lv, J., Zhang, L., Yan, F., Wang, X., 2018. Clinical lipidomics: a new way to diagnose human diseases. Clin. Transl. Med. 7, 10–12.
Magalhaes, A., Salgado, V., 1983. Critérios de diagnóstico de Esclerose Múltipla. Acta Med. Port. 4, 235–237.
Mattsson, N., Haghighi, S., Andersen, O., 2007. Elevated cerebrospinal fluid F2-isoprostane levels indicating oxidative stress in healthy siblings of multiple sclerosis patients. Neurosci. Lett. 414, 233–236.
Monteiro, A., Cruto, C., Rosado, P., Martinho, A., Rosado, L., Fonseca, M., Paiva, A., 2018. Characterization of circulating gamma-delta T cells in relapsing vs remission multiple sclerosis. J. Neuroimmunol. 318, 65–71.
Morel, A., Miller, E., Bijak, M., Saluk, J., 2016. The increased level of COX-dependent arachidonic acid metabolism in blood platelets from secondary progressive multiple sclerosis patients. Mol Cell Biochem. 420, 85–94.
Morel, A., Rywaniak, J., Bijak, M., Miller, E., Niwald, M., Saluk, J., 2017. Flow cytometric analysis reveals the high levels of platelet activation parameters in circulation of multiple sclerosis patients.

Mol Cell Biochem. 430, 69–80.
Moscatelli, E.A., Isaacson, E., 1969. Gas liquid chromatographic analysis of sphingosine bases in sphingolipids of human normal and multiple sclerosis cerebral white matter. Lipids 4, 550–555.
Navarro, X., Segura, R., 1989. Red blood cell fatty acids in multiple sclerosis. Acta Neurol. Scand. 79, 32–37.
Navarro, X., Segura, R., 1988. Plasma lipids and their fatty acid composition in multiple sclerosis. Acta Neurol. Scand. 78, 152–157.
Neu, I.S., 1983. Essential fatty acids in the serum and cerebrospinal fluid of multiple sclerosis patients. Acta Neurol. Scand. 67, 151–163.
Neu, I.S., Metzger, G., Zschocke, J., Zelezny, R., Mayatepek, E., 2001. Leukotrienes in patients with clinically active multiple sclerosis. Acta Neurol Scand. 105, 63–66.
Newcombe, J., Li, H., Cuzner, M.L., 1994. Low density lipoprotein uptake by macrophages in multiple sclerosis plaques: implications for pathogenesis. Neuropathol. Appl. Neurobiol. 20, 152–162.
Nogueras, L., Gonzalo, H., Jové, M., Sol, J., Gil-Sanchez, A., Hervás, J. V., Valcheva, P., Gonzalez-Mingot, C., Solana, M.J., Peralta, S., Pamplona, R., Brieva, L., 2019. Lipid profile of cerebrospinal fluid in multiple sclerosis patients: a potential tool for diagnosis. Sci. Rep. 9, 1–9.
Noseworthy, J.H., Lucchinetti, C., Rodriguez, M., Weinshenker, B.G., 2000. Multiple sclerosis. N. Engl. J. Med. 343, 938–952.
Ortiz, G.G., Macías-Islas, M.A., Pacheco-Moisés, F.P., 2009. Oxidative stress is increased in serum from Mexican patients with relapsing-remitting multiple sclerosis. Dis. Markers 26, 35–39.
Ortiz, G.G., Pacheco-Moisés, F.P., Bitzer-Quintero, O.K., Ramírez-Anguiano, A.C., Flores-Alvarado, L.J., Ramírez-Ramírez, V., Macias-Islas, M.A., Torres-Sánchez, E.D., 2013. Immunology and oxidative stress in multiple sclerosis: Clinical and basic approach. Clin. Dev. Immunol. 2013, 1–14.
Palumbo, S., 2017. Pathogenesis an Progression of Multiple Sclerosis: The Role of Arachidonic Acid – Mediated Neuroinflammation, in: Zagon, I., McLaughlin, P. (Eds.), Multiple Sclerosis: Perspectives in Treatment and Pathogenesis. Codon Publications, Brisbane, Australia, pp. 111–123.
Penesova, A., Vlcek, M., Imrich, R., Vernerova, L., Marko, A., Meskova, M., Grunnerova, L., Turcani, P., Jezova, D., Kollar, B., 2015. Hyperinsulinemia in newly diagnosed patients with multiple sclerosis. Metab. Brain Dis. 30, 895–901.
Pieragostino, D., Cicalini, I., Lanuti, P., Ercolino, E., Di Ioia, M., Zucchelli, M., Zappacosta, R., Miscia, S., Marchisio, M., Sacchetta, P., Onofrj, M., Del Boccio, P., 2018. Enhanced release of acid sphingomyelinase-enriched exosomes generates a lipidomics signature in CSF of Multiple Sclerosis patients. Sci. Rep. 8, 1–12.
Plum, C.M., Fog, T., 1959. Studies in multiple sclerosis. Acta psychiat. scand. 34, 13–18.
Poser, C.M., Paty, D.W., Scheinberg, L., McDonald, W.I., Davis, F.A., Ebers, G.C., Johnson, K.P., Sibley, W.A., Silberberg, D.H., Tourtellotte, W.W., 1983. New diagnostic criteria for multiple sclerosis: guidelines for research protocols. Ann. Neurol. 13, 227–231.
Prineas, J., 1968. Red blood cell size in multiple sclerosis. Acta neurol. scand. 44, 81–90.
Qin, J., Goswami, R., Balabanov, R., Dawson, G., 2007. Oxidized Phosphatidylcholine Is a Marker for Neuroinflammation in Multiple Sclerosis Brain. J. Neurosci. Res. 85, 977–984.
Rahmanzadeh, R., Brück, W., Minagar, A., Sahraian, M.A., 2019. Multiple sclerosis pathogenesis: Missing pieces of an old puzzle. Rev. Neurosci. 30, 67–83.
Rajda, C., Pukoli, D., Bende, Z., Majláth, Z., Vécsei, L., 2017. Excitotoxins, mitochondrial and redox disturbances in multiple sclerosis. Int J Mol Sci 18, 353.
Rosnowska, M., Cendrowski, W., Sobocinnska, Z., Wieczorkiewicz, A., 1981. Prostaglandins E2 and F2 alpha in the cerebrospinal fluid in patients with multiple sclerosis. Acta Med Pol. 22, 97–103.
Saluk-Juszczak, J., Wachowicz, B., Kaca, W., 2000. Endotoxins stimulate generation of superoxide radicals and lipid peroxidation in blood platelets. Microbios. 103, 17–25.
Shukla, V.K.S., Clausen, J., 1978. Linoleate and fatty acid patterns of serum lipids in multiple sclerosis. Acta Neurol. Scand. 57, 270–274.
Singh, I., Pahan, K., Khan, M., Singh, A.K., 1998. Cytokine-mediated Induction of Ceramide Production Is Redox sensitive. J. Biol. Chem. 273, 20354–20362.
Society, N.M.S., 2020. What is MS? [WWW Document]. URL https://www.nationalmssociety.org/

(accessed 3.16.20).
Thi Cuc, B., Pohar, J., Fillatreau, S., 2019. Understanding regulatory B cells in autoimmune diseases: the case of multiple sclerosis. Curr. Opin. Immunol. 61, 26–32.
Thompson, A.J., Banwell, B.L., Barkhof, F., Carroll, W.M., Coetzee, T., Comi, G., Correale, J., Fazekas, F., Filippi, M., Freedman, M.S., Fujihara, K., Galetta, S.L., Hartung, H.P., Kappos, L., Lublin, F.D., Marrie, R.A., Miller, A.E., Miller, D.H., Montalban, X., Mowry, E.M., Sorensen, P.S., Tintoré, M., Traboulsee, A.L., Trojano, M., Uitdehaag, B.M.J., Vukusic, S., Waubant, E., Weinshenker, B.G., Reingold, S.C., Cohen, J.A., 2018. Diagnosis of multiple sclerosis: 2017 revisions of the McDonald criteria. Lancet Neurol. 17, 162–173.
Usatyuk, P. V., Parinandi, N.L., Natarajan, V., 2006. Redox regulation of 4-hydroxy-2-nonenal-mediated endothelial barrier dysfunction by focal adhesion, adherens, and tight junction proteins. J. Biol. Chem. 281, 35554–35566.
Vergara, D., D'Alessandro, M., Rizzello, A., De Riccardis, L., Lunetti, P., Del Boccio, P., De Robertis, F., Trianni, G., Maffia, M., Giudetti, A.M., 2015. A lipidomic approach to the study of human CD4+ T lymphocytes in multiple sclerosis. BMC Neurosci. 16, 1–10.
Vidaurre, O.G., Haines, J.D., Katz Sand, I., Adula, K.P., Huynh, J.L., Mcgraw, C.A., Zhang, F., Varghese, M., Sotirchos, E., Bhargava, P., Bandaru, V.V.R., Pasinetti, G., Zhang, W., Inglese, M., Calabresi, P.A., Wu, G., Miller, A.E., Haughey, N.J., Lublin, F.D., Casaccia, P., 2014. Cerebrospinal fluid ceramides from patients with multiple sclerosis impair neuronal bioenergetics. Brain 137, 2271–2286.
Wang, P., Xie, K., Wang, C., Bi, J., 2014. Oxidative stress induced by lipid peroxidation is related with inflammation of demyelination and neurodegeneration in multiple sclerosis. Eur Neurol 72, 249–254.
Wheeler, D., Bandaru, V.V.R., Calabresi, P.A., Nath, A., Haughey, N.J., 2008. A defect of sphingolipid metabolism modifies the properties of normal appearing white matter in multiple sclerosis. Brain 131, 3092–3102.
Wilkins, A., Ingram, G., Brown, A., Jardine, P., Steward, C.G., Robertson, N.P., Scolding, N.J., 2009. Very long chain fatty acid levels in patients diagnosed with multiple sclerosis. Mult. Scler. 15, 1525–1527.
Zhao, Y.Y., Cheng, X. long, Lin, R.C., 2014. Lipidomics Applications for Discovering Biomarkers of Diseases in Clinical Chemistry, International Review of Cell and Molecular Biology. Elsevier Inc.

2.2 CHAPTER 2.2: LIPIDOMIC ANALYSIS IN MULTIPLE SCLEROSIS

This chapter was integrally published as follows.
Reprinted with permission from:

H.B. Ferreira, T. Melo, A. Monteiro, A. Paiva, P. Domingues, M.R. Domingues, Serum hospholipidomics reveals altered lipid profile and promising biomarkers in multiple sclerosis, *Archives of Biochemistry and Biophysics* (2021), volume 697, page 108672
https://doi.org/10.1016/j.abb.2020.108672

Abstract

Multiple sclerosis is a neurodegenerative disease causing disability in young adults. Alterations in metabolism and lipid profile have been associated with this disease. Several studies have reported changes in the metabolism of arachidonic acid and the profile of fatty acids, ceramides, phospholipids and lipid peroxidation products. Nevertheless, the understanding of the modulation of circulating lipids at the molecular level in multiple sclerosis remains unclear. In the present study, we sought to assess the existence of a distinctive lipid signature of multiple sclerosis using an untargeted lipidomics approach. It also aimed to assess the differences in lipid profile between disease status (relapse and remission). For this, we used hydrophilic interaction liquid chromatography coupled with mass spectrometry for phospholipidomic profiling of serum samples from patients with multiple sclerosis. Our results demonstrated that multiple sclerosis has a phospholipidomic signature different from that of healthy controls, especially the PE, PC, LPE, ether-linked PE and ether-linked PC species. Plasmalogen PC and PE species, which are natural endogenous antioxidants, as well as PC and PE polyunsaturated fatty acid esterified species showed significantly lower levels in patients with multiple sclerosis and patients in both remission and relapse of multiple sclerosis. Our results show for the first time that the serum phospholipidome of multiple sclerosis is significantly different from that of healthy controls and that few phospholipids, with the lowest p-value, such as PC(34:3), PC(36:6), PE(40:10) and PC(38:1) may be suitable as biomarkers for clinical applications in multiple sclerosis.

Keywords: multiple sclerosis; lipidomic; mass spectrometry; lipid profile; phospholipids; plasmalogens

1. Introduction

Multiple sclerosis is a chronic disease characterized by neurodegeneration, demyelination and (neuro)inflammation, resulting in severe neurological impact and disability in young adults [1]. This pathology is responsible for a progressive disability where the acute phases are the most debilitating for the patients. It affects approximately 2.3 million people worldwide, mostly women [2].

Four disease courses are considered for this disease, classified according with clinical signs and symptoms. These courses are clinically isolated syndrome, relapsing-remitting multiple sclerosis (RRMS), secondary progressive multiple sclerosis and primary progressive multiple sclerosis, of which RRMS is the most common [3,4]. The diagnosis of multiple sclerosis is based on clinical parameters and imaging, but it is a long and often delayed task, preventing early initiation of treatment [5]. Much effort has been made to overcome this drawback, but the early diagnosis of multiple sclerosis remains a difficult task and definitive diagnostic tests are not available. Moreover, the monitoring of disease progression and the efficacy of therapeutic approaches are also based on clinical parameters and lack specific markers or tests to predict or early detect a period of remission [6]. Thus, it is difficult if not impossible to apply early therapeutic or preventive strategies to prevent worsening of symptoms and periods of relapse. Thus, there is a need to find new reliable biomarkers not only to help and improve the diagnosis of multiple sclerosis but also for more accurate monitoring of disease progression [7].

The lack of biomarkers is mainly due to the heterogeneous pathophysiology of this disease which is not fully understood. Multiple sclerosis is a demyelinating disease in which the myelin sheath around the nerves is destroyed [8]. Myelin has a high lipid content, mainly composed of phosphatidylethanolamine, glucosyl-ceramides, phosphatidylcholine, sphingomyelin, ceramides and sulfatides. Changes in its lipid composition may be associated with impaired myelin function [9]. Therefore, lipids would be promising candidates to be useful biomarkers of this disease [10,11]. Also, lipids are key players in the regulation of inflammatory responses and can modulate activated immune cells in autoimmune diseases [12].

Changes in lipid metabolism and lipid profile have been reported in a few studies of multiple sclerosis, and it has been suggested to play a fundamental role in the pathogenesis and severity of this disease [13,14]. Although most studies have focused on the variation in fatty acid metabolism [6]. The arachidonic acid metabolic pathway has been reported to be overactivated in the central nervous system of patients with multiple sclerosis [15]. Prostaglandins and hydroxyeicosatetraenoic acids were elevated in the cerebrospinal fluid of patients with multiple sclerosis due to overactivation of arachidonic acid metabolism and neuroinflammation[16]. Deficiency of polyunsaturated fatty acids (PUFAs) and increased short-chain FA have also been reported in other studies (as recently reviewed in [6]). Omega-3 lipids, which have a protective role by preserving the blood-brain barrier, are significantly reduced in the serum of patients with multiple sclerosis [17,18].

Regarding phospholipids (PL), lyso-phosphatidylcholines are reduced in plasma [19]. Ceramides (Cer), well-known signalling molecules associated with mitochondrial dysfunction and cell apoptosis, are significantly increased in the plasma and cerebrospinal fluid of patients with multiple sclerosis [20,21]. The lipid peroxidation products of 4-hydroxynonenal, isoprostanes, malondialdehyde and cholesteryl ester hydroperoxides have been found at increased concentrations in plasma and serum of multiple sclerosis [6]. Despite studies showing a positive correlation of lipids in this disease, no study has looked for an alteration in serum PL in this pathology.

Analysis of lipid variation at the molecular level using high-throughput lipidomic techniques provides an understanding of the contribution of lipids to disease development and its molecular mechanisms, which could be useful and have a purpose for the study of several chronic diseases in clinical lipidomics [22,23].

In the present study, we sought to make a comprehensive assessment of the variation in the serum phospholipid profile of patients with multiple sclerosis compared to control patients, using an untargeted lipidomics approach. It also aimed to assess the differences in lipid profile between disease status (relapse and remission).

2. Materials and methods

2.1 Reagents

To perform the PL separation of the samples by solid-phase extraction, acetonitrile (ACN) was acquired from Fisher Scientific (Leicestershire, UK) and formic acid and ammonium hydroxide were obtained from Sigma-Aldrich Chemical Co. (St. Louis, MO, USA). To quantify the PL in each sample, dichloromethane was purchased from Fisher Scientific, 70% perchloric acid was obtained from Chem-Lab NV (Zedelgem, Belgium), $NaH_2PO_4 \cdot 2H_2O$ was purchased from Riedell-de Haën (Seelze, Germany), ammonium molybdate ($NaMoO_4 \cdot H_2O$) was acquired from Panreac (Barcelona, Spain) and the L(+)-ascorbic acid from VWR Chemicals (Leuven, Belgium). Internal standards of PL 1,2-dimyristoyl-*sn*-glycero-3-phosphocholine (dMPC, PC 14:0/14:0), 1,2-dimyristoyl-*sn*-glycero-3-phosphoethanolamine (dMPE, PE 14:0/14:0), 1,2-dimyristoyl-*sn*-glycero-3-phospho-(10-rac-)glycerol (dMPG, PG 14:0/14:0), 1,2-dimyristoyl-*sn*-glycero-3-phospho-L-serine (dMPS, PS 14:0/14:0), tetramyristoylcardiolipin (TMCL, CL 14:0/14:0/14:0/14:0), 1,2-dipalmitoyl-*sn*-glycero-3-phosphatidylinositol (dPPI, PI 16:0/16:0), N-heptadecanoyl-D-*erythro*-sphingosylphosphorylcholine (SM d18:1/17:0), 1-nonadecanoyl-2-hydroxy-*sn*-glycero-3-phosphocholine (LPC 19:0) and 1,2-dimyristoyl-*sn*-glycero-3-phosphate (dMPA, PA 14:0/14:0) for HILIC-MS analysis were obtained from Avanti® Polar Lipids, Inc (Alabaster, AI, EUA). The solvents for LC-MS were ACN, methanol (Fisher Scientific), Milli-Q water and ammonium acetate (Sigma-Aldrich). Dichloromethane was also purchased from Fisher Scientific. All solvents were of high-performance liquid chromatography (HPLC) grade and were used without any additional purification. Milli-Q water was used for all experiments, filtered through a 0.22mm filter and obtained using a Milli-Q Millipore system (Synergy®, Millipore Corporation, Billerica, MA, USA).

2.2 Serum samples

Serum samples from patients with multiple sclerosis and healthy controls were provided by Centro Hospitalar Cova da Beira (CHCB). Participating patients (n=24) were diagnosed with RRMS and were followed up at CHCB before sample collection for this study. The diagnosis was based on clinical, MRI, and biochemical criteria, according to the 2010 MacDonald criteria [24]. Exclusion criteria were active infections, local or systemic diseases that affect the immune system, pregnancy, and corticosteroids or other treatments for multiple sclerosis in addition to IFN-β. To allow participation in this study, all healthy control volunteers (HC) (n=30) were guaranteed to be healthy, showing no signs of active infection, autoimmune disease, and treatment with immunomodulatory drugs. HC samples were age- and gender-matched. The study protocol was approved by the CHCB`s Ethics Committee. Summary information on patients with multiple sclerosis and healthy controls is shown in Table 1. After collection, serum samples were stored at −80 °C until further study of the lipid profile.

Table 2.2-1. Demographic and clinical characteristics of patients with multiple sclerosis (RRMS) and healthy controls (HC).

	Remission RRMS (n=17)	Relapse RRMS (n=7)	HC (n=30)
Age (years)*	46.5 ± 12.3	40.9 ± 14.7	49.5 ± 10.1
Sex (% women)	94.1 %	71.4 %	76.7%
EDSS-score*	1.5 ± 0.8	3.0 ± 1.4	-
Disease duration (years)*	12.2 ± 7.2	4.3 ± 4.0	-

*Values represent the mean ± standard deviation.

2.3 Phospholipid extraction and phosphorus measurement

Solid-phase extraction (SPE) was used to separate PL from serum samples as previously described by Anjos *et al* [25] with modifications. The SPE procedure required three eluents prepared before the extraction of PL. Eluent 1 consisted of ACN with 1% formic acid. Eluent 2 was pure ACN. Eluent 3 was ACN with 5% ammonium hydroxide. After the preparation of the mobile phases, a volume of 100 µL of serum from each sample was mixed with 900 µL of eluent 1 in a Pyrex tube. Each tube was vortexed for 30 seconds, then centrifuged at 2000 rpm

for 5 minutes for protein precipitation. The resulting supernatant from each tube was transferred to a Hybrid SPE-PL column (HybridSPE® - Phospholipid 30 mg, SUPELCO, Sigma-Aldrich, Bellefonte, PA) that was already placed in a vacuum *Visiprep SPE Vacuum Manifold* (SUPELCO) system and previously conditioned with 1 mL of ACN. After elution of almost all the supernatant, the columns were washed with 1 mL of eluent 2 and with 1 mL of eluent 1. At this stage, the collection tubes were replaced by new ones and the PL retained on the Hybrid SPE-PL columns were eluted with two consecutive 1 mL aliquots of eluent 3. The flow-through was collected and dried under a stream of nitrogen. The samples were dissolved in 400 µL of dichloromethane and transferred individually to a HAMILTON glass syringe. All samples were filtered with a Millex® - LH 0,45 µm filter (low protein binding hydrophilic LCR Membrane for clarification of aqueous and organic solutions). The filtered samples were collected in vials and dried under a stream of nitrogen.

2.4 Phospholipid quantification by phosphorous measurement

The quantification of the total PL recovered after extraction was carried out according to the method of Bartlett & Lewis [26]. The detailed experimental procedures have been previously described by Anjos *et al* [25]. The PL extracts were dissolved in 100 µL of dichloromethane, and a volume of 10 µL was transferred, in duplicate, to a glass tube, previously washed with 5% nitric acid. The solvent was dried under a stream of nitrogen and a volume of 125 µL of 70 % perchloric acid was added to each tube. The samples were incubated in a heat block (Stuart, U.K.) for 1h at 180 °C. After cooling to room temperature, a volume of 825 µL of Milli-Q water, 125 µL of 2.5% ammonium molybdate (2.5 g/ 100 mL of Milli-Q water), and 125 µL of 10% ascorbic acid (0.1 g/1 mL of Milli-Q water) were added to each sample, with a vortex mixing between each addition. The samples were then incubated in a 100 °C water bath for 10 min. Then the samples were immediately cooled in a cold-water bath. Phosphate standards of 0.1 to 2 µg of phosphorus (P) were prepared from sodium dihydrogen phosphate dihydrate ($NaH_2PO_4 \bullet 2H_2O$, 100 µg/mL of P). The standards underwent the same experimental procedure as the samples without the heat block step. Absorbance was measured at 797 nm in a Multiskan GO 1.00.38 Microplate Spectrophotometer (Thermo Scientific, Hudson,

NH, USA) controlled by SkanIT software version 3.2 (Thermo Scientific™). The amount of P present in each sample was calculated by linear regression. For each lipid extract, the amount of total PL was calculated by multiplying the amount of phosphorus by 25.

2.5 Lipid extract analysis by Hydrophilic interaction liquid chromatography-mass spectrometry (HILIC-MS)

2.5.1 Sample preparation

The PL extracts obtained from serum samples were resuspended in dichloromethane to have a PL concentration of 1 µg PL/µL. Subsequently, in a vial with a micro-insert, 5 µL of each sample, 4 µL of a mixture of internal standards and 91 µL of the initial chromatographic phase were added. The internal standard mixture contained 0.02 µg of phosphatidylcholine (PC, 14:0/14:0), 0.02 µg of phosphatidylethanolamine (PE, 14:0/14:0), 0.012 µg of phosphatidylglycerol (PG, 14:0/14:0), 0.08 µg of phosphatidylinositol (PI, 16:0/16:0), 0.04 µg of phosphatidylserine (PS, 14:0/14:0), 0.08 µg of phosphatidic acid (PA, 14:0/14:0), 0.02 µg of lyso-PC (LPC, 19:0), 0.02 µg of sphingomyelin (SM, d18:1/17:0) and 0.08 µg of cardiolipin (CL, 14:0/14:0/14:0/14:0). The initial chromatographic phase consisted of two mobile phases at a proportion of 10% of eluent A (50% acetonitrile, 25% methanol, 25% water and 2.5 mM ammonium acetate) and 90% of eluent B (60% acetonitrile, 40% methanol and 2.5 mM ammonium acetate).

2.5.2 Data and statistical analysis

The PL were separated by HILIC, according to the polarity of the moiety group, using an Ascentis Si HPLC Pore column (100 mm x 1 mm; 3 µm, Sigma-Aldrich) inserted into an HPLC system (Ultimate 3000 Dionex, Thermo Fisher Scientific, Bremen, Germany) with an autosampler coupled online to a Q-Exactive™ Hybrid Quadrupole-Orbitrap™ Mass Spectrometer (Thermo Fisher Scientific, Bremen, Germany).

A volume of 5 µL of each sample mixture was injected into the HPLC column, at a flow rate of 50 µL/min. The temperature of the column oven was maintained at 35 °C. Elution started with 10% of mobile phase A, which was held isocratically for 2 minutes, followed by a linear

increase to 90% of mobile phase A within 13 minutes and maintained for 2 minutes. After that, conditions returned to the initial settings in 13 minutes (3 min to decrease to 10% of phase A and a re-equilibration period of 10 min prior next injection). The Q-Exactive™ orbitrap mass spectrometer with a heated electrospray ionization source was operated using a positive/negative switching toggles between positive (electrospray voltage of 3.0 kV) and negative modes (electrospray voltage of −2.7 kV). The sheath gas flow was 15 U, auxiliary gas was 5 U, the capillary temperature was 250 °C, the S-lenses RF was 50 U and the probe`s temperature was 130 °C. Full scans MS spectra were acquired both in positive and negative ionisation modes in an *m/z* range of 400-1600, with a resolution of 70.000, automatic gain control (AGC) target of $1x10^6$ and maximum injection time of 100 ms. For tandem MS (MS/MS) experiments, a top-10 data-dependent method was used. The top 10 most abundant precursor ions in full MS were selected to be fragmented in the collision cell HCD. A stepped normalized collision energy™ scheme was used and ranged between 20, 25 and 30 eV. MS/MS spectra obtained were those combining the information obtained with the three collision energies. The MS/MS spectra were obtained with a resolution of 17,500; AGC target of $1x10^5$; an isolation window of 1 *m/z*; scan range of 200-2000 *m/z*; and maximum injection time of 50 ms. The cycles consisted of one full scan mass spectrum and ten data-dependent MS/MS scans, which were repeated continuously throughout the experiments, with the dynamic exclusion of 60 s and intensity threshold of $1x10^4$. Data acquisition was carried out using the Xcalibur data system (V3.3, Thermo Fisher Scientific, USA).

LC-MS data were processed and integrated using the MZmine v2.42 software [27]. This software enabled filtering and smoothing, PL peak detection, PL peak alignment and integration, and PL assignment and identification against an in-house database, which contains information on the exact mass and retention time (RT) for each PL molecular species. The identification of the PL species was performed as described previously [25,28]. Briefly, to correctly identify the PL species, during the processing of raw data by MZmine, all peaks of raw intensity less than $1x10^4$ and error greater than 5 ppm were excluded. The assignment of each PL species was confirmed by analysis and interpretation of the MS/MS spectra. PC, LPC

and SM were analysed in the LC-MS spectra in the positive ion mode, as $[M+H]^+$ ions. The presence of the fragment ion at *m/z* 184, corresponding to the phosphocholine polar head group, in the MS/MS of $[M+H]^+$ ions allows identifying PL molecular species belonging to the PC, LPC and SM classes, which were further differentiated by the characteristic retention times. PC, LPC and SM were also analysed in the LC-MS spectra in the negative ion mode, as acetate adducts ($[M+CH_3COO]^-$ ions). MS/MS spectra of $[M+CH_3COO]^-$ ions of these three PL classes should display the typical fragment ion at *m/z* 168 (phosphocholine polar head group minus a methyl moiety). Carboxylate anions of fatty acyl chains can also be seen for PC and LPC. PE and LPE classes were analysed both in positive ($[M+H]^+$ ions) and negative ion modes ($[M-H]^-$ ions). The neutral loss of 141 Da (phosphoethanolamine polar head group) can be observed in the MS/MS acquired in the positive mode, while the fragment ion at *m/z* 140 (phosphoethanolamine polar head group) and the carboxylate anions of fatty acyl chains can be found in MS/MS data from negative ion mode. For structural identification of PC, LPC, SM, PE and LPE, the MS/MS data was analysed in positive and negative ion modes, however, for quantification purposes, only LC-MS positive ion mode data was used. PI and PG species together with the lyso forms of PI (LPI) and PG (LPG) were analysed in negative ion mode, as $[M-H]^-$ ions. These species were identified based only on the RT and exact mass measurements, no MS/MS spectrum was found. An example of the MS/MS fragmentation patterns of each PL classes analysed in the present study is available in the supplementary material.

Relative quantification was performed by exporting the peak area values to a computer spreadsheet. For normalization of the data, the peak areas of the extracted ion chromatograms (XIC) of the PL precursors of each class were divided for the peak area of the internal standards selected for the class.

The data sets composed of the XIC areas obtained by the HILIC-MS analysis were normalized to the internal standard, generalized log2, normalized with EigenMS [29], autoscaled and analysed statistically. Missing values were replaced with half of the minimum positive values detected in the data set. Principal component analysis (PCA) was performed

using the R libraries FactoMineR [30] and factoextra [31], and the ellipses were drawn assuming a multivariate normal distribution and a level of 0.95. Univariate statistical analysis was performed using the Wilcoxon or Kruskal−Wallis test following a post hoc Dunn test. A p-value < 0.05 was considered an indicator of statistical significance. Heatmaps were created using the R package pheatmap using "Euclidean" as the clustering distance and "ward.D" as the clustering method [32]. Univariate and multivariate statistical analyses were performed using R version 3.5.1 in Rstudio version 1.1.4. All graphics and boxplots were created using the R package ggplot2 [33]. Other R packages used for data management and graphics included plyr [32], dplyr [34] and tidyr [35]. The areas under curve (AUC) of Receiver operative characteristic (ROC) curves were used to determine the diagnostic effectiveness of important phospholipids using the R packages Caret [36], using a Random Forest model with the default parameters, and pROC [37].

3. Results

3.1 Characterization of the serum samples

To assess the changes in the PL profile associated with multiple sclerosis, we analysed the serum of 24 patients diagnosed with multiple sclerosis (from now on referred to as MSs) and 30 healthy controls samples (HC), as summarized in Table 1. All patients and controls were adults aged 20 to 60 years. A total of 94.1% and 71.4% of the patients in remission (MSs_Rem) and relapse (MSs_Rel), respectively, were female.

3.2 Identification of the serum phospholipid profile of patients with MSs and HC

The PL profile of MSs and HC serum was analysed by high-resolution HILIC-MS and MS/MS platform. This lipidomic analysis allowed to identify 161 different PL species (molecular ions) belonging to 9 different classes, namely phosphatidylcholine (PC) comprising diacyl, alkyl-acyl and alkenyl-acyl species, lyso PC (LPC), phosphatidylethanolamine (PE) including diacyl, alkyl-acyl and alkenyl-acyl species, lyso PE (LPE), phosphatidylglycerol (PG), lyso PG (LPG), phosphatidylinositol (PI), lyso PI (LPI) and sphingomyelin (SM) (Supplementary Table S1). PC, LPC, PE, LPE and SM species were identified by analysis of

exact mass, retention time and MS/MS spectra, while PG, LPG, PI and LPI species were identified by exact mass and retention time. Statistical analysis, including multivariate and univariate statistical analysis grouped the data as follows: 1) comparing HC with MSs (healthy *vs* overall disease) and 2) comparing HC with MSs_Rem and MSs_Rel patients.

3.2.1 Comparison of serum phospholipidome from HC versus patients with MSs (health *vs* disease)

The differences between the PL profile of HC (30 controls) and patients with MSs (24 patients), regardless the disease state (remission or relapse), were assessed using multivariate statistical analysis. Data from LC-MS analysis were auto-scaled and then subjected to principal component analysis (PCA) to show the clustering trends of the two experimental groups. The PCA plot showed that the two groups were separated in two different clusters, in a two-dimensional score plot that represented the analysis describing 31.3% of the total variance, including dimension 1 (24%) and dimension 2 (7.3%), with major discrimination in dimension 1 (Figure 1). HC samples were scattered on the right region of the PCA plot while MSs samples were scattered on the left region.

Considering the variables that contributed the most to group discrimination, 16 PL molecular species were identified that showed the most significant discriminating power between conditions using variable importance in projection (VIP) (Supplementary Figure S4). Eight of these PL species with higher discriminating potential were ether-linked (akyl-acyl and alkenyl-acyl), PC (5 species) and PE (3 species), which are generally decreased in MSs.

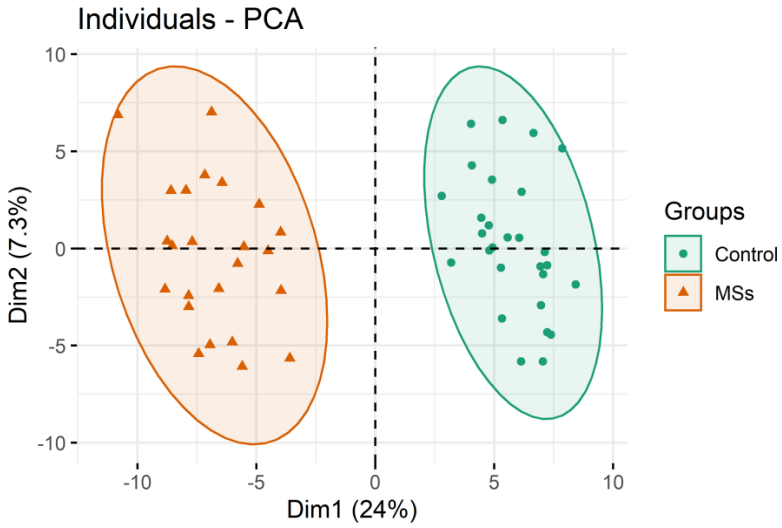

Figure 2.2-1 Principal component analysis (PCA) in a two-dimensional score scatter plot of PL profiles from serum from healthy control (Control) and disease (MSs) groups.

Also, a univariate analysis of the HILIC-MS data of the two conditions was performed (Supplementary Table S2), and the Wilcoxon test showed that the 16 major contributors with the lowest *q*-value ($q<0.05$) were selected (Figure 2) corresponding to 7 PC, 3 ether-linked PC, 3 ether-linked PE, and 3 LPE species, all with statistically significant lower levels in MSs. We predicted the test dataset using a trained model and found that the random forest predicts with an accuracy of 100%. Next, we have performed a Receiver operative characteristic (ROC) analysis to further characterize the predictive value of these top 5 PL independently (Supplementary Figure S5). We found that all 5 PL had an area under the curve (AUC) >0.96.

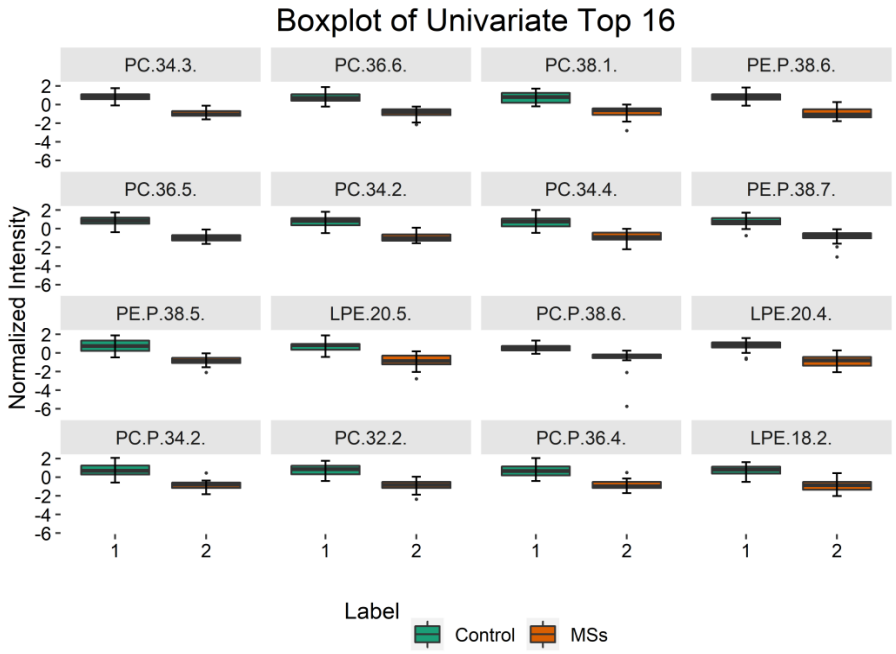

Figure 2.2-2. Box plots of the 16 most discriminating PL species with the lowest q-values obtained from a univariate analysis of HC (1) and MSs patients (2) using the Wilcoxon test. $q < 0.05$ for all comparisons.

Additionally, we carried out a hierarchical clustering analysis (HCA) on the phospholipid data sets from the two conditions (Figure 3). The results were used to create a heatmap of the top 25 PL species with the lowest q-values in the Wilcoxon test, and a dendrogram with a two-dimensional hierarchical clustering of the functional state and variables that reflect the most important native PL species contributing to differentiate MSs disease from HC. The resulting HCA dendrogram (Figure 3) showed a noticeable separation of the two data in the first dimension (upper hierarchical dendrogram) where samples are clustered independently into two groups, control and disease (MSs). Moreover, the clustering of individual PL species also shows two principal clusters: the first group includes a single PL specie, PE(40:10), which is more abundant in MSs, while the second group had 24 different PL species which are less abundant in MSs than HC, and included 11 plasmalogens species, namely 6 PE plasmalogens, 5 PC plasmalogens, 8 PC species (with 7 PC bearing PUFA), 3 LPE with PUFA, 1 PE and 1 PG species.

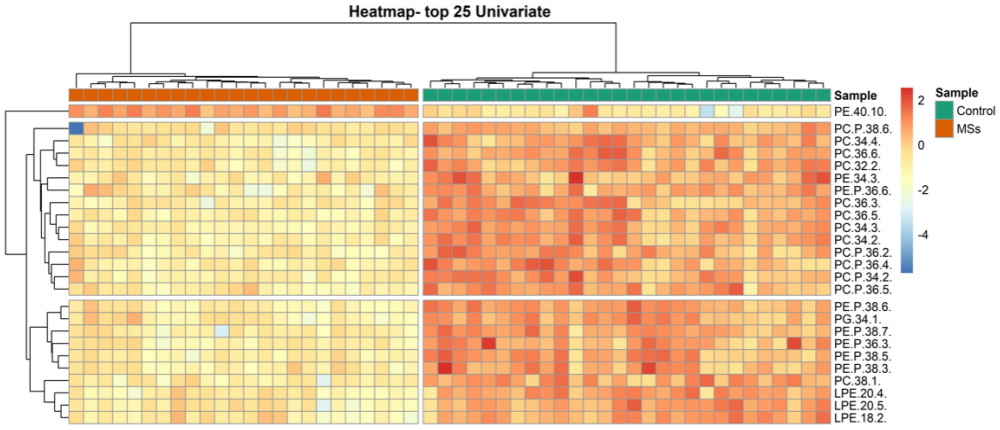

Figure 2.2-3. Two-dimensional hierarchical clustering heatmap of the 25 most discriminating PL molecular species of Control and MSs groups. Relative abundance levels are shown on the red-yellow-blue scale, with the numbers indicating the fold difference from the overall mean. The red colour of the tile indicates high abundance and blue indicates low abundance. Null values were displayed in yellow. The clustering of the control and disease groups is represented by the dendrogram at the top. The clustering of individual PL molecular species is represented by the dendrogram on the left.

3.2.2 Comparison of serum phospholipidome from HC versus patients with MSs_Rem and MSs_Rel

The PL profile was compared considering the disease status. Thus, the MSs PL profile of the serum from the two groups, MSs_Rem (n=17) and MSs_Rel (n=7), were compared to HC. Multivariate analysis of the datasets was performed and the PCA plot generated showed that, in a two-dimensional score plot, the HC group separates from the two MSs groups (Figure 4). The PCA plot also showed the separation of the two conditions, MSs_Rem and MSs_Rel, although some overlapping of the 95% confidence ellipse was observed. The PCA score plot described 32.7% of the total variance, including dimension 1 (24.8%) and dimension 2 (7.9%), where dimension 1 was the major discriminant. The HC samples were scattered in the right region of the plot while the MSs_Rem and MSs_Rel samples were scattered on the left region of the plot. The 16 PL molecular species that showed the most significant discriminating power between conditions in PCA analysis (Supplementary Figure S6), using VIP scores, included 7 PC (2 diacyl PC plus 5 alkyl-acyl PC), 4 PE (2 diacyl PE and 2 PE plasmalogens), 2 PG, 1 PI, 1 LPE and 1 LPG specie. Boxplots, which report the normalized intensities of the 16 PL species,

show the PL species with higher discriminating potential between MSs groups, such as PE (P-34:5), PE (30:2) and LPG14:0 species which were found to have lower levels in MSs_Rel than in HC and MSs_Rem.

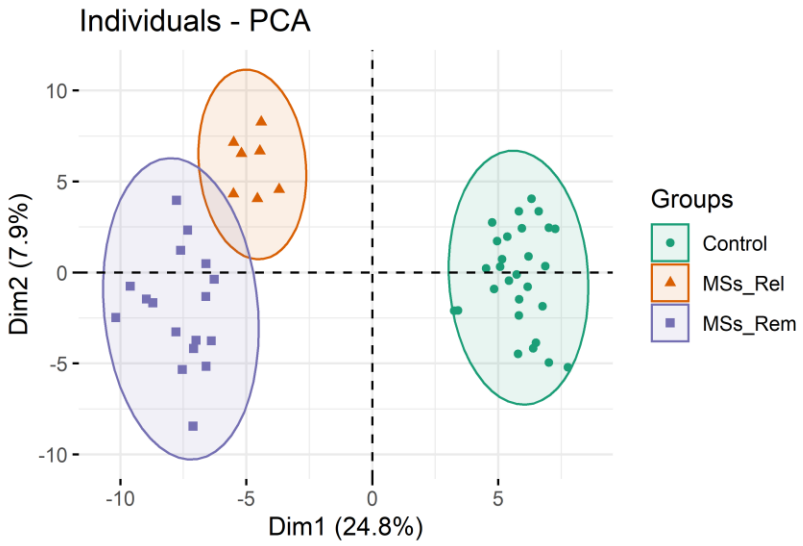

Figure 2.2-4. PCA of the serum phospholipidome from control, MSs_Rel and MSs_Rem. PCA in a two-dimensional score scatter plot of PL profiles obtained in both positive and negative modes from healthy control (Control), MSs_Rel and MSs_Rem groups.

Also, a univariate analysis (Kruskal−Wallis test followed by Dunn's multiple comparison post-hoc test) was performed on the HILIC-MS data, to test for significant differences between the three conditions (Supplementary Table S3). The main 16 contributors from the Kruskal−Wallis test with the lowest *q*-value (with $q<0.05$) were selected (Figure 5) and correspond to 7 PC, 2 ether-linked PC, 5 ether-linked PE, and 2 LPE species, all with statistically significantly higher levels in control samples. Dunn's test of multiple comparisons revealed that 16 species were significantly different between HC and MSs_REM, 15 between HC and MSs_REL, and 1 (PC 38:1) between MSs_REL and MSs_REM.

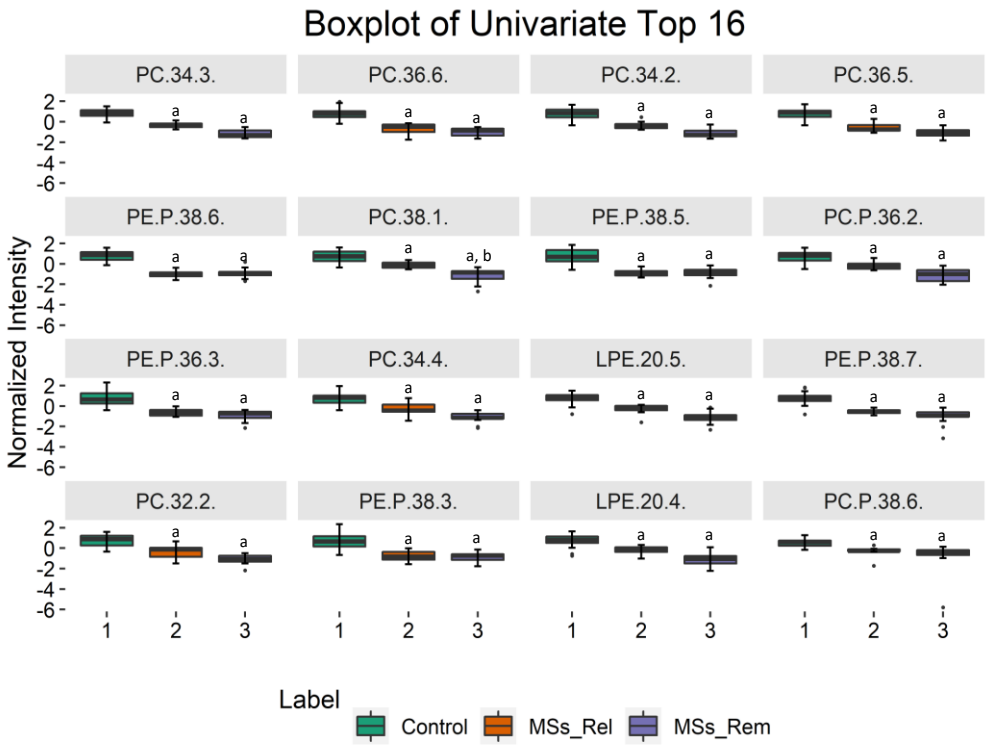

Figure 2.2-5. Box plots of PL molecular species with the lowest 16 q-values of the Kruskal-Wallis test followed by the Dunn multiple comparison tests of Control, MSs_Rel and MSs_Rem. $q < 0.05$ was considered statistically significant: a, control vs MSs_Rem and control versus MSs_Rel; b, MSs_Rel versus MSs_Rem.

The results of the Kruskal-Wallis test were also used to create a heatmap of the 25 PL species with the lowest q-values. The dendrogram with two-dimensional hierarchical clustering of disease status and variables (Figure 6) shows the most important native PL species contributing to differentiate MSs-Rel and MSs-Rem from HC samples. It is possible to observe that in the first dimension, in the top hierarchical dendrogram, the samples are clustered independently into two groups, control versus disease, and it was not possible to achieve complete discrimination between the two statuses of disease. The clustering of the individual PL species allowed for the identification of two principal clusters: the first which included 6 ether-linked PE that is more abundant in the HC group and less abundant in the disease groups, while the second contains different PL species which are also more abundant in the HC group and the MSs-Rel, but with low abundance in MSs-Rem, including 4 PC plasmalogens, 8 PC(including 6 PC bearing PUFA) and 3 LPE species and 1 LPC.

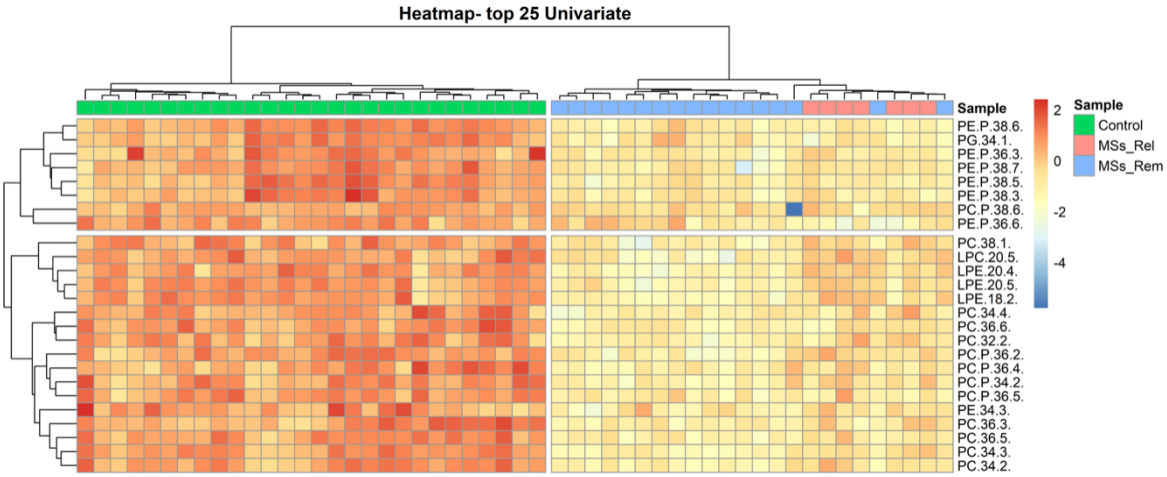

Figure 2.2-6. Two-dimensional hierarchical clustering heat map of the 25 most discriminating PL molecular species of the control, MSs_Rel and MSs_Rem groups. Relative abundance levels are shown on the red-yellow-blue scale, with the numbers indicating the fold difference from the overall mean. The red colour of the tile indicates high abundance and blue indicates low abundance. Null values were displayed in yellow. The clustering of the HC, MSs_Rel and MSs_Rem groups is represented by the dendrogram at the top. The clustering of individual PL molecular species is represented by the dendrogram on the left.

Univariate analysis (Figure 2 and Figure 5) indicates that the 16 PL molecular species that most significantly contribute to discriminating HC from MSs and HC from patients with MSs_Rem and MSs_Rel mainly include PC and PE species, bearing PUFA, and PC and PE alkyl-acyl species, and some lyso PL. There was variation in 13 PL molecular species revealing the lowest abundance of PC(34:3); PC(36:6); PC(38:1); PE(P-38:6); PC(36:5); PC(34:2); PC(34:4); PE(P-38:7); PE(P-38:5)/PE(O-38:6); LPE(20:5); PC(P-38:6); LPE(20:4) and PC(32:2) in MSs (overall disease) and MSs_Rem and MSs_Rel. ROC analysis (supplementary figure S5) have shown, that the five variables with the lowest p-value distinctive had very high AUC value (>0.96) two had a AUC > 0.99 (PC(34:3) and PC(36:6)), showing a potential high diagnostic performance of multiple sclerosis. The boxplots in Figure 2, which compared HC with MSs, also showed that PC(P-34:2)/PC(O-34:3); PC(P-36:4)/PC(O-36:5) and LPE(18:2) were significantly downregulated in MSs and contributed to differentiate the two groups. In the second analysis (Figure 5), PC(P-36:2)/PC(O-36:3); PE(P-36:3)/PE(O-36:4) and PE(P-38:3)/PE(O-38:4) were also significantly decreased in the MSs_Rem and MSs_Rel groups. The lower levels of PC(34:3); PC(34:2); PC(36:5); PC(38:1); PC(P-36:2)/PC(O-36:3); PC(34:4);

LPE(20:5); PC(32:2) and LPE(20:4) in the MSs_Rem group show a deeper alteration in lipid metabolism. The result of the hierarchical cluster analysis represented by a heatmap (Figures 3 and 6) also confirms that PC and PE are the PL classes that contribute the most to differentiate all the groups.

4. Discussion

Lipids have important biological functions with critical roles in inflammatory and immune processes and have been correlated with the pathophysiology of many diseases, including autoimmune diseases such as MSs [6]. They have been shown to contribute to the pathogenesis and severity of MSs. MSs is characterized by demyelination and myelin is mainly composed of lipids, but their role in MSs is scarcely addressed [10]. In this study, a phospholipidomic profiling of serum samples from patients with MSs was carried out, aiming to elucidate the adaptations of the PL profile concerning the health status, and associated with the different statuses of this disease. Lipidomics data were analyzed by multivariate principal component analysis (PCA) as well as univariate and hierarchical cluster analysis (HCA) for visualization and interpretation of results. Of all the patients included in this study, a total of 94.1% of MSs_Rem patients and 71.4% of MSs_Rel patients were female, which is in agreement with the epidemiological evidence indicating that MSs is three times more prevalent in women [38].

Initially, a comparison between healthy controls and patients with the disease (HC vs MSs) was performed to assess the differences between health and disease. Analysis of the PCA score plot (Figure 1) indicated that the lipidome of the two conditions differ from each other, which means that the serum PL profile of MSs is different from HC. Then the lipid profile was also compared taking into account the status of the disease. RRMS is characterized by periods of relapse and remission that affect the patient's daily life. During periods of relapse, the (neuro)inflammatory conditions worsen, so it is expected to observe major or dissimilar changes in the lipid profile. The analysis of PCA scores scatter plot (Figure 4) revealed that HC differed from MSs, however, the MSs_Rem and MSs_Rel 95% confidence ellipses partially intercept

and as such are not fully discriminated. This means that while considering that in remission there are fewer (if any) symptoms, there is also a modulation of the lipid profile which is different from typical health conditions. Even in the absence of symptoms, the lipid profile does not return to the level of healthy status and the significance of this imbalance should be carefully assessed.

In this work, patients with MSs had a lower abundance of plasmalogens PC and PE species, compared to controls, and differences were mainly observed in PC and PE species with PUFA. PC is the most abundant class of PL in cell membranes and plasma [39]. In our models, few PC species discriminated HC from MSs and HC from MSs_Rem and MSs_Rel. Different PC species have contributed to this differentiation such as plasmalogens PC(P-38:6); PC(P-36:2)/PC(O-36:3); PC(P-36:4)/PC(O-36:5); PC(P-34:2)/PC(O-34:3); PC(P-36:5) and the diacyl species PC(34:4); PC(36:6); PC(32:2); PC(36:3); PC(36:5); PC(34:3); PC(34:2) and PC(38:1). However, only PC(38:1) was statistically different between MSs_Rel and MSs_Rem, being lower in MSs_Rem (Figure 5). PC(38:1) was identified as PC(18:1/20:0), thus bearing an oleic acid (FA 18:1). Trépanier et al reported a significant reduction in oleic acid in post-mortem brain tissue from mouse models with induced demyelination and from patients with MSs [40]. In our study, comparing HC to MSs groups, we also found significantly lower levels of the molecular species PC(34:2), PC(36:3), and PC(38:1), all of which contained oleic acid in their composition. Cicalini *et al* also found a markedly decreased PC(38:1) in tears from patients with MSs [41]. The decrease in PL species may be due to a decrease in oleic acid biosynthesis which may result from the dysregulation of different pathways, such as i): formation and reduced levels of 18:1 precursors, namely palmitate (C16:0), stearate (C18:0) or palmitoleate (C16:1); ii) this may be the result of downregulation of desaturases, as Δ9-desaturase, which converts FA 18:0 into FA 18:1 n-9 and FA 16:0 into FA 16:1 n-9; or iii) it may ultimately derive from the downregulation of ELOVL6 elongase which converts FA 16:0 into FA 18:0 (Supplementary Figure S7).

PE is the second most abundant class of PL in cells and is the major class of PL in myelin sheaths. The results gathered in the present work showed that the PE species contributed

to differentiate HC from MSs and HC from MSs_Rel and MSs_Rem. These species were PE(34:3); PE(P-36:6); PE(P-38:6); PE(P-38:7); PE(P-36:3)/PE(O-36:4); PE(P-38:5)/PE(O-38:6); PE(P-38:3)/PE(O-38:4), generally lower in disease. Another feature noted when comparing MSs phospholipidome (overall disease) with HC, was the significantly higher concentrations of PE(40:10) in MSs. The majority of PC and PE species that showed variation were esterified to PUFA and were decreased in MSs. The significant reduction in serum PE and PC species in MSs has also been reported by Villoslada et al[42].

PE may have a role in the immune response by modulating CD300 receptor in chronic inflammatory diseases and are also known to participate in autoimmune diseases. However, the exact function of the receptors of this family is unclear and may upregulate or downregulate immune responses [43]. PC is fundamental in proliferative growth and programmed cell death [44]. Therefore, these alterations in phospholipidome may be correlated with increased chronic activation of the immune system in patients with MSs, in which PL have important functions [45]. In addition, we have found among the PC and PE species several ether-linked species, namely the PC and PE plasmalogens. These species had significantly lower levels in MSs, MSs_Rel and MSs_Rem, compared to controls. Plasmalogens are considered to be important endogenous antioxidants, playing a key role in cellular antioxidant defence, so their reduction in disease conditions may be an indicator of an increased oxidative environment in MSs [46,47]. Plasmalogens have also been recognised as important antioxidants in myelin [46]. Myelin is highly enriched in PE species, in particular in plasmalogens, and the decrease in PE may be due to damage to the myelin that occurs during demyelination [48,49]. Plasmalogen-deficient mammalian cells are considerably more susceptible to oxidative stress-induced death than high plasmalogen mammalian cells, corroborating the protective role of plasmalogens as antioxidants [46,50,51]. Accordingly, our results of significantly lower abundances of PC and PE plasmalogen species in MSs serum may indicate alterations of the myelin lipid-rich sheaths, making them more vulnerable to oxidative damage, known to be increased in this pathology.

In this work, we found that several PC and PE phospholipids bearing PUFA species had significantly lower abundances in MSs. This decrease could be due to degradation by lipid

peroxidation processes that can occur in MSs, in the two groups with different disease status. An increase in oxidative stress has been described in MSs, leading to exacerbation of disease activity and severity [6,52]. The identification of oxidized lipids was not the scope of our work, but oxidized PL has already been found in the plasma of patients with MSs [42,53,54].

The LPE class also contributed to the discrimination of HC and MSs and of HC, MSs_Rem and MSs_Rel, particularly with three species, LPE(20:4); LPE(20:5) and LPE(18:2). These LPE species with PUFA were shown to be significantly reduced in MSs, which correlates well to the results showing that patients with MSs have a FA 18:2, 20:4 and PUFA deficiency in plasma and serum [6]. PUFA are also known to have immunomodulatory effects which are associated with their ability to suppress T cell activation and function [55]. Thus, the reduction in PUFA levels in patients with MSs observed in our work indicates that this may contribute to the activation of T cells in this pathology. MS is mediated by effector T cells, even in remission MSs patients the IL-17 and Th/c17 cells seemed to contribute to perpetuating chronic inflammation [56]. Moreover, the decrease in LPE(20:5) in MSs is noteworthy because LPE(20:5) can arise from degradation of PE(40:10) by phospholipases [57]. In the analysis of control versus MSs, PE(40:10) shows higher abundances in patients with MSs which may indicate altered PLA2 activity in patients with MSs and decreased LPE(20:5) biosynthesis. For future work, it would be interesting to investigate PLA2 activity. In the HC vs MSs_Rem and MSs_Rel comparison, LPC(20:5) also contributes to differentiate the lipid profile, being downregulated in MSs_Rem and MSs_Rel patients.

Del Boccio *et al* [19], Kurz *et al* [20] and De Oliveira *et al* [58] also analysed MSs plasma and serum samples using LC-MS/MS techniques but these authors only explored alterations on lyso-PL[19], ceramides[20] and other lipid species[58]. To our knowledge, our study is the first to assess phospholipidome changes of several classes of PL using LC-MS/MS.

5. Conclusion

From this study, we can conclude that the pathogenesis of MSs was associated with changes in the lipid profile and that patients with MSs have a significantly different PL profile compared to healthy controls. Our results showed that the phospholipidomic signature of MSs is

significantly different from that of healthy controls, in particular for the PE, PC, LPE and ether-linked PE and PC species. Based on the comparison of MSs_Rel and MSs_Rem, our models had less discriminating power, and the species that showed significant differences were mainly PC species, particularly PC(38:1). PC and PE plasmalogens, as well as PC and PE species bearing PUFA, had significantly lower levels in MSs disease and MSs_Rel and MSs_Rem. PE(40:10) and PC(38:1) may be considered as possible serum biomarkers of this disease due to their significant variations in patients with MSs and may be suitable for clinical applications. These results provide new insights on changes in the lipidome profile in MSs and may help improve our understanding of the characteristics of MSs pathogenesis. Clinical lipidomics is one of the best approaches to better understand these disease-induced changes and find suitable biomarkers for personalized MSs medicine.

Acknowledgements

Thanks are due for the financial support to the University of Aveiro and FCT/MCT for the financial support for the CESAM (UIDB/50017/2020+UIDP/50017/2020), QOPNA (FCT UID/QUI/00062/2019), LAQV/REQUIMTE (UIDB/50006/2020) and to RNEM, Portuguese Mass Spectrometry Network (LISBOA-01-0145-FEDER-402-022125) through national funds and, where applicable, co-financed by the FEDER, within the PT2020. Tânia Melo thanks the research contract under the project OMICS 4ALGAE (POCI-01-0145-FEDER-030962).

References

[1] R. Rahmanzadeh, W. Brück, A. Minagar, M.A. Sahraian, Multiple sclerosis pathogenesis: Missing pieces of an old puzzle, Rev. Neurosci. 30 (2019) 67–83.

[2] G.G. Ortiz, F.P. Pacheco-Moisés, O.K. Bitzer-Quintero, A.C. Ramírez-Anguiano, L.J. Flores-Alvarado, V. Ramírez-Ramírez, M.A. Macias-Islas, E.D. Torres-Sánchez, Immunology and oxidative stress in multiple sclerosis: Clinical and basic approach, Clin. Dev. Immunol. 2013 (2013) 1–14.

[3] B.J. Hurwitz, The diagnosis of multiple sclerosis and the clinical subtypes, Ann. Indian Acad. Neurol. 12 (2009) 226–230.

[4] A.J. Thompson, B.L. Banwell, F. Barkhof, W.M. Carroll, T. Coetzee, G. Comi, J. Correale, F. Fazekas, M. Filippi, M.S. Freedman, K. Fujihara, S.L. Galetta, H.P. Hartung, L. Kappos, F.D. Lublin, R.A. Marrie, A.E. Miller, D.H. Miller, X. Montalban, E.M. Mowry, P.S. Sorensen, M. Tintoré, A.L. Traboulsee, M. Trojano, B.M.J. Uitdehaag, S. Vukusic, E. Waubant, B.G.

Weinshenker, S.C. Reingold, J.A. Cohen, Diagnosis of multiple sclerosis: 2017 revisions of the McDonald criteria, Lancet Neurol. 17 (2018) 162–173.
[5] C. Tur, A.J. Thompson, Early accurate diagnosis crucial in multiple sclerosis, Practitioner. 259 (2015) 21–27.
[6] H.B. Ferreira, B. Neves, I.M. Guerra, A. Moreira, T. Melo, A. Paiva, M.R. Domingues, An overview of lipidomic analysis on different human matrices of multiple sclerosis, Mult. Scler. Relat. Disord. 44 (2020) 102189.
[7] O. Ciccarelli, A. Thompson, Managing the complexity of multiple sclerosis., Nat. Rev. Neurol. 12 (2016) 70–72.
[8] S. Love, Demyelinating diseases., J Clin Pathol. 59 (2006) 1151–1159.
[9] S. Schmitt, L.C. Castelvetri, M. Simons, Metabolism and functions of lipids in myelin, Biochim. Biophys. Acta - Mol. Cell Biol. Lipids. 1851 (2015) 999–1005. http://dx.doi.org/10.1016/j.bbalip.2014.12.016.
[10] G. Cermenati, N. Mitro, M. Audano, R.C. Melcangi, M. Crestani, E. De Fabiani, D. Caruso, Lipids in the nervous system: From biochemistry and molecular biology to patho-physiology, Biochim. Biophys. Acta - Mol. Cell Biol. Lipids. 1851 (2015) 51–60.
[11] C.E. Hayes, J.M. Ntambi, Multiple sclerosis: Lipids, Lymphocytes and Vitamin D, Immunometabolism. 2 (2020) 1–53.
[12] H.B. Ferreira, A.M. Pereira, T. Melo, A. Paiva, M.R. Domingues, Lipidomics in autoimmune diseases with main focus on systemic lupus erythematosus, J. Pharm. Biomed. Anal. 174 (2019) 386–395.
[13] H. Lassmann, W. Brück, C.F. Lucchinetti, The Immunopathology of Multiple Sclerosis: An Overview., Brain Pathol. 17 (2007) 210–218.
[14] A.P. Corthals, Multiple Sclerosis is Not a Disease of the Immune System., Q. Rev. Biol. 86 (2011) 287–321.
[15] S. Palumbo, Pathogenesis an Progression of Multiple Sclerosis: The Role of Arachidonic Acid – Mediated Neuroinflammation, in: I. Zagon, P. McLaughlin (Eds.), Mult. Scler. Perspect. Treat. Pathog., Codon Publications, Brisbane, Australia, 2017: pp. 111–123.
[16] N. Mattsson, M. Yaong, L. Rosengren, K. Blennow, J.-E. Månsson, O. Andersen, H. Zetterberg, S. Haghighi, I. Zho, D. Pratico, Elevated cerebrospinal fluid levels of prostaglandin E2 and 15-(S)-hydroxyeicosatetraenoic acid in multiple sclerosis., J. Intern. Med. 265 (2009) 459–464.
[17] S. Bittner, T. Ruck, M.K. Schuhmann, A.M. Herrmann, H.M. ou Maati, N. Bobak, K. Göbel, F. Langhauser, D. Stegner, P. Ehling, M. Borsotto, H.-C. Pape, B. Nieswandt, C. Kleinschnitz, C. Heurteaux, H.-J. Galla, T. Budde, H. Wiendl, S.G. Meuth, Endothelial TWIK-related potassium channel-1 (TREK1) regulates immune-cell trafficking into the CNS., Nat. Med. 19 (2013) 1161–1165.
[18] R.T. Holman, S.B. Johnson, E. Kokmen, Deficiencies of polyunsaturated fatty acids and replacement by nonessential fatty acids in plasma lipids in multiple sclerosis, Proc. Natl. Acad. Sci. U. S. A. 86 (1989) 4720–4724.
[19] P. Del Boccio, D. Pieragostino, M. Di Ioia, F. Petrucci, A. Lugaresi, G. De Luca, D. Gambi, M. Onofrj, C. Di Ilio, P. Sacchetta, A. Urbani, Lipidomic investigations for the characterization of circulating serum lipids in multiple sclerosis, J. Proteomics. 74 (2011) 2826–2836.
[20] J. Kurz, R. Brunkhorst, C. Foerch, L. Blum, M. Henke, L. Gabriel, T. Ulshöfer, N. Ferreirós, M.J. Parnham, G. Geisslinger, S. Schiffmann, The relevance of ceramides and their synthesizing enzymes for multiple sclerosis, Clin. Sci. 132 (2018) 1963–1976.
[21] O.G. Vidaurre, J.D. Haines, I. Katz Sand, K.P. Adula, J.L. Huynh, C.A. Mcgraw, F. Zhang, M. Varghese, E. Sotirchos, P. Bhargava, V.V.R. Bandaru, G. Pasinetti, W. Zhang, M. Inglese, P.A. Calabresi, G. Wu, A.E. Miller, N.J. Haughey, F.D. Lublin, P. Casaccia, Cerebrospinal fluid ceramides from patients with multiple sclerosis impair neuronal bioenergetics, Brain. 137 (2014) 2271–2286.
[22] Y.Y. Zhao, X. long Cheng, R.C. Lin, Lipidomics Applications for Discovering Biomarkers of Diseases in Clinical Chemistry, Elsevier Inc., 2014.
[23] J. Lv, L. Zhang, F. Yan, X. Wang, Clinical lipidomics: a new way to diagnose human diseases,

Clin. Transl. Med. 7 (2018) 10–12.
[24] C.H. Polman, S.C. Reingold, B. Banwell, M. Clanet, J.A. Cohen, M. Filippi, K. Fujihara, E. Havrdova, M. Hutchinson, L. Kappos, F.D. Lublin, X. Montalban, P. O'Connor, M. Sandberg-Wollheim, A.J. Thompson, E. Waubant, B. Weinshenker, J.S. Wolinsky, Diagnostic criteria for multiple sclerosis: 2010 Revisions to the McDonald criteria, Ann. Neurol. 69 (2011) 292–302.
[25] S. Anjos, E. Feiteira, F. Cerveira, T. Melo, A. Reboredo, S. Colombo, R. Dantas, E. Costa, A. Moreira, S. Santos, A. Campos, R. Ferreira, P. Domingues, M.R.M. Domingues, Lipidomics Reveals Similar Changes in Serum Phospholipid Signatures of Overweight and Obese Pediatric Subjects, J. Proteome Res. 18 (2019) 3174–3183.
[26] E.M. Bartlett, D.H. Lewis, Spectrophotometric determination of phosphate esters in the presence and absence of orthophosphate, Anal. Biochem. 36 (1970) 159–167.
[27] T. Pluskal, S. Castillo, A. Villar-Briones, M. Oresĭc, MZmine 2: Modular Framework for Processing, Visualizing, and Analyzing Mass Spectrometry-Based Molecular Profile Data., BMC Bioinf. 11 (2010) 395.
[28] S. Colombo, T. Melo, M. Martínez-López, M.J. Carrasco, M.R. Domingues, D. Pérez-Sala, P. Domingues, Phospholipidome of endothelial cells shows a different adaptation response upon oxidative, glycative and lipoxidative stress, Sci. Rep. 8 (2018) 1–13.
[29] Y. V. Karpievitch, S.B. Nikolic, R. Wilson, J.E. Sharman, L.M. Edwards, Metabolomics data normalization with EigenMS, PLoS One. 9 (2014) 1–10.
[30] S. Le, J. Josse, F. Husson, FactoMineR: An R Package for Multivariate Analysis., J. Stat. Softw. 25 (2008) 1–18.
[31] A. Kassambara, F. Mundt, factoextra: Extract and Visualize the Results of Multivariate Data Analyses. R package version 1.0.7., (2020).
[32] R. Kolde, Kolde, R. Pheatmap: Pretty Heatmaps. R package version 1.0.12., (n.d.).
[33] H. Wickham, ggplot2 – Elegant Graphics for Data Analysis., 2nd Editio, Springer Nature, 2016.
[34] H. Wickham, R. François, L. Henry, K. Müller, dplyr: A Grammar of Data Manipulation. R package version 0.7.7., (2018).
[35] H. Wickham, L. Henry, tidyr: Easily Tidy Data with "spread()" and "gather()" Functions., (2018).
[36] M. Kuhn, caret: Classification and Regression Training. R package version 6.0-86., (2020).
[37] X. Robin, N. Turck, A. Hainard, N. Tiberti, F. Lisacek, J.-C. Sanchez, M. Müller, pROC: an open-source package for R and S+ to analyze and compare ROC curves, BMC Bioinformatics. 12 (2011) 77.
[38] N.M.S. Society, What is MS?, (2020). https://www.nationalmssociety.org/ (accessed March 16, 2020).
[39] P. Risé, S. Eligini, S. Ghezzi, S. Colli, C. Galli, Fatty acid composition of plasma, blood cells and whole blood: relevance for the assessment of the fatty acid status in humans, Prostaglandins Leukot. Essent. Fat. Acids. 76 (2007) 363–369.
[40] M.O. Trépanier, K.D. Hildebrand, S.D. Nyamoya, S. Amor, R.P. Bazinet, M. Kipp, Phosphatidylcholine 36:1 concentration decreases along with demyelination in the cuprizone animal model and in post-mortem multiple sclerosis brain tissue, J. Neurochem. 145 (2018) 504–515.
[41] I. Cicalini, C. Rossi, D. Pieragostino, L. Agnifili, L. Mastropasqua, M. di Ioia, G. De Luca, M. Onofrj, L. Federici, P. Del Boccio, Integrated Lipidomics and Metabolomics Analysis of Tears in Multiple Sclerosis: An Insight into Diagnostic Potential of Lacrimal Fluid, Int. J. Mol. Sci. 20 (2019) 1–16.
[42] P. Villoslada, C. Alonso, I. Agirrezabal, E. Kotelnikova, I. Zubizarreta, I. Pulido-Valdeolivas, A. Saiz, M. Comabella, X. Montalban, L. Villar, J.C. Alvarez-Cermeño, O. Fernández, R. Alvarez-Lafuente, R. Arroyo, A. Castro, Metabolomic signatures associated with disease severity in multiple sclerosis, Neurol. Neuroimmunol. NeuroInflammation. 4 (2017) 1–10.
[43] J. Vitallé, I. Terrén, A. Orrantia, O. Zenarruzabeitia, F. Borrego, CD300 receptor family in viral infections, Eur. J. Immunol. 49 (2019) 364–374.
[44] O. Zenarruzabeitia, J. Vitallé, C. Eguizabal, V.R. Simhadri, F. Borrego, The Biology and Disease Relevance of CD300a, an Inhibitory Receptor for Phosphatidylserine and

Phosphatidylethanolamine, J. Immunol. 194 (2015) 5053–5060.
[45] L.A. O'Neill, R.J. Kishton, J. Rathmell, A guide to immuno-metabolism for immunologists., Nat Rev Immunol. 16 (2016) 553–565.
[46] A.M. Luoma, F. Kuo, O. Cakici, M.N. Crowther, A.R. Denninger, R.L. Avila, P. Brites, D.A. Kirschner, Plasmalogen phospholipids protect internodal myelin from oxidative damage., Free Radic Biol Med. 84 (2015) 296–310.
[47] S. Wallner, G. Schmitz, Plasmalogens the neglected regulatory and scavenging lipid species., Chem. Phys. Lipids. 164 (2011) 573–589.
[48] K.J. Smith, R. Kapoor, P.A. Felts, Demyelination: the role of reactive oxygen and nitrogen species., Brain Pathol. 9 (1999) 69–92.
[49] S. Aggarwal, L. Yurlova, M. Simons, Central nervous system myelin: structure, synthesis and assembly., Trends Cell Biol. 21 (2011) 585–593.
[50] O.H. Morand, R.A. Zoeller, C.R. Raetz, Disappearance of plasmalogens from membranes of animal cells subjected to photosensitized oxidation., J. Biol. Chem. 263 (1988) 11597–11606.
[51] R.A. Zoeller, O.H. Morand, C.R. Raetz, A possible role for plasmalogens in protecting animal cells against photosensitized killing., J. Biol. Chem. 263 (1988) 11590–11596.
[52] R. Padureanu, C.V. Albu, R.R. Mititelu, M.V. Bacanoiu, A.O. Docea, D. Calina, V. Padureanu, G. Olaru, R.E. Sandu, R.D. Malin, A.-M. Buga, Oxidative Stress and Inflammation Interdependence in Multiple Sclerosis, J. Clin. Med. 8 (2019) 1815.
[53] J. Qin, R. Goswami, R. Balabanov, G. Dawson, Oxidized Phosphatidylcholine Is a Marker for Neuroinflammation in Multiple Sclerosis Brain, J. Neurosci. Res. 85 (2007) 977–984.
[54] L. Haider, M.T. Fischer, J.M. Frischer, J. Bauer, R. Höftberger, G. Botond, H. Esterbauer, C.J. Binder, J.L. Witztum, H. Lassmann, Oxidative damage in multiple sclerosis lesions, Brain. 134 (2011) 1914–1924.
[55] T.M. Stulnig, J. Huber, N. Leitinger, E.M. Imre, P. Angelisová, P. Nowotny, W. Waldhäusl, Polyunsaturated Eicosapentaenoic Acid Displaces Proteins from Membrane Rafts by Altering Raft Lipid Composition, J. Biol. Chem. 276 (2001) 37335–37340.
[56] A. Monteiro, P. Rosado, L. Rosado, A.M. Fonseca, A. Paiva, Alterations in circulating T cell functional subpopulations in interferon-beta treated multiple sclerosis patients: A pilot study, J. Neuroimmunol. 339 (2020) 577113.
[57] A. Trotter, E. Anstadt, R.B. Clark, F. Nichols, A. Dwivedi, K. Aung, J.L. Cervantes, The role of phospholipase A2 in multiple Sclerosis: A systematic review and meta-analysis, Mult. Scler. Relat. Disord. 27 (2019) 206–213.
[58] E.M.L. De Oliveira, D.A. Montani, D. Oliveira-Silva, A.F. Rodrigues-Oliveira, S.L.D.A. Matas, G.B.P. Fernandes, I.D.C.G. Da Silva, E.G. Lo Turco, Multiple sclerosis has a distinct lipid signature in plasma and cerebrospinal fluid, Arq. Neuropsiquiatr. 77 (2019) 696–704.

2.3 CHAPTER 2.3: LIPIDOMIC ANALYSIS IN SYSTEMIC LUPUS ERYTHEMATOSUS AND SYSTEMIC SCLEROSIS

This chapter was integrally published as follows.
Reprinted with permission from:

H. B. Ferreira, T. Melo, I. M. S. Guerra, A. S. P. Moreira, P. Laranjeira, A. Paiva, L. Goracci, S. Bonciarelli, P. Domingues, M. R. Domingues, Whole Blood and Plasma-Based Lipid Profiling Reveals Distinctive Metabolic Changes in Systemic Lupus Erythematosus and Systemic Sclerosis, *Journal of proteome research* (2023), volume 22, issue 9, pages 2995-3008
https://doi.org/10.1021/acs.jproteome.3c00321

Abstract

Autoimmune diseases (AID), such as systemic lupus erythematosus (SLE) and systemic sclerosis (SS), are complex conditions involving immune system dysregulation. Diagnosis is challenging, requiring biomarkers for improved detection and prediction of relapses. Lipids have emerged as potential biomarkers due to their role in inflammation and immune response. This study uses an untargeted C18 RP-LC-MS lipidomics approach to comprehensively assess changes in lipid profiles in patients with SLE and SS. By analyzing whole blood and plasma, the study aims to simplify the lipidomic analysis, explore cellular-level lipids, and compare lipid signatures of SLE and SS with healthy controls, enhancing understanding of these AID. Our findings showed variations in the lipid profile of SLE and SS, particularly in sphingomyelins (SM), ceramides (Cer), phosphatidylserines (PS), and phospholipid species bearing polyunsaturated fatty acids (PUFAs). SM and Cer molecular species showed significant increases in plasma samples from SS patients, suggesting an atherosclerotic profile and potentially serving as future lipid biomarkers. PS species in whole blood from SLE patients exhibited elevated levels supporting previously reported dysregulated processes of cell death and defective clearance of dying cells in this AID. Moreover, decreased phospholipids bearing PUFA were observed, potentially attributed to the degradation of these species through lipid peroxidation processes. This observation is consistent with the increased oxidative stress environment associated with persistent inflammatory states in SLE and SS. Further studies are needed to better understand the role of the plasticity of lipids in the pathological mechanisms underlying SLE and SS.

Keywords: Systemic Lupus Erythematosus; Systemic Sclerosis; Lipid metabolism; Lipidomic signature; Autoimmune diseases; Lipidomics; Mass spectrometry

1. Introduction

Autoimmune diseases (AID) are a heterogeneous group of conditions in which the immune system attacks the body´s tissues and organs without an apparent trigger[1]. Systemic AID are characterized by the presence of autoantigens that are distributed throughout the body, leading to the involvement of multiple organs and tissues[2]. Systemic lupus erythematosus (SLE) and systemic sclerosis (SS) are two of the most prevalent AID worldwide, with reported prevalence rates of 43.7 per 100 000[3] and 17.6 per 100 000 individuals[4], respectively.

In SLE, pathogenic autoantibodies are generated by dysfunctional immunocompetent cells, including T cells, B cells, and dendritic cells, which are distributed throughout the body[5,6]. This chronic and debilitating disease is characterized by systemic inflammation in multiple organs, and its primary clinical features include fatigue and musculoskeletal symptoms[7]. SLE is more prevalent in women, with a female-to-male ratio of 9:1. Diagnosis of SLE is a complex process that involves the use of the Systemic Lupus International Collaborating Clinics (SLICC) classification criteria, which encompasses a set of immunological and clinical criteria that the patient must meet to be diagnosed with SLE[8].

SS is a connective tissue AID characterized by a complex interplay of immune system activation, vasculopathy, and generalized tissue fibrosis[9]. As a systemic AID, it can affect all major organs, with vascular disease being the most common early manifestation[10]. SS is a relatively rare rheumatological disorder that is also more prevalent in women than men, with reported female-to-male ratios ranging from 3:1 to 8:1[11]. Diagnosis of SS is challenging and usually requires fulfilment of the 2013 European League Against Rheumatism (EULAR) and American College of Rheumatology (ACR) classification criteria, which include immunological and clinical signs and symptoms[12].

SLE and SS are both debilitating systemic AID that significantly impacts patients, society, and health care systems. Although they exhibit distinct clinical phenotypes, there are some pathogenic features that they share, including loss of tolerance against self-nuclear antigens, activation of plasmacytoid dendritic cells, T cells, and B cells, auto-antibody production, platelet activation, and increased tissue damage[13].

Despite the international guidelines, the diagnosis of SLE and SS can be difficult due to the low specificity and predictive value of the immunological parameters used to diagnose them[14]. Therefore, it is important to find biomarkers that can ease the diagnosing process, be used to evaluate the outcome of the therapeutics of the disease, and predict relapse episodes. Lipids have been considered promising molecules in the research of biomarkers of chronic diseases associated with inflammation. Lipids play biological functions that are related to the maintenance of cell and tissue homeostasis and have a key signalling role in inflammation and immune response. Disrupting lipid homeostasis can have a severe impact on the onset and progression of several pathologies.

There is evidence of dysregulation in lipid metabolism in patients with SLE and SS, indicating the importance of lipid regulation in the pathogenesis of these AID. In the case of SLE, some molecular lipid species, such as plasmalogens, fatty acids (FA), and oxidized phospholipids, have been reported to be altered, although results are not consistent and different studies show contradictory findings as reviewed recently[1]. FA, specifically C20:4, C20:5, and C22:6, are either increased or decreased depending on the study and type of sample[15–18]. Triglycerides (TG) also display dissimilar behaviour based on the esterified FA. TG endowed with C18:2 fatty acyl moieties were decreased in the serum of SLE patients, while C22:6 TG were increased[19]. Regarding phospholipids (PL), lysophosphatidylethanolamine (LPE) with C20:4 and C22:6[19], phosphatidylethanolamine (PE) species with C18:2 and C22:6 and phosphatidylinositol (PI) species with C18:2[20] were increased in SLE. In contrast, PE with C20:419,20, phosphatidylcholine (PC) with C18:0 and C18:2[19], PI with C20:4 and lysophosphatidylcholine (LPC) with C18:2[20] were significantly reduced in these patients. Sphingomyelins (SM) with N18:1 and N18:0 and ceramides with N24:1 were significantly increased in SLE serum, while ceramides with N22:0-N24:0 (with hydroxyl groups) were found to be reduced[20]. As for SS, there are limited studies on lipid alterations. Nevertheless, increased serum levels of lysophosphatidic acid (20:4) and sphingosine 1-phosphate have been reported[21]. PC plasmalogen species and SM were found to be significantly increased in the plasma of SS patients, while PE plasmalogen species were significantly reduced[22]. The profiles of plasma FA

and acylcarnitine (CAR) are also altered, with reported increases of FA C12:0, C14:0 and C20:0, CAR and CAR 5:0, and reduction in CAR 8:0 and CAR 16:0[23]. Other lipid molecules characteristic of inflammatory and oxidative stress conditions, such as leukotrienes and isoprostanes, have also been found to be elevated in both diseases. Leukotriene B4[24] and cysteinyl leukotriene[25] were found to be elevated in the serum and exhaled breath condensate of patients with SLE and SS, respectively. Isoprostanes, such as F2-isoprostane and 8-isoprostane, also had increased concentrations in both diseases[26–28].

It is crucial to improve the screening methodologies for evaluating changes in the lipid profile of SLE and SS due to the contradictory or limited results and investigations. To this aim, lipidomics represents the best methodological tool for studying the lipidome of AID and its modifications, enabling the identification of potential disease biomarkers. The identification of the lipid profile and its variations at the molecular level is accomplished using high-throughput lipidomic techniques and can be used to identify lipid biomarkers, which provide an understanding of the contribution of lipids to disease development and its molecular mechanisms. This clinical lipidomic information could be useful and contribute to the study of chronic diseases such as AID[29,30].

In this study, our objective was to comprehensively assess and compare the changes in the lipid profile of patients with Systemic Lupus Erythematosus (SLE) and Systemic Sclerosis (SS) by using an untargeted C18 RP-LC-MS lipidomic approach in both whole blood and plasma. We aimed to simplify the lipidomic analysis in clinical settings by analysing whole blood, eliminating the need for centrifugation to collect the plasma, and to determine whether lipids at the cellular level experienced any changes. Plasma samples were also analysed as they are the most commonly used fluid in research. The lipidomic signatures of both AID were then compared with those of healthy controls.

2. Materials and methods

2.1 Reagents

To perform the lipid extraction by Methyl tert-butyl ether (MTBE) method, methanol (MeOH) was acquired from Fisher Scientific (Leicestershire, UK) and MTBE was obtained from Merck KgaA (Germany). To quantify the PL in each sample, dichloromethane (CH_2Cl_2) was purchased from Fisher Scientific, 70% perchloric acid was obtained from Chem-Lab NV (Zedelgem, Belgium), $NaH_2PO_4 \bullet 2H_2O$ was purchased from Riedell-de Haën (Seelze, Germany), ammonium molybdate (NaMoO4·H2O) was acquired from Panreac (Barcelona, Spain) and the L(+)-ascorbic acid from VWR Chemicals (Leuven, Belgium). Internal standards of PL 1,2-dimyristoyl-sn-glycero-3-phosphocholine (dMPC, PC 14:0/14:0), 1,2-dimyristoyl-*sn*-glycero-3-phosphoethanolamine (dMPE, PE 14:0/14:0), 1,2-dimyristoyl-*sn*-glycero-3-phospho-(10-rac-)glycerol (dMPG, PG 14:0/14:0), 1,2-dimyristoyl-*sn*-glycero-3-phospho-L-serine (dMPS, PS 14:0/14:0), tetramyristoylcardiolipin (TMCL, CL 14:0/14:0/14:0/14:0), 1,2-dipalmitoyl-*sn*-glycero-3-phosphatidylinositol (dPPI, PI 16:0/16:0), N-heptadecanoyl-D-erythro-sphingosylphosphorylcholine (SM d18:1/17:0), N-heptadecanoyl-D-erythro-sphingosine (Cer d18:1/17:0), 1-nonadecanoyl-2-hydroxy-$_{sn}$-glycero-3-phosphocholine (LPC 19:0) and 1,2-dimyristoyl-$_{sn}$-glycero-3-phosphate (dMPA, PA 14:0/14:0) for RP-LC-MS analysis were obtained from Avanti® Polar Lipids, Inc (Alabaster, AI, EUA). Solvents for LC-MS were acetonitrile (ACN), MeOH, isopropanol (Fisher Scientific), Milli-Q water, and CH_2Cl_2. All solvents were of high-performance liquid chromatography (HPLC) grade and were used without any additional purification. Ammonium acetate (Sigma-Aldrich) was also used for LC-MS. Milli-Q water was used for all experiments, filtered through a 0.22 mm filter and obtained using a Milli-Q Millipore system (Synergy®, Millipore Corporation, Billerica, MA, USA).

2.2 Whole blood/plasma samples

Whole blood and plasma samples were obtained from individuals diagnosed with systemic lupus erythematosus (SLE) and Systemic sclerosis (SS) at Centro Hospitalar e

Universitário de Coimbra (CHUC). The inclusion criteria for SLE and SS patients (n=11 for SLE, n=10 for SS) were based on clinical and biochemical criteria according to the Systemic Lupus International Collaborating Clinics (SLICC) classification criteria (for SLE)[8] and the 2013 European League Against Rheumatism/American College of Rheumatology (EULAR/ACR) classification criteria (for SS)[12]. Exclusion criteria included active infections, local or systemic diseases affecting the immune system, pregnancy, corticosteroid use, and relapse phases. Healthy control volunteers (n=10) were carefully selected to ensure their overall health status, absence of active infections, AID, immunomodulatory drug treatment, and lipoprotein profiles within the reference range. Age and gender were matched between the control group and the patient groups. The study protocol was approved by the Ethics Committees of both CHUC. Following collection, whole blood and plasma samples were stored at -80°C until subsequent analysis of the lipid profile.

2.3 Lipid extraction

The MTBE method was used to separate the lipids from whole blood/plasma samples31. Briefly, 200 µL of the samples were transferred to a glass tube to which was added 750 µL of cold MeOH. Each tube was vortex for 20 s and sonicate for 10 min in ice. Then, 2.5 mL of cold MTBE was added and the tubes were incubated for 30 min in ice, under stiring (75 rpm) with vortex every 5 min. After the 30 min incubation, 625 µL of milli-Q water were added to each tube, vortex for 20 s and incubated again for 10 min in ice at 75 rpm. Finally, the extracts were centrifuged at 2000 rpm for 10 min and the upper phase (lipids) was collected into a new glass tube. The extracts were dried under a nitrogen stream. The extracts were then filtered by dissolving them into 400 µL of CH_2Cl_2 and transferring them into a HAMILTON glass syringe with a filter (low protein binding hydrophilic LCR Membrane for clarification of aqueous and organic solutions). The filtered samples were collected in vials, dried under a stream of nitrogen, and stored at -80ºC.

2.4 Phospholipid quantification by phosphorous measurement

The quantification of the total PL recovered after extraction was carried out according to the method of Bartlett & Lewis[32]. The detailed experimental procedures have been previously described by Ferreira *et al*[33]. The PL extracts were dissolved in 200 µL of dichloromethane, and a volume of 10 µL was transferred, in duplicate, to a glass tube, previously washed with 5% nitric acid. The solvent was dried under a stream of nitrogen and a volume of 125 µL of 70 % perchloric acid was added to each tube. The samples were incubated in a heat block (Stuart, U.K.) for 1h at 180°C. After cooling to room temperature, a volume of 825 µL of Milli-Q water, 125 µL of 2.5% ammonium molybdate (2.5 g/ 100 mL of Milli-Q water), and 125 µL of 10% ascorbic acid (0.1 g/1 mL of Milli-Q water) were added to each sample, with a vortex mixing between each addition. The samples were then incubated in a 100°C water bath for 10 min. Then the samples were immediately cooled in a cold-water bath. Phosphate standards of 0.1 to 2 µg of phosphorus (P) were prepared from sodium dihydrogen phosphate dihydrate ($NaH_2PO_4 \bullet 2H_2O$, 100 µg/mL of P). The standards underwent the same experimental procedure as the samples without the heat block step. Absorbance was measured at 797 nm in a Multiskan GO 1.00.38 Microplate Spectrophotometer (Thermo Scientific, Hudson, NH, USA) controlled by SkanIT software version 3.2 (Thermo Scientific™). The amount of P present in each sample was calculated by linear regression. For each lipid extract, the amount of total PL was calculated by multiplying the amount of phosphorus by 25.

2.5 Lipid extract analysis by C18 Reverse-phase liquid chromatography-mass spectrometry (RP-LC-MS)

2.5.1 Sample preparation

The lipid extracts obtained from whole blood/plasma samples were resuspended in dichloromethane to have a PL concentration of 1 µg PL/µL. Subsequently, in a vial with a micro-insert, 10 µL of each sample, 8 µL of a mixture of internal standards and 82 µL of isopropanol:MeOH (1:1) were added. The internal standard mixture contained 0.04 µg of phosphatidylcholine (PC, 14:0/14:0), 0.04 µg of phosphatidylethanolamine (PE, 14:0/14:0), 0.024 µg of phosphatidylglycerol (PG, 14:0/14:0), 0.08 µg of phosphatidylinositol (PI,

16:0/16:0), 0.08 µg of phosphatidylserine (PS, 14:0/14:0), 0.16 µg of phosphatidic acid (PA, 14:0/14:0), 0.04 µg of lyso-PC (LPC, 19:0), 0.04 µg of sphingomyelin (SM, d18:1/17:0), 0.08 µg of ceramide (d18:1/17:0) and 0.16 µg of cardiolipin (CL, 14:0/14:0/14:0/14:0). The initial chromatographic phase consisted of two mobile phases at a proportion of 68% of eluent A (60% acetonitrile, 40% methanol, 10 mM ammonium formate and 0.1% formic acid) and 32% of eluent B (90% isopropanol, 10% acetonitrile, 10 mM ammonium formate and 0.1% formic acid).

2.5.2 Data and statistical analysis

Lipids were separated by a C18 reverse phase column, using an Ascentis® Express 90 Å C18 HPLC column (15 cm x 2.1 mm; 2.7 µm, Supelco®) inserted into an HPLC system (Ultimate 3000 Dionex, Thermo Fisher Scientific, Bremen, Germany) with an autosampler coupled online to a Q-Exactive™ Hybrid Quadrupole-Orbitrap™ Mass Spectrometer (Thermo Fisher Scientific, Bremen, Germany).

A volume of 5 µL of each sample mixture was injected into the HPLC column, at a flow rate of 260 µL/min. The temperature of the column oven was maintained at 50 °C. Elution started with 32% of mobile phase B, and the gradient used was: 45% B (1.5 min), 52% B (4 min), 58% B (5 min), 66% B (8 min), 70% B (11 min), 85% B (14 min), 97% B (18 min, maintained for 7 min), and 32% B (25.01 min, followed by a re-equilibration period of 8 min prior next injection). The Q-Exactive™ orbitrap mass spectrometer with a heated electrospray ionization source was operated in the positive mode (electrospray voltage of 3.0 kV) and negative modes (electrospray voltage of -2.7 kV). The sheath gas flow was 35 U, the auxiliary gas was 3 U, the capillary temperature was 320 °C, the S-lenses RF was 50 U and the probe`s temperature was 300 °C. Full scans MS spectra were acquired both in positive and negative ionisation modes in an *m/z* range of 300-1600, with a resolution of 70.000, automatic gain control (AGC) target of $3x10^6$ and maximum injection time of 100 ms. For tandem MS (MS/MS) experiments, a top-10 data-dependent method was used. The top 10 most abundant precursor ions in full MS were selected to be fragmented in the collision cell HCD, with the dynamic exclusion of 30 s and an intensity threshold of $8x10^4$. The MS/MS spectra were

obtained with a resolution of 17,500; an AGC target of $1x10^5$; an isolation window of 1 *m/z*; and a maximum injection time of 100 ms. A stepped normalized collision energy™ scheme was used and ranged between 25 and 30 eV for the positive ion mode and between 20, 24 and 28 for the negative ion mode. The MS/MS spectra obtained were those combining the information obtained with the different collision energies applied to each ionization mode. Data acquisition was carried out using the Xcalibur data system (V3.3, Thermo Fisher Scientific, USA). PC, LPC and SM were analysed in the LC-MS spectra in the positive ion mode, as $[M+H]^+$ ions. The presence of the fragment ion at *m/z* 184, corresponding to the phosphocholine polar head group, in the MS/MS of $[M+H]^+$ ions allows identifying PL molecular species belonging to the PC, LPC and SM classes, which were further differentiated by the characteristic retention times. The identification of PC, LPC and SM classes was confirmed in the LC-MS spectra in the negative ion mode, as formate adducts ($[M+HCOO]^-$ ions). MS/MS spectra of $[M+HCOO]^-$ ions of these three PL classes should display the typical fragment ion at *m/z* 168 (phosphocholine polar head group minus a methyl moiety). Carboxylate anions of fatty acyl chains can also be seen for PC and LPC. PE and LPE classes were analysed in negative ion mode ($[M-H]^-$ ions). The fragment ion at *m/z* 140 (phosphoethanolamine polar head group) and the carboxylate anions of fatty acyl chains can be found in the MS/MS data from negative ion mode. PI and PS species were analysed in negative ion mode, as $[M-H]^-$ ions. The presence of the fragment ion at *m/z* 241, corresponding to the phosphoinositol polar head group, in the MS/MS of $[M-H]^-$ ions, allows the identification of PI molecular species. PS species were identified in the MS/MS of $[M-H]^-$ ions by the neutral loss of -87Da from the molecular ion. The identification of the remaining lipid species belonging to the classes of carnitines (CAR), ceramides (Cer), cholesteryl esters (CE, fragment ion at *m/z* 369), diacylglycerols (DG) and triacylglycerols (TG), was made in LC-MS spectra in the positive ion mode, as $[M+H]^+$ ions (CAR and Cer), $[M+NH_4]^+$ ions (CE) and $[M+NH_4]^+$ ions (DG and TG) respectively.

LC-MS data were processed using the Lipostar software (version 2.1.1 x64)[34]. This software was used for raw data import, peak detection, and identification. Lipid assignment and identification was made against a database created from LIPID MAPS structure database

(version December 2022), that was then fragmented using the DM Manager Module in Lipostar, according to Lipostar fragmentation rules. The raw files were imported directly and aligned using the settings according to Lange *et al*[35]. Briefly, automatic peak picking was performed with SDA smoothing level set to high and minimum S/N ratio 3. Automatic isotope clustering settings were set to 7 ppm with an RT tolerance of 0.2 min. The MS/MS filter was applied to keep only features with MS/MS spectra for identification. Lipid identification was made according to the following parameters: 5 ppm precursor ion mass tolerance and 10 ppm product ion mass tolerance. The automatic approval was performed to keep structures with a quality of 2-4 stars. The lists with the identified and approved species results were exported and we used MZmine software (v2.42)[36] to perform relative quantification.

Relative quantification was performed by exporting the peak area values to a computer spreadsheet. For data normalization, the peak areas of the extracted ion chromatograms (XIC) of the lipid precursors of each class were divided by the peak areas of the internal standards selected for the class. Missing values were replaced by 1/5 of the minimum positive values detected in the data set. Univariate and multivariate statistical analyses were performed using R version 3.5.1 in Rstudio version 1.1.4. The data sets were then normalized to the internal standard, generalized log2, and EigenMS[37]. Principal component analysis (PCA) was performed using the R libraries FactoMineR[38] and factoextra[39]. Heatmaps were created using the R package pheatmap using "Euclidean" as the clustering distance and "ward.D" as the clustering method[40]. The normality of the data was tested with the Shapiro−Wilk test. To test the significance of the differences between conditions, we used either the ANOVA or Kruskal−Wallis test, followed by Tukey's or Dunn's test, respectively, using the R package Rstatix[41]. A p-value < 0.05 was considered an indicator of statistical significance. All graphics and boxplots were created using the R package ggplot2[42].

3. Results

3.1 Characterization of the whole blood/plasma samples

We conducted a study to assess the changes in the lipid profile associated with systemic lupus erythematosus (SLE) and systemic sclerosis (SS) by analysing whole blood and plasma samples (62 samples, 31 blood and 31 plasma) from 11 SLE patients, 10 SS patients and 10 healthy control samples, as summarized in Table 1. All patients and controls were adults aged between 19 and 82 years old. A total of 90.9% in SLE and 100% of the patients in SS were female, with ages of 40.2 ± 13.7 and 54.2 ± 17.9 years, respectively.

Table 2.3-1. Demographic and clinical characteristics of patients with systemic lupus erythematosus (SLE), systemic sclerosis (SS) and controls.

	SLE (n=11)	SS (n=10)	Controls (n=10)
Age (years)*	40.2 ± 13.7	54.2 ± 17.9	65.2 ± 11.4
Sex (% women)	90.9%	100%	80%

*Values represent the mean ± standard deviation.

3.2 Lipid profile in SLE and SS patients

The lipid profile of both whole blood and plasma samples from SLE and SS patients, as well as healthy control subjects was analysed using a high-resolution C18 RP-LC-MS/MS platform. This comprehensive lipidomic analysis allowed for the identification of 246 distinct lipid species (molecular ions) in the whole blood samples and 245 lipid species in the plasma samples (Supplementary Table S1). These identified species belonged to 13 different lipid classes, namely phosphatidylcholine (PC) comprising of diacyl, alkyl-acyl and alkenyl-acyl species, lyso PC (LPC), phosphatidylethanolamine (PE) including diacyl, alkyl-acyl and alkenyl-acyl species, lyso PE (LPE), phosphatidylinositol (PI), phosphatidylserine (PS), sphingomyelin (SM), ceramide (Cer), galactosylceramide (GalCer), fatty acylcarnitine (CAR), cholesteryl ester (CE), diacylglycerol (DG) and triacylglycerol (TG). The lipid species from all classes were identified through analysis of exact mass, retention time and MS/MS spectra (Supplementary Table S1).

3.2.1 Comparison of the whole blood lipidome of SLE and SS patients versus Controls

We compared the lipid profile of patients diagnosed with SLE (n=11), SS (n=10) and health controls (n=10) using statistical analysis. Data from LC-MS analysis were analysed with principal component analysis (PCA) to visualize the clustering trends of the three experimental groups. The PCA scores plot revealed that the three groups formed three different clusters (95% confidence interval), in a two-dimensional score plot describing 28.6% of the total variance, including dimension 1 (19.7%) and dimension 2 (8.9%) (Figure 1). Control samples were scattered in the right region of the PCA plot, while SLE and SS samples were scattered in the left region with a small overlap between the two diseases. It should be noted that, after careful consideration and treatment of the statistical data, it was confirmed that the triangle at the top of the score plot belonging to SLE whole blood group is not an outlier and it falls under the 95% confidence ellipse.

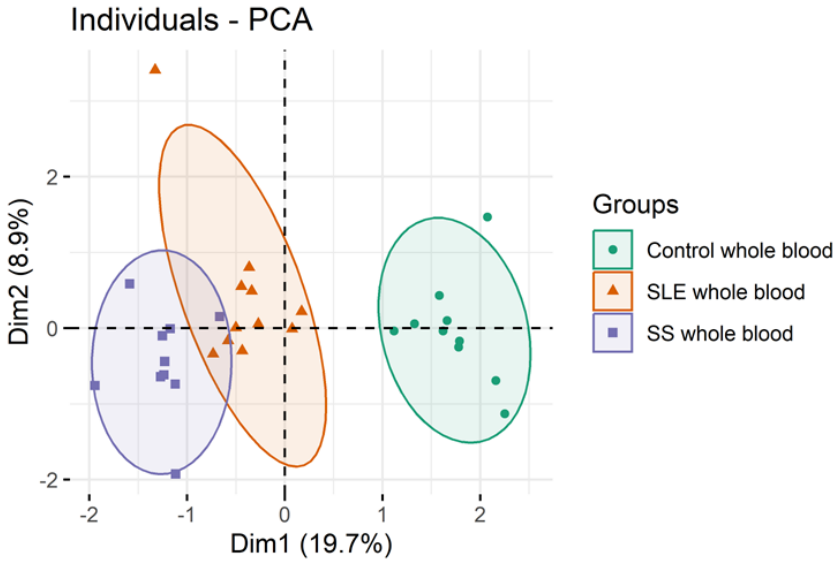

Figure 2.3-1. Two-dimensional principal component analysis (PCA) score plot generated based on the lipid profiles extracted from whole blood samples for Controls, SLE and SS patients` samples.

To test for significant differences between the three groups, univariate analysis was conducted on the LC-MS data. The analysis revealed that the 16 major contributors with the lowest *q*-value ($q<0.05$) (Figure 2) corresponded to 1 Cer, 6 PC, 1 PE, 2 ether-linked PE, 2 PS and 4 TG species. All these species showed statistically significant differences between the

groups. The 16 species include 11 PL (PC, PE and PS), 1 sphingolipid (Cer) and 4 neutral lipids (TG). Of the 16 identified species, Cer, TG and ether-linked PE exhibited increased abundances in SLE and SS compared to the control group, whereas PC species and PS(40:5) showed decreased concentrations in both diseases. PE(36:4) and PS(40:4) showed opposite behaviours in SLE and SS diseases, with significant increases in SLE and marked decreases in SS.

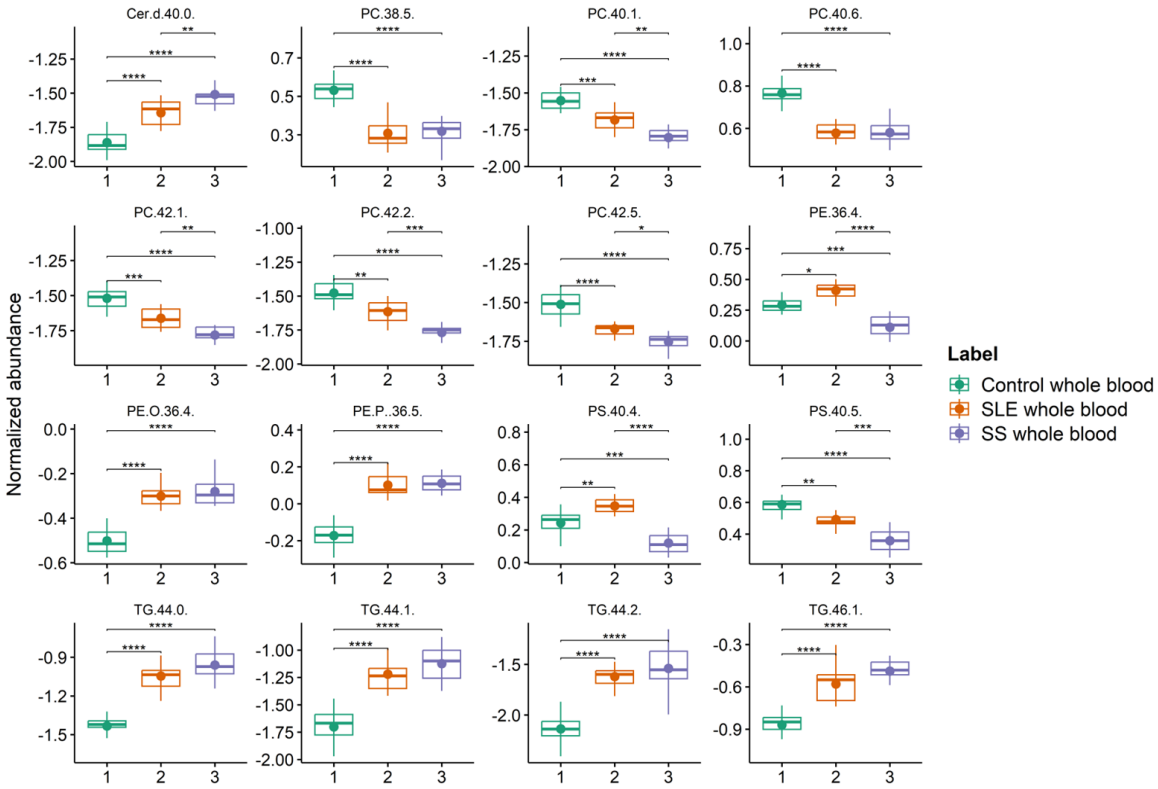

Figure 2.3-2. Box plots of the 16 most discriminative lipid species in whole blood with the lowest q-values obtained from a univariate analysis of Controls, patients with SLE and with SS using ANOVA and Tukey tests. *q < 0.05, **q < 0.01, ***q < 0.001, and ****q < 0.0001.

Lastly, a hierarchical clustering analysis (HCA) was performed on the lipid data sets from the three groups (Figure 3). The resulting heatmap depicts the top 50 lipid species with the lowest *q*-values in the ANOVA test, and a dendrogram displaying a two-dimensional hierarchical clustering of the condition (health *vs* disease) and variables that reflect the most important lipid species that differentiate SLE and SS from controls. The HCA dendrogram

(Figure 3) exhibits a clear separation between healthy and disease states in the first leaf (upper hierarchical dendrogram) where samples are clustered independently into two groups, control (green) and disease, SLE (orange) and SS (purple), while patients with SLE and SS were independently clustered in the second leaf. The clustering of individual lipid species in the second dimension shows two principal clusters in the first leaf, with species displaying a dissimilar trend depending on the disease. The first group included 13 lipid species, namely 10 TG, 1 Cer and 2 ether PE, all of which were significantly more abundant in SS, followed by SLE. The second group consisted of 37 different lipid species, which show markedly lower abundances in SS, compared to controls, and included 5 PE, 3 SM, 4 PS, 13 PC species, 6 ether species including 5 PC and 1 PE, 2 CAR, 1 LPE with essential PUFA and 3 TG species.

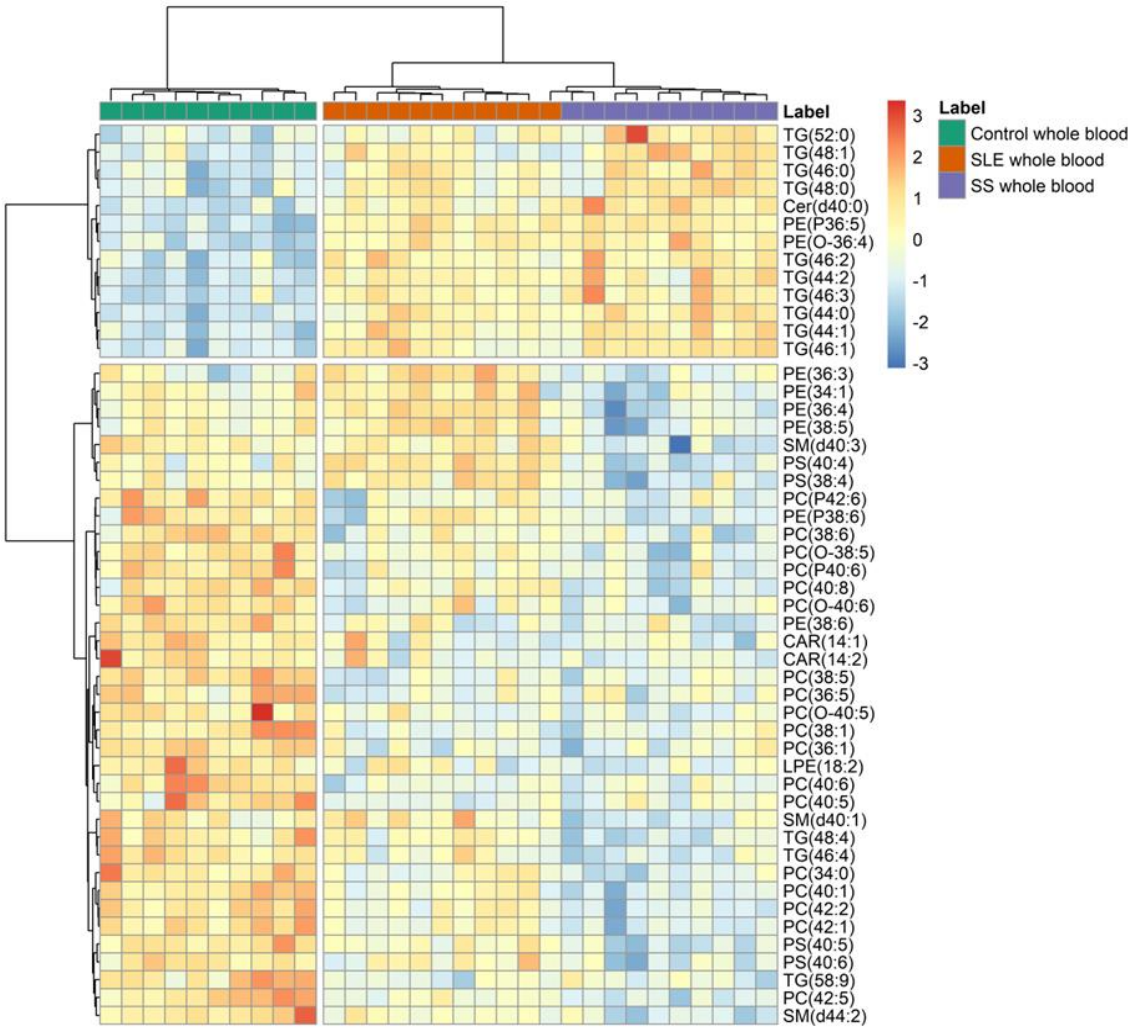

Figure 2.3-3. Two-dimensional hierarchical clustering heatmap of the 50 most discriminating lipid molecular species in whole blood of Control, SLE and SS groups. Relative abundance levels are shown on the red-yellow-blue scale, with the numbers indicating the fold difference from the overall mean. The red colour of the tile indicates high abundance and blue indicates low abundance. Null values were displayed in yellow. The clustering of the control and disease groups is represented by the dendrogram at the top. The clustering of individual lipid molecular species is represented by the dendrogram on the left.

3.2.2 Comparison of plasma lipidome from SLE/SS patients versus Controls

The plasma lipid profile was also compared to have a better understanding of the lipid alterations without the influence of the cellular components of blood. A multivariate analysis of the datasets was performed and the PCA plot generated showed a separation of the Control group from SLE and SS along the first principal component (PC1, Figure 4). The PCA plot also showed the separation of the two AID, SLE and SS along the second principal component

(PC2), although some overlapping of the 95% confidence ellipse was observed. The PCA score plot described 30.7.% of the total variance, including PC1 (18.1%) and PC2 (12.6%). Control samples were scattered in the right region of the plot while SLE and SS samples were scattered on the left region of the plot.

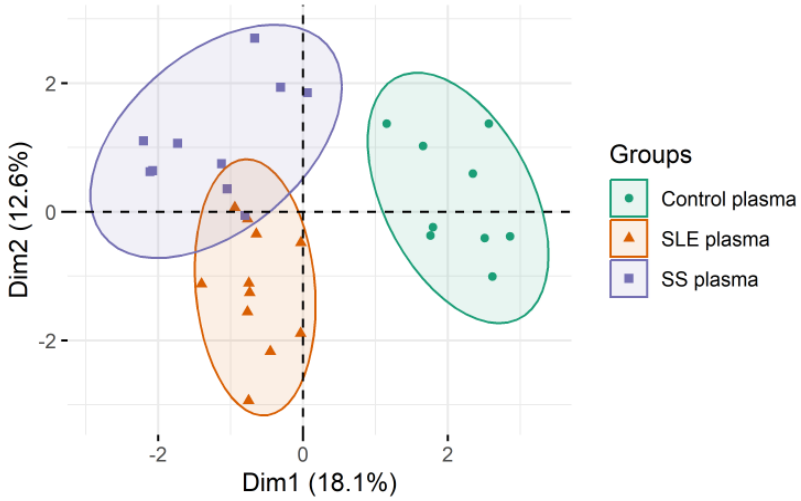

Figure 2.3-4. Two-dimensional principal component analysis (PCA) score plot generated based on the lipid profiles obtained in both positive and negative modes from plasma lipidome for Controls, SLE and SS patients` samples.

Also, a univariate analysis (ANOVA test followed by Tukey test) was performed on the RP-LC-MS data, to test for significant differences between the three conditions. The main 16 contributors with the lowest *q*-value (with $q<0.05$) were selected (Figure 5) corresponding to 6 Cer, 1 PC, 1 ether PE and 8 SM species, all statistically different. The 16 species include 2 PL (PC and PE), 8 sphingolipids (SM) and 6 sphingolipids (Cer). From these identified species, Cer and SM were significantly higher in SS patients and lower in SLE regarding control while ether PC and ether PE plasmalogen showed reduced abundances in both SLE and SS.

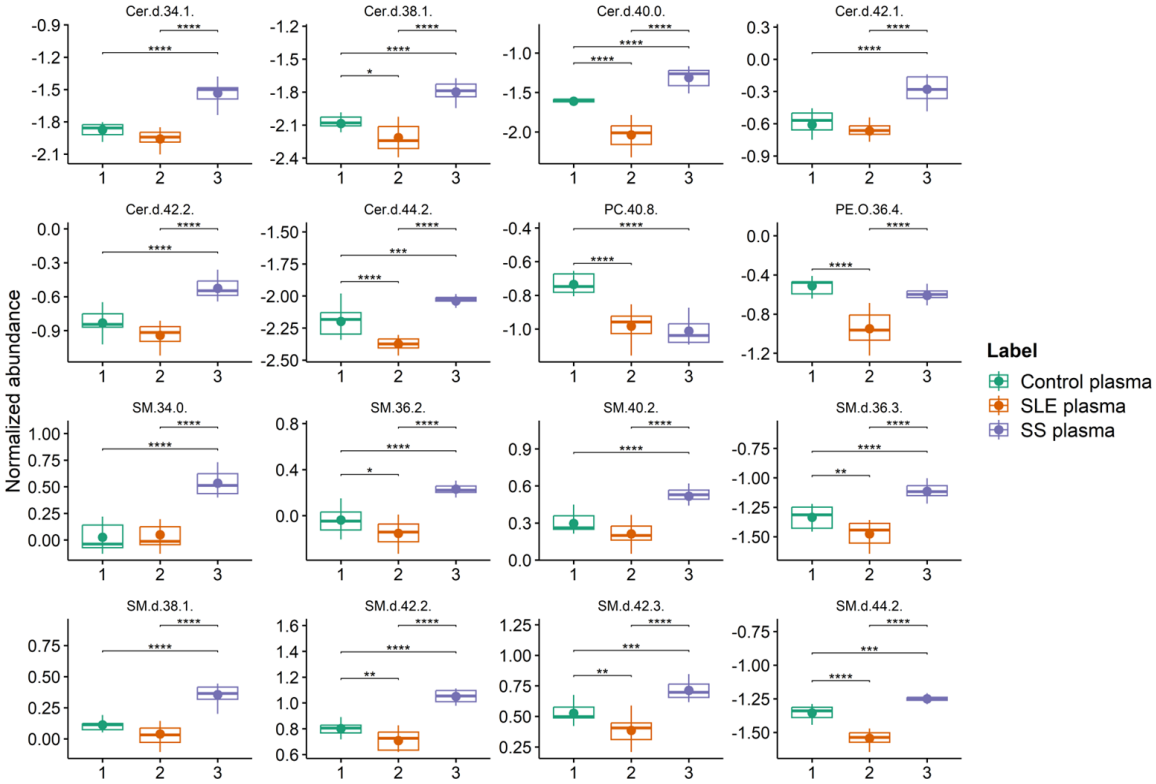

Figure 2.3-5. Box plots of lipid molecular species in plasma with the lowest 16 q-values of the Anova test followed by the Tukey test of Control, SLE and SS groups. *q < 0.05, ** q < 0.01, ***q < 0.001, and ****q < 0.0001.

Finally, HCA analysis of the plasma data set was used to create a heatmap of the top 50 lipid species with the lowest *q*-values. The dendrogram with two-dimensional hierarchical clustering of condition (health *vs* disease) and variables (Figure 6) shows the most important lipid species contributing to differentiate SLE and SS from Control samples. It is possible to observe that in the first dimension, in the top hierarchical dendrogram, the samples are clustered independently into two groups, being the Control group (green) clustered with SLE (orange). The clustering of Controls and SLE samples was not expected. In the second dimension, there are two principal clusters: the first which included 3 LPC, 2 CAR, 1 TG, 10 PC, 1 ether-linked PE, 3 ether-linked PC and 1 PS that are all more abundant in the Control group and less abundant in the disease groups, while the second cluster contains different sphingolipids(SM and Cer) and neutral lipid species which are significantly more abundant in the SS group comparing with SLE and the Control group, including 5 TG, 14 SM, 9 Cer and 1 GalCer species.

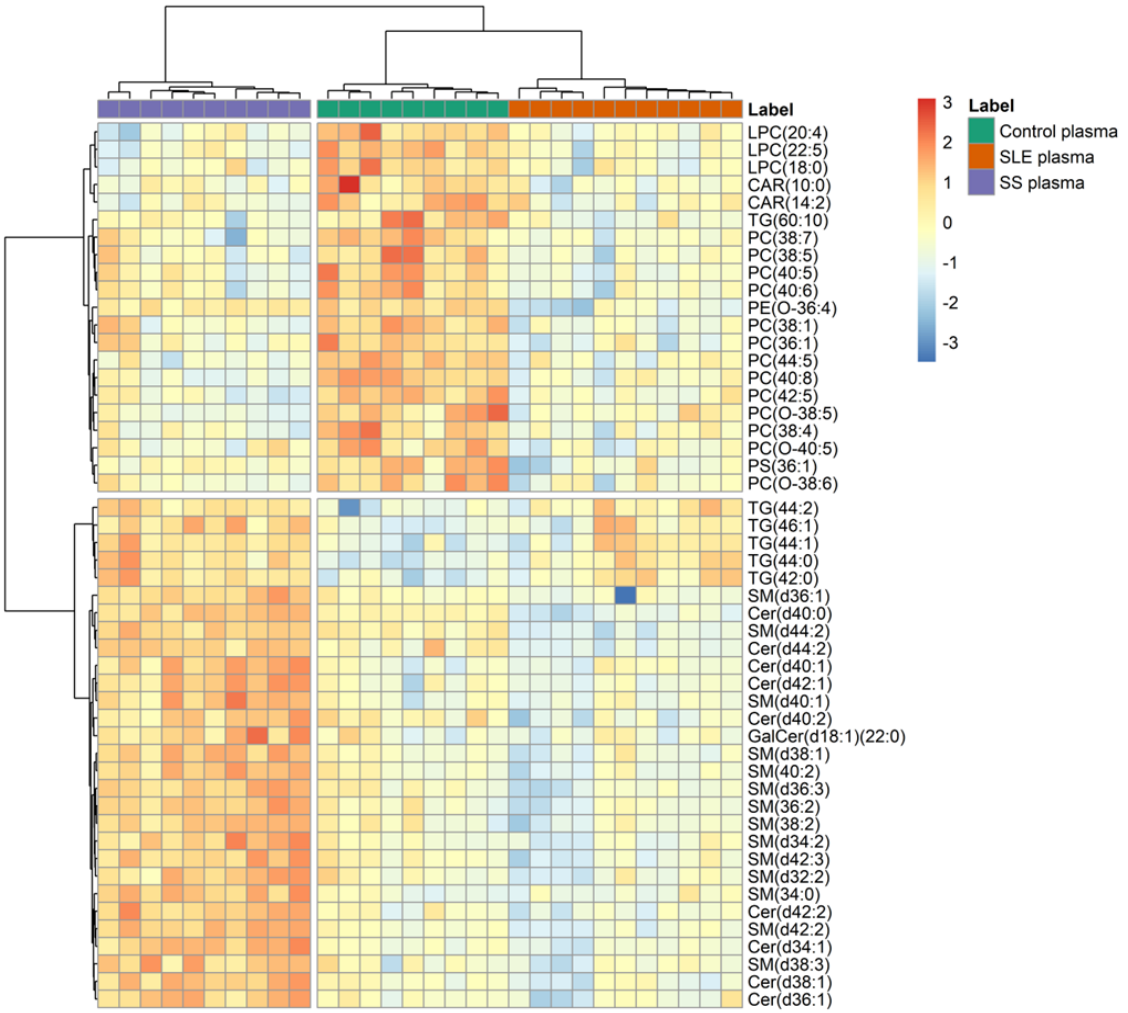

Figure 2.3-6. Two-dimensional hierarchical clustering heat map of the 50 most discriminating lipid molecular species of the Control, SLE and SS groups. Relative abundance levels are shown on the red-yellow-blue scale, with the numbers indicating the fold difference from the overall mean. The red colour of the tile indicates high abundance and blue indicates low abundance. Null values were displayed in yellow. The clustering of the Control, SLE and SS groups is represented by the dendrogram at the top. The clustering of individual lipid molecular species is represented by the dendrogram on the left.

4. Discussion

Clinical lipidomics is an emerging scientific discipline that seeks to merge the field of lipidomics with clinical medicine through the comprehensive analysis of an extensive range of lipid molecular species present in biological patient samples, such as plasma and whole blood. This approach aims to elucidate the underlying mechanisms of pathological conditions and identify potential biomarkers for diagnosis, prognosis, and therapeutics[30]. Although the

application of clinical lipidomics in AID remains limited, there is already some available information regarding lipid alterations in SLE and SS, however showing some dissimilar results. Nonetheless, further research on this subject is urgently needed.

One of the primary objectives of clinical lipidomics is to establish standardized and harmonized protocols to ensure consistent results across different studies. Accordingly, the primary goal of this investigation was to gain a better understanding of the lipid profile alterations occurring in both whole blood and plasma samples from patients with SLE and SS. By employing identical protocols, we aimed to shed light on potential discriminatory lipid markers. Analysis of whole blood samples served two purposes: firstly, to evaluate lipid variations at the cellular level and, secondly, to avoid the need for centrifugation to collect plasma, thereby facilitating lipidomic analysis in clinical settings. Moreover, this approach could potentially lead to future applications of whole blood analysis using dried blood spots. Nevertheless, we also analysed plasma samples, as they represent the most commonly studied biofluid in lipidomic investigations and are routinely utilized in clinical settings for biochemical analyses.

Within our study cohort, it is noteworthy that 90.9% and 100% of SLE and SS patients, respectively, were of the female gender, thus corroborating the well-established notion that these diseases predominantly affect females[43,44]. The average age of the patients was 40.2 ± 13.7 years for SLE and 54.2 ± 17.9 years for SS. To analyse the lipidomics data, we employed multivariate principal component analysis (PCA) in addition to univariate and hierarchical cluster analysis (HCA) for visualization and interpretation of the results. Examination of the PCA score plots (Figure 1 and Figure 4) revealed that the three conditions are similarly clustered. In both cases, plasma and blood samples differ from controls. However, it should be noted that the lipid profiles of SLE and SS exhibit partial overlap, as evidenced by the partial intersection of the 95% confidence ellipses in the PCA score plots (Figure 1 and Figure 4). This partial overlap can be attributed to the inherent biological heterogeneity associated with human samples as well as the inflammatory conditions characteristic of AID diseases.

The application of univariate and hierarchical cluster analysis (HCA) provided insights into the specific lipid species that exhibit distinct modulation in AID. In the analysis of whole blood samples, the phosphatidylcholine (PC) class displayed the highest number of discriminant species among the top 50 discriminant ones. This class comprised 18 species, predominantly diacyl species with polyunsaturated fatty acids (PUFAs) (7 out of 13 species) and 5 ether-linked species, all of which were significantly reduced in both SLE and SS compared to the control group (Figure 3). However, the decrease in these species was more pronounced in SS patients than in SLE patients. Notably, PC(40:1), PC(42:1), PC(42:2), and PC(42:5) species exhibited statistically significant differences among the three groups (Controls vs SLE, Controls vs SS, and SLE vs SS) according to univariate analysis of blood samples, while only PC(38:5) and PC(40:6) showed statistically significant differences between Controls vs SLE and Controls vs. SS (Figure 2).

Interestingly, in plasma samples, the PC class was the second most discriminatory in both AID groups, contributing with 10 diacyl species and 3 plasmanyl (-O) species. Like the findings in blood samples, all these PC species were significantly reduced in both AID conditions (SLE and SS) (Figure 6). However, only PC(40:8) showed statistically significant differences between Controls vs SLE and Controls vs SS (Figure 5).

Several lipid species demonstrated similar trends in both AID conditions, regardless of the type of sample analysed (plasma or whole blood). PC(38:1) was consistently found to be significantly reduced in SLE and SS in both whole blood and plasma analyses. This lipid species has been previously reported as decreased in a lipidomic study of multiple sclerosis[33], suggesting that PC(38:1) holds promise as a potential biomarker for AID in general. PC(38:4), PC(38:5), PC(38:6), and PC(36:5) were identified as containing C18:2, an essential fatty acid, and exhibited marked reductions in both SS and SLE (in plasma and whole blood). It should be noted that the majority of these discriminatory PC species contain long-chain PUFAs. This observation may indicate alterations in the incorporation of these fatty acids into cellular membranes, deficiencies in the elongation process, or degradation due to oxidative modifications, as increased oxidative stress has been reported in both diseases[5,45,46]. Reactive

oxygen species (ROS) generated under conditions of oxidative stress can attack unsaturated lipid species, leading to lipid peroxidation of PUFAs and also the formation of potentially toxic aldehydes[47]. Oxidative stress may also account for the reduction in ether PC species in both types of samples and in both AID. Ether-linked species, including plasmanyl (-O) and plasmenyl (-P) species, constitute a significant proportion (20%) of total PL content in mammals and are considered crucial endogenous antioxidants, playing a pivotal role in cellular antioxidant defence mechanisms[48]. Therefore, their reduction in SLE and SS may also serve as an indicator of an increased oxidative environment in these pathologies[49–52]. Aging, stress, and inflammatory stimuli have been shown to decrease the content of ether-linked species in cells. Conversely, the addition of these species to cells has been found to inhibit the development of inflammatory processes. Thus, the reduction of ether-linked species may be considered a potential risk factor for inflammatory diseases such as SLE and SS[48].

Triglycerides (TGs) are circulating lipids and serve as the primary source of energy for the body[53]. In the analysis of blood samples, TGs emerged as the second most discriminant lipid class in whole blood, comprising 13 species (Figure 3), each exhibiting distinct behaviour. Ten TG species demonstrated significantly higher levels in both SLE and SS compared to the control group, with SS patients showing the most elevated values. Among these species, only TG(44:0), TG(44:1), TG(44:2), and TG(46:1) exhibited statistically significant differences between the groups Controls vs SLE and Controls vs SS (Figure 2). On the other hand, three TG species containing PUFAs were significantly reduced in both SLE and SS groups, with the lowest values observed in SS samples. Similarly, TG species in plasma samples were found to be significantly increased in both SLE and SS groups. These results align with the findings regarding PC species bearing PUFAs, which were also found to be reduced in SLE and SS, particularly in SS. SLE patients often experience dyslipoproteinemia, characterized by low levels of HDL cholesterol and elevated levels of VLDL cholesterol and TGs[54]. Therefore, the elevated levels of TGs observed in SLE patients in this study are consistent with previously reported findings[1,19,54]. Although there is no consensus on TG levels in SS, another study has reported higher levels of TGs in the plasma of SS patients[55].

The phosphatidylethanolamine (PE) class, which is the second most abundant in cellular membranes, contributed eight species to the differentiation of the three groups in the whole blood analysis, including three ether-linked species. PE(P-36:5) and PE(O-36:4) were found to be significantly elevated in SS patients, followed by SLE patients, compared to the control group. Conversely, PE(P-38:6) exhibited the lowest relative abundances in SS patients, followed by SLE patients, when compared to healthy volunteers. Both PE(P-36:5) and PE(O-36:4) were considered statistically significant (Figure 2) in differentiating the control group from the SLE and SS groups. In the analysis of plasma samples, PE(O-36:4) was found to have significantly lower levels in SLE patients, followed by SS patients, compared to the control group. These findings indicate opposing trends for this plasmanyl species in blood and plasma samples, which supports the hypothesis of an altered antioxidant defence system in SLE and SS patients. Further investigation is necessary to understand this contrasting behaviour across different sample matrices. Ether-linked PE species, except for PE(P-38:6), displayed the opposite behaviour to ether-linked PC species. Ether-linked PC and PE species are in the outer and inner leaflets of the cell membrane, respectively, and have distinct functions[48]. However, it is currently unknown whether plasmanyl and plasmenyl lipids serve different functions. It was also found from the results gathered in this work that diacyl species of PE exhibited varying behaviours in blood samples depending on the disease. They were significantly increased in SLE and reduced in SS when compared to the control group, suggesting that these diacyl species, along with PE(P-36:5) and PE(O-36:4), could serve as discriminatory markers for SS. Meanwhile, PE(38:6) showed marked reduction in both AID conditions. Among the three groups (Controls vs SLE, Controls vs SS, and SLE vs SS), only PE(36:4) exhibited statistically significant differences (Figure 2).

The PE species PE(36:3), PE(36:4), PE(38:5), and PE(38:6) were identified as containing linoleic acid (C18:2), and their decrease in the SS group supports the findings of a few PC species, which were also found to have C18:2 esterified and were markedly reduced in SS, and their reduction can also be associated with increased oxidative stress in AID. PE species serve as important structural phospholipids (PL) and potentially contribute to the immune response by

modulating CD300 receptors in chronic inflammatory diseases, such as autoimmune diseases (AID). However, the exact function of receptors in this family, which may induce up or downregulation of immune responses, remains unclear[56].

Lysophospholipids (Lyso PL) are significant signalling lipids in the inflammatory cascade and cellular processes such as plasma membrane remodelling, cell growth, and cell death[57]. These lipids are derived from the hydrolysis of their diacyl precursors through the action of phospholipases. Lyso phosphatidylcholine (PC) species are derived from PC, and this PL class plays a crucial role in the development of various diseases, including AID[58,59]. The LPC class also distinguished the three groups based on three species: LPC(20:4), LPC(22:5), and LPC(18:0), which were found to be significantly reduced in the plasma of patients with SLE and SS. LPC species containing PUFA are known to exhibit anti-atherogenic properties as they modulate the inflammatory response triggered by LPC species with saturated or monounsaturated fatty acids[60]. LPC species with PUFA are considered anti-inflammatory60, hence their decrease in SLE and SS patients is likely associated with an enhanced inflammatory state in these AID. Furthermore, this finding aligns with the atherogenic lipoprotein profile characteristic of SLE[54]. LPE(18:2) also displayed significantly lower relative abundances in both AID. The reduction of this lipid coincides with the decrease of C18:2, which has been reported for PC and PE classes and may be associated with impaired cellular processes.

Phosphatidylserines (PS) represent the most abundant negatively charged PL in the inner leaflet of the bilayer cellular membrane[61]. In both blood and plasma samples, PS levels were significantly reduced in SS and followed by SLE when compared to the Control group. Consistent with the findings for PC species, these PS species contain long-chain PUFA, suggesting a possible impairment in the metabolism of these fatty acids or an increase in fatty acid oxidation. The slight but noticeable increase in PS(40:4) and PS(38:4) in blood samples of SLE compared to Controls may indicate an elevation in cell apoptosis. Apoptotic cells express "eat me" signals, including the exposure of PS and PE lipid species on the outer leaflet of the membrane[62]. The exposure of PS on the cell surface serves as a critical signal for efferocytosis and apoptosis and correlates with other major indicators of dying cells[63].

Sphingomyelins (SM) are predominantly located in plasma membranes, lipoproteins (particularly LDL), and other lipid-rich tissue structures such as myelin. This lipid class plays a crucial role in maintaining cell membrane structure and contributes to group differentiation in whole blood with three species[64]. All SM species were found to be significantly increased in the plasma of patients with SS and decreased in both SLE and Control groups (Figure 6). A similar decreasing trend was observed for SM species in both AID when analysing whole blood. Among these species, SM(d36:2), SM(d36:3), SM(d42:2), SM(d42:3), and SM(d44:2) showed statistically significant differences between the three groups: Controls vs. SS, Controls vs. SLE, and SS vs. SLE. On the other hand, SM(d34:0), SM(d40:2), and SM(d38:1) exhibited statistical differences only between Controls vs. SS and SS vs. SLE, indicating that the plasma profile of SM in SLE does not undergo significant alterations compared to Controls (Figure 5). Our findings align with the existing literature regarding the increase of SM in the plasma of SS patients[22]. Elevated levels of SM species may be associated with atherogenesis. The hydrolysis of SM into ceramides (Cer) in atherogenic lipoproteins like LDL leads to lipoprotein aggregation and fusion, resulting in the formation of large lipoprotein aggregates resembling those found in extracellular regions of atherosclerotic lesions[64]. Fernandez et al. determined that SM(d38:2) was the only SM species associated with an increased risk of future cardiovascular disease[65]. In our study, we also observed an increase in SM(d38:2). Indeed, cardiovascular involvement in SS patients is well-documented, and the risk of atherosclerotic disease is high in this pathology[10,66]. Hence, our findings support an elevated risk of atherosclerotic events in SS disease.

If the SM class is augmented, ceramides (Cer) are also expected to be increased[67]. Our results demonstrated that Cer exhibited the same behaviour as SM, with significantly higher abundances in the SS group compared to the SLE and Control groups (Figure 6). Among these Cer species, Cer(d38:1), Cer(d40:0), and Cer(d44:2) played a statistically important role in the plasma analysis to differentiate between the three groups: Controls vs. SS, Controls vs. SLE, and SS vs. SLE. However, Cer(d34:1), Cer(d42:1), and Cer(42:2) showed statistical differences only between Controls vs. SS and SS vs. SLE, indicating that, similar to the SM profile, the

profile of Cer in SLE does not undergo significant alterations compared to Controls (Figure 5). The increase in Cer species also supports the hypothesis of cellular apoptosis proposed for the observed variation of PS in SLE. Increased and accelerated apoptosis of immune cells, which is essential for the removal of apoptotic debris, has been observed in SLE patients. This may lead to inefficient clearance of dying cells and chronic exposure to intracellular autoantigens[68]. Various key immune cells in SLE patients experience accelerated apoptosis, including phagocytes (monocytes, macrophages, neutrophils, and immature dendritic cells), which are crucial for debris clearance[68].

Carnitine plays a crucial role in energy production as a vital cofactor in the transport of long-chain fatty acids (FA) into the mitochondria for oxidation and energy generation[69]. In our study, we observed a significant reduction of CAR(10:0), CAR(14:1), and CAR(14:2) in both AID, in both blood and plasma samples. Patients with SS exhibit altered lipid metabolism, including mitochondrial beta-oxidation of short-chain saturated FA, FA metabolism, beta-oxidation of very long-chain FA, and carnitine synthesis pathways[23]. The modified profile of carnitine species may be indicative of dysregulated FA oxidation[23]. Malfunctioning of FA oxidation has been reported as a major contributor to the development of renal fibrosis[70]. Both inflammation and FA oxidation promote the production of pro-inflammatory cytokines, creating a vicious circle of chronic inflammation and fibrosis in SS[71].

Analysing the top 16 species with the lowest q-values from both sample types (Figures 2 and 5), we observed that only Cer(d40:0) and PE(O-36:4) were common to both analyses, exhibiting the same variation. In whole blood samples, both species showed increased abundances in SLE and SS, while in plasma samples, the abundance of both lipid species increased in SS and decreased in SLE. These results indicate that the variation of Cer(d40:0) and PE(O-36:4) is not limited to the cellular level but also has physiological implications. In plasma samples, where cellular content does not influence the results, the variation suggests that the lipid profile is different from that of typical healthy conditions. PE(36:4) and PS(40:4) exhibited different behaviour according to the disease (increased in SLE and decreased in SS), suggesting that these species may serve as discriminatory markers for each disease.

Furthermore, our study revealed significantly lower abundances of several lipid molecular species containing polyunsaturated fatty acids (PUFA) in both AID. It has been shown that PUFA possesses immunomodulatory effects and are capable of suppressing T-cell activation and function[72]. Therefore, the decrease in PUFA levels in patients with SLE and SS may indicate increased T cell activation, which is a hallmark of AID[13]. We hypothesize that the decrease in PUFA levels could be attributed to the degradation of these species through lipid peroxidation processes, which occur in both SLE and SS due to the enhanced oxidative stress environment associated with persistent inflammation. Additionally, evidence suggests that SLE is characterized by dysregulated cell death processes and defective clearance of dying cells, as reflected in the lipid profile of blood samples by the increase in PS species, while the SM species in SS are highly suggestive of an atherosclerotic profile of the disease.

5. Conclusion

The pathology of SLE and SS exerts a significant influence on lipid metabolism, leading to marked changes in the lipid profile of affected patients. Our findings demonstrate that the lipidomic signature of SLE and SS differs significantly from that of a healthy state, particularly in terms of SM, Cer, and PL bearing PUFA species. The elevated levels of specific SM and Cer molecular species in the plasma of SS patients make them potential lipid biomarkers for the disease. Additionally, the significant variations of PC(38:1) in patients with AID suggest its potential as a plasma biomarker for AID.

This study underscores the importance of conducting further investigations using whole blood samples rather than plasma/serum, as it enables the detection of lipid alterations at the cellular level. Moreover, blood samples are more practical for clinical purposes as they do not require centrifugation, thus reducing processing time. Nevertheless, the results obtained from this study contribute valuable insights into the metabolic changes in the lipid profile associated with SLE and SS, enhancing our understanding of the underlying mechanisms of AID pathogenesis.

AUTHOR INFORMATION

Corresponding Author

Helena B. Ferreira, Chemistry Department of University of Aveiro,

Campus Universitário de Santiago, 3810-193 Aveiro, Portugal.

E-mail: helenabeatrizferreira@ua.pt

Author Contributions

The manuscript was written through contributions of all authors. All authors have given approval to the final version of the manuscript.

Acknowledgements

Thanks are due for the financial support to the University of Aveiro and to PT national funds (FCT/MCTES, Fundação para a Ciência e Tecnologia and Ministério da Ciência, Tecnologia e Ensino Superior) through the projects UIDB/50006/2020 and UIDP/50006/2020, to the research unit CESAM (UIDB/50017/2020+UIDP/50017/2020+LA/P/0094/2020) and to RNEM, Portuguese Mass Spectrometry Network (LISBOA-01-0145-FEDER-402-022125) through national funds and, where applicable, co-financed by the FEDER, within the PT2020. Helena Beatriz Ferreira thanks FCT/MCTES (Fundação para a Ciência e Tecnologia and Ministério da Ciência, Tecnologia e Ensino Superior) and ESF (European Social Fund) through NORTE 2020 (Programa Operacional Região Norte) for her PhD grant (2020.04611.BD). Inês M. S. Guerra thanks FCT/MCTES (Fundação para a Ciência e Tecnologia and Ministério da Ciência, Tecnologia e Ensino Superior) and ESF (European Social Fund) through NORTE 2020 (Programa Operacional Região Norte) for her PhD grant (2021.04754.BD). Tânia Melo thanks FCT (Fundação para a Ciência e Tecnologia) for funding through the Scientific Employment Stimulus - Individual Call (CEECIND/01578/2020). The authors are thankful to the COST Action EpiLipidNET, CA19105 - Pan-European Network in Lipidomics and EpiLipidomics.

References

(1) Ferreira, H. B.; Pereira, A. M.; Melo, T.; Paiva, A.; Domingues, M. R. Lipidomics in Autoimmune Diseases with Main Focus on Systemic Lupus Erythematosus. J. Pharm. Biomed. Anal. 2019, 174, 386–395.

(2) Raval, P. Systemic (Non-Organ Specific) Autoimmune Disorders. In xPharm: The Comprehensive Pharmacology Reference.; Enna, S. J., Bylund., D. B., Eds.; Elsevier Inc., 2011; pp 1–6.

(3) Tian, J.; Zhang, D.; Yao, X.; Huang, Y.; Lu, Q. Global Epidemiology of Systemic Lupus Erythematosus: A Comprehensive Systematic Analysis and Modelling Study. Ann. Rheum. Dis. 2023, 82 (3), 351–356. https://doi.org/10.1136/ard-2022-223035.

(4) Bairkdar, M.; Rossides, M.; Westerlind, H.; Hesselstrand, R.; Arkema, E. V.; Holmqvist, M. Incidence and Prevalence of Systemic Sclerosis Globally: A Comprehensive Systematic Review and Meta-Analysis. Rheumatol. (United Kingdom) 2021, 60 (7), 3121–3133. https://doi.org/10.1093/rheumatology/keab190.

(5) Lee, H. T.; Wu, T. H.; Lin, C. S.; Lee, C. S.; Wei, Y. H.; Tsai, C. Y.; Chang, D. M. The Pathogenesis of Systemic Lupus Erythematosus - From the Viewpoint of Oxidative Stress and Mitochondrial Dysfunction. Mitochondrion 2016, 30, 1–7.

(6) Perl, A. Pathogenic Mechanisms in Systemic Lupus Erythematosus. Autoimmunity 2010, 43 (1), 1–6. https://doi.org/10.3109/08916930903374741.

(7) Lang, K. S.; Burow, A.; Kurrer, M.; Lang, P. A.; Recher, M. The Role of the Innate Immune Response in Autoimmune Disease. J. Autoimmun. 2007, 29 (4), 206–212.

(8) Petri, M.; Orbai, A.-M.; Alarcón, G. S.; Gordon, C.; Merrill, J. T.; Fortin, P. R.; Bruce, I. N.; Isenberg, D.; Wallace, D. J.; Nived, O.; Sturfelt, G.; Ramsey-Goldman, R.; Bae, S.-C.; Hanly, J. G.; Sánchez-Guerrero, J.; Clarke, A.; Aranow, C.; Manzi, S.; Urowitz, M.; Gladman, D.; Kalunian, K.; Costner, M.; Werth, V. P.; Zoma, A.; Bernatsky, S.; Ruiz-Irastorza, G.; Khamashta, M. A.; Jacobsen, S.; Buyon, J. P.; Maddison, P.; Dooley, M. A.; van Vollenhoven, R. F.; Ginzler, E.; Stoll, T.; Peschken, C.; Jorizzo, J. L.; Callen, J. P.; Lim, S. S.; Fessler, B. J.; Inanc, M.; Kamen, D. L.; Rahman, A.; Steinsson, K.; Franks, A. G.; Sigler, L.; Hameed, S.; Fang, H.; Pham, N.; Brey, R.; Weisman, M. H.; McGwin, G.; Magder, L. S. Derivation and Validation of the Systemic Lupus International Collaborating Clinics Classification Criteria for Systemic Lupus Erythematosus. Arthritis Rheum. 2012, 64 (8), 2677–2686. https://doi.org/10.1002/art.34473.

(9) Katsumoto, T. R.; Whitfield, M. L.; Connolly, M. K. The Pathogenesis of Systemic Sclerosis. Annu. Rev. Pathol. Mech. Dis. 2011, 6 (1), 509–537. https://doi.org/10.1146/annurev-pathol-011110-130312.

(10) Hughes, M.; Herrick, A. L. Systemic Sclerosis. Br. J. Hosp. Med. 2019, 80 (9), 530–536. https://doi.org/10.12968/hmed.2019.80.9.530.

(11) Valentini, G.; Black, C. Systemic Sclerosis. Best Pract. Res. Clin. Rheumatol. 2002, 16 (5), 807–816. https://doi.org/10.1053/berh.2002.0258.

(12) van den Hoogen, F.; Khanna, D.; Fransen, J.; Johnson, S. R.; Baron, M.; Tyndall, A.; Matucci-Cerinic, M.; Naden, R. P.; Medsger, T. A.; Carreira, P. E.; Riemekasten, G.; Clements, P. J.; Denton, C. P.; Distler, O.; Allanore, Y.; Furst, D. E.; Gabrielli, A.; Mayes, M. D.; van Laar, J. M.; Seibold, J. R.; Czirjak, L.; Steen, V. D.; Inanc, M.; Kowal-Bielecka, O.; Müller-Ladner, U.; Valentini, G.; Veale, D. J.; Vonk, M. C.; Walker, U. A.; Chung, L.; Collier, D. H.; Csuka, M. E.; Fessler, B. J.; Guiducci, S.; Herrick, A.; Hsu, V. M.; Jimenez, S.; Kahaleh, B.; Merkel, P. A.; Sierakowski, S.; Silver, R. M.; Simms, R. W.; Varga, J.; Pope, J. E. 2013 Classification Criteria for Systemic Sclerosis: An American College of Rheumatology/European League Against Rheumatism Collaborative Initiative. Arthritis Rheum. 2013, 65 (11), 2737–2747. https://doi.org/10.1002/art.38098.

(13) Bruni, C.; Shirai, Y.; Kuwana, M.; Matucci-Cerinic, M. Cyclophosphamide: Similarities and Differences in the Treatment of SSc and SLE. Lupus 2019, 28 (5), 571–574. https://doi.org/10.1177/0961203319840433.

(14) Santhosh, P.; Ajithkumar, K. Anti-Nuclear Antibodies: A Practical Approach to Testing and Interpretation. J. Ski. Sex. Transm. Dis. 2020, 3, 175. https://doi.org/10.25259/JSSTD_40_2020.

(15) Aghdassi, E.; Ma, D. W. L.; Morrison, S.; Hillyer, L. M.; Clarke, S.; Gladman, D. D.; Urowitz, M. B.; Fortin, P. R. Alterations in Circulating Fatty Acid Composition in Patients with Systemic Lupus Erythematosus : A Pilot Study. J. Parenter. Enter. Nutr. 2011, 35 (2), 198–208.

(16) Clark, W. F.; Parbtani, A.; Huff, M. W.; Reid, B.; Holub, B. J.; Falardeau, P. Omega-3 Fatty Acid Dietary Supplementation in Systemic Lupus Erythematosus. Kidney Int. 1989, 36 (4), 653–660.

(17) Nakamura, N.; Kumasaka, R.; Osawa, H.; Yamabe, H.; Shirato, K.-I.; Fujita, T.; Murakami, R.-I.; Shimada, M.; Nakamura, M.; Okumura, K.; Hamazaki, K.; Hamazaki, T. Effects of Eicosapentaenoic Acids on Oxidative Stress and Plasma Fatty Acid Composition in Patients with Lupus Nephritis. In Vivo 2005, 19 (5), 879–882.

(18) Shin, T. H.; Kim, H. A.; Jung, J. Y.; Baek, W. Y.; Lee, H. S.; Park, H. J.; Min, J.; Paik, M. J.; Lee, G.; Suh, C. H. Analysis of the Free Fatty Acid Metabolome in the Plasma of Patients with Systemic Lupus Erythematosus and Fever. Metabolomics 2018, 14 (1), 1–10.

(19) Hu, C.; Zhou, J.; Yang, S.; Li, H.; Wang, C.; Fang, X.; Fan, Y.; Zhang, J.; Han, X.; Wen, C. Oxidative Stress Leads to Reduction of Plasmalogen Serving as a Novel Biomarker for Systemic Lupus Erythematosus. Free Radic. Biol. Med. 2016, 101 (July), 475–481.

(20) Lu, L.; Hu, C.; Zhao, Y.; He, L.; Zhou, J.; Li, H.; Du, Y.; Wang, Y.; Wen, C.; Han, X.; Fan, Y. Shotgun Lipidomics Revealed Altered Profiles of Serum Lipids in Systemic Lupus Erythematosus Closely Associated with Disease Activity. Biomolecules 2018, 8 (4), E105.

(21) Tokumura, A.; Carbone, L. D.; Yoshioka, Y.; Morishige, J.; Kikuchi, M.; Postlethwaite, A.; Watsky, M. A. Elevated Serum Levels of Arachidonoyl-Lysophosphatidic Acid and Sphingosine 1-Phosphate in Systemic Sclerosis. Int. J. Med. Sci. 2009, 6 (4), 168–176.

(22) Geroldinger-Simić, M.; Bögl, T.; Himmelsbach, M.; Sepp, N.; Buchberger, W. Changes in Plasma Phospholipid Metabolism Are Associated with Clinical Manifestations of Systemic Sclerosis. Diagnostics 2021, 11 (11). https://doi.org/10.3390/diagnostics11112116.

(23) Ottria, A.; Hoekstra, A. T.; Zimmermann, M.; van der Kroef, M.; Vazirpanah, N.; Cossu, M.; Chouri, E.; Rossato, M.; Beretta, L.; Tieland, R. G.; Wichers, C. G. K.; Stigter, E.; Gulersonmez, C.; Bonte-Mineur, F.; Berkers, C. R.; Radstake, T. R. D. J.; Marut, W. Fatty Acid and Carnitine Metabolism Are Dysregulated in Systemic Sclerosis Patients. Front. Immunol. 2020, 11 (May), 1–12. https://doi.org/10.3389/fimmu.2020.00822.

(24) Wu, T.; Xie, C.; Han, J.; Ye, Y.; Weiel, J.; Li, Q.; Blanco, I.; Ahn, C.; Olsen, N.; Putterman, C.; Saxena, R.; Mohan, C. Metabolic Disturbances Associated with Systemic Lupus Erythematosus. PLoS One 2012, 7, e37210.

(25) Tufvesson, E.; Bozovic, G.; Hesselstrand, R.; Bjermer, L.; Scheja, A.; Wuttge, D. M. Increased Cysteinyl-Leukotrienes and 8-Isoprostane in Exhaled Breath Condensate from Systemic Sclerosis Patients. Rheumatology 2010, 49 (12), 2322–2326. https://doi.org/10.1093/rheumatology/keq271.

(26) Jovanovic, V.; Aziz, N. A.; Lim, Y.; Poh, A. N. A.; Chan, S. J. H.; Pei, E. H. X.; Lew, F.; Shui, G.; Jenner, A.; Bowen, L.; McKinney, E.; Lyons, P.; Kemeny, M.; Smith, K.; Wenk, M.; Macary, P. Lipid Anti-Lipid Antibody Responses Correlate with Disease Activity in Systemic Lupus Erythematosus. PLoS One 2013, 8 (2), e55639.

(27) Ogawa, F.; Shimizu, K.; Muroi, E.; Hara, T.; Hasegawa, M.; Takehara, K.; Sato, S. Serum Levels of 8-Isoprostane, a Marker of Oxidative Stress, Are Elevated in Patients with Systemic Sclerosis. Rheumatology 2006, 45 (7), 815–818. https://doi.org/10.1093/rheumatology/kel012.

(28) Cracowski, J.-L.; Carpentier, P. H.; Imbert, B.; Cachot, S.; Stanke-Labesque, F.; Bessard, J.; Bessard, G. Increased Urinary F2-Isoprostanes in Systemic Sclerosis, but Not in Primary Raynaud's Phenomenon: Effect of Cold Exposure. Arthritis Rheum. 2002, 46 (5), 1319–1323. https://doi.org/10.1002/art.10261.

(29) Zhao, Y. Y.; Cheng, X. long; Lin, R. C. Lipidomics Applications for Discovering Biomarkers of Diseases in Clinical Chemistry. Int. Rev. Cell Mol. Biol. 2014, 313, 1–26.

(30) Lv, J.; Zhang, L.; Yan, F.; Wang, X. Clinical Lipidomics: A New Way to Diagnose Human Diseases. Clin. Transl. Med. 2018, 7 (1), 10–12. https://doi.org/10.1186/s40169-018-0190-9.

(31) Matyash, V.; Liebisch, G.; Kurzchalia, T. V.; Shevchenko, A.; Schwudke, D. Lipid Extraction by Methyl-Tert-Butyl Ether for High-Throughput Lipidomics. J. Lipid Res. 2008, 49 (5), 1137–1146. https://doi.org/10.1194/jlr.D700041-JLR200.

(32) Bartlett, E. M.; Lewis, D. H. Spectrophotometric Determination of Phosphate Esters in the Presence and Absence of Orthophosphate. Anal. Biochem. 1970, 36 (1), 159–167.

(33) Ferreira, H. B.; Melo, T.; Monteiro, A.; Paiva, A.; Domingues, P.; Domingues, M. R. Serum Phospholipidomics Reveals Altered Lipid Profile and Promising Biomarkers in Multiple Sclerosis. Arch. Biochem. Biophys. 2021, 697. https://doi.org/10.1016/j.abb.2020.108672.

(34) Goracci, L.; Tortorella, S.; Tiberi, P.; Pellegrino, R. M.; Di Veroli, A.; Valeri, A.; Cruciani, G. Lipostar, a Comprehensive Platform-Neutral Cheminformatics Tool for Lipidomics. Anal. Chem. 2017, 89 (11), 6257–6264. https://doi.org/10.1021/acs.analchem.7b01259.

(35) Lange, M.; Angelidou, G.; Ni, Z.; Criscuolo, A.; Schiller, J.; Blüher, M.; Fedorova, M. AdipoAtlas: A Reference Lipidome for Human White Adipose Tissue. Cell Reports Med. 2021, 2 (10), 100407. https://doi.org/10.1016/j.xcrm.2021.100407.

(36) Pluskal, T.; Castillo, S.; Villar-Briones, A.; Oresĭc, M. MZmine 2: Modular Framework for Processing, Visualizing, and Analyzing Mass Spectrometry-Based Molecular Profile Data. BMC Bioinf 2010, 11, 395.

(37) Karpievitch, Y. V.; Nikolic, S. B.; Wilson, R.; Sharman, J. E.; Edwards, L. M. Metabolomics Data Normalization with EigenMS. PLoS One 2014, 9 (12), 1–10.

(38) Le, S.; Josse, J.; Husson, F. FactoMineR: An R Package for Multivariate Analysis. J. Stat. Softw. 2008, 25 (1), 1–18.

(39) Kassambara, A.; Mundt, F. Factoextra: Extract and Visualize the Results of Multivariate Data Analyses. R Package Version 1.0.7.; 2020.

(40) Kolde, R. Kolde, R. Pheatmap: Pretty Heatmaps. R Package Version 1.0.12. pheatmap Pretty Heatmaps. R Packag. 2019, CRAN. R-pr (version 1.0.12), version 1.0.12.

(41) Kassambara A. Rstatix: Pipe-Friendly Framework for Basic Statistical Tests_. R Package Version 0.7.2, <https://CRAN.R-Project.Org/Package=rstatix>. 2023.

(42) Wickham, H. Ggplot2 – Elegant Graphics for Data Analysis., 2nd Editio.; Springer Nature, 2016.

(43) Pons-Estel, G. J.; Alarcón, G. S.; Sconfield, L.; Reinlib, L.; Cooper, G. S. Understanding the Epidemiology and Progression of Systemic Lupus Erythematosus. Semin Arthritis Rheum 2010, 39 (4), 257–268.

(44) Khan, D.; Ahmed, S. A. The Immune System Is a Natural Target for Estrogen Action: Opposing Effects of Estrogen in Two Prototypical Autoimmune Diseases. Front. Immunol. 2015, 6, 635.

(45) Doridot, L.; Jeljeli, M.; Chêne, C.; Batteux, F. Implication of Oxidative Stress in the Pathogenesis of Systemic Sclerosis via Inflammation, Autoimmunity and Fibrosis. Redox Biol. 2019, 25, 101122. https://doi.org/10.1016/j.redox.2019.101122.

(46) Shah, D.; Mahajan, N.; Sah, S.; Nath, S. K.; Paudyal, B. Oxidative Stress and Its Biomarkers in Systemic Lupus Erythematosus. J. Biomed. Sci. 2014, 21 (1), 1–13.

(47) Yadav, U. C. S. Oxidative Stress-Induced Lipid Peroxidation: Role in Inflammation. In Free Radicals in Human Health and Disease; Springer India: New Delhi, 2015; pp 119–129. https://doi.org/10.1007/978-81-322-2035-0_9.

(48) Hossain, M. S.; Mawatari, S.; Fujino, T. Biological Functions of Plasmalogens. In Peroxisome Biology: Experimental Models, Peroxisomal Disorders and Neurological Diseases; Lizard, G., Ed.; Springer Nature Switzerland AG 2020, 2020; pp 171–193. https://doi.org/10.1007/978-3-030-60204-8_13.

(49) Luoma, A. M.; Kuo, F.; Cakici, O.; Crowther, M. N.; Denninger, A. R.; Avila, R. L.; Brites, P.; Kirschner, D. A. Plasmalogen Phospholipids Protect Internodal Myelin from Oxidative Damage. Free Radic Biol Med 2015, 84, 296–310.

(50) Wallner, S.; Schmitz, G. Plasmalogens the Neglected Regulatory and Scavenging Lipid Species. Chem. Phys. Lipids 2011, 164 (6), 573–589.

(51) Zoeller, R. A.; Morand, O. H.; Raetz, C. R. A Possible Role for Plasmalogens in Protecting Animal Cells against Photosensitized Killing. J. Biol. Chem. 1988, 263, 11590–11596.

(52) Morand, O. H.; Zoeller, R. A.; Raetz, C. R. Disappearance of Plasmalogens from Membranes of Animal Cells Subjected to Photosensitized Oxidation. J. Biol. Chem. 1988, 263, 11597–11606.

(53) Robinson, J. G. Disorders of Lipid Metabolism. In Goldman-Cecil Medicine; Elsevier, 2020; Vol. 2-volume S, pp 1355-1365.e2.

(54) Reichlin, M.; Fesmire, J.; Quintero-Del-Rio, A. I.; Wolfson-Reichlin, M. Autoantibodies to Lipoprotein Lipase and Dyslipidemia in Systemic Lupus Erythematosus. Arthritis Rheum. 2002, 46, 2957–2963.

(55) Gogulska, Z.; Smolenska, Z.; Turyn, J.; Mika, A.; Zdrojewski, Z. Lipid Alterations in Systemic Sclerosis. Front. Mol. Biosci. 2021, 8 (December), 1–7. https://doi.org/10.3389/fmolb.2021.761721.

(56) Vitallé, J.; Terrén, I.; Orrantia, A.; Zenarruzabeitia, O.; Borrego, F. CD300 Receptor Family in Viral Infections. Eur. J. Immunol. 2019, 49, 364–374.

(57) Cas, M. D.; Roda, G.; Li, F.; Secundo, F. Functional Lipids in Autoimmune Inflammatory Diseases. Int. J. Mol. Sci. 2020, 21 (9), 1–19.

(58) Grossmayer, G. E.; Keppeler, H.; Boeltz, S.; Janko, C.; Rech, J.; Herrmann, M.; Lauber, K.; Muñoz, L. E. Elevated Serum Lysophosphatidylcholine in Patients with Systemic Lupus Erythematosus Impairs Phagocytosis of Necrotic Cells In Vitro. Front. Immunol. 2018, 8. https://doi.org/10.3389/fimmu.2017.01876.

(59) Liu, P.; Zhu, W.; Chen, C.; Yan, B.; Zhu, L.; Chen, X.; Peng, C. The Mechanisms of Lysophosphatidylcholine in the Development of Diseases. Life Sci. 2020, 247, 117443. https://doi.org/https://doi.org/10.1016/j.lfs.2020.117443.

(60) Akerele, O. A.; Cheema, S. K. Fatty Acyl Composition of Lysophosphatidylcholine Is Important in Atherosclerosis. Med. Hypotheses 2015, 85 (6), 754–760.

(61) Leventis, P. A.; Grinstein, S. The Distribution and Function of Phosphatidylserine in Cellular Membranes. Annu. Rev. Biophys. 2010, 39 (1), 407–427. https://doi.org/10.1146/annurev.biophys.093008.131234.

(62) Munoz, L. E.; Gaipl, U. S.; Franz, S.; Sheriff, A.; Voll, R. E.; Kalden, J. R.; Herrmann, M. SLE—a Disease of Clearance Deficiency? Rheumatology 2005, 44 (9), 1101–1107. https://doi.org/10.1093/rheumatology/keh693.

(63) Birge, R. B.; Boeltz, S.; Kumar, S.; Carlson, J.; Wanderley, J.; Calianese, D.; Barcinski, M.; Brekken, R. A.; Huang, X.; Hutchins, J. T.; Freimark, B.; Empig, C.; Mercer, J.; Schroit, A. J.; Schett, G.; Herrmann, M. Phosphatidylserine Is a Global Immunosuppressive Signal in Efferocytosis, Infectious Disease, and Cancer. Cell Death Differ. 2016, 23 (6), 962–978. https://doi.org/10.1038/cdd.2016.11.

(64) Tabas, I. Lipids and Atherosclerosis. In Biochemistry of Lipids, Lipoproteins and Membranes; Elsevier, 2008; pp 579–605. https://doi.org/10.1016/B978-044453219-0.50023-4.

(65) Fernandez, C.; Sandin, M.; Sampaio, J. L.; Almgren, P.; Narkiewicz, K.; Hoffmann, M.; Hedner, T.; Wahlstrand, B.; Simons, K.; Shevchenko, A.; James, P.; Melander, O. Plasma Lipid Composition and Risk of Developing Cardiovascular Disease. PLoS One 2013, 8 (8), e71846. https://doi.org/10.1371/journal.pone.0071846.

(66) Man, A.; Zhu, Y.; Zhang, Y.; Dubreuil, M.; Rho, Y. H.; Peloquin, C.; Simms, R. W.; Choi, H. K. The Risk of Cardiovascular Disease in Systemic Sclerosis: A Population-Based Cohort Study. Ann. Rheum. Dis. 2013, 72 (7), 1188–1193. https://doi.org/10.1136/annrheumdis-2012-202007.

(67) D'Angelo, G.; Moorthi, S.; Luberto, C. Role and Function of Sphingomyelin Biosynthesis in the Development of Cancer; Inc., E., Ed.; 2018; pp 61–96. https://doi.org/10.1016/bs.acr.2018.04.009.

(68) Mistry, P.; Kaplan, M. J. Cell Death in the Pathogenesis of Systemic Lupus Erythematosus and Lupus Nephritis. Clin. Immunol. 2017, 185, 59–73. https://doi.org/10.1016/j.clim.2016.08.010.

(69) Adeva-Andany, M. M.; Calvo-Castro, I.; Fernández-Fernández, C.; Donapetry-García, C.; Pedre-Piñeiro, A. M. Significance of L-Carnitine for Human Health. IUBMB Life 2017, 69 (8), 578–594. https://doi.org/https://doi.org/10.1002/iub.1646.

(70) Allison, S. J. Dysfunctional Fatty Acid Oxidation in Renal Fibrosis. Nat. Rev. Nephrol. 2015, 11 (2), 64–64. https://doi.org/10.1038/nrneph.2014.244.

(71) Lee, S. B.; Kalluri, R. Mechanistic Connection between Inflammation and Fibrosis. Kidney Int. 2010, 78, S22–S26. https://doi.org/10.1038/ki.2010.418.

(72) Stulnig, T. M.; Huber, J.; Leitinger, N.; Imre, E. M.; Angelisová, P.; Nowotny, P.; Waldhäusl, W. Polyunsaturated Eicosapentaenoic Acid Displaces Proteins from Membrane Rafts by Altering Raft Lipid Composition. J. Biol. Chem. 2001, 276 (40), 37335–37340.

3. CHAPTER 3: CLINICAL LIPIDOMICS, AUTOIMMUNE DISEASES AND OXIDATIVE STRESS

3.1 CHAPTER 3.1: CURRENT KNOWLEDGE ON LIPIDOMICS AND OXIDATIVE STRESS IN RHEUMATOID ARTHRITIS

This chapter was integrally published as follows.
Reprinted with permission from:

H.B. Ferreira, T. Melo, A. Paiva, M.R. Domingues, Insights in the Role of Lipids, Oxidative Stress and Inflammation in Rheumatoid Arthritis Unveiled by New Trends in Lipidomic Investigations, *Antioxidants* (2021), volume 10 (1), page 45
https://doi.org/10.3390/antiox10010045

Abstract

Rheumatoid arthritis (RA) is a highly debilitating chronic inflammatory autoimmune disease most prevalent in women. The true etiology of this disease is complex, multifactorial, and is yet to be completely elucidated. However, oxidative stress and lipid peroxidation are associated with the development and pathogenesis of RA. In this case, oxidative damage biomarkers have been found to be significantly higher in RA patients, associated with the oxidation of biomolecules and the stimulation of inflammatory responses. Lipid peroxidation is one of the major consequences of oxidative stress, with the formation of deleterious lipid hydroperoxides and electrophilic reactive lipid species. Additionally, changes in the lipoprotein profile seem to be common in RA, contributing to cardiovascular diseases and a chronic inflammatory environment. Nevertheless, changes in the lipid profile at a molecular level in RA are still poorly understood. Therefore, the goal of this review was to gather all the information regarding lipid alterations in RA analyzed by mass spectrometry. Studies on the variation of lipid profile in RA using lipidomics showed that fatty acid and phospholipid metabolisms, especially in phosphatidylcholine and phosphatidylethanolamine, are affected in this disease. These promising results could lead to the discovery of new diagnostic lipid biomarkers for early diagnosis of RA and targets for personalized medicine.

Keywords: Rheumatoid arthritis; lipidomics; mass spectrometry; biomarkers; lipid peroxidation

1. Rheumatoid Arthritis

Rheumatoid arthritis (RA) is a chronic inflammatory autoimmune disease (AID) affecting almost 1% of the population worldwide and is most prevalent in women [1]. In RA, chronic inflammation of the synovium membrane is the crucial pathologic feature, leading to progressive and irreversible joint destruction, deformity, and disability, if left untreated [2]. Increased autoantibody production is another hallmark of RA, in particular, the rheumatoid factor (RF) and the anticitrullinated protein antibodies (ACPA) [3]. Both RF and ACPA have predictive, diagnostic, and prognostic roles, since it is possible to detect these autoantibodies prior to RA onset and their presence positively correlates with disease severity and joint destruction [4,5]. However, only about 70% of RA patients produce RF or ACPA [6], thus revealing that the diagnosis of RA cannot be based solely on these biomarkers.

Besides the presence of autoantibodies, the etiology of RA is complex, multifactorial, and is yet to be completely elucidated. The main physiological characteristics of RA (joint inflammation and cartilage destruction) are the result of the infiltration of immune cells into the synovial joint lining and the associated complex network of cytokines [3,7,8]. Impaired adaptive immune responses are considered keys in RA pathogenesis. In brief, activated T helper cells release several pro-inflammatory cytokines into the synovial membrane and fluid [9]. Another set of pro-inflammatory cytokines is secreted by recently activated macrophages contributing to a self-amplifying pro-inflammatory loop. This induces the proliferation and differentiation of B cells, resulting in the production of RF and ACPA autoantibodies [3]. Fibroblasts from the synovial membrane produce matrix metalloproteinases that will destroy the cartilage and activate osteoclasts, promoting bone resorption. The release of such pro-inflammatory mediators induces protein modifications that enhance the immune response and chronic inflammation [10,11].

Additional pivotal cells for RA pathogenesis are monocytes and neutrophils. It has been suggested that an increased turnover of monocytes, migrating from the bone marrow into the inflamed synovia, occurs in RA [12]. The process of recruiting neutrophils into the synovium is a key feature of inflammatory responses in RA, and it is propelled, once more, by an intricate

network of cytokines [3]. The aforementioned pro-inflammatory cytokines released by macrophages and T cells serve as a primer of the infiltrated neutrophils. Once primed, neutrophils will foster joint destruction by inducing synthesis of proteins that can upregulate and extend neutrophil ability to secrete a large quantity of cytokines and chemokines [13,14]. Furthermore, neutrophils contribute to cartilage destruction in the synovial fluid, damage surrounding tissues, induce oxidative stress conditions due to the release of reactive oxygen species (ROS), increasing the inflammation status, and may be a source of ACPA contributing for the impaired immune response in RA [15–17].

Given the complex character of RA, it is believed that genetic and environmental factors also take part in the pathogenesis of this disease. RA susceptibility is strongly associated with major histocompatibility complex genes, and the genetic factors have a straight connection with the environmental factors [18]. The production of ACPA may be triggered by silica exposure, microbiota, infections, epigenetic modifications and environmental risk factors, specially cigarette smoking [19]. The microbiota of RA patients differs from that of the general population and is associated with the inflammatory conditions of this disease, while viral and bacterial infections contribute for the development of the autoimmune response in RA [20]. Additionally, RA has an increased heritability that is estimated to be 50% for ACPA-seronegative and 70% for ACPA-seropositive [21,22]. The expression of ACPA in RA patients is associated with the presence of shared epitope alleles (SE) which, in turn, are associated with disease severity [23]. In genetically predisposed individuals, the environmental factors have a high impact on the risk of developing RA by inducing molecular changes to proteins that trigger a loss of immunological self-tolerance [3].

Systemic effects linked to inflammation are responsible for severe physical disability of RA patients, diminishing their life quality. Impaired muscle function may be considered a hallmark of RA and several factors contribute to this process. Pro-inflammatory cytokines, as mentioned before, are highly involved in RA pathogenesis. Cytokines are responsible for low skeletal muscle function in RA patients by reducing muscle fibers contractility due to increased oxidant activity in the system [24]. Cytokines were found to be two times higher in RA patients' muscle

compared with systemic cytokines levels [25]. The chronic inflammation in RA is also involved in skeletal muscle pathology. Inflammation and insulin resistance are correlated with diminished mitochondrial function and content, thus disrupting muscle oxidative metabolic capacity and increasing levels of intramyocellular lipid content [26,27]. RA patients have an increased risk for developing insulin resistance, which is influenced by RF seropositivity, higher disease activity, prednisone use, and visceral and thigh intermuscular adiposity [24,28]. The increased accumulation of toxic lipid mediators and consequent lipotoxicity in skeletal muscles may also stimulate mitochondrial dysfunction, that, together with insulin resistance, contribute to cardiovascular disorders and sarcopenia [29]. Insulin resistance, cardiovascular disorders, and sarcopenia, associated with an increased intramuscular fat compared to healthy subjects, are frequently associated with RA [30].

Although the true etiology of this chronic inflammatory, rheumatic and immune-mediated disease remains unknown, several factors are known to contribute to the development and pathogenesis of RA, (Figure 1), namely inflammation exacerbation, oxidative stress and lipid peroxidation, as will be detailed in the following chapters.

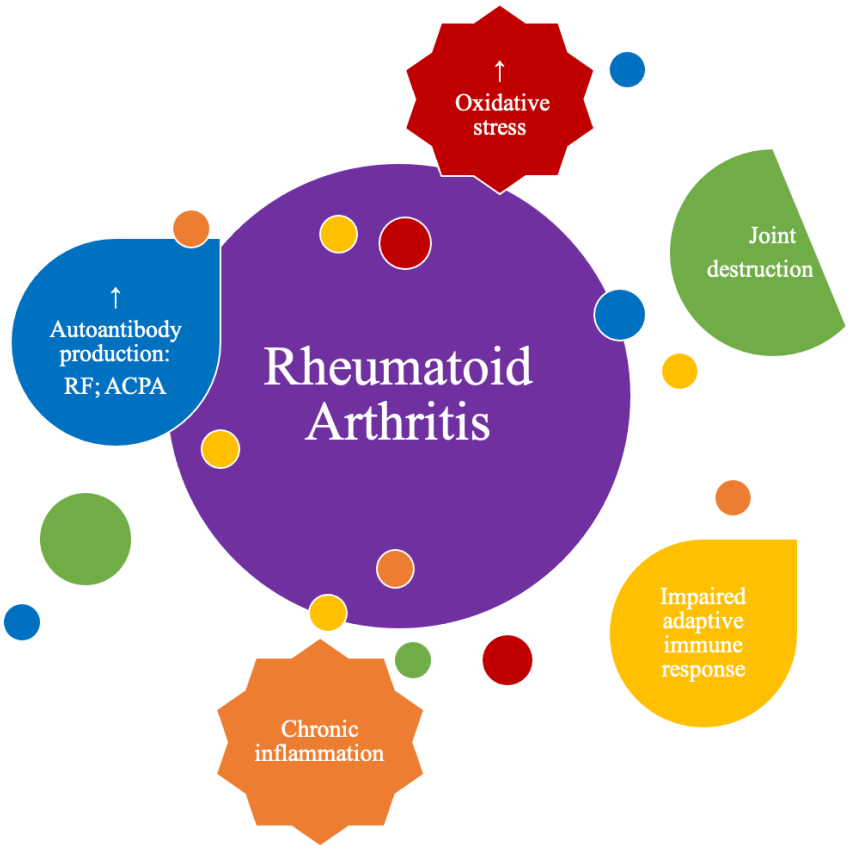

Figure 3.1-1 Main physio-pathological alterations that occur in rheumatoid arthritis (RA).

2. Oxidative Stress in Rheumatoid Arthritis

RA pathogenesis is associated with increased oxidative stress, decreased antioxidant levels, and impaired antioxidant defenses [20]. Reactive nitrogen species (RNS) and ROS have been implicated in RA pathogenesis, when they exceed physiological concentrations, especially through the damage of lipids of plasmatic membranes, proteins, and nucleic acids [31]. In fact, a fivefold increase in mitochondrial ROS production has been identified in whole blood and monocytes from RA patients, suggesting oxidative stress to be a pathogenic characteristic in RA [32].

The release of cytokines by T cells induces oxidative stress, thus antioxidants, such as glutathione, are important to reduce the oxidative status. Vitamin C and vitamin E are important non-enzymatic antioxidants essential to, for instance, immune system functions, repair body tissues and protect cell membranes from oxidative damages. However, evidence suggests that the antioxidant system in RA has been compromised. Serum vitamin C levels [33] and plasma

concentration of vitamin E [34] were significantly lower in RA patients, re-enforcing the fact that oxidative stress impairs the antioxidant system in RA. Additionally, low levels of tocopherols, β-carotene, retinols, SH groups and L-γ-glutamyl-L-cysteinylglycine have been found in RA patients along with low activity levels of glutathione reductase and superoxide dismutase [35,36]. However, these findings are not consistent in every study on enzymatic activity in RA patients. Superoxide dismutase, glutathione peroxidase, catalase, glutathione reductase, NADPH oxidase, myeloperoxidase, and arylesterase have been found to be increased, decreased or even without altered activity in different investigations (for further information, please consult the review article [32]). Nitric oxide (NO•) free radical negatively correlates with glutathione, which could be a compensatory effect of intracellular non-enzymatic antioxidative mechanisms to an increased nitrogen dioxide (NO2•) production in RA [37]. Also, the suppression of endothelial NO• synthase activity was found to be considered a characteristic of endothelial injury, leading to atherosclerosis, which is common in RA [38]. By these contradictory results, it is possible to assume that the antioxidant systems of RA patients are impaired, requiring more studies to clarify this matter.

The immune response may become abnormal due to T cell exposure to increased oxidative stress by disturbing growth and death stimuli [39]. Furthermore, neutrophils from RA produce higher quantities of neutrophil extracellular traps (NET), ROS, and RNS than healthy people [3]. NETosis, the process of NET formation, is augmented in both circulating and synovial neutrophils of RA and is linked with ACPA seropositivity and inflammatory markers. NETosis contributes to the production of ACPA, which results in pro-inflammatory molecules synthesis [16]. This way, NET may be considered a potential biomarker of RA early diagnosis because the concentration of plasma levels of cell-free nucleosomes shows high sensitivity (91%) and specificity (92%) [40,41].

DNA oxidation products, such as 8-oxo-7-hydro-deoxyguanosine, are produced due to the reaction between hydroxyl radicals and deoxyguanosine and are found in serum and lymphocytes of RA [42,43]. The levels of oxidation of uric acid were higher in RA patients as well [44]. Protein oxidation has also been reported in RA. Oxidative stress leads to an

accumulation of advanced oxidation protein products [45]. Protein oxidation markers have been found in higher concentrations in plasma and synovial fluid of RA patients and were correlated with disease progress and development [44,46–49]. Higher levels of protein carbonyls and 3-chlorotyrosine were detected in synovial fluid, and other types of RA samples, along with increased activity of myeloperoxidase, which catalyzes the reaction between hydrogen peroxide (H_2O_2) and chloride anion (Cl-) producing hypochlorous acid (HOCl) that can cause oxidative damage in the host tissue. This way, the increase of myeloperoxidase activity suggests a pronounced oxidative stress environment [44,50]. Hypochlorous acid can react with nitrite (NO^{2-}), resulting in nitrate (NO^{3+}), which was found to be increased in serum of RA patients [51]. Moreover, myeloperoxidase is known to convert low-density lipoproteins (LDL) into a foam cell forming LDL isoform and promote the formation of dysfunctional high-density lipoproteins (HDL), thus not only contributing for oxidative stress conditions but also for a dysregulated lipid metabolism and an atherogenic environment [52]. Synovial fluid is rich in hyaluronic acid (2–3 mg/mL), a glycosaminoglycan (GAG) which is a linear homopolymer of the disaccharide repeating units of [D-glucuronic acid-beta-(1-3)-N-acetyl-D-glucosamine] linked together with beta-(1-4) glycosidic linkages. Hyaluronic acid, like other GAGs and proteins, is highly reactive with ROS and RNS. The modifications of hyaluronan in synovial fluid are highly informative about the pathophysiological condition of synovial joints [53]. The balance between the superoxide anion radical and NO radical precursors, the intermediates such as H_2O_2, and the degradation products like the hydroxyl radical, determines which GAG component (i.e., hyaluronan, heparan sulphate, chondroitin sulphate) of the extracellular matrix is predominantly degraded and may be important in regulating disease processes.

This way, oxidative damage biomarkers have been consistently found to be significantly higher in RA patients than in controls in any type of sample analyzed. Altogether, it is well established that prevails an oxidative stress environment in RA, leading to biomolecules oxidation and stimulating inflammatory responses in this debilitating pathology. Lipids are biomolecules that are very susceptible to the attack of ROS and RNS under oxidative stress conditions. Therefore, lipid peroxidation is one of the major consequences of oxidative stress.

Cigarette smoking for instance, which is an environmental factor that triggers RA development, is a source of exogenous lipid peroxidation products, which are capable not only of promoting the depletion of serum antioxidants that normally act as radical scavengers, but also of affecting directly biological macromolecules, by introducing third-party carbonyl groups into a wide array of proteins, such as cytoskeletal proteins, glycolytic enzymes, antioxidant enzymes, and endoplasmic reticulum proteins, and by attacking the free amino-groups of DNA bases [54–56]. Lipids, including phospholipid oxidation products, are important in the modulation in an inflammatory response [57]. In addition, oxidative stress and inflammation may also be associated with an increased dysregulation of the lipid metabolism, which is also found in RA. Thus, in the next chapter we will detail the role of lipids in RA.

3. Lipids Are Key Players in Rheumatoid Arthritis

Lipid metabolism alterations have been suggested to participate on RA pathogenesis and to contribute to disease severity. Lipid peroxidation is also an important consequence of oxidative stress. When lipids are oxidized, fluidity, and permeability of plasmatic membranes are altered, and membrane-bound enzymes may become dysfunctional [32]. Oxidation of lipids leads to the formation of lipid hydroperoxides, which are quite unstable molecules, and can decompose and lead to the formation of several bioactive aldehydes like 4-hydroxynonenal (HNE), malondialdehyde (MDA), which are electrophilic molecules that can react with proteins, leading to changes in their function [58]. MDA levels have been reported to be significantly higher in RA whole blood, plasma, serum, synovial fluid, erythrocytes and urine [34,39,42,59–64]. MDA levels have also been positively correlated with disease activity and levels of ROS [49]. MDA is highly reactive and can spontaneously break, resulting in acetaldehyde. MDA and acetaldehyde can react with each other, leading to the formation of malondialdehyde-acetaldehyde (MAA) protein adducts, which the production was increased in RA synovial tissue [65]. Besides, a correlation was also found between increased levels of anti-MAA antibodies and seropositivity for RF and ACPA, revealing a potential pathogenic role of this biomarker. Additionally, ACPA seropositivity was linked with increased MDA and myeloperoxidase levels in RA synovial fluid [59]. Thiobarbituric acid reactive substances (TBARS), usually used to measure the levels of

lipid oxidation and lipid carbonylated species, were found markedly elevated in RA blood as well [37,46,66]. Isoprostanes, formed by enzymatic oxidation of lipids, excretion, and plasmatic concentrations were identified as significantly higher in RA patients than in controls [64,67,68]. Isoprostanes excretion was also positively correlated with diminished HDL protective effect against coronary calcification in patients with RA [67].

The overproduction of eicosanoids, like the ones observed in RA, could be correlated with dietary polyunsaturated fatty acids (PUFA). Eicosanoids directly derive from ω-3 and ω-6 PUFA esterified to phospholipids (PL) of the plasmatic membranes of immune cells and were correlated with PUFA dietary intake [69]. It is well established that arachidonic acid (AA, fatty acid (FA) 20:4) derived metabolites have a pro-inflammatory effect while eicosapentaenoic acid (EPA, FA 20:5) and docosahexaenoic acid (DHA, FA 22:6) derivatives promote an anti-inflammatory environment. Therefore, dietary ω-3 PUFA may have favorable clinical applications in patients with RA [70]. Evidence suggests that there is an inverse correlation between the intake of ω-3 PUFA, and RA prevalence. Populations whose intake of ω-3 PUFA is higher have a lower incidence of RA [71,72]. A similar correlation was found to olive oil consumption, however in this case it is due to the increase of C18:1 consumption, which is less prone to oxidation, than the increased intake of ω-3 PUFA [73,74]. Clinically, ω-3 PUFA supplementation has been shown to reduce morning stiffness, lower tender, swollen, and painful joints, improve global arthritic activity, ameliorate biological parameters of inflammation and reduce drug requirement for disease management (for further information, please see review article [70]). ω-3 PUFA supplementation has beneficial effects reducing the symptoms of RA. However, it cannot be considered a standard treatment of this pathology.

Dyslipidemia as an Important Contributor to RA Pathogenesis

The increased concentrations of pro-inflammatory cytokines reported throughout the previous chapters are responsible not only for favoring oxidative stress conditions but also for contributing to dyslipidemia in RA patients [45]. Dyslipidemia is prevalent in 55–65% of RA patients and it can be detected in its early stages or even before the diagnosis of clinical RA, a

time in which both inflammation and autoimmunity (RF, ACPA) are typically elevated [75,76]. Both active or untreated RA is associated with an unfavorable lipoprotein profile, which is essentially characterized by decreased serum levels of HDL, and variation in levels of LDL and total cholesterol (TC) [77,78]. LDL and TC levels have contrasting results in several studies [79–81]. These discrepancies may be due to differences in the study designs such as samples sizes, populations, treatment effects and unconsidered confounders. The reduction of HDL leads to the increase of TC/HDL ratio which was correlated with disease activity and representative of an atherogenic index, thus being a relevant prognostic marker for the risk of cardiovascular diseases [81]. Moreover, a variation was reported in the composition of HDL PL that may be accountable for the decrease in its atheroprotective function, besides explaining the higher cardiovascular risk in RA [64,82].

Singh et al. saw significantly decreased levels of HDL and TC and increased levels of LDL in RA [83]. The reduction of TC levels was less pronounced than the HDL levels, resulting in an increase of both TC/HDL (atherogenic index) and LDL/HDL ratios [83]. Lower levels of TC and HDL were associated with TNF-α and higher levels of disease activity, which could be an explanation for the correlation between disease activity and lipoprotein levels [83]. Cacciapaglia et al. observed significantly lower levels of TC, LDL, triglycerides, and atherogenic index in RA patients with low disease activity when compared with patients with moderate/high disease activity [84]. It should be noted that there is a lipid paradox in RA where the conventional hypercholesterolemia link with cardiovascular diseases is not straight forward. It has been reported that patients with lower levels of TC, LDL, and atherogenic index had an increased risk of cardiovascular diseases than those with higher levels of lipoproteins, suggesting that hypercholesterolemia as a risk factor for cardiovascular diseases may not be applicable in RA [85]. Moreover, growing evidence suggests that specific lipoprotein subfractions are altered as well, which may contribute to the initiation and progression of atherosclerosis in RA patients [86]. All things considered, although TC and LDL levels are inconsistent in several studies, and may resemble those of the healthy population, the

lipoprotein sizes, the apolipoprotein cargo of lipoproteins and the lower levels of HDL in RA patients are enhancers of a pro-atherogenic dyslipidemia [78].

Oxidized LDL (ox-LDL) has also been reported in RA. A significant elevation of the ox-LDL fraction has been found in RA patients with and without carotid plaques [87,88], enhancing pro-atherogenic events, inflammatory responses through upregulation of chemokines, adhesion molecules and production of advanced glycation end-products, improving the risk of RA patients to develop cardiovascular complications [45,83,89]. Chronic inflammation also leads to HDL oxidation and reduced apolipoprotein-A-I in patients with active RA [90].

Changes in the lipoprotein profile seem to be a hallmark of RA and lipid peroxidation is also present in this disease. Dyslipidemia may, in fact, be responsible for the increased risk for cardiovascular diseases in RA. Nevertheless, the interaction between oxidative stress, inflammation and changes in the lipid profile, and the functionality of lipoproteins in RA are still poorly understood, and there are still conflicting results between studies revealing the need for more research in this field. Thus, dysregulation of lipid homeostasis and lipid metabolism at a molecular level was also reported, as will be detailed in the next chapter.

4. Lipidomic Studies in Rheumatoid Arthritis

From the evidence described in the previous chapter, it is accepted that, in fact, there are changes in the lipid metabolism in this pathology. The correct regulation of the lipid metabolism is vital for the homeostasis of the organism, thus avoiding pathological states. The dysregulation of lipid homeostasis affects several processes of inter and intracellular signaling and regulation of the immune response. Thus, the analysis of lipids and their variation is fundamental for a better understanding of the pathogenesis of several chronic diseases such as RA. Personalized medicine is the utmost tailored approach to disease management. Although the routine substances work for the general population, there are some patients to whom the drug effects are not the desired ones. To overcome this setback, biomarkers are of extreme importance to exclude the undesired effects of the drug treatment. These biomarkers may be autoantibodies, genes, or even biomolecules such as lipids. It should be noted that RA treatment involves corticosteroids, which are used as a powerful anti-inflammatory drug, but their effect in the lipid

profile is unknown. Thus, clinical lipidomics is the utmost approach to evaluate the variation of lipids at a molecular level in several chronic diseases, including AID [91]. The aim of clinical lipidomics is to understand lipid metabolism and mechanisms and identify new putative diagnostic biomarkers and therapeutic targets [92]. Clinical lipidomics is a reliable source of information regarding lipidic alterations and, hopefully, it can be seen as a promising approach to disease diagnostics and therapy monitorization in the near future.

Studies on the variation of RA lipid profile at a molecular level using lipidomics were gathered in this review. English language publications were identified through a computerized search (using PubMed database) until 2020 using the following keywords: lipidomic(s), lipid profile, fatty acid(s), phospholipid(s), sphingolipid(s), ceramide(s), and oxidized, combined with rheumatoid arthritis. Studies that did not report the use of mass spectrometry (MS) techniques were not taken into consideration. To structure this review, the studies were divided in three sections: lipidomic studies on RA serum/plasma samples; lipidomic studies on other types of samples from RA patients; and lipidomic studies on high-risk patients to develop RA.

a. Lipidomic Analysis of Serum/Plasma in Rheumatoid Arthritis Patients

Serum/plasma is the most important body fluid to portray metabolic changes. The analysis of serum/plasma sheds light on alterations induced by a pathological environment. The majority of the lipidomic studies on RA has been performed in human serum/plasma samples using mainly gas chromatography-mass spectrometry (GC-MS) for FA profiling, comparing RA patients with healthy controls, also including studies that evaluated the effect of FA diet, but not the effect of disease state. Few studies used liquid chromatography-mass spectrometry (LC-MS) for PL profiling, free fatty acids (FFA) and oxidized FA, also comparing data from plasma/serum from RA patients and controls (Table 1).

i. Fatty Acid Profiling Analysis

The studies that reported the changes in FA profile in RA patients, compared with non-disease subjects, reported similar trends in some FA while opposite trends were reported in other studies. This can also be due to different experimental approaches since some studies

investigate the variation of FA in plasma [93–96], while others reported in phosphatidylcholine (PC) [97] or in total PL [98–102]. The majority of the studies reported a decrease of ω-3 FA, namely a decrease of 18:3 ω-3, 20:5 ω-3 or/and 22:6 ω-3. A decrease of palmitic acid (16:0) was seen in some studies, but was increased in others, while the saturated FA 18:0 was reported to decrease or not change in different studies. The ω-6 FA, such as the arachidonic acid (20:4), showed also contradictory variations. Other FA were also affected by disease, as will be described.

Bruderlein and colleagues investigated the FA profile of serum PL of RA patients [98]. They determined significant decreases of FA 16:0; 18:2 ω-6 and 18:3 ω-3, and significant increases of FA 18:1 ω-9; 20:3 ω-6; 20:3 ω-9 and (20:3 + 20:4) ω-6/18:2 ω-6 ratio [98]. It was suggested that the ω-6 metabolic pathway is altered in RA patients, and it was induced by the persistent inflammation of this disease. The sum of ω-6 FA was constant, thus the disease seemed to stimulate an alteration in the content of different ω-6 FA towards higher unsaturated species, namely 20:3 and 20:4 [98]. When in a cell membrane, 20:3 ω-6 and 20:4 ω-6, have a much higher distortion, conformation wise, than that of 18:2 ω-6, due to the presence of a higher number of unsaturations. Changes in the abundance of these FA may affect membrane properties [103]. Jacobsson and co-workers analyzed the FA composition of serum PC (the major PL class in plasma/serum lipid profile) in RA patients of short and long disease duration [97]. It was verified a significant decrease of FA 16:1; 18:0; 18:2 ω-6; 18:3 ω-3; 20:5 ω-3; 22:5 ω-3; 18:2/20:4 ratio and Σ ω-6 and a significant increase of FA 14:0; 16:0; 18:1 and Σ saturated FA. These changes became more evident with the increase of disease duration [97]. The disturbances in FA of the ω-6 series are in agreement with the previous findings of Bruderlein [98]. The reduced 18:2/20:4 ratio in RA patients was suggested to be related to the degree of inflammation, due to an increase in the FA desaturation/elongation process, which could be the result of higher insulin levels (stimulates desaturation) that have been found in RA patients, or due to an increased synthesis of eicosanoids [104,105]. Suryaprabha and colleagues studied plasma concentrations of essential FA of PL and determined a marked decrease of FA 18:0; 18:3 ω-6; 18:3 ω-3; 20:3 ω-6; 20:5 ω-3 and 22:6 ω-3 [99]. Interleukin-2 dependent T-cell

proliferation and tumour necrosis factor and interleukin-2 production can be blocked by PUFA, thus, the reduction of essential FA and their metabolites may contribute to increase the chronic inflammation once T-cell proliferation, tumour necrosis factor and interleukin-2 production may not be inhibited [106]. The low levels of EPA and DHA also contribute to the inflammatory state [99].

Non-esterified FA/FFA profile of serum in RA was also evaluated by using LC-MS lipidomic approaches, and revealed a significant reduction of FA 16:0; 16:1 ω-7; 18:1 ω-9 and 20:4 ω-6 when compared with healthy controls [93]. The FA 20:5 ω-3 and 22:6 ω-3 were reported to have significantly lower concentrations in RA patients as well [93]. These results were associated with SE presence, which suggests that non-esterified FA alterations could be on the onset of RA development.

ii. FA Analysis after a Fasting Period

Changes in FA profile in RA with different diets or in a fasting/non-fasting regimen was also evaluated, since fasting has been shown to have significant beneficial effects in clinical manifestations in RA [107]. Hafström et al. evaluated the serum levels of FA of membrane PL of RA patients after a fasting period [100] and observed markedly reduced levels of FA 20:3 ω-6 and markedly elevated levels of FA 20:4 ω-6 and 20:5 ω-3 comparing with RA patients before fasting and healthy control's levels [100]. Haugen et al. investigated the possible impact on disease activity of fasting and one-year vegetarian diet in patients with RA [101]. The results showed that, after a vegan diet period, several FA of plasma PL were significantly decreased, such as FA 14:0; 16:0; 16:1; 18:0; 18:1; 18:3 ω-3; 20:1; 20:3 ω-9; 20:3 ω-6; 20:4 ω-6; 20:5 ω-3; 22:0; 22:1 ω-11; 22:4 ω-6; 22:5 ω-6; 22:5 ω-3; 22:6 ω-3; Σ ω-6; Σ ω-3 and Σ saturated FA [101]. A few years forward, Fraser and co-workers evaluated free FA changes in plasma of RA subjects after fasting and assessed the effects upon T lymphocyte proliferation [94]. Long chain ω-3 and ω-6 FA are linked with the inhibition of T lymphocyte function [108–110]. However, it is unclear if alterations on total concentration of circulating FFA would influence the immune response. Firstly, Fraser determined marked increases of FFA 14:0; 16:0; 16:1 ω-7; 18:0; 18:1 ω-9; 18:2 ω-6; 18:3 ω-3 and total FFA after a fasting period [94]. Secondly, it was shown that

the proliferative response of T lymphocytes was higher with the increase of FA levels. Lastly, in vitro tests revealed that the ratio of unsaturated/saturated FFA had a significant effect upon lymphocyte proliferation. Lymphocyte proliferative responses, after mitogenic stimulation in the presence of 1) only unsaturated FA or 2) only saturated FA, were significantly lower than when stimulated in the presence of a mixture of unsaturated/saturated FA [94]. The practical implications of this finding to in vivo situations remains uncertain.

iii. FA Analysis after Supplementation Intake

The effect of dietary fatty acid was also evaluated in a few studies, and dissimilar variations were found, which may be due to different supplements, methods, and samples. Kremer and co-workers examined the effect of manipulation of dietary FA comparing plasma of RA patients with and without EPA supplementation [95]. As expected, patients taking EPA supplementation had significantly higher levels of plasma EPA than the patients not taking the supplementation [95]. Remans et al. had similar results as obtained by Kremer's team. Remans compared the FA profile of PL of active RA patients receiving nutrient supplementation containing PUFA, including EPA, and micronutrients, with a group of active RA patients receiving placebo [102]. All patients receiving nutrient supplementation had significant increases of total ω-3 PUFA (20:5; 22:5; 22:6) and decrease of AA [102]. Although there were significant changes in plasma FA, the nutritional supplementation did not improve signs and symptoms of RA patients. On the other side, Jäntti et al. also evaluated the influence of supplementation with evening primrose oil (rich in FA 18:3 ω-6) and determined significantly lower concentrations of serum FA 18:1 and EPA; and markedly increased levels of serum FA 18:2; 18:3; 20:3 and 20:4 [96]. The intake of evening primrose oil had contradictory effects, increasing both anti-inflammatory FA 18:3 and pro-inflammatory AA. The increase of FA 18:3 may be regarded as favorable to help reduce the inflammatory status. However, the increase of AA may be considered as harmful since it is the precursor of pro-inflammatory prostaglandins and leukotrienes [96]. Proudman [111] analyzed the results of an investigation conducted previously by other authors, and therefore did not mention original results to be discussed in this review. PUFA supplementation should have, in theory, beneficial results and improve clinical symptoms because EPA and DHA compete

with AA for incorporation in cellular membranes, which leads to a reduction in the synthesis of prostaglandins and leukotrienes, thus reducing the inflammatory state [112]. However, investigators struggle to find the correct dosage of PUFA supplementation proven by different studies (with unequal doses) having different results. Having said that, more studies are needed to ascertain the quantity of PUFA supplementation should be administered to RA patients in order to maximize the results.

iv. Phospholipidomic Profiling Analysis by LC-MS

To our knowledge, there is only one study that reported untargeted lipidomic analysis of plasma PL of RA subjects. Łuczaj et al. [113] determined alterations on the PL profile that reflected a decrease on PC(40:2); PC(40:3) and PC(42:3), and an increase on lyso-PC (LPC) species LPC(16:1); LPC(24:3); PC(34:3); PC(36:3); PC(38:2); PC(38:3); PC(38:4); lyso-phosphatidylethanolamine (LPE) species LPE(16:0); LPE(18:0); phosphatidylethanolamine (PE) specie PE(30:1); phosphatidylinositol (PI) species PI(36:1); PI(36:2); PI(36:3); PI(36:4); PI(38:3); PI(38:4) and sphingomyelin (SM) species SM(d34:2); SM(d38:1); SM(d40:1) and SM(d40:2) [113]. The results suggest a significantly altered PE and PC metabolism with enhanced PL hydrolysis by phospholipase A_2. In addition, the increase of LPC in RA has already been associated with the induction of cyclooxygenase 2 hence contributing to systemic inflammation [114,115]. PC and PE can also be modified by ROS in oxidative stress conditions [116]. Although the main targets of oxidation are the unsaturated FA chains and PC is more abundant than PE, PE is more reactive over PC since it has a free amino group in the polar head, being a preferable target to suffer modifications induced by oxidative stress conditions and ROS which are enhanced in inflammation. Sphingolipids have pleotropic pro-inflammatory effects. Therefore, the study of its metabolism is very important. Regarding sphingolipids metabolism, other findings worth mentioning are the detection of increased levels of total monohexosylceramides (HexCer, as a sum of HexCer16:0; HexCer16:1; HexCer18:0; HexCer20:0; HexCer22:0; HexCer23:0; HexCer24:0 and HexCer24:1), total ceramides (Cer, as a sum of Cer16:0; Cer18:0; Cer20:0; Cer22:0; Cer23:0; Cer24:0; Cer24:1; Cer25:0 and Cer26:0;) and sphingosine (d18:1) in serum of established RA patients [117].

v. Identification of Lipid Peroxidation Products by LC-MS

Lipid peroxidation products of AA and linoleic acid in RA patients were evaluated through LC-MS techniques by Charles-Schoeman and co-workers [118]. It was analyzed the presence of hydroxyeicosatetraenoic acids (HETE) and hydroxyoctadecadienoic acids (HODE) in plasma lipoproteins HDL and LDL. The results showed markedly increase levels of oxidation products 5-HETE; 15-HETE; 9-HODE and 13-HODE in both HDL and LDL fractions of RA patients [118]. HETE and HODE contribute to LDL oxidation which, together with their accumulation in HDL particles, may inhibit HDL beneficial function increasing the risk of developing atherosclerotic events [119,120]. Higher concentrations of these lipid peroxidation products in HDL are associated with the decreased antioxidant capacity of such particles. Thus, the raised levels of systemic inflammation, also determined in this investigation, positively correlates with the increased levels of free oxidized FA in HDL and LDL, reassuring the fact that RA is an AID with an exacerbated oxidative environment [118].

Overall, the serum/plasma lipidomic analysis of the studies reported above suggest that RA is characterized by an altered lipid metabolism. Plasma FA alterations were observed and revealed as significant lower levels of FA 20:5 ω-3 and 22:6 ω-3, although some contradictory variations were reported, as for other FA. The plasma PL profile was found to be changed with manifestations on PE and PC metabolism with enhanced PL hydrolysis, in a solely study that used lipidomic approaches.

Some attempts were made regarding the effects of PUFA supplementation to compensate the lower level of ω-3 PUFA in RA, but more studies are needed to understand exactly which dose should be administrated and if, besides FA alterations, there are, in fact, changes concerning disease activity.

Nonetheless, lipid metabolism is undeniably affected in RA. Considering the important role of lipids in inflammation, more studies are needed, particularly using modern lipidomics, which could contribute to unveil the pathophysiology of this disease, find new biomarkers, and also to develop better therapeutic approaches.

Table 3.1-1. Main lipid variations observed in serum/plasma of RA patients reported in published lipidomic studies, available in PubMed database, using MS approaches.

Reference	Analytical Method	Lipid Extraction Method	N° and Age (Years) of RA Patients	Extra Details of the Study	Molecular Specie	Results	
						↓ Decrease	↑ Increase
FA profiling analysis							
Bruderlein et al. [98]	GC-MS	Gloster and Fletcher method	20 RA Age: 25–66	NSAID treatment.	FA esterified to PL	16:0; 18:2 ω-6; 18:3 ω-3	18:1 ω-9; 20:3 ω-6; 20:3 ω-9; (20:3 + 20:4) ω-6/18:2 ω-6 ratio
Jacobsson et al. [97]	GC-MS	INF	Two groups: 21 RA Age: 25–78 21 RA Age: 3–43	NSAID treatment.	FA esterified to PC	16:1; 18:0; 18:2 ω-6; 18:3 ω-3; 20:5 ω-3; 22:5 ω-3; 18:2/20:4 ratio; Σ ω-6	14:0; 16:0; 18:1; Σ saturated FA
Suryaprabha et al. [99]	GC-MS	Methanol:Chloroform (1:2, *v/v*)	14 RA Mean age: 33 ± 9	Not on drugs when sample collection.	FA esterified to PL	18:0; 18:3 ω-6; 18:3 ω-3; 20:3 ω-6; 20:5 ω-3; 22:6 ω-3	-
Rodríguez-Carrio et al. [93]	LC-MS/MS	MTBE	124 RA Mean age: 52.47 ± 12.76	43 patients with smoking habits.	Plasma FFA	16:0; 16:1 ω-7; 18:1 ω-9; 20:4 ω-6; 20:5 ω-3; 22:6 ω-3	-
Analysis after a fasting period							
Hafström et al. [100]	GC-MS	Methanol:Chloroform (2:1, *v/v*)	14 RA Age: 34–65	No steroids/NSAID treatment for the previous 3 months. 7 days of fasting.	FA esterified to PL	20:3 ω-6	20:4 ω-6; 20:5 ω-3
Haugen et al. [101]	GC-MS	n-butanol (butyl alcohol)	53 RA Mean age: 51	Fasting period of 7–10 days followed by 1-year vegetarian diet.	FA esterified to PL	<u>After vegan diet</u> 14:0; 16:0; 16:1; 18:0; 18:1; 18:3 ω-3; 20:1; 20:3 ω-9; 20:3 ω-6; 20:4 ω-6; 20:5 ω-3; 22:0; 22:1 ω-11; 22:4 ω-6; 22:5 ω-6; 22:5 ω-3; 22:6 ω-3; Σ ω-6; Σ ω-3; Σ saturated FA	-
Fraser et al. [94]	GC-MS	n-hexane	9 RA Age: 31–65	Steroids/NSAID treatment. 7 days of fasting.	Plasma FFA	-	14:0; 16:0; 16:1 ω-7; 18:0; 18:1 ω-9; 18:2 ω-6; 18:3 ω-3; Σ FFA
Analysis after supplementation intake							
Kremer et al. [95]	GC-MS	INF	37 RA Age: INF	NSAID treatment. EPA supplementation.	Plasma FFA	-	<u>With supplementation</u> 20:5

Remans et al. [102]	GC-MS	Bligh & Dyer method	26 RA Mean age: 59.5 ± 11.0	Steroids treatment. Nutritional supplement with PUFA and micronutrients.	FA esterified to PL	With supplementation 20:4	With supplementation Σ ω-3 PUFA (20:5; 22:5; 22:6)
Jäntti et al. [96]	GC-MS	Methanol:Chloroform (1:1, *v/v*)	Two groups: 10 RA Mean age: 50 10 RA Mean age: 38	No NSAID treatment for the previous 7 days. Evening primrose oil/olive oil supplementation.	Plasma FFA	With supplementation 18:1; 20:5	With supplementation 18:2; 18:3; 20:3; 20:4
Phospholipidomic profiling analysis by LC-MS							
Łuczaj et al. [113]	LC-MS	Modified Folch method	9 RA Age: 23–79	No steroids/NSAID treatment. Excluded heavy smokers.	Plasma PL	PC(40:2); PC(40:3); PC(42:3)	LPC(16:1); LPC(24:3); PC(34:3); PC(36:3); PC(38:2); PC(38:3); PC(38:4); LPE(16:0); LPE(18:0); PE(30:1); PI(36:1); PI(36:2); PI(36:3); PI(36:4); PI(38:3); PI(38:4); SM(d34:2); SM(d38:1); SM(d40:1); SM(d40:2)
Identification of lipid peroxidation products by LC-MS							
Charles-Schoeman et al. [118]	LC-MS/MS	Methanol/water	10 RA Mean age: 49.6 ± 11.8	10% of the patients with smoking habits.	Plasma HDL + LDL	-	5-HETE; 15-HETE; 9-HODE; 13-HODE

INF: information not found.

b. Lipidomic Analysis of Other Types of Samples of Rheumatoid Arthritis Patients

Serum/plasma is undoubtedly the best source of information regarding pathologically induced metabolic alterations. However, the lipidomic analysis of other types of samples (body fluids) and also blood cells offer valuable insights into the disease as well. The works published to date and found in the literature describe changes in lipids, in particular FA, in synovial fluid, platelets, erythrocytes, PBMC, and adipose tissue of human samples (Table 2).

Synovial fluid is extremely important in RA diagnosis. When there is a joint problem, synovial fluid can accumulate, causing stiffness, pain, and inflammation, therefore its analysis should reveal interesting results. Synovial fluid can physiologically change in volume and content which can occur in response to trauma, inflammation, or bacterial/fungal/viral penetrance, leading to an accumulation of selected molecules [121]. Thus, synovial fluid may be considered the body fluid of choice to obtain crucial information. Nevertheless, the collection of synovial fluid (arthrocentesis) is a difficult process for RA patients and even more for healthy volunteers. To the best of our knowledge, no studies reported the comparison of synovial fluids between RA patients and healthy volunteers. There is only one study that used GC-MS to evaluate the FA profile of the synovial fluid comparing it with the FA profile of serum from the same RA patient [122]. Quantitatively (% of total FA esters), the FA composition of the synovial fluid of RA patients was significantly lower, approximately one third of that of serum samples. In both biofluids, the major FA were FA 16:0; 18:1 and 18:2 (the sum of the relative abundances of these FA accounted for nearly 80% of FA composition) while FA 14:0; 16:1; 18:0 and 20:4 were less abundant [122]. The synovial fluid membrane significantly contributes to local lipid content, by releasing lipids to the synovial fluid. Thus, the qualitative composition of synovial fluid and serum of RA is similar [123].

Platelets release pro-inflammatory microparticles after being activated, which in turn interact with leucocytes, promoting joint and systemic inflammation in RA [124]. Hafström and colleagues determined the FA profile of platelets (by GC-MS), after a fasting period and found markedly reduced levels of FA 20:3 ω-6 while AA and 20:5 ω-3 showed the opposite trend,

being markedly increased in RA subjects [100]. In this study, the composition of serum and platelets concerning the FA profile was equivalent, suggesting a fast exchange of lipids between platelets membrane and serum.

Erythrocytes are likewise involved in RA pathobiology. Erythrocytes count is positively correlated with joint pathology, as well as with inflammatory biomarkers. There is also an alteration in the lipid distribution within erythrocytes membranes [125]. Masoom-Yasinzai et al. assessed the status of EPA in the membrane of RA erythrocytes and found markedly decreased levels of 20:5 ω-3, as compared with controls, which may suggest an impaired EPA metabolism in these cells [126]. Lee and colleagues investigated if erythrocyte levels of ω-3 PUFA were linked with disease activity and the risk of developing RA [127]. It was found significantly lower concentrations of FA 18:1 ω-9; 18:2 ω-6; 18:3 ω-3; 20:5 ω-3; ω-3 index and 20:5/20:4 ratio, and significantly higher concentrations of FA 14:0; 16:0; 16:1 ω-7; 18:0 and 18:3 ω-6 [127]. The authors determined that the risk of RA was positively correlated with the levels of saturated FA; 14:0; 16:0; 18:0; 16:1 ω-7; 18:3 ω-6; ω-6 PUFA; *trans* 18:2 and *trans* FA and disease activity was positively associated with age [127]. Lastly, Park and co-workers aimed to determine if ω-3 PUFA supplementation improved the clinical outcomes of RA patients [128]. The results showed a significant decrease of FA 18:1 ω-9; 18:2 ω-6; 20: 4 ω-6; total ω-6 PUFA and ω-6/ω-3 ratio, and a significant increase of FA 20:5 ω-3 and total ω-3 PUFA after supplementation [128]. Nevertheless, ω-3 PUFA supplementation did not ameliorate the clinical outcomes, both clinical symptoms and laboratory parameters, of RA patients.

Unlike the previously described investigations, some studies with immune cells, neutrophils [100] and peripheral blood mononuclear cells [94] (PBMC, which include lymphocytes and monocytes), did not reveal statistically significant results, as will be described. Neutrophils are key players in RA pathogenesis, favoring, among others, an oxidative environment and cartilage destruction, as explained before. Hafström and collaborators determined the FA profile of neutrophils after a fasting period. However, the investigation did not report significant results [100]. Changes in the PL composition of the membrane of PBMC directly influence immune cell functions [129] and thus, Fraser et al. evaluated the FA profile of PBMC cellular

membranes, but no statistically significant differences in the amount of FA as a percentage of total cellular lipids between RA and healthy subjects were found [94].

Adipose tissue reflects the long-term FA status. Hence, its analysis would indicate if the lipid metabolism alterations derive from the onset of RA, or if they are established later in RA development. Jacobsson and co-workers analyzed the FA composition of adipose tissue of patients with RA which showed a significant decrease of FA 18:2 ω-6; 18:3 ω-3 and total ω-6 [97]. These abnormalities were found to be more severe with the increase of disease duration.

From the results described above, it cannot be concluded if different types of samples show the same metabolic alterations at a lipid level. However, the low levels of FA 18:2 ω-6 and 20:5 ω-3 in erythrocytes are in agreement with the low levels found in adipose tissue and PL serum of RA subjects [97,98]. Furthermore, the increased levels of saturated FA are consistent with previous studies that also found higher levels of these FA in plasma PL of RA [97,130] and lower levels of EPA and other ω-3 FA. Further studies are needed to confirm or not this trend. Changes in PL were not studied at all besides plasma/serum.

Table 3.1-2. Main lipid variations observed in synovial fluid [122], platelets [100], erythrocytes [126–128], neutrophils [100], PBMC [94], and adipose tissue [97] of RA patients reported in published lipidomic studies, available in PubMed database, using MS approaches.

Reference	Analytical Method	Lipid Extraction Method	N° and Age (Years) of RA Patients	Extra Details of the Study	Molecular Specie	Results	
						↓ Decrease	↑ Increase
Kim et al. [122]	GC-MS	Folch method	10 RA Age: INF	-	FFA	-	-
Hafström et al. [100]	GC-MS	Methanol:Chloroform (2:1, *v/v*)	14 RA Age: 34–65	No steroids/NSAID treatment for the previous 3 months. 7 days of fasting.	Membrane FA	Neutrophils: NSD Platelets: 20:3 ω-6	Neutrophils: NSD Platelets: 20:4 ω-6; 20:5 ω-3
Masoom-Yasinzai [126]	GC-MS	Chloroform:Methanol (2:1, *v/v*)	15 RA Age: INF	No steroids/hypolipidemic treatment.	Membrane FA	20:5 ω-3	-
Lee et al. [127]	GC-MS	INF	100 RA Mean age: 48.39 ± 9.69	Steroids/NSAID treatment. 13% of the patients with smoking habits.	Membrane FA	18:1 ω-9; 18:2 ω-6; 18:3 ω-3; 20:5 ω-3; ω-3 index; 20:5/20:4 ratio	14:0; 16:0; 16:1 ω-7; 18:0; 18:3 ω-6
Park et al. [128]	GC-MS	INF	Two groups: 41 RA Mean age: 49.24 ± 10.46 40 RA Mean age: 47.63 ± 8.78	Steroids/NSAID treatment. 15 patients with smoking habits. ω-3 PUFA supplementation.	Membrane FA	<u>With supplementation</u> 18:1 ω-9; 18:2 ω-6; 20: 4 ω-6; Σ ω-6 PUFA; ω-6/ω-3 ratio	<u>With supplementation</u> 20:5 ω-3; Σ ω-3 PUFA
Fraser et al. [94]	GC-MS	Benzene	9 RA Age: 31–65	Steroids/NSAID treatment. 7 days of fasting.	Membrane FA	NSD	NSD
Jacobsson et al. [97]	GC-MS	2% Sulfuric acid in Methanol:Toluene (1:1, *v/v*)	Two groups: 21 RA Age: 25–78 21 RA Age: 3–43	NSAID treatment.	FA	18:2 ω-6; 18:3 ω-3; Σ ω-6	-

NSD: no significant differences; INF: information not found.

c. Lipidomic Analysis of Erythrocytes from Pre-Clinical Rheumatoid Arthritis Subjects

Accumulating evidence suggests that there is a pre-clinical period of increased levels of RA-related autoantibodies that precedes RA development [131]. This type of antibodies is usually detected 3–5 years prior to RA onset [132,133]. This pre-clinical phase of RA re-enforces the multifactorial aspect of RA pathogenesis by suggesting that genetic and environmental factors act previously to the development of classifiable RA, leading to autoantibodies production [134]. This way, lipidomic investigations in pre-clinical RA subjects, which are considered to have a high risk of developing RA forward in their lives, may reveal promising results that could ultimately lead to preventive interventions (Table 3).

As far as our knowledge goes, there are only three lipidomic studies on pre-clinical RA patients that used GC-MS approaches. Gan and colleagues conducted two different investigations, only one of which obtained reportable results [135,136]. The first study described significantly lower levels of 22:6; 20:5 + 22:6 and total ω-3 FA% in erythrocytes of patients who tested positive for anti-CCP2 autoantibodies (an RA-specific autoantibody) [135]. The results suggest an inverse correlation between ω-3 FA and anti-CCP2 positivity. In the second study, Gan and his team tested the seropositivity for several antibodies and determined that pre-clinical RA patients who were positive for RF and SE showed significantly decreased concentrations of FA 22:5 ω-3; 22:6 ω-3; total ω-3 FA% and 20:5 + 22:6 [136]. Similarly, pre-clinical RA patients who tested positive for anti-CCP2 and SE also had markedly reduced levels of FA 20:5 ω-3; 22:6 ω-3; total ω-3 FA% and 20:5 + 22:6 [136]. Resembling the first investigation, the authors concluded that RF, anti-CCP2 and SE positivity is accompanied by low levels of ω-3 FA, which may be linked with RA pathogenesis and RA-related autoimmunity in the pre-clinical phase of this disease. Recently, Pablo et al. tested the hypothesis that higher levels of long-chain ω-3 PUFA were associated with a lower risk of developing RA [137]. The study found significantly increased levels of FA 20:3 ω-6 and 22:5 ω-3, which were increasing with the approaching of the time of the diagnosis [137]. It was also observed that erythrocyte membrane levels of FA 18:2 ω-6 were inversely correlated with the risk of developing RA,

meaning that higher levels of 18:2 ω-6 were associated with a lower risk of RA [137]. The hypothesis proposed by the authors was not confirmed.

In summary, lipidomic analysis on erythrocytes add valuable information to the existing knowledge on the lipid profile of RA and pre-clinical RA. The studies of Gan et al. [135,136] corroborate previous findings in erythrocytes of RA patients who determined low levels of 20:5 ω-3 and ω-3 index [126,127]. However, the investigations of Pablo et al. [137] and Gan et al. [136] present opposing results regarding the FA 22:5 ω-3, revealing the intricacy of the lipid metabolism under both pre-pathological and pathological conditions.

Table 3.1-3. Main lipid variations observed in erythrocytes from subjects with high risk of developing RA reported in published lipidomic studies, available in PubMed database, using MS approaches.

Reference	Analytical Method	Lipid Extraction Method	N° and Age (Years) of RA Patients	Extra Details of the Study	Results	
					↓ Decrease	↑ Increase
Gan et al. [135]	GC-MS	INF	30 pre-RA Mean age: 45.6 ± 16.5	2 patients with smoking habits.	Anti-CCP2 + 22:6; Σ ω-3 FA%; 20:5 + 22:6	-
Gan et al. [136]	GC-MS	INF	Two groups: 40 pre-RA Mean age: 43.7 ± 15.4 27 pre-RA Mean age: 48.1 ± 13.2	5 patients with smoking habits.	RF + and SE + 22:5 ω-3; 22:6 ω-3; Σ ω-3 FA%; 20:5 + 22:6 Anti-CCP2 + and SE + 20:5 ω-3; 22:6 ω-3; Σ ω-3 FA%; 20:5 + 22:6	-
Pablo et al. [137]	GC-MS	Chloroform:Methanol (2:1, *v/v*)	96 pre-RA Mean age: 51 ± 7.56	29 patients with smoking habits.	-	20:3 ω-6; 22:5 ω-3

NSD: no significant differences; INF: information not found.

5. Concluding Remarks and Future Perspectives

By the evidence reported in this review, alteration of the lipid metabolism seems to be a characteristic of RA that is far from being completely elucidated. For some cases, dissimilar lipid changes were reported. Variations between studies may also be related to the experimental approach (whether the data are from the analysis of total FA or only from the esterified fraction) and data analysis process, hence the need for further studies based on standardized protocols. The upcoming studies should be standardized so that the results obtained are more robust and more easily comparable, making possible the identification of reliable biomarkers.

Lipid alterations can be observed even before disease manifestations, which suggests that these molecules are closely linked to the most widespread metabolic changes caused by inflammation (associated with TNF-α) [138,139]. As a result, it is important to study in deep the lipid modulation by RA as it can provide potential markers for early diagnosis of this disease. New biomarker discovery is important once early diagnosis is essential for an early treatment of RA and even for a better prognosis of the disease. All of the reviewed investigations clearly validate the importance of lipids in inflammation, autoimmunity and in the onset (pre-clinical RA) and development of RA. In particular, FA and PE and PC metabolism are primarily affected in this disease, namely a decrease of ω-3 FA, in particular 20:5 ω-3 and 22:6 ω-3 in serum/plasma, increase/decrease of PC and PE species, the increase of oxidized PL and the increase of polar lipids in their lyso form (Figure 2). Additionally, more studies are needed to clarify the effect of lipid supplementation on disease onset and follow-up.

Lipids are important players in inflammation and are modulated in RA. It is very important to continue to advance in this research field: 1) lipidomics of plasma/serum/lipoproteins of patients with RA to characterize the lipidomic signature typical of RA, and in the different stages of the disease to unveil biomarker discovery; 2) lipidomics of immune cells for detailed characterization of changes in their lipid profile to understand how they can correlate with the dysfunction of these cells and the development of RA. In this way, clinical lipidomics, by allowing a detailed lipidome profiling of RA, could be a great contributor and add value on the personalized medical field, leading to a more precise and early diagnosis, management of disease progression, and evaluation of therapy strategies and outcomes.

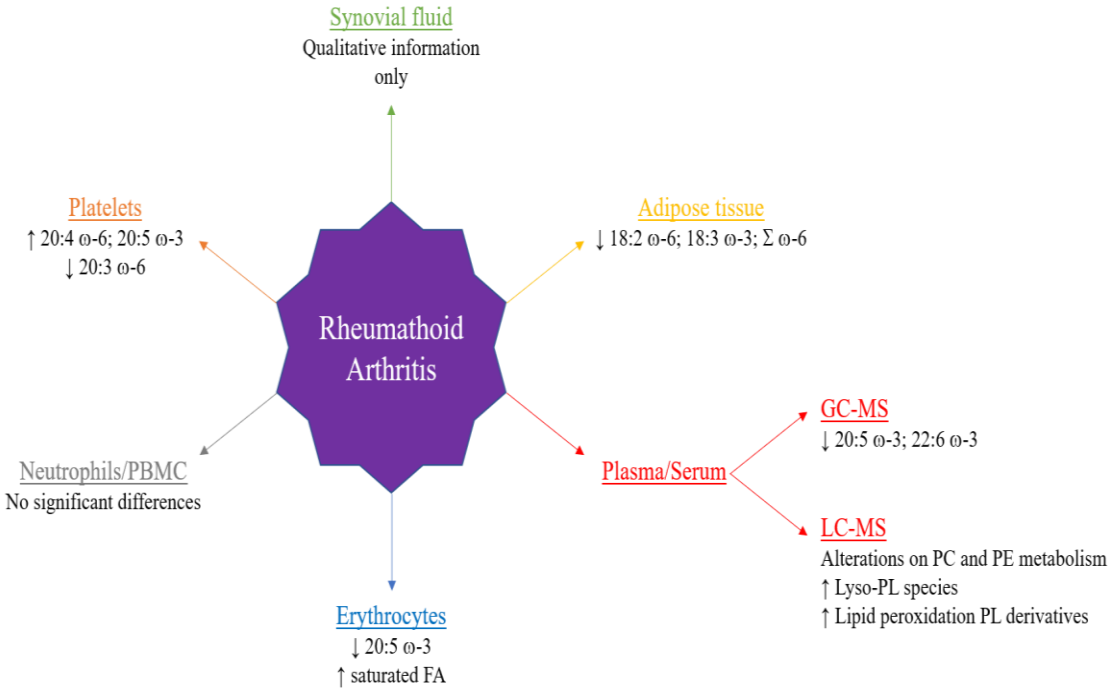

Figure 3.1-2. Main lipidomic alterations described in several studies reported in this review. PBMC: peripheral blood mononuclear cells; GC-MS: gas-chromatography mass spectrometry; LC-MS: liquid-chromatography mass spectrometry.

Funding: Thanks are due for the financial support to the University of Aveiro and FCT/MCT for the financial support to CESAM (UIDB/50017/2020 + UIDP/50017/2020), QOPNA (FCT UID/QUI/00062/2019), LAQV/REQUIMTE (UIDB/50006/2020), and to RNEM, Portuguese Mass Spectrometry Network (LISBOA-01-0145-FEDER-402-022125) through national founds and, where applicable, cofinanced by the FEDER, within the PT2020. Helena Beatriz Ferreira (2020.04611.BD) is grateful to FCT (Fundação para a Ciência e Tecnologia) for her Phd Grant.

Institutional Review Board Statement: Not applicable.

Informed Consent Statement: Not applicable.

Data Availability Statement: Not applicable.

Conflicts of Interest: The authors declare no conflict of interests regarding the publication of this paper.

References

1. Alamanos, Y.; Voulgari, P.V.; Drosos, A.A. Incidence and prevalence of rheumatoid arthritis, based on the 1987 American College of Rheumatology criteria: A systemic review. *Sem. Arthritis Rheum.* **2006**, *36*, 182–188.

2. Sandoughi, M.; Kaykhaei, M.A.; Shahrakipoor, M.; Darvishzadeh, R.; Nikbakht, M.; Shahbakhsh, S.; Zakeri, Z. Clinical manifestations and disease activity score of rheumatoid arthritis in southeast of Iran. *Rheumatol. Res.* **2017**, *2*, 61–64.
3. Jung, N.; Bueb, J.L.; Tolle, F.; Bréchard, S. Regulation of neutrophil pro-inflammatory functions sheds new light on the pathogenesis of rheumatoid arthritis. *Biochem. Pharmacol.* **2019**, *165*, 170–180.
4. Aletaha, D.; Blüml, S. Therapeutic implications of autoantibodies in rheumatoid arthritis. *RMD Open* **2016**, *2*, e000009.
5. Aggarwal, R.; Liao, K.; Nair, R.; Ringold, S.; Costenbader, K.H. Anti-citrullinated peptide antibody assays and their role in the diagnosis of rheumatoid arthritis. *Arthritis Rheum.* **2009**, *61*, 1472–1483.
6. Aletaha, D.; Neogi, T.; Silman, A.J.; Funovits, J.; Felson, D.T.; Bingham, C.O.; Birnbaum, N.S.; Burmester, G.R.; Bykerk, V.P.; Cohen, M.D.; et al. 2010 Rheumatoid arthritis classification criteria: An American College of Rheumatology/European League Against Rheumatism collaborative initiative. *Arthritis Rheum.* **2010**, *62*, 2569–2581.
7. Bartok, B.; Firestein, G.S. Fibroblast-like synoviocytes: Key effector cells in rheumatoid arthritis. *Immunol. Rev.* **2010**, *233*, 233–255.
8. Marston, B.; Palanichamy, A.; Anolik, J.H. B cells in the pathogenesis and treatment of rheumatoid arthritis. *Curr. Opin. Rheumatol.* **2010**, *22*, 307–315.
9. Su, Z.; Yang, R.; Zhang, W.; Xu, L.; Zhong, Y.; Yin, Y.; Cen, J.; DeWitt, J.P.; Wei, Q. The synergistic interaction between the calcineurin B subunit and IFN-γ enhances macrophage antitumor activity. *Cell Death Dis.* **2015**, *6*, e1740.
10. Tolboom, T.C.; Pieterman, E.; Laan, W.H. Van Der; Toes, R.E.; Huidekoper, A.L.; Nelissen, R.G.; Breedveld, F.C.; Huizinga, T.W. Invasive properties of fibroblast-like synoviocytes: Correlation with growth characteristics and expression of MMP-1, MMP-3, and MMP-10. *Ann. Rheum. Dis.* **2002**, *61*, 975–980.
11. Sabeh, F.; Fox, D.; Weiss, S.J. Membrane-type I matrix metalloproteinase-dependent regulation of rheumatoid arthritis synoviocyte function. *J. Immunol.* **2010**, *184*, 6396–6406.
12. Smiljanovic, B.; Radzikowska, A.; Kuca-Warnawin, E.; Kurowska, W.; Grün, J.R.; Stuhlmüller, B.; Bonin, M.; Schulte-Wrede, U.; Sörensen, T.; Kyogoku, C.; et al. Monocyte alterations in rheumatoid arthritis are dominated by preterm release from bone marrow and prominent triggering in the joint. *Ann. Rheum. Dis.* **2018**, *77*, 300–308.
13. Cascão, R.; Moura, R.A.; Perpétuo, I.; Canhão, H.; Vieira-Sousa, E.; Mourão, A.F.; Rodrigues, A.M.; Polido-Pereira, J.; Queiroz, M.V.; Rosário, H.S.; et al. Identification of a cytokine network sustaining neutrophil and Th17 activation in untreated early rheumatoid arthritis. *Arthritis Res. Ther.* **2010**, *12*, R196.
14. Wright, H.L.; Moots, R.J.; Bucknall, R.C.; Edwards, S.W. Neutrophil function in inflammation and inflammatory diseases. *Rheumatology* **2010**, *49*, 1618–1631.
15. Larbre, J.P.; Moore, A.R.; Silva, J.A. Da; Iwamura, H.; Ioannou, Y.; Willoughby, D.A. Direct degradation of articular cartilage by rheumatoid synovial fluid: Contribution of proteolytic enzymes. *J. Rheumatol.* **1994**, *21*, 1796–1801.
16. Khandpur, R.; Carmona-Rivera, C.; Vivekanandan-Giri, A.; Gizinski, A.; Yalavarthi, S.; Knight, J.S.; Friday, S.; Li, S.; Patel, R.M.; Subramanian, V.; et al. NETs are a source of citrullinated autoantigens and stimulate inflammatory responses in rheumatoid arthritis. *Sci. Transl. Med.* **2013**, *5*, 178ra40.
17. Bala, A.; Mondal, C.; Haldar, P.K.; Khandelwal, B. Oxidative stress in inflammatory cells of patient with rheumatoid arthritis: Clinical efficacy of dietary antioxidants. *Inflammopharmacology* **2017**, *25*, 595–607.
18. Karami, J.; Aslani, S.; Jamshidi, A.; Garshasbi, M.; Mahmoudi, M. Genetic implications in the pathogenesis of rheumatoid arthritis; an updated review. *Gene* **2019**, *702*, 8–16.
19. Takeno, M.; Kitagawa, S.; Yamanaka, J.; Teramoto, M.; Tomita, H.; Shirai, N.; Itoh, S.; Hida, S.; Hayakawa, K.; Onozaki, K.; et al. 5-Hydroxy-2-methylpyridine isolated from cigarette smoke condensate aggravates collagen-induced arthritis in mice. *Biol. Pharm. Bull.* **2018**, *41*, 877–884.

20. Croia, C.; Bursi, R.; Sutera, D.; Petrelli, F.; Alunno, A.; Puxeddu, I. One year in review 2019: Pathogenesis of rheumatoid arthritis. *Clin. Exp. Rheumatol.* **2019**, *37*, 347–357.
21. Knevel, R.; De Rooy, D.P.; Saxne, T.; Lindqvist, E.; Leijsma, M.K.; Daha, N.A.; Koeleman, B.P.; Tsonaka, R.; Houwing-Duistermaat, J.J.; Schonkeren, J.J. A genetic variant in osteoprotegerin is associated with progression of joint destruction in rheumatoid arthritis. *Arthritis Res. Ther.* **2014**, *16*, R108.
22. de Rooy, D.P.; Tsonaka, R.; Andersson, M.L.; Forslind, K.; Zhernakova, A.; Frank-Bertoncelj, M.; de Kovel, C.G.; Koeleman, B.P.; van der Heijde, D.M.; Huizinga, T.W. Genetic factors for the severity of ACPA-negative rheumatoid arthritis in 2 cohorts of early disease: A genome-wide study. *J. Rheumatol.* **2015**, *42*, 1383–1391.
23. Van Vollenhoven, R.F. Progress in RA genetics, pathology and therapy. *Nat. Rev. Rheumatol.* **2013**, *9*, 70–72.
24. Hanaoka, B.Y.; Ithurburn, M.P.; Rigsbee, C.A.; Bridges, S.L.; Moellering, D.R.; Gower, B.; Bamman, M. Chronic inflammation in RA: Mediator of skeletal muscle pathology and physical impairment. *Arthritis Care Res.* **2020**, *71*, 173–177.
25. Huffman, K.M.; Jessee, R.; Andonian, B.; Davis, B.N.; Narowski, R.; Huebner, J.L.; Kraus, V.B.; McCracken, J.; Gilmore, B.F.; Tune, K.N.; et al. Molecular alterations in skeletal muscle in rheumatoid arthritis are related to disease activity, physical inactivity, and disability. *Arthritis Res. Ther.* **2017**, *19*, 12.
26. VanderVeen, B.N.; Fix, D.K.; Carson, J.A. Disrupted skeletal muscle mitochondrial dynamics, mitophagy, and biogenesis during cancer cachexia: A role for inflammation. *Oxid. Med. Cell. Longev.* **2017**, *2017*, 3292087.
27. Petersen, K.F.; Dufour, S.; Befroy, D.; Garcia, R.; Shulman, G.I. Impaired mitochondrial activity in the insulin-resistant offspring of patients with type 2 diabetes. *N. Engl. J. Med.* **2004**, *350*, 664–671.
28. Giles, J.T.; Danielides, S.; Szklo, M.; Post, W.S.; Blumenthal, R.S.; Petri, M.; Schreiner, P.J.; Budoff, M.; Detrano, R.; Bathon, J.M. Insulin resistance in rheumatoid arthritis: Disease-related indicators and associations with the presence and progression of subclinical atherosclerosis. *Arthritis Rheumatol.* **2015**, *67*, 626–636.
29. Lanchais, K.; Capel, F.; Tournadre, A. Could omega 3 fatty acids preserve muscle health in rheumatoid arthritis? *Nutrients* **2020**, *12*, 223.
30. Baker, J.F.; Mostoufi-Moab, S.; Long, J.; Zemel, B.; Ibrahim, S.; Taratuta, E.; Leonard, M.B. Intramuscular fat accumulation and associations with body composition, strength, and physical functioning in patients with rheumatoid arthritis. *Arthritis Care Res.* **2018**, *70*, 1727–1734.
31. Filippin, L.I.; Vercelino, R.; Marroni, N.P.; Xavier, R.M. Redox signalling and the inflammatory response in rheumatoid arthritis. *Clin. Exp. Immunol.* **2008**, *152*, 415–422.
32. Quinonez-Flores, C.M.; Gonzalez-Chavez, S.A.; Del Rio Najera, D.; Pacheco-Tena, C. Oxidative stress relevance in the pathogenesis of the rheumatoid arthritis: A systematic review. *Biomed Res. Int.* **2016**, *2016*.
33. Das, D.C.; Jahan, I.; Uddin, M.G.; Hossain, M.M.; Chowdhury, M.A.Z.; Fardous, Z.; Rahman, M.M.; Kabir, A.K.M.H.; Deb, S.R.; Siddique, M.A.B.; et al. Serum CRP, MDA, Vitamin C, and trace elements in Bangladeshi patients with rheumatoid arthritis. *Biol. Trace Elem. Res.* **2021,** *199***,** 76-84.
34. Aryaeian, N.; Djalali, M.; Shahram, F.; Jazayeri, S.H.; Chamari, M.; Nazari, S.A. Beta-carotene, vitamin E, MDA, glutathione reductase and arylesterase activity levels in patients with active rheumatoid arthritis. *Iran. J. Public Health* **2011**, *40*, 102–109.
35. Hassan, M.Q.; Hadi, R.A.; Al-Rawi, Z.S.; Padron, V.A.; Stohs, S.J. The glutathione defense system in the pathogenesis of rheumatoid arthritis. *J. Appl. Toxicol.* **2001**, *21*, 69–73.
36. Kalpakcioglu, B.; Senel, K. The interrelation of glutathione reductase, catalase, glutathione peroxidase, superoxide dismutase, and glucose-6-phosphate in the pathogenesis of rheumatoid arthritis. *Clin. Rheumatol.* **2008**, *27*, 141–145.
37. Veselinovic, M.; Barudzic, N.; Vuletic, M.; Zivkovic, V.; Tomic-Lucic, A.; Djuric, D.; Jakovljevic, V. Oxidative stress in rheumatoid arthritis patients: Relationship to diseases activity. *Mol. Cell. Biochem.* **2014**, *391*, 225–232.

38. Hansson, G.K.; Libby, P. The immune response in atherosclerosis: A double-edged sword. *Nat. Rev. Immunol.* **2006**, *6*, 508–519.
39. Hassan, S.Z.; Gheita, T.A.; Kenawy, S.A.; Fahim, A.T.; Sorougy, I.M.E.-; Abdou, M.S. Oxidative stress in systemic lupus erythematosus and rheumatoid arthritis patients: Relationship to disease manifestations and activity. *Int. J. Rheum. Dis.* **2011**, *14*, 325–331.
40. Chowdhury, C.S.; Giaglis, S.; Walker, U.A.; Buser, A.; Hahn, S.; Hasler, P. Enhanced neutrophil extracellular trap generation in rheumatoid arthritis: Analysis of underlying signal transduction pathways and potential diagnostic utility. *Arthritis Res. Ther.* **2014**, *16*, R122.
41. Pérez-Sánchez, C.; Ruiz-Limón, P.; Aguirre, M.A.; Jiménez-Gómez, Y.; Rosa, I.A. la; Ábalos-Aguilera, M.C.; Rodriguez-Ariza, A.; Castro-Villegas, M.C.; Ortega-Castro, R.; Segui, P.; et al. Diagnostic potential of NETosis-derived products for disease activity, atherosclerosis and therapeutic effectiveness in Rheumatoid Arthritis patients. *J. Autoimmun.* **2017**, *82*, 31–40.
42. Karaman, A.; Binici, D.N.; Melikoğlu, M.A. Comet assay and analysis of micronucleus formation in patients with rheumatoid arthritis. *Mutat. Res. Toxicol. Environ. Mutagen.* **2011**, *721*, 1–5.
43. Hajizadeh, S.; DeGroot, J.; TeKoppele, J.M.; Tarkowski, A.; Collins, L.V. Extracellular mitochondrial DNA and oxidatively damaged DNA in synovial fluid of patients with rheumatoid arthritis. *Arthritis Res. Ther.* **2003**, *5*, R234–R240.
44. Stamp, L.K.; Khalilova, I.; Tarr, J.M.; Senthilmohan, R.; Turner, R.; Haigh, R.C.; Winyard, P.G.; Kettle, A.J. Myeloperoxidase and oxidative stress in rheumatoid arthritis. *Rheumatology* **2012**, *51*, 1796–1803.
45. Phull, A.-R.; Nasir, B.; Haq, I. ul; Kim, S.J. Oxidative stress, consequences and ROS mediated cellular signaling in rheumatoid arthritis. *Chem. Biol. Interact.* **2018**, *281*, 121–136.
46. García-González, A.; Gaxiola-Robles, R.; Zenteno-Savín, T. Oxidative stress in patients with rheumatoid arthritis. *Rev. Invest. Clin.* **2015**, *67*, 46–53.
47. Tetik, S.; Ahmad, S.; Alturfan, A.A.; Fresko, I.; Disbudak, M.; Sahin, Y.; Aksoy, H.; Yardimci, K.T. Determination of oxidant stress in plasma of rheumatoid arthritis and primary osteoarthritis patients. *Indian, J. Biochem. Biophys.* **2010**, *47*, 353–358.
48. Toukap, A.N.; Delporte, C.; Noyon, C.; Franck, T.; Rousseau, A.; Serteyn, D.; Raes, M.; Vanhaeverbeek, M.; Moguilevsky, N.; Nève, J.; et al. Myeloperoxidase and its products in synovial fluid of patients with treated or untreated rheumatoid arthritis. *Free Radic. Res.* **2014**, *48*, 461–465.
49. Datta, S.; Kundu, S.; Ghosh, P.; De, S.; Ghosh, A.; Chatterjee, M. Correlation of oxidant status with oxidative tissue damage in patients with rheumatoid arthritis. *Clin. Rheumatol.* **2014**, *33*, 1557–1564.
50. Dalle-Donne, I.; Rossi, R.; Colombo, R.; Giustarini, D.; Milzani, A. Biomarkers of oxidative damage in human disease. *Clin. Chem.* **2006**, *52*, 601–623.
51. Ersoy, Y.; Ozerol, E.; Baysal, O.; Temel, I.; MacWalter, R.S.; Meral, U.; Altay, Z.E. Serum nitrate and nitrite levels in patients with rheumatoid arthritis, ankylosing spondylitis, and osteoarthritis. *Ann. Rheum. Dis.* **2002**, *61*, 76–78.
52. Nicholls, S.J.; Hazen, S.L. Myeloperoxidase, modified lipoproteins, and atherogenesis. *J. Lipid Res.* **2009**, *50*, S346–S351.
53. Šoltés, L.; Mendichi, R.; Kogan, G.; Schiller, J.; Stankovská, M.; Arnhold, J. Degradative action of reactive oxygen species on hyaluronan. *Biomacromolecules* **2006**, *7*, 659–668.
54. Bello, H.; Dandare, A.; Danmaliki, G. Effects of cigarette smoking on lipid peroxidation and serum antioxidant vitamins. *IOSR J. Pharm. Biol. Sci.* **2017**, *12*, 40–44.
55. Gornati, R.; Colombo, G.; Clerici, M.; Rossi, F.; Gagliano, N.; Riva, C.; Colombo, R.; Dalle-Donne, I.; Bernardini, G.; Milzani, A. Protein carbonylation in human endothelial cells exposed to cigarette smoke extract. *Toxicol Lett.* **2013**, *218*, 118–28.
56. Colombo, G.; Garavaglia, M.L.; Astori, E.; Giustarini, D.; Rossi, R.; Milzani, A.; Dalle-Donne, I. Protein carbonylation in human bronchial epithelial cells exposed to cigarette smoke extract. *Cell Biol. Toxicol.* **2019**, *35*, 345–360.
57. Bochkov, V.N.; Oskolkova, O.V.; Birukov, K.G.; Levonen, A.-L.; Binder, C.J.; Stöckl, J. Generation and biological activities of oxidized phospholipids. *Antioxid. Redox Signal.* **2009**, *12*, 1009–1059.

58. Phaniendra, A.; Jestadi, D.B.; Periyasamy, L. Free radicals: Properties, sources, targets, and their implication in various diseases. *Indian, J. Clin. Biochem.* **2015**, *30*, 11–26.
59. Ediz, L.; Hiz, O.; Ozkol, H.; Gulcu, E.; Toprak, M.; Ceylan, M.F. Relationship between anti-CCP antibodies and oxidant and anti-oxidant activity in patients with rheumatoid arthritis. *Int. J. Med. Sci.* **2011**, *8*, 139–147.
60. Mishra, R.; Singh, A.; Chandra, V.; Negi, M.P.S.; Tripathy, B.C.; Prakash, J.; Gupta, V. A comparative analysis of serological parameters and oxidative stress in osteoarthritis and Rheumatoid arthritis. *Rheumatol. Int.* **2012**, *32*, 2377–2382.
61. Alver, A.; Şentürk, A.; Çakirbay, H.; Menteşe, A.; Gökmen, F.; Keha, E.E.; Uçar, F. Carbonic anhydrase II autoantibody and oxidative stress in rheumatoid arthritis. *Clin. Biochem.* **2011**, *44*, 1385–1389.
62. Shah, D.; A. Wanchu; Bhatnagar, A. Interaction between oxidative stress and chemokines: Possible pathogenic role in systemic lupus erythematosus and rheumatoid arthritis. *Immunobiology* **2011**, *216*, 1010–1017.
63. Desai, P.B.; S. Manjunath; Sumangala, K.; Chetana, K.; Vanishree, J. Oxidative stress and enzymatic antioxidant status in rheumatoid arthritis: A case control study. *Eur. Rev. Med. Pharmacol. Sci.* **2010**, *14*, 959–967.
64. Łuczaj, W.; Gindzienska-Sieskiewicz, E.; Jarocka-Karpowicz, I.; Andrisic, L.; Sierakowski, S.; Zarkovic, N.; Waeg, G.; Skrzydlewska, E. The onset of lipid peroxidation in rheumatoid arthritis: Consequences and monitoring. *Free Radic. Res.* **2016**, *50*, 304–313.
65. Thiele, G.M.; Duryee, M.J.; Anderson, D.R.; Klassen, L.W.; Mohring, S.M.; Young, K.A.; Benissan-Messan, D.; Sayles, H.; Dusad, A.; Hunter, C.D.; et al. Malondialdehyde-acetaldehyde adducts and anti-malondialdehyde-acetaldehyde antibodies in rheumatoid arthritis. *Arthritis Rheumatol.* **2015**, *67*, 645–655.
66. Staro´n, A.; G. Mąkosa; Koter-Michalak, M. Oxidative stress in erythrocytes from patients with rheumatoid arthritis. *Rheumatol. Int.* **2012**, *32*, 331–334.
67. Rho, Y.H.; Chung, C.P.; Oeser, A.; Solus, J.F.; Gebretsadik, T.; Shintani, A.; Raggi, P.; Milne, G.L.; Stein, C.M. Interaction between oxidative stress and high-density lipoprotein cholesterol is associated with severity of coronary artery calcification in rheumatoid arthritis. *Arthritis Care Res.* **2010**, *62*, 1473–1480.
68. Kwaśny-Krochin, B.; Głuszko, P.; Undas, A. Plasma asymmetric dimethylarginine in active rheumatoid arthritis: Links with oxidative stress and inflammation. *Pol. Arch. Med. Wewn.* **2012**, *122*, 270–276.
69. Calder, P.C. n-3 polyunsaturated fatty acids, inflammation, and inflammatory diseases. *Am. J. Clin. Nutr.* **2006**, *83*, 1505S–19.
70. Ruggiero, C.; Lattanzio, F.; Lauretani, F.; Gasperini, B.; Andres-Lacueva, C.; Cherubini, A. n-3 polyunsaturated fatty acids and immune-mediated diseases: Inflammatory bowel disease and rheumatoid arthritis. *Curr. Pharm. Des.* **2009**, *15*, 4135–4148.
71. Cleland, L.G.; James, M.J. Rheumatoid arthritis and the balance of dietary n-6 and n-3 essential fatty acids. *Br. J. Rheumatol.* **1997**, *36*, 513–514.
72. Kromann, N.; Green, A. Epidemiological studies in the Upernavik district, Greenland. Incidence of some chronic diseases 1950-74. *Acta Med* **1980**, *208*, 401–406.
73. Linos, A.; Kaklamani, V.G.; Kaklamani, E.; Koumantaki, Y.; Giziaki, E.; Papazoglou, S.; Mantzoros, C.S. Dietary factors in relation to rheumatoid arthritis: A role for olive oil and cooked vegetables? *Am. J. Clin. Nutr.* **1999**, *70*, 1077–1082.
74. Linos, A.; Kaklamanis, E.; Kontomerkos, A.; Koumantaki, Y.; Gazi, S.; Vaiopoulos, G.; Tsokos, G.C.; Kaklamanis, P. The effect of olive oil and fish consumption on rheumatoid arthritis—A case control study. *Scand. J. Rheumatol.* **1991**, *20*, 419–426.
75. Kavanaugh, A. Dyslipoproteinaemia in a subset of patients with rheumatoid arthritis. *Ann. Rheum. Dis.* **1994**, *53*, 551–552.
76. Dessein, P.H.; Joffe, B.I.; Veller, M.G.; Stevens, B.A.; Tobias, M.; Reddi, K.; Stanwix, A.E. Traditional and nontraditional cardiovascular risk factors are associated with atherosclerosis in rheumatoid arthritis. *J. Rheumatol.* **2005**, *32*, 435–442.

77. Curtis, J.R.; John, A.; Baser, O. Dyslipidemia and changes in lipid profiles associated with rheumatoid arthritis and initiation of anti-tumor necrosis factor therapy. *Arthritis Care Res.* **2012**, *64*, 1282–1291.
78. Bag-Ozbek, A.; Giles, J.T. Inflammation, adiposity, and atherogenic dyslipidemia in rheumatoid arthritis: Is there a paradoxical relationship? *Curr. Allergy Asthma Rep.* **2015**, *15*, 1–10.
79. Park, Y.B.; Lee, S.K.; Lee, W.K.; Suh, C.H.; Lee, C.W.; Lee, C.H.; Song, C.H.; Lee, J. Lipid profiles in untreated patients with rheumatoid arthritis. *J. Rheumatol.* **1999**, *26*, 1701–1704.
80. Kowsalya, R.; Sreekantha; Chandra, V.; Remya Dyslipidemia with altered oxidant– antioxidant status in rheumatoid arthritis. *Int. J. Pharma Bio Sci.* **2011**, *2*, 424–428.
81. Boers, M.; Nurmohamed, M.T.; Doelman, C.J.A.; Lard, L.R.; Verhoeven, A.C.; Voskuyl, A.E.; Huizinga, T.W.J.; Stadt, R.J.; Dijkmans, B.A.C.; Linden, S. Influence of glucocorticoid and disease activity on total and high density lipoprotein cholesterol in patients with rheumatoid arthritis. *Ann Rheum Dis* **2003**, *62*, 842–845.
82. Charles-schoeman, C.; Fleischmann, R.; Davignon, J.; Schwartz, H.; Turner, S.M.; Beysen, C.; Milad, M.; Hellerstein, M.K.; Luo, Z.; Kaplan, I. V; et al. Potential mechanisms leading to the abnormal lipid profile in patients with rheumatoid arthritis versus healthy volunteers and reversal by Tofacitinib. *Arthritis Rheumatol.* **2015**, *67*, 616–625.
83. Singh, H.V.; Shrivastava, A.K.; Raizada, A.; Singh, S.K.; Pandey, A.; Singh, N.; Yadav, D.; Sharma, H. Atherogenic lipid profile and high sensitive C-reactive protein in patients with rheumatoid arthritis. *Clin. Biochem.* **2013**, *46*, 1007–1012.
84. Cacciapaglia, F.; Anelli, M.G.; Rinaldi, A.; Serafino, L.; Covelli, M.; Scioscia, C.; Iannone, F.; Lapadula, G. Lipid profile of rheumatoid arthritis patients treated with anti-tumor necrosis factor-alpha drugs changes according to disease activity and predicts clinical response. *Drug Dev. Res.* **2014**, *75*, S77–S80.
85. Myasoedova, E.; Crowson, C.S.; Kremers, H.M.; Roger, V.L.; Fitz-gibbon, P.D.; Therneau, T.M.; Gabriel, S.E. Lipid paradox in rheumatiod arthritis: The impact of serum lipid measures and systemic inflammation on the risk of cardiovascular disease. *Ann. Rheum. Dis.* **2012**, *70*, 482–487.
86. Carmena, R.; Duriez, P.; Fruchart, J.C. Atherogenic lipoprotein particles in atherosclerosis. *Circulation* **2004**, *109*, III–2–III–7.
87. Nowak, B.; Madej, M.; Łuczak, A.; Małecki, R.; Wiland, P. Disease activity, oxidized-LDL fraction and anti-oxidized LDL antibodies influence cardiovascular risk in rheumatoid arthritis. *Adv. Clin. Exp. Med.* **2016**, *25*, 43–50.
88. Ajeganova, S.; Faire, U. de; Jogestrand, T.; Frostegård, J.; Hafström, I. Carotid atherosclerosis, disease measures, oxidized low-density lipoproteins, and atheroprotective natural antibodies for cardiovascular disease in early rheumatoid arthritis—An inception cohort study. *J. Rheumatol.* **2012**, *39*, 1146–1154.
89. Hitchon, C.A.; El-Gabalawy, H.S. Oxidation in rheumatoid arthritis. *Arthritis Res. Ther.* **2004**, *6*, 265–278.
90. Charles-Schoeman, C.; Watanabe, J.; Lee, Y.Y.; Furst, D.E.; Amjadi, S.; Elashoff, D.; Park, G.; McMahon, M.; Paulus, H.E.; Fogelman, A.M.; et al. Abnormal function of high-density lipoprotein is associated with poor disease control and an altered protein cargo in rheumatoid arthritis. *Arthritis Rheum.* **2009**, *60*, 2870–2879.
91. Zhao, Y.Y.; Cheng, X. long; Lin, R.C. Lipidomics Applications for Discovering Biomarkers of Diseases in Clinical Chemistry; *Int. Rev. Cell Mol. Biol.* **2014**; *313*, 1-26.
92. Lv, J.; Zhang, L.; Yan, F.; Wang, X. Clinical lipidomics: A new way to diagnose human diseases. *Clin. Transl. Med.* **2018**, *7*, 10–12.
93. Rodríguez-Carrio, J.; Alperi-López, M.; López, P.; Ballina-García, F.J.; Suárez, A. Non-esterified fatty acids profiling in rheumatoid arthritis: Associations with clinical features and Th1 response. *PLoS ONE* **2016**, *11*, 1–17.
94. Fraser, D.A.; Thoen, J.; Rustan, A.C.; Førre, Ø.; Kjeldsen-Kragh, J. Changes in plasma free fatty acid concentrations in rheumatoid arthritis patients during fasting and their effects upon T-lymphocyte proliferation. *Rheumatology* **1999**, *38*, 948–952.

95. Kremer, J.M.; Michalek, A.V.; Lininger, L.; Huyck, C.; Bigauoette, J.; Timchalk, M.A.; Rynes, R.I.; Zieminski, J.; Bartholomew, L.E. Effects of manipulation of dietary fatty acids on clinical manifestations of rheumatoid arthritis. *Lancet* **1985**, *1*, 184–187.
96. Jäntti, J.; Nikkari, T.; Solakivi, T.; Vapaatalo, H.; Isomaki, H. Evening primrose oil in rheumatoid arthritis: Changes in serum lipids and fatty acids. *Ann. Rheum. Dis.* **1989**, *48*, 124–127.
97. Jacobsson, L.; Lindgarde, F.; Manthorpe, R.; Akesson, B. Correlation of fatty acid composition of adipose tissue lipids and serum phosphatidylcholine and serum concentrations of micronutrients with disease duration in rheumatoid arthritis. *Ann. Rheum. Dis.* **1990**, *49*, 901–905.
98. Bruderlein, H.; Daniel, R.; Boismenu, D.; Julien, N.; Couture, F. Fatty acid profiles of serum phospholipids in patients suffering rheumatoid arthritis. *Prog. Lipid Res.* **1981**, *20*, 625–631.
99. Suryaprabha, P.; Das, U.N.; Ramesh, G.; Kumar, K.V.; Kumar, G.S. Reactive oxygen species, lipid peroxides and essential fatty acids in patients with rheumatoid arthritis and systemic lupus erythematosus. *Prostaglandins Leukot. Essent. Fat. Acids* **1991**, *43*, 251–255.
100. Hafström, I.; Ringertz, B.; Gyllenhammar, H.; Palmblad, J.; Harms-Ringdahl, M. Effects of fasting on disease activity, neutrophil function, fatty acid composition, and leukotriene biosynthesis in patients with rheumatoid arthritis. *Arthritis Rheum.* **1988**, *31*, 585–592.
101. Haugen, M.A.; Kjeldsen-Kragh, J.; Bjervea, K.S.; Høstmark, A.T.; Førre, Ø. Changes in plasma phospholipid fatty acids and their relationship to disease activity in rheumatoid arthritis patients treated with a vegetarian diet. *Br. J. Nutr.* **1994**, *72*, 555–566.
102. Remans, P.H.J.; Sont, J.K.; Wagenaar, L.W.; Wouters-Wesseling, W.; Zuijderduin, W.M.; Jongma, A.; Breedveld, F.C.; van Laar, J.M. Nutrient supplementation with polyunsaturated fatty acids and micronutrients in rheumatoid arthritis: Clinical and biochemical effects. *Eur. J. Clin. Nutr.* **2004**, *58*, 839–845.
103. Ferber, E.; De Pasquale, G.G.; Resch, K. Phospholipid metabolism of stimulated lymphocytes. Composition of phospholipd fatty acids. *Biochim. Biophys. Acta*. **1975**, *398*, 364–376.
104. Svensson, K.; Lundqvist, G.; Wide, L.; Hallgren, R. Impaired glucose handling in active rheumatoid arthritis: Relationship to the secretion of insulin and counter-regulatory hormones. *Metabolism* **1987**, *36*, 944–948.
105. Brenner, R. Nutritional and hormonal factors influencing desaturation of essential fatty acids. *Prog Lipid Res* **1982**, *20*, 41–48.
106. Santoli, D.; Phillips, P.D.; Colt, T.L.; Zurier, R.B. Suppression of interleukin-2 dependent human T cell growth in vitro by Prostaglandin E and their precursor fatty acids. *J. Clin. Invest.* **1990**, *85*, 424–432.
107. Athanassiou, P.; Athanassiou, L.; Kostoglou-Athanassiou, I. Nutritional pearls: Diet and rheumatoid arthritis. *Mediterr. J. Rheumatol.* **2020**, *31*, 319–324.
108. Rossetti, R.; Seiler, C.; DeLuca, P.; Laposata, M.; Zurier, R. Oral administration of unsaturated fatty acids: Effects on human peripheral blood T lymphochyte proliferation. *J. Leukoc. Biol.* **1997**, *62*, 438–443.
109. Purasiri, P.; McKechnie, A.; Heys, S.; Eremin, O. Modulation in vitro of human natural cytotoxicity, lymphocyte proliferative response to mitogens and cytokine production by essential fatty acids. *Immunology* **1997**, *92*, 166–172.
110. Søyland, E.; Nenseter, M.; Braathen, L.; Drevon, C. Very long chain n-3 and n-6 polyunsaturated fatty acids inhibit proliferation of human T-lymphocytes in vitro. *Eur. J. Clin. Invest.* **1993**, *23*, 112–121.
111. Proudman, S.M.; Cleland, L.G.; Metcalf, R.G.; Sullivan, T.R.; Spargo, L.D.; James, M.J. Plasma n-3 fatty acids and clinical outcomes in recent-onset rheumatoid arthritis. *Br. J. Nutr.* **2015**, *114*, 885–890.
112. Kremer, J.M. n-3 fatty acid supplements in rheumatoid arthritis. *Am. J. Clin. Nutr.* **2000**, *71*, 349S–351S.
113. Łuczaj, W.; Moniuszko-Malinowska, A.; Domingues, P.; Domingues, M.R.; Gindzienska-Sieskiewicz, E.; Skrzydlewska, E. Plasma lipidomic profile signature of rheumatoid arthritis versus Lyme arthritis patients. *Arch. Biochem. Biophys.* **2018**, *654*, 105–114.

114. Fuchs, B.; Schiller, J.; Wagner, U.; Häntzschel, H.; Arnold, K. The phosphatidylcholine/ lysophosphatidylcholine ratio in human plasma is an indicator of the severity of rheumatoid arthritis: Investigations by 31 P NMR and MALDI-TOF MS. *Clin. Biochem.* **2005**, *38*, 925–933.
115. Rikitake, Y.; Hirata, K.; Kawashima, S.; Takeuchi, S.; Shimokawa, Y.; Kojima, Y.; Inoue, N.; Yokoyama, M. Signaling mechanism underlying COX-2 induction by lysophosphatidylcholine. *Biochem. Biophys. Res. Commun.* **2001**, *281*, 1291–1297.
116. Domingues, M.R.M.; Reis, A.; Domingues, P. Mass spectrometry analysis of oxidized phospholipids. *Chem. Phys. Lipids* **2008**, *156*, 1–12.
117. Miltenberger-Miltenyi, G.; Cruz-Machado, A.R.; Saville, J.; Conceição, V.A.; Calado, Â.; Lopes, I.; Fuller, M.; Fonseca, J.E. Increased monohexosylceramide levels in the serum of established rheumatoid arthritis patients. *Rheumatology* **2020**, *59*, 2085–2089.
118. Charles-Schoeman, C.; Meriwether, D.; Lee, Y.Y.; Shahbazian, A.; Reddy, S.T. High levels of oxidized fatty acids in HDL are associated with impaired HDL function in patients with active rheumatoid arthritis. *Clin. Rheumatol.* **2018**, *37*, 615–622.
119. Morgantini, C.; Natali, A.; Boldrini, B.; Imaizumi, S.; Navab, M.; Fogelman, A.M.; Ferrannini, E.; Reddy, S.T. Anti-inflammatory and antioxidant properties of HDLs are impaired in type 2 diabetes. *Diabetes* **2011**, *60*, 2617–2623.
120. Imaizumi, S.; Grijalva, V.; Navab, M.; Lenten, B.J. Van; Wagner, A.C.; Anantharamaiah, G.M.; Fogelman, A.M.; Reddy, S.T. L-4F differentially alters plasma levels of oxidized fatty acids resulting in more anti-inflammatory HDL in mice. *Drug. Metab. Lett.* **2010**, *4*, 139–148.
121. Seidman, A.J.; Limaiem, F. Synovial Fluid Analysis. In *StatPearls*; Treasure Island (FL), StatPearls Publishing: 2020.
122. Kim, I.C.; Cohen, A.S. Synovial fluid fatty acid composition in patients with rheumatoid arthritis, gout and degenerative joint disease. *Proc. Soc. Exp. Biol. Med.* **1966**, *123*, 77–80.
123. Newcombe, D.S.; Cohen, A.S. Chylous synovial effusion in rheumatoid arthritis: Clinical and pathogenetic significance. *Am. J. Med.* **1965**, *38*, 156–164.
124. Harifi, G.; Sibilia, J. Pathogenic role of platelets in rheumatoid arthritis and systemic autoimmune diseases: Perspectives and therapeutic aspects. *Saudi Med. J.* **2016**, *37*, 354–360.
125. Olumuyiwa-Akeredolu, O.-O.O.; Pretorius, E. Platelet and red blood cell interactions and their role in rheumatoid arthritis. *Rheumatol. Int.* **2015**, *35*, 1955–1964.
126. Masoom-Yasinzai, M. Altered fatty acid, cholesterol and Na+/K+ ATPase activity in erythrocyte membrane of rheumatoid arthritis patients. *Z. Nat. C. J. Biosci.* **1996**, *51*, 401–403.
127. Lee, A.L.; Park, Y. The association between n-3 polyunsaturated fatty acid levels in erythrocytes and the risk of rheumatoid arthritis in Korean Women. *Ann. Nutr. Metab.* **2013**, *63*, 88–95.
128. Park, Y.; Lee, A.R.; Shim, S.C.; Lee, J.H.; Choe, J.Y.; Ahn, H.; Choi, C.B.; Sung, Y.K.; Bae, S.C. Effect of n-3 polyunsaturated fatty acid supplementation in patients with rheumatoid arthritis: A 16-week randomized, double-blind, placebo-controlled, parallel-design multicenter study in Korea. *J. Nutr. Biochem.* **2013**, *24*, 1367–1372.
129. Calder, P.C. Immunomodulation by omega-3 fatty acids. *Prostaglandins Leukot Essent Fat. Acids* **2007**, *77*, 327–335.
130. Gu, Y.; Lu, C.; Zha, Q.; Kong, H.; Lu, X.; Lu, A.; Xu, G. Plasma metabonomics study of rheumatoid arthritis and its Chinese medicine subtypes by using liquid chromatography and gas chromatography coupled with mass spectrometry. *Mol. Biosyst.* **2012**, *8*, 1535–1543.
131. Deane, K.D.; Norris, J.M.; Holers, V.M. Preclinical rheumatoid arthritis: Identification, evaluation, and future directions for investigation. *Rheum. Dis. Clin. N. Am.* **2010**, *36*, 213–241.
132. Deane, K.D.; El-Gabalawy, H. Pathogenesis and prevention of rheumatic disease: Focus on preclinical RA and SLE. *Nat. Rev. Rheumatol.* **2014**, *10*, 212–228.
133. Deane, K.D.; O'Donnell, C.I.; Hueber, W.; Majka, D.S.; Lazar, A.A.; Derber, L.A.; Gilliland, W.R.; Edison, J.D.; Norris, J.M.; Robinson, W.H.; et al. The number of elevated cytokines and chemokines in preclinical sero-positive rheumatoid arthritis predicts time to diagnosis in an age-dependent manner. *Arthritis Rheum.* **2010**, *62*, 3161–3172.
134. Greenblatt, H.K.; Kim, H.A.; Bettner, L.F.; Deane, K.D. Preclinical rheumatoid arthritis and rheumatoid arthritis prevention. *Curr. Opin. Rheumatol.* **2020**, *32*, 289–296.

135. Gan, R.W.; Young, K.A.; Zerbe, G.O.; Kristen Demoruelle, M.; Weisman, M.H.; Buckner, J.H.; Gregersen, P.K.; Mikuls, T.R.; O'Dell, J.R.; Keating, R.M.; et al. Lower omega-3 fatty acids are associated with the presence of anti-cyclic citrullinated peptide autoantibodies in a population at risk for future rheumatoid arthritis: A nested case-control study. *Rheumatology* **2016**, *55*, 367–376.
136. Gan, R.W.; Demoruelle, M.K.; Deane, K.D.; Weisman, M.H.; Buckner, J.H.; Gregersen, P.K.; Mikuls, T.R.; O'Dell, J.R.; Keating, R.M.; Fingerlin, T.E.; et al. Omega-3 fatty acids are associated with a lower prevalence of autoantibodies in shared epitope-positive subjects at risk for rheumatoid arthritis. *Ann. Rheum. Dis.* **2017**, *76*, 147–152.
137. Pablo, P. de; Romaguera, D.; Fisk, H.L.; Calder, P.C.; Quirke, A.M.; Cartwright, A.J.; Panico, S.; Mattiello, A.; Gavrila, D.; Navarro, C.; et al. High erythrocyte levels of the n-6 polyunsaturated fatty acid linoleic acid are associated with lower risk of subsequent rheumatoid arthritis in a Southern European nested case–control study. *Ann. Rheum. Dis.* **2018**, *77*, 981–987.
138. McGrath, C.M.; Young, S.P. Lipid and metabolic changes in rheumatoid arthritis. *Curr. Rheumatol. Rep.* **2015**, *17*, 57.
139. Cas, M.D.; Roda, G.; Li, F.; Secundo, F. Functional lipids in autoimmune inflammatory diseases. *Int. J. Mol. Sci.* **2020**, *21*, 1-19.

3.2. CHAPTER 3.2: LOOKING IN DEPTH AT OXIDIZED CHOLESTERYL ESTERS

This chapter was integrally published as follows.
Reprinted with permission from:

H. B. Ferreira, C. Barros, T. Melo, A. Paiva, M. R. Domingues, Looking in Depth at Oxidized Cholesteryl Esters by LC−MS/MS: Reporting Specific Fragmentation Fingerprints and Isomer Discrimination, *Journal of the American Society for Mass Spectrometry* (2022), volume 33, issue 5, pages 793-802
https://doi.org/10.1021/jasms.1c00370

Abstract

Cholesteryl esters (CE) are prone to oxidation under increased oxidative stress conditions, but little is known about oxidized CE species (oxCE). To date, only a few oxCE have been identified, however mainly based on the detection of molecular ions by mass spectrometry (MS) or target approaches for specific oxCE. The study of oxCE occurring from radical oxidation is still scarcely addressed. In this work, we made a comprehensive assessment of oxCE derivatives and their specific fragmentation patterns to identify detailed structural features and isomer differentiation, using high resolution C18 HPLC-MS and MS/MS based lipidomic approaches. The LC-MS/MS analysis allowed to pinpoint oxCE structural isomers of long-chain and short-chain species, eluting at different RT. Data analysis revealed that oxCE can be modified either in the fatty acyl moiety or in the cholesterol ring. The location of the hydroxy/hydroperoxy group originates character-istic fragment ions, namely the unmodified cholestenyl cation (m/z 369) for the isomer with oxidation in the fatty acyl chain, or ions at m/z 367 and m/z 385 (369+16) when oxygenation occurs in the cholesterol ring. Additionally, we identified CE 18:2 and 20:4 aldehydic and carboxylic short-chain products that showed a clear fragmentation pattern that confirmed the modification in the fatty acyl chain. Specific fragmentation fingerprinting allowed discrimination of the isobaric short-chain species, namely carboxylic short-chain products, from hydroxy-aldehyde short-chain products, with hydroxy-cholesterol moiety. This new information is important to identify different oxCE in biological samples and will contribute to unravel their role in biological conditions and diseases, like cardiovascular disease.

Keywords: cholesteryl esters oxidation, mass spectrometry, lipidomics, fragmentation, isomers

1. Introduction

Cholesteryl esters (CE) are derivatives of cholesterol esterified to a saturated or unsaturated long-chain fatty acid (FA). They are main constituents of circulating lipoproteins, but CE biological roles are not fully understood[1]. However, CE are mostly considered as a preferred way to transport polyunsaturated fatty acids (PUFA), resembling the function of phosphatidylcholines (PC)[2]. In serum, enzyme lecithin-cholesterol acyl transferase associates preferentially with discoid HDL and catalyses the transfer of the *sn*-2 FA of PC to cholesterol, both constituents of the same particle, to produce CE and lysophosphatidylcholines[3]. In fact, due to its mechanism of synthesis, CE concentrations are strongly correlated with the corresponding PC subspecies concentrations in plasma and lipoproteins. Also, plasma CE composition is similar to that of PC, containing reasonably high proportions of the polyunsaturated moieties[4,5]. The presence of PUFA makes CE quite prone to oxidation under increased oxidative stress conditions associated with several diseases, generating oxidized species of CE (oxCE)[4]. oxCE may be formed by an enzymatic reaction with 15-lipoxygenase, or through lipid peroxidation induced by free radicals, like hydroxyl radical formed under oxidative stress conditions, affecting preferably the PUFA side chain[6,7]. oxCE have dissimilar properties from the non-oxidized CE[1].

Disturbed homeostasis of CE and formation of oxCE may be a consequence of disease. For instance, in cardiovascular disease oxCE are found in deposits in the fatty lesions of atherosclerotic plaques playing an important role in the disease pathology and in being a major risk of complications[8]. oxCE have been detected in lipoproteins, especially in LDL, in human blood and atherosclerotic lesions, and have been shown to initiate proinflammatory macrophage activation and foam cell formation, thus being considered a promoter of inflammation[8,9]. oxCE can also decompose to produce electrophilic reactive species, like malondialdehyde or 4-hydroxy-2-nonenal, that are able to covalently modify phosphatidylethanolamines and proteins[10,11]. Moreover, when oxCE are intracellularly hydrolysed, they release oxidized fatty acyl chains that when re-esterified can produce oxidized phospholipids, as oxidized PC[6]. However, oxCE are scarcely studied as opposed to what happens with oxidized PC.

Oxidized PC is widely studied by mass spectrometry (MS) based approaches either in biomimetic systems or in biological samples[1], and the formation of a great variety of oxidation products have been identified and characterized[12–14]. Oxidized products of PC were found to be dependent on the esterified PUFA, leading to different products with dissimilar biological functions. The successful identification of PC oxidation products and MS fingerprinting reveals itself to be important to effectively demonstrated the presence and biological role of oxidized PC and other phospholipids, using lipidomics based on MS. This is nowadays the most important methodology to study lipid modifications at a molecular level[12–14]. But there are few MS and tandem mass spectrometry (MS/MS) studies of CE and even fewer regarding oxCE[8,15–20]. oxCE were identified using MS methodologies in human atherosclerotic lesions, estimating that 23% of cholesteryl linoleate, 16% of cholesteryl arachidonate and 12% of cholesteryl docosahexaenoate are oxidized[13]. In another MS study, oxCEs have accounted for 11 to 92% of the CE bearing PUFA pool in atherosclerotic plaques[8]. However, most of the MS studies detected the presence of oxCE only through exact mass measurements of their molecular ions or target lipidomic approaches for the quantification of specific oxCE species. Those studies did not explore in detail the fragmentation patterns of such molecules to unequivocally determine the oxCE structural features and separate isomers with different locations of the oxidized moiety (either on the FA or on the cholesterol ring).

In the present study, we sought to make a comprehensive assessment of oxCE derivatives and their specific fragmentation patterns to pinpoint detailed structural features and isomer differentiation. For that, we analysed the oxidized derivatives of CE 18:1 (cholesteryl oleate), CE 18:2 (cholesteryl linoleate) and CE 20:4 (cholesteryl arachidonate) using C18 HPLC-MS and MS/MS based lipidomic approaches.

2. Methods

2.1 Reagents

Cholesteryl ester standards CE18:1 was purchased from Sigma-Aldrich and CE 18:2 (Item No. 22597) and CE 20:4 (Item No. 22595) were purchased from Cayman Chemical Company

(Michigan, USA). 1,2-dimyristoyl-*sn*-glycero-3-phosphocholine (dMPC) and 1-palmitoyl-2-linoleoyl-*sn*-glycero-3-phosphocholine (PLPC) were obtained from Avanti®. For CE oxidation, ammonium hydrogen carbonate (NH_4HCO_3) was acquired from Riedel-de Haën (Germany) and $FeCl_2 \cdot 4H_2O$ and hydrogen peroxide 30 wt.% solution in water (H_2O_2) from Sigma-Aldrich®. To analyse cholesteryl ester fragmentation by MS and MS/MS, dichloromethane and methanol were obtained from Fisher Scientific. All solvents were of high-performance liquid chromatography (HPLC) grade and were used without any additional purification.

2.2 Cholesteryl esters oxidation

Non-oxidized CE standards were incorporated in liposomes, with PC species (dMPC and PLPC) and the oxidation was induced by Fenton reaction. For that, it was transferred into a glass vial 25 µL of dMPC, 50 µL of PLPC and 50 µL of CE standard and dried under a nitrogen stream. To the dried glass vial was added 55.75 µL of NH_4HCO_3 buffer (5 mM, pH 7.4), 0.5 µL of $FeCl_2 \cdot 4H_2O$ solution (5 mM) and 6.25 µL of H_2O_2 solution (500 mM, stock solution of 30% m/v). The glass vial was vortexed for 2 minutes and sonicated for 1 minute for the formation of the vesicles. This procedure was made for each CE standard (CE 18:1, CE 18:2 and CE 20:4). The vials were placed in a vortex mixer (Thermomixer compact, Eppendorf) at 37ºC during 72h. After 72h the lipids were extracted by Folch method. Briefly, it was added 166.7 µL of dichloromethane and 83.3 µL of methanol to the glass vials with the liposomes. The mixture was vortexed and transferred into an eppendorf and centrifuged (Fisherbrand®) for 5 minutes at 4000 rpm. The organic phase (lower phase) was collected into a clean glass vial, dried under nitrogen, and stored at -20ºC.

2.3 Cholesteryl esters analysis by reverse phase LC-MS and MS/MS

oxCE extracts were dissolved in dichloromethane to have a lipid concentration of 1 µg/µL. To perform liquid chromatography-mass spectrometry (LC-MS), an aliquot of 2.6 µL of each CE was mixed with 97.4 µL of a 50/50 mixture of isopropanol/methanol. The chromatographic phase consisted of two mobile phases: eluent A (60% acetonitrile, 40% water, 10 mM ammonium formate and 0.1% formic acid) and eluent B (90% isopropanol, 10% acetonitrile, 10 mM ammonium formate and 0.1% formic acid).

CE standards and oxCE were separated by C18, using an Ascentis® Express 90 Å C18 HPLC column (15 cm x 2.1 mm; 2.7 μm, Supelco®) inserted into an HPLC system (Ultimate 3000 Dionex, Thermo Fisher Scientific, Bremen, Germany) with an autosampler coupled online to a Q-Exactive™ hybrid quadrupole Orbitrap™ mass spectrometer (Thermo Fisher Scientific, Bremen, Germany). A volume of 10 μL of each sample mixture was injected into the HPLC column, at a flow rate of 260 μL/min. The temperature of the column oven was maintained at 50 °C. The 33 minutes gradient was: 32% of mobile phase B (0 min), 45% B (1.5 min), 52% B (4 min), 58% B (5 min), 68% B (8 min), 70% B (11 min), 85% B (14 min), 97% B (18 min, held for 7 min), 32% B (25.01 min, held for 8 min). The Q-Exactive™ orbitrap mass spectrometer with a heated electrospray ionization source was operated in positive mode (electrospray voltage of 3.0 kV). The sheath gas flow was 35 U, auxiliary gas was 3 U, the capillary temperature was 320 °C, the S-lenses RF was 50 U and the probe`s temperature was 300 °C. Full scans MS spectra were acquired in positive ionisation mode in an *m/z* range of 300-1600, with a resolution of 70.000 (at *m/z* 200), automatic gain control (AGC) target of $1x10^6$ and maximum injection time of 100 ms. For tandem MS (MS/MS) experiments, a top-10 data-dependent acquisition (DDA) method was used. The top 10 most abundant precursor ions in full MS were selected to be fragmented in the collision cell using higher energy dissociation (HCD). A stepped normalized collision energy™ scheme was used and ranged between 25 and 30 eV. MS/MS spectra obtained were those combining the information obtained with the three collision energies. The MS/MS spectra were obtained with a resolution of 17,500; AGC target of $1x10^5$; an isolation window of 1 *m/z*; scan range of 200-2000 *m/z*; and maximum injection time of 100 ms. The cycles of one full scan mass spectrum and ten data-dependent MS/MS scans were repeated continuously throughout the experiments, with the dynamic exclusion of 30 s and intensity threshold of $8x10^4$. Data acquisition was carried out using the Xcalibur data system (V3.3, Thermo Fisher Scientific, USA).

3. Results

According with the main goal of this study, we evaluated the fragmentation under HCD-MS/MS and the structural features of oxidized derivatives of CE (CE 18:1, CE 18:2 and CE 20:4) formed by radical oxidation and identified by MS[8,15–20], which fragmentation has not been reported yet. The oxCE studied were the CE+O and CE+2O, corresponding respectively to the hydroxy derivative and di-hydroxy or hydroperoxy derivatives, the main long-chain oxidation products formed by hydroxyl radical as reported for PC species bearing the same unsaturated fatty acyl chain[21,22]. We also studied short-chain products that result from the cleavage of the unsaturated FA, from degradation of long-chain oxCE bearing 18:2 and 20:4, in analogy to what was reported for PC bearing the same FA[23].

Cholesteryl esters with two oxygens (CE+2O) on the sterol moiety have already been identified in several studies, however only through exact mass measurements, and no MS/MS studies were done to confirm the structural features. In fact, CE+2O can be assign as a di-hydroxy or a hydroperoxy CE derivative. CE-OOH were identified in oxidized LDL however its levels are relatively low comparing with other oxidation products like hydroxy and keto[24,25]. This seems to suggest that in biological samples there is a fast conversion of CE-OOH into its subproducts, which may hinder its detection and characterization. Hydroperoxy derivatives are the first oxidation products of free radical oxidation of PUFA. These long-chain oxidation products are formed by the addition of oxygen to the CE, preserving the backbone structure of the CE molecule. The hydroperoxy derivatives can decompose and generate other long chain products like the hydroxy and keto derivatives, among others. The long-chain product CE hydroperoxyde (CE-OOH) can also suffer cleavage of the oxidized fatty acyl chain to generate the short-chain oxidation products, where the fatty acyl chain is truncated (Figure 1)[26].

The oxidation products of CE 18:1, CE 18:2 and CE 20:4 were analysed by LC-MS after 72h of oxidation (Supporting Information Figure S1). oxCE were identified in MS as ammonium adducts, $[M+NH_4]^+$, by the RT of each oxCE species and mass accuracy (Table 1). The information regarding the RT was used to confirm the presence of oxCE isomers, namely oxCE eluting in two or more peaks at different RT.

In the analysis of the reconstructed ion chromatogram (RIC) obtained for the long-chain oxidation products (Supporting Information Figure S1), hydroxy (CE with addition of one oxygen atom, +O, +16 Da) and di-hydroxy and/or hydroperoxy (CE with addition of two atoms oxygen, +2O, +32 Da) derivatives, it was seen that, concerning oxCE 18:1, each eluted in two peaks, with shorter retention time when compared with the unmodified CE18:1. In the case of oxCE 18:2 long-chain oxidation products, CE 18:2+O eluted in two peaks and C18:2+2O eluted in three peaks. Regarding oxCE 20:4, the CE 20:4+O eluted in one peak, while C20:4+2O eluted in three unresolved peaks, probably due to the formation of several isomeric oxidation products. All the long-chain products eluted with shorter RT when compared with the unmodified ones, as expected, since the presence of oxygenated moieties in lipids are usually associated with higher polarity thus being less retained in the RP columns, when compared with the unmodified lipids. In general, oxCE with +O has shorter RT when compared with unmodified CE and the +2O has shorter RT than the CE+O. To confirm if different RT correspond to different structural isomers, all long-chain oxCE were characterized by LC-MS/MS analysis.

Short-chain products, which are formed due to cleavage of the FA chain in the vicinity of the oxidative modification, were identified by LC-MS for CE 18:2 and CE 20:4 (Supporting Information Figure S2). They were formed in lower abundances, and some also eluted in peaks with different RT suggesting the presence of structural isomers as well. The majority eluted in only one peak each, with exception of CE 18:2 C9 short-chain at *m/z* 574 that eluted in two peaks. Short-chain oxidation products of CE 18:2 were those with C9 terminal aldehyde (*m/z* 558) and carboxylic moiety (*m/z* 574) or hydroxyaldehyde (*m/z* 574), while the short oxidation products of CE 20:4 were the ones with the shorted fatty acyl chain in C9, C10 and C12 with terminal aldehyde (Table 1). All short-chain products were characterized by MS/MS and the fragmentation pathways identified will be detailed below.

3.1 Fragmentation and structural features of oxidation products of CE

Unmodified CE molecules are characterized for having a specific fragmentation pattern in the MS/MS spectra of $[M+NH_4]^+$ adducts, formed in LC-MS analysis. In the LC-HCD-MS/MS spectra it is possible to observe a major product ion at *m/z* 369.35 corresponding to the base peak of the MS/MS spectra (100% relative abundance (RA)), assigned as the cholestenyl positive ion and that is formed by the cleavage of the ester bond between the fatty acyl chain and the cholesterol ring. This fragmentation pattern confirms the presence of CE species[17,27].

The fragmentation patterns of CE oxidation products were analysed by LC-MS/MS of the corresponding $[M+NH_4]^+$ adducts. The dissociation of oxCE adducts originates several product ions in the MS/MS spectra that are diagnostically significant ions of oxCE products as will be detailed.

3.1.1 LC-MS/MS of CE 18:1 oxidation products

CE 18:1+O were assigned as the CE hydroxy derivatives (CE 18:1-OH) confirmed by exact mass measurements (Table 1), with a mass increase of +16 Da regarding the mass of the unmodified CE 18:1. The MS/MS of $[M+NH_4]^+$ ions of the two isomers of CE 18:1+O were acquired and analysed. The isomers that eluted at RT 17.25 min and 17.52 min, showed different fragmentation patterns (Supporting Information Figure S1). The isomer that eluted at shorter RT (17.25 min) showed the presence of the unmodified cholestenyl cation, at *m/z* 369.35, confirming that the oxidation occurs in the fatty acyl chain (Supporting Information Figure S3-A). The isomer that eluted at longer RT (17.52 min) showed the ion at *m/z* 385.35, that is formed by the cleavage of the ester bond with loss of the unmodified FA, indicating that CE is oxidized in the cholesterol ring $[Cholestenyl+O]^+$. The product ion at *m/z* 367.34, formed by loss of H_2O from $[Cholestenyl+O]^+$ (Supporting Information Figure S3-B), corroborates the presence of a hydroxy derivative linked to the cholesterol ring. Curiously, the isomer with oxidation in the cholesterol moiety showed higher abundance than the isomer with oxidation in the FA.

CE18:1+2O have a mass increase of +32 Da regarding the mass of the unmodified CE 18:1 and can be attributed to CE di-hydroxy derivatives (CE 18:1+$(OH)_2$), and/or to the CE

hydroperoxy derivatives. CE 18:1+2O oxidation products were confirmed by exact mass measurements and eluted in two peaks, RT 16.19 min and RT 16.56 min (Supporting information Figure S1, Table 1). The MS/MS spectrum obtained at RT 16.19 min showed the unmodified cholestenyl cation, at *m/z* 369.35, confirming the oxidation in the fatty acyl chain (Supporting information Figure S3-C). In these spectra we do not see loss of H_2O or the loss of HOOH to confirm if it is a hydroperoxy or a di-hydroxy derivatives as reported for oxidized PC in low CID MS/MS instruments[12,13]. However, it is expected to be hydroperoxy derivatives with FA bearing the hydroperoxy group since they are the main products formed in ·OH radical conditions. The isomer that eluted at RT 16.56 min showed the ion at *m/z* 367.34, that is proposed to be formed either by: i) loss of modified fatty acyl chain with a hydroxy group combined with loss of H_2O, from the hydroxycholestenyl or ii) loss of unmodified fatty acid combined with loss of HOOH from the hydroperoxycholestenyl (Supporting Information Figure S3-D). Thus, this derivative with 2 oxygens can be a di-hydroxy product with one hydroxy in the cholestenyl and the other hydroxy group in fatty acyl chain. However, the hypothesis of the hydroperoxy derivative cannot be discarded. In this manner, this detailed analysis allowed to pinpoint two isomers for the CE 18:1+2O one isomer with a hydroperoxy group linked to the FA 18:1 and another isomer most probably as a di-hydroxy derivative.

3.1.2 LC-MS/MS of CE 18:2 long-chain oxidation products

CE 18:2+O eluted in one major peak at RT 16.92 min and a minor peak at RT 17.03 min (Supporting Information Figure S1). The MS/MS spectrum of the isomer that eluted at RT 16.92 min showed the product ion at *m/z* 369.35 that confirmed the presence of an isomer with oxidation on the FA (Figure 2-A). The isomer that eluted at longer RT (17.03 min) showed the product ion at *m/z* 385.35, that is formed by the cleavage of the ester bond with loss of the unmodified FA, indicating that CE is oxidized on the cholesterol ring. This is also corroborated by the ion at *m/z* 367.34, that is formed by loss of H_2O from hydroxycholestenyl ion combined with loss of unmodified FA. The product ion at *m/z* 664.51, formed by loss of H_2O from the precursor ion $[M+NH_4]^+$, also corroborates the presence of the hydroxy moiety (Figure 2-B).

CE 18:2+2O oxidation products were also confirmed by exact mass and eluted in three peaks at RT 14.74 min, RT 15.77 min and RT 16.02 min (Supporting Information Figure S1). The most abundant isomer eluted at RT 15.77 min and the MS/MS showed the ion at *m/z* 369.35 (Figure 2-C). Interestingly, the MS/MS of the isomer at RT 14.74 min is similar, with oxidation on the FA. Therefore, the isomer that elutes with shorter retention time, thus being more polar, should be the di-hydroxy derivative (CE 18:2+$(OH)_2$), with di-hydroxy FA similar as reported for PC(16:0/18:2)-$(OH)_2$ [12], while the isomer that elutes at RT 15.77 min should be the hydroperoxy derivative with the hydroperoxy group linked to the FA. The last isomer that eluted at RT 16.02 min showed the ion at *m/z* 367.34 which is attributed to a di-hydroxy isomer with a hydroxy group linked to the cholestenyl and other to the FA. The ion at *m/z* 383 suggests the formation of a hydroperoxy isomer with loss of H_2O [Cholestenyl+OO-H_2O]$^+$ (369+32-18) where the hydroperoxy group is on the cholestenyl cation (Figure 2-D). The detailed analysis allowed to pinpoint three isomers for the CE 18:2, two isomers oxidized in FA 18:2 and other two isomers with oxidation on the cholesterol ring. To confirm the fragmentation pattern of oxCE with OOH on the FA, we performed MS/MS analysis of a commercial oxCE-OOH standard where we identified the presence of the ion at *m/z* 369 and the absence of the ion at *m/z* 367 (data not shown) corroborating our results.

3.1.3 LC-MS/MS of CE 20:4 long-chain oxidation products

The CE 20:4 hydroxy derivative eluted in one major peak at RT 16.88 min (Supporting Information Figure S1). The MS/MS spectrum revealed the presence of the ion at *m/z* 369.35, corresponding to the unmodified cholestenyl cation, indicating that the OH group is on the fatty acyl chain (Supporting Information Figure 4-A).

Regarding the CE 20:4+2O, most probably a di-hydroxy derivative, the RIC suggests the presence of several isomers eluting at different RT, however we could only obtain the MS/MS spectra for RT 15.73 min because in other RT the peak intensity of the ions were too low and we could not obtain a good MS/MS data in DDA (Supporting Information Figure S1). Nonetheless, in the MS/MS spectra of RT 15.73 min, we were able to detect several product ions that suggested the presence of two isomers that could not be isolated. The product ions

identified were: i) the ion at *m/z* 369.35 (unchanged cholestenyl cation), which indicates that the hydroperoxy group is on the FA and thus allowing to assign a hydroperoxy CE and ii) the ion at *m/z* 367.34 corresponding to an isomer with one hydroxy group linked to the cholestenyl and other hydroxy to the FA, and this justifies the loss of the hydroxy fatty acid combined with loss of water from the hydroxy cholestenyl cation (Supporting Information Figure S4-B) (the hypothesis of this isomer being a hydroperoxy derivative cannot be excluded and may be considered as well).

3.1.4 LC-MS/MS of CE 18:2 of short-chain oxidation products

Few short-chain oxidation products formed by degradation of oxCE 18:2–OOH were observed for oxCE 18:2[23]. Through LC-MS we were able to detect C9 aldehyde and carboxylic acid short-chain products of CE 18:2, with the identification of the ions at *m/z* 558.49 and *m/z* 574.48, respectively (Supporting Information Figure S2). The ion at *m/z* 558.49 eluted in one peak at RT 13.53 min while the ion at *m/z* 574.48 eluted in two peaks, at RT 10.27 min and RT 12.34 min (Supporting Information Figure S2). The relative abundances were lower compared with the hydroxy and hydroperoxy derivatives.

The LC-MS/MS spectrum of CE 18:2 C9-aldehyde at *m/z* 558.49 (RT 13.53 min) showed the presence of the unmodified cholestenyl ion, at *m/z* 369.35, confirming that the carbon chain was cleaved in C9, and without any modification on the cholesterol ring (Figure 3-A). The type of short-chain product with a terminal aldehyde was one of the products reported during Fenton oxidation of PC(16:0/18:2)[12].

In the case of CE 18:2 short-chain at *m/z* 574.48 (RT 10.27 min and RT 12.34 min), the isomer that elutes at RT 12.34 min showed, in the MS/MS, the unmodified cholestenyl ion at *m/z* 369.35 indicating the presence of a shortened C9 acyl chain with a terminal carboxylic group (COOH) as reported for the oxidation of PC(16:0-18:2)[12] (Figure 3-B). In the MS/MS spectra of the most abundant isomer at RT 10.27 min, the unmodified cholestenyl ion is absent, but instead it showed the fragment ion at *m/z* 385.35, attributed to the hydroxycholestenyl cation (*m/z* 369+O, *m/z* 369+16). This ion is indicative that, in this case, we should have an isomer with a shortened fatty acyl chain in C9 with a terminal aldehyde, and the hydroxy group being

linked to the cholesterol ring (Figure 3-C). The ion at *m/z* 367.34 is formed by loss of water from the ion at *m/z* 385.35 [Cholestenyl+O]$^+$, corroborating the modification of the cholesterol moiety. Thus, it is a hydroxyaldehyde short chain products isomer of the carboxylic short chain oxCE.

The cholestenyl ion at *m/z* 369.35 was identified in the MS/MS spectra of [M+NH_4]$^+$ ions of the short chain products at RT 12.34 min and 13.53 min indicating that the modification is in the acyl chain (Figure 3A and B). The results also showed that oxCE bearing modifications in the acyl chain and cholesterol can also be formed by radical oxidation, that is characterized to be a non-target oxidation, in opposition to enzymatically induced peroxidation, in a similar trend as previously reported for PC, phosphatidylethanolamines (PE) and phosphatidylserines oxidation induced by the hydroxyl radical[26,28,29].

Some of the short-chain products of oxCE were already reported in the literature but were only identified through exact mass measurements by precursor-ion scanning and no MS/MS information was pinpointed[8,15]. Thus, some structural information was missing, which could be important to understand the biological function of these oxCE species. CE 18:2 C9-aldehyde products were identified *in vivo* samples from percutaneous coronary and peripheral arterial interventions in humans[8] and CE 18:2 C3-C9-aldehydes were identified also *in vivo* within human atherosclerotic plaques from femoral artery endarterectomy samples[15]. In both studies the formation of oxCE was proposed as a result of non-enzymatic oxidation, not ruling out enzymatic initiation or amplification of the oxidation process.

3.1.5 LC-MS/MS of CE 20:4 short-chain oxidation products

Few short-chain products of CE 20:4 were detected by LC-MS and MS/MS as well. These were identified as [M+NH_4]$^+$ ions at *m/z* 558.49, 568.47 and 596.50 and correspond to the short-chain products formed by cleavage of the arachidonic acid at C9, C10 and C12, respectively, all with a terminal aldehyde in the shortened FA chain (Supporting Information Figure 5). The cholestenyl ion, at *m/z* 369.35, was identified in all MS/MS spectra of [M+NH_4]$^+$, confirming the identification of short-chain species with modification only in the acyl chain.

Several short-chain oxidation products were already reported to be formed from CE 20:4 but were identified only through exact mass measurements[8,15]. CE 20:4 fatty acyl chain can be cleaved, most commonly, in carbon 5 (C5) and originate C5-aldehyde/carboxylic acid products[26]. Contrarily to what was expected, we could not detect C5 short-chain products, instead, we found the short-chain products with shortened chain with a terminal aldehyde in C9, C10 and C12. Different short-chain products with fatty acyl chain with different carbon length were reported to be formed from PAPC[22,30]. In these publications, the shortened chains in C9, C10 and C12 were also reported similarly as we have seen. In fact, C10 is a bis-allylic position, thus it is expected to be one of the firsts to be oxidized by abstraction of a hydrogen by the hydroxyl radical, leading to the formation of carbon centered radicals, that after reaction with O_2, lead to the formation of CE-OO$^{\cdot}$. This hydroperoxyl radical can also decompose to yield the alkoxy derivative that will lead to CE shortened in C10. The radical in C10 can migrate to C9 or C11 originating the other shortened CE products. C12 short-chain products can be formed by initial oxidation in C13 with migration of the radical to C12.

4. Discussion

Most of the MS studies detected the presence of oxCE only through exact mass measurements and do not analyse in detail the fragmentation of such molecules to determine oxCE structural features and differentiate the isomers. In this study, we focused on the MS/MS analysis of oxCE, allowing the identification of several isomers. The analysis of the RIC and MS/MS spectra allowed the identification of isomeric oxCE, namely the discrimination of isomer with the oxidized moiety in the FA or with the hydroxy/hydroperoxy group in the cholesterol moiety.

Firstly, we identified long-chain oxidation products of CE 18:1, 18:2 and 20:4. This analysis revealed the presence of different structural isomers, either with oxidation in the FA (shorter RT) or in the cholesterol moiety (longer RT). On the literature, the oxidation of CE is reported to be on the FA. In fact, those species have been identified by targeted analysis using precursor-ion scanning of the ion at *m/z* 369 (cholestenyl cation)[8,15–20]. However, this fragment ion is only

observed when the oxidation is in the FA. When there is oxidation in the cholestenyl moiety it is seen the typical ions [Cholestenyl+nO]$^+$ (which means 369+16 or 369+32 Da, in the case of hydroxy or hydroperoxy derivatives). The loss of H_2O or HOOH combined with loss of FA from oxCE+O or oxCE+2O, respectively, leads to the formation of ions at *m/z* 367 and *m/z* 383, which can be seen in the MS^2 spectrum rather than the ion at *m/z* 369. Nevertheless, and to the best of our knowledge, there are no studies performing precursor-ion scan of *m/z* 367 and only one study performs precursor-ion scan of *m/z* 385 (369+16 Da)[15], thus, oxCE modified on the cholesterol ring have been overlooked. These isomers of oxCE were observed for every combination with FA 18:1, 18:2 and 20:4. We were not able to detect the loss of HOOH (-34Da) from oxCE+2O $[M+NH_4]^+$ ion which may be due to the high energy HCD-MS of Orbitrap mass spectrometer, as reported for aminophospholipids[31]. In the MS/MS of HCD mode, there is a preference for the formation of ions with lower *m/z* while in CID the preference is for ions formed by low weight neutral loss[31,32].

We have identified short-chain oxidation products as well. Short-chain oxidation products were not observed for CE 18:1, similarly as in the case of PC bearing 18:1, due to the low oxidation propensity of oleic acid. On the contrary, short-chain products were seen for oxCE 18:2 and 20:4. In the case of CE 18:2, both aldehydic and carboxylic derivatives were detected, as also the hydroxy aldehyde (isomeric of the carboxylic), with aldehyde in C9 terminal and the OH group in the cholesterol ring. This finding corroborates the possibility of oxidation in the two moieties of CE (FA and cholesterol ring). Regarding CE 20:4, we only detected short-chain aldehydes in C9, C10 and C12, rather than in C5 which is the most reported short-chain oxidation product for FA 20:4. In this case, we did not identify structural isomers with oxidation in the cholestenyl moiety, suggesting that the FA oxidizes first, as expected.

Oddly, CE oxidation has been exclusively considered to happen in the fatty acyl chain, maybe because the majority of the studies only measure the exact mass or consider enzymatic oxidation. CE are integrated in LDL particles that may suffer modifications during oxidative stress conditions, where there is an increase of reactive oxygen species production, namely hydroxyl radical[33]. These environmental conditions are suitable to the occurrence of oxidative

modifications in CE, similarly to what happens with the oxidation of PC. Hence, oxCE may, likewise what has been reported for oxPC, be one of the oxidized lipids of oxLDL that may play an important role in the inflammatory response as well as in the development of cardiovascular diseases. In fact, CE with 2 oxygens (CE 18:1+OOH, CE 18:2+OOH and CE 20:4+OOH) were reported in the core of lipoproteins and are known to accumulate in atherosclerotic tissue[18,34], modulate cholesterol levels and inhibit cholesterol uptake in hepatocytes and macrophages[35].

5. Conclusions

Specific oxCE molecular species can be identified by specific fragmentation fingerprinting of ammoniated adducts by C18 LC-MS/MS. The fragmentation of $[M+NH_4]^+$ CE molecular species originates a cholestenyl product, which can be used to primarily detect CE species in a consistent manner. The RP-LC-MS analysis was a key approach to pinpoint the presence of oxCE species structural isomers, eluting at different RT. These isomers were structurally identified by reporter fragmentation patterns obtained from tandem MS analysis. MS/MS data of oxCE revealed that the hydroxy/hydroperoxy can be either in the fatty acyl moiety or in the cholesterol ring leading to the formation of characteristic ions. In our study, we also identified CE 18:2 and 20:4 short-chain products that showed a clear fragmentation pattern that confirmed the modification in the fatty acyl chain. Some of the oxCE were not reported before, maybe because structural analysis by MS/MS have not been performed. To our knowledge this is the first study on the fragmentation of oxCE by radical oxidation, thus more studies are needed to understand the ionization and fragmentation of OxCE species. High resolution LC-MS/MS shed light on the characteristic fragmentation patterns of several oxCE species, that should be used to detect these species in biological samples of disease conditions, contributing for the evolution of knowledge on the biological role of oxCE.

ASSOCIATED CONTENT

Supporting Information

The Supporting Information is available free of charge on the ACS Publications website.
MS and MS/MS data (PDF)

AUTHOR INFORMATION
Corresponding Author
*M. Rosário Domingues,
Chemistry Department of University of Aveiro, Campus Universi-tário de Santiago, 3810-193 Aveiro, Portugal.
E-mail: mrd@ua.pt
Tel.:+351 234 370 698

Author Contributions
All authors have given approval to the final version of the manu-script.

ACKNOWLEDGMENT
Thanks are due for the financial support to the University of Aveiro and FCT/MCT for the financial support for the CESAM (UIDB/50017/2020+UIDP/50017/2020+LA/P/0094/2020), LAQV/REQUIMTE (UIDB/50006/2020) and to RNEM, Portu-guese Mass Spectrometry Network (LISBOA-01-0145-FEDER-402-022125) through national funds and, where applicable, co-financed by the FEDER, within the PT2020. Helena Beatriz Fer-reira is grateful to FCT for her PhD Grant (2020.04611.BD). Tânia Melo thanks the junior research contract in the scope of the Indi-vidual Call to Scientific Employment Stimulus 2020 [CEECIND/01578/2020]. The authors would also like to thank the COST Action CA 191055 EpiLipidNet.

References

1. Gonen, A. & Miller, Y. I. From inert storage to biological activity - in search of identity for oxidized cholesteryl esters. Front. Endocrinol. (Lausanne). 11, 1–8 (2020).
2. Brown, A. J. & Sharpe, L. J. Cholesterol synthesis. in Biochemistry of Lipids, Lipoproteins and Membranes (eds. Ridgway, N. D. & McLeod, R. S.) 327–358 (Elsevier Science, 2015).
3. Nakamura, Y. Molecular mechanism of reverse cholesterol transport: reaction of pre-beta-migrating high-density lipoprotein with plasma lecithin/cholesterol acyltransferase. Biochemistry 14811–14820 (2004).
4. Korber, M., Klein, I. & Daum, G. Steryl ester synthesis, storage and hydrolysis: A contribution to sterol homeostasis. Biochim. Biophys. Acta - Mol. Cell Biol. Lipids 1862, 1534–1545 (2017).
5. Luo, J., Yang, H. & Song, B. L. Mechanisms and regulation of cholesterol homeostasis. Nat. Rev. Mol. Cell Biol. 21, 225–245 (2020).
6. Hutchins, P. M. & Murphy, R. C. Cholesteryl ester acyl oxidation and remodeling in murine macrophages: formation of oxidized phosphatidylcholine. J Lipid Res 53, 1588–97 (2012).
7. Belkner, J., Stender, H. & Kuhn, H. The rabbit 15-lipoxygenase preferentially oxygenates LDL cholesterol esters, and this reaction does not require vitamin. E. J Biol Chem 273, 23225–32 (1998).
8. Ravandi, A. Release and capture of bioactive oxidized phospholipids and oxidized cholesteryl esters during percutaneous coronary and peripheral arterial interventions in humans. J. Am. Coll. Cardiol. 63, 1961–1971 (2014).
9. Huber, J. Oxidized cholesteryl linoleates stimulate endothelial cells to bind monocytes via the extracellular signal-regulated kinase 1/2 pathway. Arterioscler. Thromb. Vasc. Biol. 22, 581–586 (2002).

10. Miller, Y. I. & Shyy, J. Y. Context-dependent role of oxidized lipids and lipoproteins in inflammation. Trends Endocrinol Metab 28, 143–152 (2017).
11. Matsuura, E., Hughes, G. R. & Khamashta, M. A. Oxidation of LDL and its clinical implication. Autoimmun Rev 7, 558–66 (2008).
12. Domingues, M. R. M., Reis, A. & Domingues, P. Mass spectrometry analysis of oxidized phospholipids. Chem. Phys. Lipids 156, 1–12 (2008).
13. Khoury, S., Pouyet, C., Lyan, B. & Pujos-Guillot, E. Evaluation of oxidized phospholipids analysis by LC-MS/MS. Anal. Bioanal. Chem. 410, 633–647 (2018).
14. Villaseñor, A. Analytical approaches for studying oxygenated lipids in the search of potential biomarkers by LC-MS. TrAC Trends Anal. Chem. 143, 116367 (2021).
15. Hutchins, P. M., Moore, E. E. & Murphy, R. C. Electrospray MS/MS reveals extensive and nonspecific oxidation of cholesterol esters in human peripheral vascular lesions. J. Lipid Res. 52, 2070–2083 (2011).
16. Bowden, J. A. Electrospray ionization tandem mass spectrometry of sodiated adducts of cholesteryl esters. Lipids 46, 1169–1179 (2011).
17. Bowden, J. A., Albert, C. J., Barnaby, O. S. & Ford, D. A. Analysis of cholesteryl esters and diacylglycerols using lithiated adducts and electrospray ionization tandem mass spectrometry. Anal. Biochem. 417, 202–210 (2011).
18. Hui, S. P. Detection and characterization of cholesteryl ester hydroperoxides in oxidized LDL and oxidized HDL by use of an Orbitrap mass spectrometer. Anal. Bioanal. Chem. 404, 101–112 (2012).
19. Shrestha, R. Identification of molecular species of cholesteryl ester hydroperoxides in very low-density and intermediate-density lipoproteins. Ann. Clin. Biochem. 51, 662–671 (2014).
20. Ito, J., Shimizu, N., Kato, S., Ogura, Y. & Nakagawa, K. Direct separation of the diastereomers of cholesterol ester hydroperoxide using LC-MS/MS to evaluate enzymatic lipid oxidation. Symmetry (Basel). 12, 1127 (2020).
21. Reis, A., Domingues, M. R. M., Amado, F. M. L., Ferrer-Correia, A. J. & Domingues, P. Radical peroxidation of palmitoyl-lineloyl-glycerophosphocholine liposomes: Identification of long-chain oxidised products by liquid chromatography-tandem mass spectrometry. J. Chromatogr. B. Analyt. Technol. Biomed. Life Sci. 855, (2007).
22. Reis, A., Domingues, P. & Domingues, M. R. M. Structural motifs in primary oxidation products of palmitoyl-arachidonoyl-phosphatidylcholines by LC-MS/MS. J. Mass Spectrom. 48, (2013).
23. Reis, A., Domingues, P., Ferrer-Correia, A. J. V & Domingues, M. R. M. Fragmentation study of short-chain products derived from oxidation of diacylphosphatidylcholines by electrospray tandem mass spectrometry: identification of novel short-chain products. Rapid Commun. Mass Spectrom. 18, (2004).
24. Brown, A. J. & Jessup, W. Oxysterols and atherosclerosis. Atherosclerosis 142, 1–28 (1999).
25. Brown, A. J., Leong, S. L., Dean, R. T. & Jessup, W. 7-Hydroperoxycholesterol and its products in oxidized low density lipoprotein and human atherosclerotic plaque. J. Lipid Res. 38, 1730–45 (1997).
26. Reis, A. & Spickett, C. M. Chemistry of phospholipid oxidation. Biochim. Biophys. Acta - Biomembr. 1818, 2374–2387 (2012).
27. Liebisch, G. High throughput quantification of cholesterol and cholesteryl ester by electrospray ionization tandem mass spectrometry (ESI-MS/MS). Biochim. Biophys. Acta - Mol. Cell Biol. Lipids 1761, 121–128 (2006).

28. Colombo, S. Electrochemical oxidation of phosphatidylethanolamines studied by mass spectrometry. J. Mass Spectrom. 53, 223–233 (2018).
29. Colombo, S. Modulation of the inflammatory response of immune cells in human peripheral blood by oxidized arachidonoyl aminophospholipids. Arch. Biochem. Biophys. 660, 64–71 (2018).
30. Ni, Z. Evaluation of air oxidized PAPC: A multi laboratory study by LC-MS/MS. Free Radic. Biol. Med. 144, 156–166 (2019).
31. Colombo, S., Domingues, P. & Domingues, M. R. Mass spectrometry strategies to unveil modified aminophospholipids of biological interest. Mass Spectrom. Rev. 1–33 (2019).
32. Neves, B. Advancing target identification of nitrated phospholipids in biological systems by HCD specific fragmentation fingerprinting in orbitrap platforms. Molecules 25, (2020).
33. Leopold, J. A. & Loscalzo, J. Oxidative mechanisms and atherothrombotic cardiovascular disease. Drug Discov. Today. Ther. Strateg. 5, 5–13 (2008).
34. Harkewicz, R. Cholesteryl ester hydroperoxides are biologically active components of minimally oxidized low density lipoprotein. J. Biol. Chem. 283, 10241–10251 (2008).
35. Guo, S. Endogenous cholesterol ester hydroperoxides modulate cholesterol levels and inhibit cholesterol uptake in hepatocytes and macrophages. Redox Biol. 21, 101069 (2019).

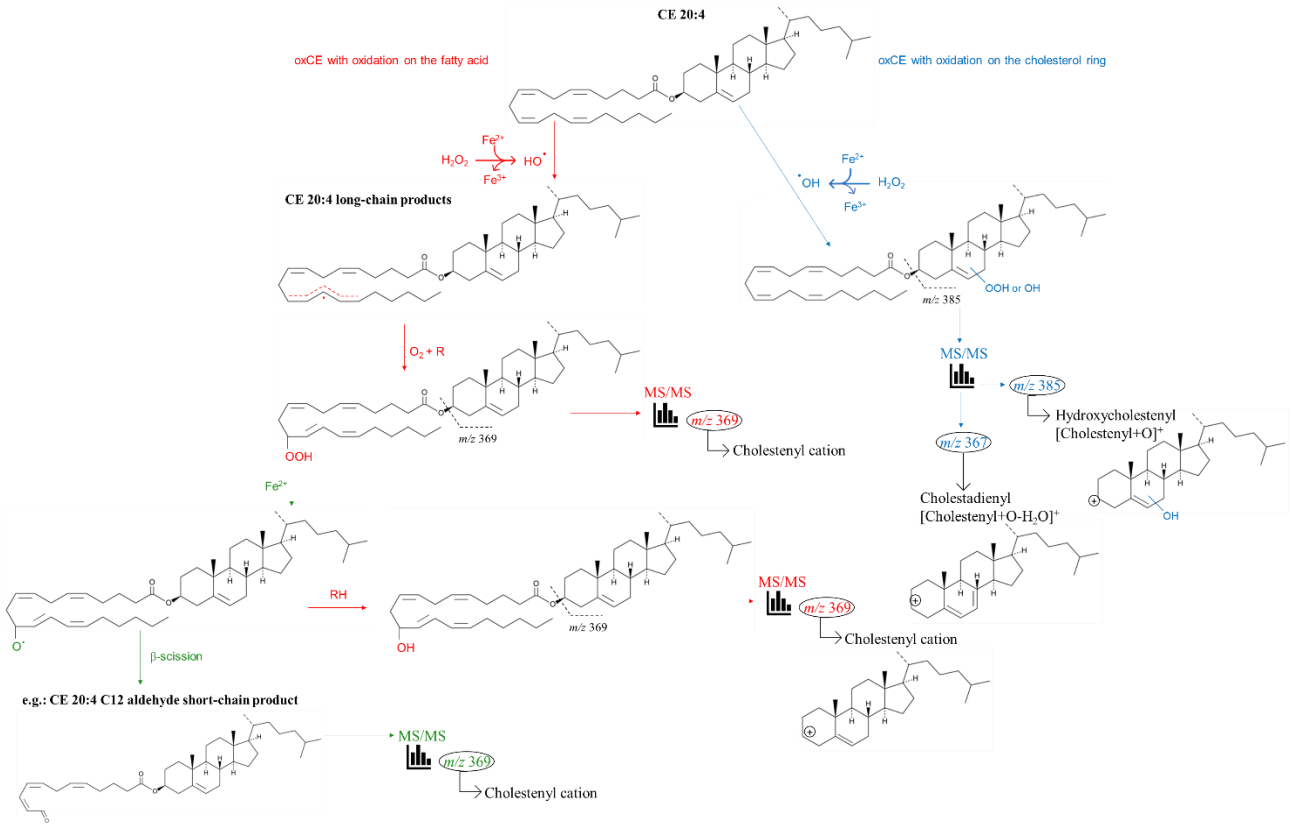

Figure 3.2-1 Schematic representation of the oxidation process and formation of the long- and short-chain products of oxCE (CE 20:4 given as an example).

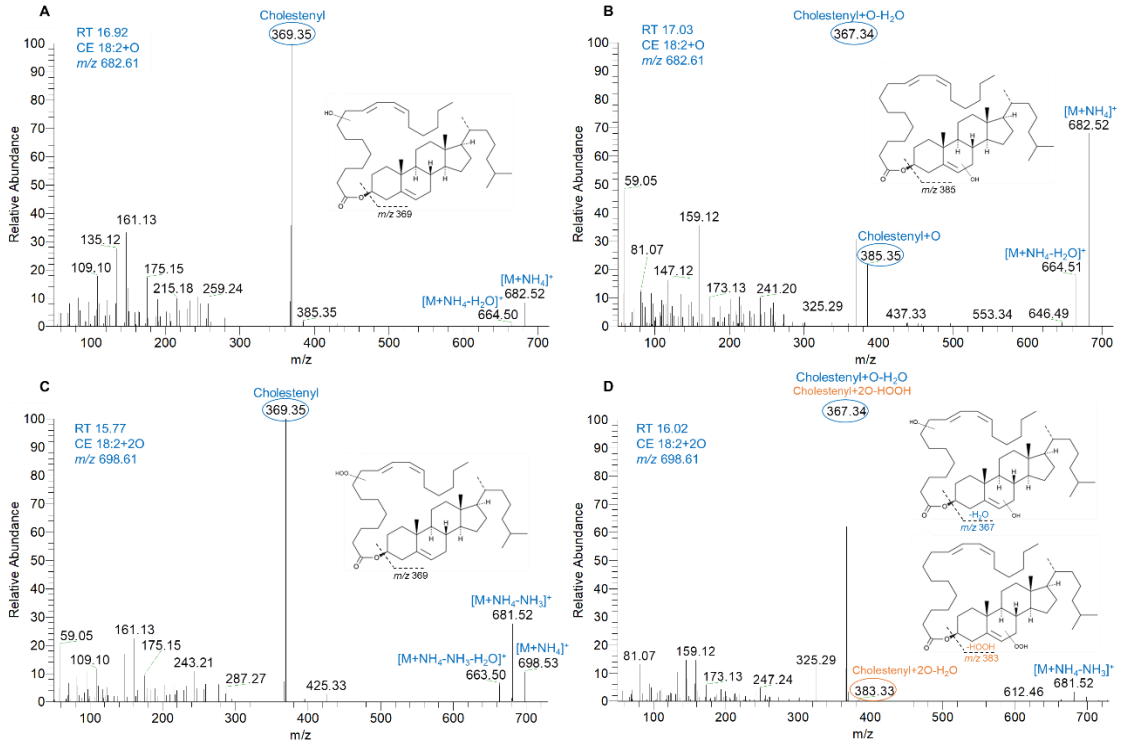

Figure 3.2-2 LC-MS/MS spectra of CE 18:2 long-chain oxidation products. Diagnostic product ions are circled in blue. A: CE 18:2 hydroxy isomer ($[M+NH_4]^+$ at *m/z* 682.62) with the hydroxy group on the fatty acyl chain confirmed by the presence of the ion at *m/z* 369.35. Loss of H_2O from the $[M+NH_4]^+$ identified at *m/z* 664.50. B: CE 18:2 hydroxy isomer ($[M+NH_4]^+$ at *m/z* 682.62) with the hydroxy group on the cholesterol ring, confirmed by the ions at *m/z* 385.35 $[Cholestenyl+O]^+$ and at *m/z* 367.34 $[Cholestenyl+O-H_2O]^+$. The ion at *m/z* 664.50 corresponds to the loss of H_2O from the $[M+NH_4]^+$. C: CE 18:2 hydroperoxy isomer ($[M+NH_4]^+$ at *m/z* 698.61) with the hydroperoxy group on the fatty acyl chain confirmed by the presence of the ion at *m/z* 369.35. The MS/MS spectrum also revealed the ions at *m/z* 681.52 and at *m/z* 663.50 corresponding, respectively, to the loss of NH_3 and conjugated loss of NH_3+H_2O. D: CE 18:2 di-hydroxy isomer (a hydroperoxy isomer structure (in orange) is also considered) ($[M+NH_4]^+$ at *m/z* 698.61) with a hydroxy group on the cholesterol ring and the other in the fatty acyl chain, confirmed by the ion at *m/z* 367.34 $[Cholestenyl+O-H_2O]^+$ (or $[Cholestenyl+2O-HOOH]^+$ highlighted in orange). The ion at *m/z* 383.33 also confirms the presence of an hydroperoxy isomer $[Cholestenyl+OO-H_2O]^+$, with the hydroperoxy group linked to the cholestenyl moiety. Loss of NH_3 from the $[M+NH_4]^+$ identified at *m/z* 681.52.

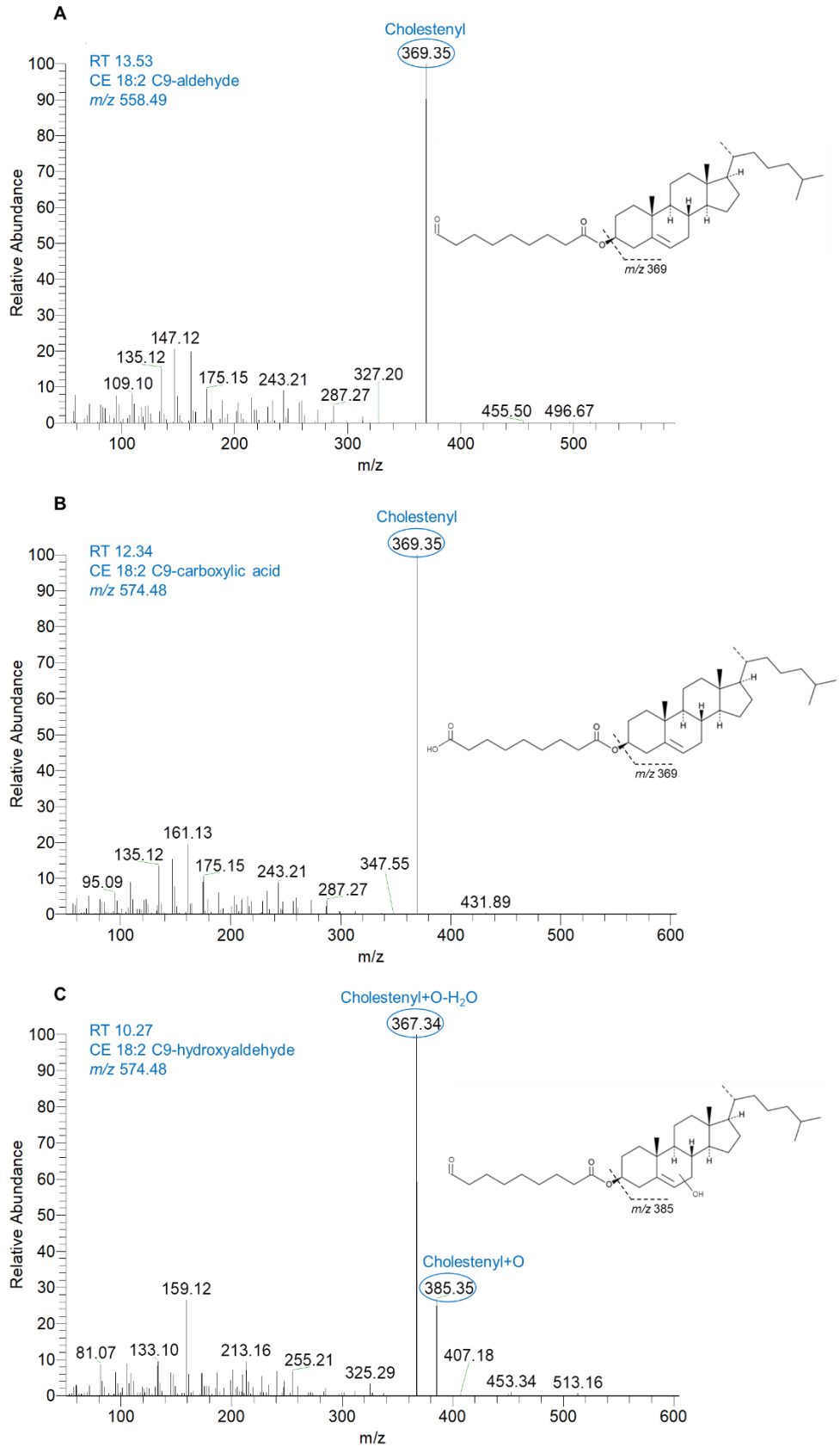

Figure 3.2-3 LC-MS/MS of oxCE 18:2 short-chain products. Diagnostic ions are circled in blue. A: CE 18:2 C9-aldehyde ($[M+NH_4]^+$ at m/z 558.49) with oxidation on the fatty acyl chain (m/z 369.35). B: CE 18:2 C9-carboxylic acid ($[M+NH_4]^+$ at m/z 574.48) with oxidation on the fatty acyl chain (m/z 369.35). C: CE 18:2 C9-hydroxyaldehyde ($[M+NH_4]^+$ at m/z 574.48) with

an OH group linked to the cholestenyl moiety, identified by the ions at m/z 367.34 and m/z 385.35.

Table 3.2-1. Identification by LC-MS and MS/MS of long- and short-chain oxCE products of CE 18:1; CE 18:2 and CE 20:4 formed by the hydroxyl radical oxidation (in bold the RT of the most intense peak).

Lipid class*	Species level*	Common name*	oxCE	Formula	Change in mass (Da)	$[M+NH_4]^+$			
						Theoretical m/z	Observed m/z	Mass error (<5ppm)	RT
CE 18:1									
SE	SE 27:1/18:1	Cholesteryl oleate	CE 18:1	$C_{45}H_{78}O_2$	-	668.6346	668.6358	-1.7947	19.12
SE	SE 27:1/18:1;O	Hydroxy cholesteryl oleate	CE 18:1 + O	$C_{45}H_{78}O_3$	+16 (+O)	684.6295	684.6308	-1.8988	17.27; **17.52**
SE	SE 27:1/18:1;O2	Di-hydroxy cholesteryl oleate	CE 18:1 + 2O	$C_{45}H_{78}O_4$	+32 (+2O)	700.6244	700.6268	-3.4255	**16.19**; 16.56
CE 18:2									
SE	SE 27:1/18:2	Cholesteryl linoleate	CE 18:2	$C_{45}H_{76}O_2$	-	666.6189	666.6206	-2.5502	18.66
SE	SE 27:1/18:2;O	Hydroxy cholesteryl linoleate	CE 18:2 + O	$C_{45}H_{76}O_3$	+16 (+O)	682.6138	682.6150	-1.7579	**16.92**; 17.03
SE	SE 27:1/18:2;O2	Di-hydroxy cholesteryl linoleate	CE 18:2 + 2O	$C_{45}H_{76}O_4$	+32 (+2O)	698.6087	698.6095	-1.1451	14.74; **15.77**; 16.02
SE	SE 27:1/9:1;O2	C9-carboxylic acid cholesteryl linoleate	C9-carboxylic acid	$C_{36}H_{60}O_4$	-92	574.4835	574.4841	-1.0444	10.27; 12.34
SE	SE 27:1/9:1;O	C9-aldehyde cholesteryl linoleate	C9-aldehyde	$C_{36}H_{60}O_3$	-108	558.4886	558.4892	-1.0743	13.53
CE 20:4									
SE	SE 27:1/20:4	Cholesteryl arachidonate	CE 20:4	$C_{47}H_{76}O_2$	-	690.6189	690.6187	0.2896	18.40
SE	SE 27:1/20:4;O	Hydroxy cholesteryl arachidonate	CE 20:4 + O	$C_{47}H_{76}O_3$	+16 (+O)	706.6138	706.6138	0.0000	16.88

SE	SE 27:1/20:4;O2	Di-hydroxy cholesteryl arachidonate	CE 20:4 + 2O	$C_{47}H_{76}O_4$	+32 (+2O)	722.6087	722.6083	0.5535	[14.66-15.88]; **15.73**
SE	SE 27:1/9:2;O	C9-aldehyde cholesteryl arachidonate	C9-aldehyde	$C_{36}H_{60}O_3$	-132	558.4886	558.4904	-3.2230	13.50
SE	SE 27:1/10:2;O	C10-aldehyde cholesteryl arachidonate	C10-aldehyde	$C_{37}H_{58}O_3$	-122	568.4730	568.4731	-0.1759	12.32
SE	SE 27:1/12:3;O	C12-aldehyde cholesteryl arachidonate	C12-aldehyde	$C_{39}H_{62}O_3$	-94	596.5043	596.5048	-0.8382	12.32

***According with the LipidMaps shorthand notation.**

4. CHAPTER 4: NOVEL PRE-ANALYTICAL METHODS IN CLINICAL LIPIDOMICS

4.1 CHAPTER 4.1: CLINICAL LIPIDOMICS AND THE USE OF DRIED BLOOD SPOTS

This chapter was integrally published as follows.

Reprinted with permission from:

H.B. Ferreira, I.M. Guerra, T. Melo, H. Rocha, A. S. P. Moreira, A. Paiva, M.R. Domingues, Dried blood spots in clinical lipidomics: optimization and recent findings, *Analytical and Bioanalytical Chemistry* (2022) 414, 7085–7101

https://doi.org/10.1007/s00216-022-04221-1

Abstract

Dried blood spots (DBS) are being considering as an alternative sampling method of blood collection that can be used in combination with lipidomic and other omics analysis. DBS are successfully used in the clinical context to collect samples for newborn screening for the measurement of specific fatty acid derivatives, as acylcarnitines, and lipids from whole blood for diagnostics purposes. However, DBS are scarcely used for lipidomic analysis and investigations. Lipidomic studies using DBS are starting to emerge as a powerful method for sampling and storage in clinical lipidomics analysis, but the major research work is being done in the pre- and analytical steps and procedures, and few in clinical applications. This review presents a description of the impact factors and variables that can affect DBS lipidomic analysis, such as the type of DBS card, hematocrit, homogeneity of the blood drop, matrix/chromatographic effects and the chemical and physical properties of the analyte. Additionally, a brief overview of the lipidomic studies using DBS to unveil its application in clinical scenarios is also presented, considering the studies of method development and validation and, to a less extent, for clinical diagnosis using clinical lipidomics. DBS combined with lipidomics approaches proved to be as effective as whole blood samples, achieving high levels of sensitivity and specificity during MS and MS/MS analysis, which could be a useful tool for biomarkers identification. Lipidomic profiling using MS/MS platforms enables significant insights into physiological changes, which could be useful in precision medicine.

Keywords: dried blood spots; mass spectrometry; lipidomics, disease biomarkers

1. Introduction

Dried blood spots (DBS) are a less invasive method for blood collection and is being considered as an alternative to whole blood samples obtained by venipuncture or arterial sampling. DBS are widely used in clinical environment to collect samples for newborn screening, as a part of public health policies[1]. This method is also considered promising for clinical diagnostics and for precision medicine, since it has been reported as an effective method for pre-analytic stages of diagnostics[2, 3]. Research on DBS for application in medicine is growing and is being explored in combination with mass spectrometry[1] (MS) and in the context of different omics, like metabolomics[4, 5], proteomics[6] and more recently lipidomics. While DBS is already well established in metabolomics analysis, its use in proteomics seems to face some challenges regarding protein analysis and degradation. Lipidomics is starting to be associated with DBS, once lipids are reported to be stable enough to endure the timespan between sample collection and lipid extraction, even more stable than in traditional samples (plasma/serum/whole blood). The major research work on this method has been done concerning pre-analytical and analytical steps and procedures, and very few in application to real clinical investigations.

Despite being a field scarcely studied, lipidomic analysis with DBS show promising results, revealing the need for more work to be done. In this review, we will address the most important findings from the use of DBS in lipidomics, highlighting as well future perspectives and development needed to pinpoint DBS as a good sampling and storage method, prior to lipid analysis for biomarker discovery, and application in clinics, diagnostics and/or therapeutic drug monitoring.

2. Advantages and applications of DBS to study lipids in biological samples

The DBS is a microsampling method that is very simple and easy to perform, as it requires only the depositing of small volumes (µL) of capillary blood onto DBS cards[1]. The collection of blood is easier therefore the sample can be collected at home, and it does not demand

specialized entities to do so. The patient can perform the sample collection by its own (or the parents, in the case of small children). The blood is placed directly onto the DBS card until the drawn circle area is full. Yet, the skin must not be punctured with the same lancet more than once due to risk of bacterial contamination and infection[7]. Contrarily to venipuncture and arterial sampling, DBS samples do not need to be immediately stored in refrigerated conditions after its collection. This way, the transport and accommodation of these type of samples is very straightforward which allows the creation of simplified biobanking facilities for storage[8]. Venipuncture and arterial blood collection are the most common blood collection methods, however, they are not considered to be the best way to collect a blood samples[9]. These methods have to be performed exclusively by personnel who have received proper training. Many patients find it inconvenient (due to dietary restrictions) and disturbing. Also, there are also risks related with the puncture site cleansing, storage, transportation, and potential loss or contamination of the blood samples once they are collected[9]. Thus, DBS have several advantages when compared with arterial sampling and venipuncture, as described in Figure 1.

DBS samples enable longitudinal studies without sample degradation if they are stored under the right conditions according with the analyte of interest. Due to high stability of several blood components, like lipids, it is possible the detection of a high number of analytes in a single analysis. The physician has a broader understanding of the patient`s metabolism and can reach a more fitting diagnosis[10].

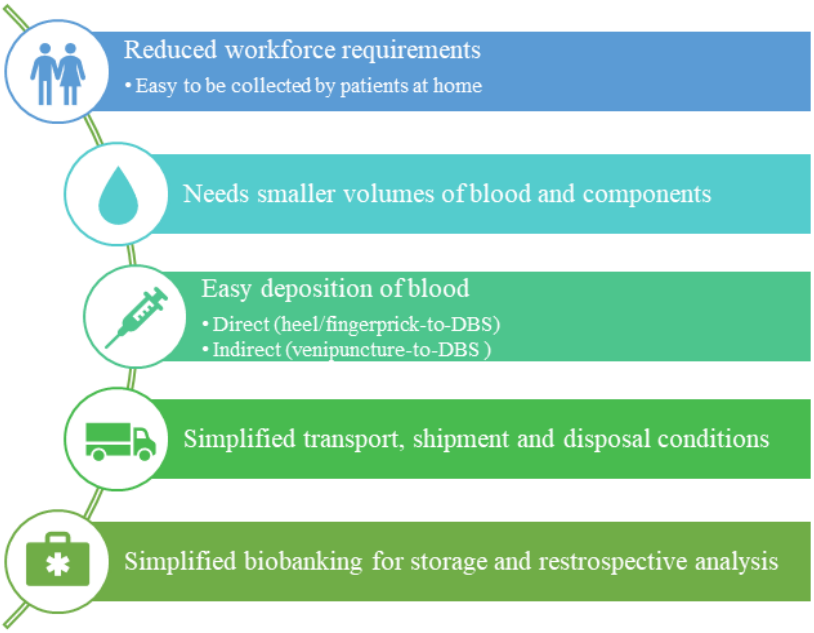

Figure 4.1-1 Dried blood spots (DBS) sampling method offers several advantages comparing with arterial/venipuncture samples. It is a minimally invasive sampling process, which can be performed by the patient on their own, and it is convenient to store and transfer allowing long distance shipments.

DBS have three primary applications (Figure 2): in health-care services (in a clinical scenario for screening/diagnostics/follow-up), in research and surveillance studies into undeveloped populations, and in drug development/monitoring[10, 11].

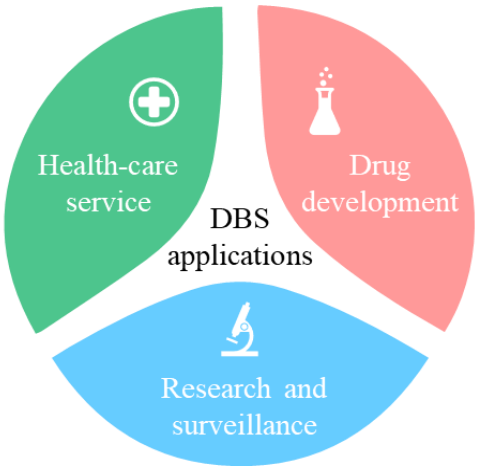

Fig 4.1-2 Dried blood spots (DBS) main applications: health-care services (in a clinical scenario for screening/diagnostics/follow-up), research and surveillance studies, and drug development/monitoring.

Lipids are important mediators in pathological conditions therefore its analysis could detect the early development of some diseases or even be considered as biomarkers of disease status, and be useful to evaluate the therapeutic outcomes[12]. Lipids are promising in the search of new putative biomarkers for diagnosis and evaluation of disease progression or to unravel the role of lipids in the disease pathophysiology. As pointed out before, all the advantages that DBS offers combined with the fact that lipids are quite stable in DBS[13], makes DBS suitable for its use in lipidomic analysis. It is a promising field of research, with potentially favourable applications in clinical environments. However, the association of DBS with lipid/lipidomics analysis is still in its infancy, mostly because lipidomics is an Omics field still in the early stage of development but with high potential applications [13], and there is not much information regarding its use in this area. DBS method is well-established in other omics, especially metabolomics[14], and there is a need for more investigation on its applicability on the lipidomics field.

In this review, we aimed to gather lipidomic investigations using DBS cards. For that, English language publications were identified through a computerized search (PubMed database) until June 2021 using the following keywords: lipidomic(s), lipid(s), lipid profile(s), phospholipid(s), fatty acid(s) and sphingomyelin(s) combined with dried blood spot(s). A total of 26 publications were found. From those, a total of 21 papers were selected according with the

eligibility criteria chosen. We only considered research studies that used gas chromatography coupled with mass spectrometry (GC-MS), gas chromatography-flame ionization detection (GC-FID), liquid chromatography coupled with mass spectrometry (LC-MS), direct injection mass spectrometry (DI-MS) and supercritical fluid chromatography coupled with mass spectrometry (SFC-MS). Studies that did not report the use of those techniques, or were review papers, were not taken into consideration. From the 21 eligible studies, most of them focused on methodology/protocol optimization, from pre-analytical parameters evaluation to analysis optimization, and very few in actual clinical lipidomics investigations, as will be described.

Most of the papers on the evaluation of pre-analytical variables that can affect the quality of the results of lipid analysis were focused on: i) the extraction efficiency of different methods, ii) factors that may affect the recovery rate of the lipids, like the type of DBS card, storage with antioxidants, matrix effects, and iii) lipid stability over a period of time. Others studied the DBS method validation in clinical cases as a possible candidate to future clinical applications by comparing the results with traditional methods (plasma, serum, or whole blood)[13, 15–29].

3. Pre-analytical parameters that may affect lipid extraction from DBS

The workflow of DBS starts with blood collection in the paper card, followed by storage/transport, lipid extraction and analysis. After blood collection, the analyte extraction procedure starts by punching a circle (with a set diameter) from the DBS card. Then, the analyte is extracted with selected extraction solvents and protocols that must be carefully chosen according with the physico-chemical properties of the analyte. Nonetheless, different pre-analytical parameters may affect the amount of compound and the lipid extract recovered from DBS. The parameters include the transport and storage conditions, the type and quality of the paper of the DBS card (variations in the matrix affects the blood volume, the extraction efficiency as well as the chromatographic results) and hematocrit (Hct). These are probably the most impactful factors to significantly affect the results, this way, the procedures must be optimized and standardized to increase the reliability and reproducibility of the assay and allow

the comparison of research work data between different labs, promoting harmonization of lipidomic investigations.

Storage of DBS and stability of lipids

The solid nature of DBS paper cards and adsorption capacity make analytes less reactive (thus more stable) than in whole blood, plasma or serum samples thus having higher stability at room temperature, at least for a week[30]. It is also an advantage to monitor metabolic diseases diagnosed in newborn screening programs and could be promising for sample collection for other diseases that need monitoring. To maintain analyte stability and to control storage conditions, to make the sample stable during longer times, transport to the laboratory should be made as soon as possible. Storage conditions must account for several variables such as temperature, humidity and time within field, transport, and laboratory settings[31]. Temperature and humidity conditions have a direct impact on the stability of several analytes including lipids, amino acids, and DNA[32–34]. Temperature effect can be prevented by keeping samples in refrigerated/cooled conditions. However, reducing the storage temperature is not always the solution for all analytes as it is described for polyunsaturated fatty acids (PUFA). It was reported that few PUFA (20:4, 20:5 and 22:6) suffer significant degradation after 10 days of storage at -28 ºC[33]. Humidity, which can also cause lipid degradation by hydrolysis reactions, can be avoided by confining DBS cards in sealed bags with desiccants while transportation or storage[1]. Nonetheless, optimal storage settings must be determined for the analyte in question and the purpose of the study (momentary or longitudinal). In the case of lipids stability in DBS, studies reported that PUFA are stable between 21 days and 2 months at room temperature[21, 23] and, in the case of phospholipids (PL), up to 2 weeks at 4 ºC or room temperature[13]. Nonetheless, there is a need for more studies on the stability of molecular species since most of the studies were performed on FA.

Type of DBS cards

There are plenty of DBS cards available on the market, and different studies used DBS cards from different manufacturers (Table 1). The difference on the card type between studies may explain the variance of results due to matrix effects. Each manufacturer produces the DBS

cards with a specific chemical composition, fiber density and network. This way, the same sample could present dissimilar results depending on the DBS card type, and consequently, on the matrix effect. Liu *et al* intended to develop a lipidomic DBS method that would allow samples to be stored at room temperature for at least two months[23]. For that, the team compared four different DBS card types: Fluka blood collection paper (Sigma-Aldrich, Switzerland); Whatman 903™ specimen collection paper; Whatman 3MM chromatography paper and Whatman ion exchange paper (46x57cm^2, Whatman, United Kingdom). Changes on the concentration of saturated fatty acids (FA), 16:0, 18:0, 22:0 and 24:0, monounsaturated FA, 16:1*n*-7, 18:1*n*-7, 18:1*n*-9 and 24:1*n*-9, and PUFA, 18:2 *n*-6, 20:3 *n*-6, 20:4 *n*-6 (arachidonic acid, AA), 22:4 *n*-6, 18:3 *n*-3, 20:5 *n*-3 (eicosapentaenoic acid, EPA), 22:5 *n*-3 and 22:6 *n*-3 (docosahexaenoic acid, DHA), were observed according with the type of paper card used and the presence/absence of antioxidants[23]. It was observed a significant decrease of PUFA in DBS samples over 4 weeks of storage at room temperature, even though the papers were impregnated with butylated hydroxytoluene (BHT, an antioxidant agent) and regardless the DBS card type. FA composition of DBS between samples collected on Fluka blood collection paper, Whatman 3MM paper, and Whatman 903 paper did not suffer significant alterations at any time point over the storage period. However, it was noticed a lower decline in the levels of all long chain PUFA in the DBS samples collected on the paper card Whatman ion exchange when compared to the other types of papers following 4 weeks of storage at room temperature[23]. As far as our knowledge goes, this is the only lipidomic study comparing lipid stability on different card types.

DBS cards using stabilizers

DBS paper cards are often impregnated with stabilizers or modifiers to increase analyte stability and recovery efficiency (Table 1)[1]. The addition of chemicals to DBS paper may directly influence the results due to matrix effects. Two studies performed stability analysis focusing on the efficiency of adding antioxidants to prevent lipid degradation[20, 21]. Metherel and co-workers assessed the efficiency of adding different concentrations of BHT [0 mg/mL (control), 2.5 mg/mL and 5 mg/mL] to the DBS paper cards to prevent PUFA degradation and

test its stability[21]. The study showed that BHT provides significant protection against PUFA degradation in a DBS sample, in open air and room temperature storage, and that PUFA losses are dependent on BHT concentrations. The analysis by GC-MS showed that the degradation of highly unsaturated FA (AA; EPA; DHA); *n*-3 FA; *n*-6 FA and total PUFA differs with BHT concentrations (the ability to prevent PUFA degradation increases with higher BHT concentrations)[21]. The same PUFA are detected in DBS in the presence of BHT for up to 21 days in open air. However, total PUFA levels significantly decrease after 3 and 14 days of storage. Also, storing DBS adsorbed in BHT in sealable containers further prevents PUFA loss up to 8 weeks[21].

On the other side, Marino and colleagues validated the use of different antioxidants to prevent FA degradation after 15 days of blood collection[20]. The study revealed that, in general, antioxidants (pure or in mixtures) are not useful to accurately measure individual FA. However, the use of sodium sulphite or ascorbic acid or their mixture with BHT, ascorbic acid or gallic acid, in some cases enabled the assessment of FA. The results obtained by GC-FID showed that the levels of saturated FA (14:0, 16:0, 18:0 and 24:0) and unsaturated FA (*trans*-16:1, 16:1, *trans*-18:1, 18:1, *trans*-18:2, 18:2, α-18:3, γ-18:3, 20:1, 20:2, 20:3, AA, EPA, 22:4, 24:1, 22:5 and DHA) were different according with the antioxidant applied on the DBS paper card[20]. Although storage conditions and BHT concentration were not the same, contrarily to what was reported by Metherel[21], the use of BHT in this study did not prevent FA degradation.

Table 4.1-1. Analysis of the selected studies according with the type of DBS card, punch diameter, use of stabilizers and lipidomic approach.

DBS card type	Diameter of the punched disk	Stabilizers	Lipidomic approach	Reference
Guthrie cards				
Commercially available Guthrie spot cards	3.2 mm	Chaeotropic buffer	DI-MS	Furse *et al* (2020)[16]
Whatman 903 ™				
Whatman 903™ protein saver cards	3.0 mm	-	LC-MS	Primassin *et al* (2010)[17]
Whatman chromatography paper	100 mm^2	BHT	GC-MS	Metherel *et al* (2013)[21]
Whatman 903® specimen collection paper	3.2 mm	-	LC-MS	Chuang *et al* (2014)[35]
Whatman 903™ CF12® protein saver cards	144 mm^2	-	LC-MS	Luginbühl *et al* (2016)[22]
Whatman 903™ filter paper cards with BHT antioxidant	144 mm^2	BHT	GC-MS	Mashavave *et al* (2016)[36]
Whatman 903™ protein saver cards	144 mm^2	-	GC-MS	Drzymała-Czyz *et al* (2017)[25]
Whatman 903™ filter paper cards	6.0 mm	LiCl	DI-MS	Gao *et al* (2017)[13]
Whatman 903™ protein saver cards	3.0 mm	-	LC-MS	Liao *et al* (2018)[27]
Whatman 903™ filter paper cards	160 mm^2	Different antioxidants (pure/mixture)	GC-FID	Marino *et al* (2018)[20]
Whatman 903™ protein saver cards; 10 µL Mitra® Microsampling Device	6.0 mm	-	LC-MS	Gunash *et al* (2019)[29]
Whatman 903™ filter paper cards	3.2 mm	-	DI-MS	Snowden *et al* (2020)[19]
Whatman 903™ paper (#10531018, GE Healthcare)	Corresponding to 2.5 µL of blood	-	SFC-MS	Le Faouder *et al* (2021)[37]
Others				
Filter papers (PKU card, Tokyo, Japan)	3.0 mm	-	GC-MS	Kimura *et al* (2002)[38]
Whatman FTA DMPK-A cards	3.0 mm	-	LC-MS	Ismaiel *et al* (2012)[15]
Filter paper cards Ahlstram 226, ID Biological Systems	3.2 mm	-	LC-MS	Koulman *et al* (2014)[24]
✓ Fluka blood collection paper ✓ Whatman 903™ specimen collection paper ✓ Whatman 3MM chromatography paper ✓ Whatman ion exchange paper (46x57 cm^2)	~225 mm^2	BHT	GC-MS	Liu *et al* (2014)[23]
INF	3.0 mm	-	DI-MS	Al-Thihli *et al* (2014)[18]
Whatman cellulose chromatography paper strips	100 mm^2	-	LC-MS	Henao *et al* (2016)[28]
Whatman FTA Classic Card	¼" diameter punch	-	LC-MS	Kyle *et al* (2017)[39]

PUFAcoat™ paper	6.0 mm	-	LC-MS	Hewawasam *et al* (2017)[26]

BHT: butylated hydroxytoluene; PKU: Phenylketonuria; DMPK: drug metabolism and pharmacokinetics; INF: Information not found

Matrix effects in DBS

In what concerns DBS matrix effects, these can be qualitatively assessed by analysing a blank DBS card[40], but also quantitatively determined by comparing the signals obtained from solvent extraction of a blank DBS. However, matrix effects from DBS cards are dependent on the type of analyte and can cause interference in the extraction efficiency, stability and contribute to ionization suppression or enhancement in the analysis of the extracts from DBS by MS lipidomic approaches[41]. Phosphatidylcholines are well known as the primary cause of matrix effects in LC-MS/MS and cholesterol, cholesterol esters, and triacylglycerols, when present at relatively high concentrations can also result in significant ion suppression effects[15, 42]. An additional problem is the potential adsorption and non-specific binding of the lipids to the sampling card. DBS paper cards contain cellulose that have several -OH groups and these can interact with the hydrophilic head of the lipid molecules[43, 44]. This phenomenon has also been reported for proteins in DBS[45, 46]. When analysing samples from DBS cards, it is generally assumed that blood and analytes spread homogeneously. However, when the spread is heterogenous, which it is called chromatographic effect[1], we could have dissimilar extractions yield, depending on the punched circle of the blood card analysed. Chromatographic effects lead to significantly different results from punch to punch and it can be induced by many factors, for instance, the type of DBS card[47], Hct levels, portioning of cell components[48] and sample integrity and preparation[49]. The commercialization of DBS cards with the same chemical composition (to prevent matrix effects and the drawbacks associated), as well as the development of lipid extraction guidelines (to prevent chromatographic effects) would facilitate the dissemination of unbiased results.

Haematocrit interference

The haematocrit (Hct) is a parameter that can affect the amount of lipids and their recovery from DBS. Hct may be considered the major factor of variability, when using DBS for metabolite analysis. Higher Hct levels are associated with increased viscosity of the blood drop, thus having a lower spread rate of the blood onto the paper card[50]. More viscous blood has been shown to have an heterogenous spread across the paper than samples with lower Hct

levels, which is expected to translate into analytical biases[50–52]. The variation of the Hct value directly affects the total amount of analytes and their extraction recovery rate from DBS (lower extraction recoveries at higher Hct levels)[53]. When Hct values are high, sonication of the DBS sample has proven to be valuable to improve extraction recovery[54]. The lipidomic approaches were used in a study aiming to find lipid species` markers for quantification of Hct using DBS samples[27]. Through LC-ESI-MS, Liao *et al* identified 189 lipid species belonging to PC and SM classes. The study showed that three SM, specifically SM 44:1, SM 44:2, and SM 44:3, had potential to be Hct estimation markers. The results revealed that the estimation errors for the Hct values were less than 20%, demonstrating the viability of using the identified SM markers to estimate the Hct values in DBS samples[27]. From the eligible studies in this review, the common diameter of the punch is around 3 mm. Increasing the punch diameter would be expected to increase the amount of lipid extract recovered.

Overall, DBS are a promising method for a less invasive blood collection and are being considered as a favourable method for clinical lipidomic studies. Nonetheless, there are specific factors like the size of DBS punch, effect of matrix, stability, methods of extraction, among others that can influence the identification and quantification of the lipids. It has been demonstrated that Hct, blood viscosity, type of DBS card, chromatographic/matrix effects, and storage conditions (temperature, humidity) can induce changes in the size of the blood spots and an irregular distribution of the sample[55]. At the present time Hct is recognized as the most relevant factor that affects the characteristics of the blood spot, but other factor can have influence as well such as drying time, blood spreading, homogeneity, and also affects the reproducibility of the extraction procedures and further analysis[8]. To overcome these challenges, it must be considered an accurate blood spotting, possible extraction of the whole DBS (not a punch with a specific diameter), and other pre-analytical parameters that need to be optimized and harmonized like the quality of the paper card and the lipid extraction protocol (detailed in the next chapter).

4. Extraction of lipids from DBS

The extraction of lipids from DBS is most-often performed with organic solvents, such as methanol (MeOH), dichloromethane (CH_2Cl_2) or chloroform ($CHCl_3$), under adjusted proportions. It is important to emphasize the fact that, when being analysed by MS, the lipid signal directly reflects the amount of the initial sample, the efficiency of the extraction recovery and matrix effects[56]. There is not a standardized protocol to extract lipids from DBS, however, it is known that, depending on the polarity and composition of the lipid specie to analyse, there is a preferential extraction with different solvents[57].

Several studies compared the extraction efficiency of different solvents (isolated and in systems) and gathered significant differences (general dry time was 3 hours after blood collection and storage at room temperature)[15, 26]. The ability of different absolute organic solvents [MeOH, acetonitrile (ACN), isopropyl alcohol (IPA), CH_2Cl_2, methyl tertiary-butyl ether (MTBE), ether or *n*-hexane] to extract phosphatidylcholine (PC), cholesterol (Chol), cholesteryl esters (CE) and triacylglycerols (TG) was investigated by Ismaiel and co-workers[15]. The study determined that MeOH extracted the highest amount of PC comparing with the other organic solvents. However, when lipids were extracted from DBS with IPA and ACN, contained approximately, 16.0% and 2.5% of PC levels that were found in MeOH extracts, respectively. Ether, *n*-hexane and CH_2Cl_2 showed less than 1.0% of PC levels in the MeOH extract. Among other species, PC were also quantified to evaluate the lipid recovery rate, since it is the major phospholipid class present in blood[15]. Lyso-PC presented the same behaviour as well. Regarding Chol and CE, ether extracts contained the highest concentrations when compared to the other extraction solvents - MeOH, MTBE, *n*-hexane, IPA, ACN and CH_2Cl_2 extracts – which contained approximately 88, 80, 70, 38, 26, and 13% of Chol and CE levels in ether extracts, respectively. Extracted TG showed the same tendency, since ether extracts presented the highest levels of the TG whereas MeOH extracts demonstrated reduced levels. The remaining organic solvents - MTBE, *n*-hexane, IPA, ACN and CH_2Cl_2 extracts - contained approximately 89, 77, 43, 21, and 18% of TG levels that were found in ether extracts, respectively. These results showed that more apolar solvents are more efficient to extract apolar

lipids (Chol, CE and TG). Therefore, the use of MeOH extracts better PL when compared with other solvents.

In the same line, Hewawasam *et al* analysed the extraction efficiency of five different extraction solvent systems (80% aqueous MeOH; 70% aqueous ACN + 12 mM ammonium formate + 0.02% acetic acid; 80% aqueous ACN; 80% aqueous ACN + 0.02% formic acid; 80% aqueous ACN + 0.05% formic acid), but in this case the efficiency of free PUFA recovery was evaluated by LC-MS[26]. The use of 80% aqueous MeOH resulted in a significantly higher extraction of the FA 18:2, EPA, DHA, and AA from DBS. Also, free PUFA in 80% aqueous MeOH remained stable up to 1 week of storage inside the autosampler, showing no significant changes[26].

Additionally, some studies used other strategies to increase the lipid extraction efficiency, as sonication or addition of buffers. Henao *et al* determined that adding sonication/homogenization and acidification of pH steps can improve the extraction efficiency of certain lipid classes, such as phosphatidylserines (PS)[28]. Additionally, Furse *et al* discovered that treating DBS paper cards with a chaeotropic buffer [guanidinium chloride (6 M) and thiourea (1.5 M)] for decoagulating blood, for 24 hours prior lipid extraction, considerably improved the extraction efficiency of DBS. This study determined over 200 lipid species belonging to the classes of TG and PL[16]. Both the number and total signal intensity of lipid species were higher than DBS samples without the pre-treatment[16]. Gao and partners established a high-throughput DI-MS/MS lipidomics platform to analyse the blood lipidome from DBS samples[13]. To the extraction protocol it was added a lithium chloride (LiCl) solution to improve the extraction efficiency of acidic lipids, prevent the degradation of plasmalogen molecular species, and decrease spectral complexity. This method was able to identify and quantify, in a single DBS sample, more than 1200 lipid molecular species belonging to PL, glycerides, glycolipids, SM, acylcarnitines and ceramides (CER) lipid class. The lipid species identified and the class distribution using DBS were analogous to whole blood samples, but it was reported that DBS extracts contained more PL and less TG than those recovered using plasma and serum samples[13].

To sum up, different extraction solvent systems have different polarities, therefore the extracted lipids will be in accordance with the polarity of the solvent. The studies agree that MeOH (absolute or aqueous) is the best solvent to extract PL and FA from DBS. Moreover, these studies do not compare the extraction efficiency of the traditional methods such as Bligh & Dyer[58] or Folch[59], thus, with the published data it is not possible to conclude in fact which is the best extraction method. More studies are needed to determine the best solvent/solvent system so that the extraction efficiency/recovery is maximized. Also, a standardization and harmonization of extraction protocols (including type of DBS cards and solvent quantity) is required to allow the comparison of data between different investigations.

5. Lipidomics analytical methodology to screen lipids from DBS

Initially in the sixties, the analysis of DBS was made using bacterial inhibition tests for the detection of phenylketonuria in newborns. Another established technique was immunoassays, where the production of monoclonal antibodies led to development of several diagnostic kits[1]. However, immunoassays have some limitations, like a possible lack of selectivity, the rather elevated cost of reagents per sample and the long time required for development of a new assay. Later in the nineties, MS-based approaches have emerged as a significant advance in clinical diagnosis and investigation, allowing the monitoring of several biomarkers at the same time, and were established as the detection technique in DBS analysis[60]. Lipid extracts are nowadays efficiently analysed using lipidomic approaches. Lipidomics is a field of research that is growing in a fast speed. It aims to understand lipids biological functions by describing and quantifying all lipid molecular species[61]. The sensitivity of MS instruments has significantly improved and nowadays it is common to analyse the lipid extract directly through LC-MS after its extraction or in some specific cases by DI-MS.

5.1 MS lipidomic approach

The combination of lipidomics and DBS follows the normal MS workflow (lipid extraction, data acquisition by MS approaches and data analysis). The lipidomic analysis can be untargeted,

aiming to identify and quantify as much lipid species as possible, and is often used for screening and usually for comparing different groups or biological conditions. On the other side, lipidomics can be used as a targeted approach, for the identification and quantification of specific lipids, aiming to unravel specific pathways, or profiling specific markers. The lipid identification can be done with the data-dependent MS/MS files that are matched against spectral databases and libraries search (e.g. LipidMaps, MSDial) to match known fragmentations from reference compounds. Quantification of each lipid species can be done using bioinformatics tools (e.g. MZmine and MSDial), as recently reviewed[62, 63]. Despite having some studies that consider lipidomics using GC-MS for FA profiling, the true lipidomics is based on LC-MS or DI-MS analysis. Other than identify lipid species from DBS samples, lipidomics also aims to quantify the molecular species present in each sample and disease conditions.The GC-MS or GC-FID approaches have been used combined with DBS to analyse the FA profiles [11, 12, 17, 18, 23, 26, 34]. GC-MS and GC-FID typically require sample derivatization prior extract injection, to enable the detection of hydrophilic, non-volatile and/or thermolabile compounds[64]. These studies mainly analysed either free or esterified FA and used different chromatographic columns as well as lipid extraction protocols, as reported in Table 2, which made the standardization and comparison for this review a rather difficult task. Thus, this reinforces the fact that there should be a normalization of the protocols regarding lipidomic analysis of DBS samples.

From the 21 studies gathered in this review it is seen a preference for LC-MS and DI-MS approaches (10 and 5 studies, respectively), mostly due to its high sensitivity and precision (Figure 3)[1]. Reverse phase (RP) high-performance liquid chromatography (RP-HPLC) and hydrophilic interaction liquid chromatography (HILIC-LC), where used coupled to MS in DBS lipidomic studies. HILIC-LC-MS approaches are widely used in lipidomics to analyse polar lipids like PL[65]. However, from all the eligible studies, RP columns were the most used in LC-MS (RP-LC-MS) for DBS studies.

In DI-MS the sample of the total lipid extract is directly injected in the MS without prior chromatographic separation and can be used as a real-time monitoring method. The published

works on DBS and LC/DI-MS were mainly used to identify the composition of different classes such as PL, sphingolipids, TG and CE and, in a few cases, carnitines, acylcarnitines or FA[13, 15–19, 22, 24, 26–29, 35, 39].

The SFC-MS approach is slowly reappearing after a period shadowed by the commercial success of LC-MS. This technique is suitable for lipid analysis and allows for a shorter separation than in LC[66]. It uses CO_2 under pressure as an eluent because CO_2 exhibits favourable properties, such as being non-flammable, chemically inert, relatively nontoxic, easy to handle and inexpensive. The separation of oxidized lipids as well as the study of positional isomers can benefit from SFC-MS approaches due to the properties of this lipidomic approach[66]. From the eligible studies, only one study using SFC-MS matched the selection criteria and focused on method development and detection of complex lipids[37]. It allowed the identification from DBS of 500 lipid species from several classes of lipids, such as phospholipids,

sphingolipids, free fatty acids, sterols, and fatty acyl-carnitines.

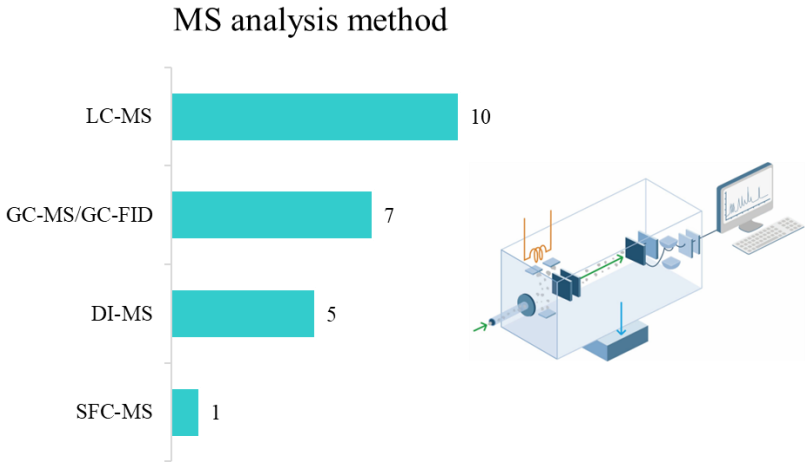

Figure 4.1-3 Number of eligible studies according with the mass spectrometry (MS) analysis method used in studies combining DBS, lipid analysis and lipidomics. Liquid chromatography coupled with mass spectrometry (LC-MS) is the approach of choice, followed by gas chromatography coupled with mass spectrometry (GC-MS)/gas chromatography with flame ionization detection (GC-FID), direct injection-mass spectrometry (DI-MS) and lastly supercritical fluid chromatography coupled with mass spectrometry (SFC-MS).

5.2 Lipid profile identified from DBS samples

Considering the identification of DBS lipid species, different lipid classes were analysed and identified, such as FA, PUFA[20–23, 26, 29, 36, 38], or acylcarnitines[17, 18], mainly analysed by GC-MS with a few studies by LC-MS. Other classes of complex lipids like sphingolipids[27, 35], PL, Chol, TG, prenols, CER and sterols[13, 15, 19, 24, 25, 28, 37, 39] were analysed either by LC-MS, DI-MS or SFC-MS. However, only one study solely reported the identification of several variables of the lipid fraction, not specifying lipid classes or species (Table 2)[16].

The lipids identified in these studies also depend a lot on the objective of the work. Some studies identify FA or PC, as major lipids, or other specific classes, for pre-analytical process optimization, as described in the previous chapter. Others identify the lipidome, as for example in studies that compare whole blood with DBS, or even some when the goal is to evaluate the applicability of DBS and lipidomics in clinical settings, as we will describe.

5.3 Lipidomics comparing DBS with whole blood or plasma/serum

DBS was compared in several studies with whole blood/plasma/serum using FA profiling or complex lipids identification, by GC-MS/GC-FID, LC-MS, DI-MS and SFC-MS(Table 2). Most of the studies identified complex lipids from specific classes but with different levels of coverage and goals. Both neutral lipids, like TG, Chol and CE, and PL were identified in DBS lipid extracts. Only few studies identified specific classes like PC, SM, TG, either when testing stability or other goals like sensitivity/specificity or method optimization. Even when looking for specific lipid classes, the number of species identified per class was different between studies, mainly because in most cases the goal of the study was not a full lipid profiling. In other studies, it was used the quantification of lipid species to evaluate the extraction recovery, or other pre-analytical parameters, as buffers, addition of antioxidants and type of paper cards, as reported in chapter 3.

Comparison of free FA profiling in DBS and blood was done by Gunash and co-workers[29]. They have compared the free FA quantification ability of DBS with a novel

wicking device designed to collect a known volume of blood (10 µL Mitra® Microsampling Device)[29]. Free FA 16:0 and 18:0 were detected on the blank DBS and after using wicking device. The concentrations of the FA 16:0 were considerably higher on the wicking device tip when compared with the 6 mm DBS punch. The presence of free FA 16:0 and 18:0 in both materials was confirmed by ultra-high performance liquid chromatography-tandem mass spectrometer (UHPLC-MS/MS). This study proved that DBS has the FA 16:0 and FA 18:0 as contaminants, however they are present in such low abundances (lower than their presence in blood) that do not influence the results of DBS blood analysis[29].

Acylcarnitines profiling in DBS and plasma, associated with different metabolic disorders, were assessed by Primassin and partners. They showed that free carnitine concentrations in plasma were generally 3.12 (±0.13) times higher than free carnitine concentrations in DBS samples, in patients with fatty acid β-oxidation disorders with and without an L-carnitine supplement[17]. In the case of patients with carnitine palmitoyltransferase I – deficiency, free carnitine concentrations were higher in DBS samples compared to plasma samples. Indeed, plasma acylcarnitine analysis have a higher sensitivity for the diagnosis of CPT2/CACT deficiencies while DBS acylcarnitine analysis have a higher sensitivity for CPT1 deficiencies[67]. Also, regarding fatty acid oxidation β-disorders, Al-Thihli *et al* found by using DI-MS analysis that the sensitivity of DBS acylcarnitine profile of patients with history of rhabdomyolysis was lower than serum acylcarnitine profile[18]. DBS presented a sensitivity of 71.4%, compared to serum that presented a sensitivity of 100%. Regarding specificity, the results showed the opposite trend. DBS acylcarnitine profile had a specificity of 100% while the specificity of the serum was 94.7%. The study concluded that serum acylcarnitine profile can be more sensitive than DBS in detecting milder forms of fatty acid oxidation β-disorders, however less specific[18].

The lipid profile of plasma, whole blood, and DBS samples of healthy breast-fed infants at 3 and 12 months of age were compared using DI-MS and by LC-MS to perform lipid profile identification[24]. The lipid species identified were from the classes of TG, SM and PC. Oxidized derivatives of CE, TG, PC, SM, and phosphatidylethanolamines (PE) were also

identified. Notably, the lipid species identified in DBS samples were not different to that of whole blood samples, but as expected both were different from plasma due to the presence of different lipid classes in whole blood. When analysing the pattern of inter-subject variability, the lipid profiles of plasma, whole blood and DBS revealed the same trend and the results from DBS were comparable or even with better precision[24].

The composition of DBS lipidome was also compared with whole blood using untargeted lipidomic profiling, allowing the identification and quantification of lipid species of the main classes found in blood, such as PC, PE, lysophosphatidylcholine (LPC), TG and CE[25]. The study identified, by UHPLC-MS/MS, the following acyl species: PC(16:0/18:2; 16:0/20:4; 16:0/20:5; 16:0/22:6; 18:0/20:5; 18:0/22:6; 18:1/22:6), LPC(16:0), PE(16:0/18:2; 16:0/22:6); Plasmenyl PE((P)-16:0/20:5; P-16:0/22:6; P-18:0/20:4), phosphatidylserines (PS) (18:0/18:1; 18:0/20:3; 18:0/20:4; 18:0/22:6), TG (16:0/18:1/18:1; 16:0/18:2/20:5; 16:0/18:2/22:6; 18:1/18:2/20:5; 16:0/18:1/22:6) and CE(18:2; 20:5; 22:6). The same lipid species were qualitatively and quantitatively identified in both samples showing that DBS can be used for comprehensive, untargeted lipidomics of the most abundant lipid species in whole blood. However, the number of identified species in this study is far from the average number of a lipidomic analysis by LC-MS, which suggests that the analysis and interpretation of the LC-MS results was limited. On the same line of work, the DBS blood lipidome was also studied by high-throughput DI-MS[26], which allowed the identification of more than 1200 lipid molecules. The lipids were extracted using a modified Bligh & Dyer extraction protocol to which was added a LiCl solution to improve the extraction efficiency of acidic lipids, prevent the degradation of plasmalogen molecular species, and decrease spectral complexity. This method was able to identify and quantify, in a single DBS sample, molecular species belonging to PL, glycerides, glycolipids, SM, acylcarnitines and Cer lipid class. DBS results for the identified lipid species and class distribution was analogous to whole blood samples, containing more PL and less TG, as opposed to plasma and serum samples, as expected, but similarly to blood due to the contribution of blood cells for the higher content in PL[13].

Lipidomic profiling from DBS and serum was compared, after analysis by LC-MS of samples collected in 2000-2001, to confirm lipid composition and stability of DBS and to assess if DBS would be useful time points for future use in larger cohorts of longitudinal studies of metabolic disease progression[39]. A total of 336 lipids were identified, from those, 194 were identified in the DBS and 280 were identified in the serum with 140 in common. On one side, PL were the most commonly identified lipids in both types of samples, with the greatest number of identified species belonging to PC, SM and LPC. On the other side, monoacylglycerol and PS classes were identified only in DBS while phosphatidic acid and vitamin E were not observed in DBS samples. The presence of PS only on DBS was understandable as PS lipids are present in the lipid membrane of erythrocytes and platelets, however PS is known to be a minor lipid class in lipoproteins. The study concludes that, since most lipid changes were preserved, DBS samples could be used in lipidomic longitudinal studies[39].

Machine learning was also used to predict 'clinical lipid' concentration from lipid profile data when compared lipid profiling from DBS with lipid profiling from plasma[19]. In this study, 118 lipid species from 11 classes were identified in DBS samples with 71% of the lipids measured in DBS also measured in plasma samples. However, the lipid classes identified were not listed in the published work. Of the 44 lipid associations from the 4 predictive panels [TG, high density lipoproteins (HDL), low density lipoprotein (LDL) and total Chol] 82% were measured in DBS samples and successfully validated with a strong correlation ($r = 0.917$) observed between the individual lipid abundance and lipoprotein concentration in both DBS and plasma samples. When applying random forest machine learning to the lipid profile data, the authors obtained good estimates ($r > 0.7$) of the concentration of TG and HDL and modest estimates ($r > 0.4$) of LDL and total Chol. However, although the obtained accuracies are significantly high, they are not suitable to be used in clinical practice, evidencing that there is room to improvement[19].

SFC-MS was used to develop a new analytical strategy for a high-throughput and comprehensive lipidomic analysis[37]. The researchers developed and optimized a new method that allowed the separation of 17 classes of lipids by SFC-MS-Q-TOF. However, when this

method was applied to the evaluation of the lipidomic profile of DBS and whole blood, they could only detect 13 lipid classes (CE, Chol, TG, free FA, Cer, SM, PC, PE, phosphatidylinositol (PI), phosphatidylglycerol (PG), LPC, LPE, acylcarnitines). In the comparison of these two types of samples, the authors noticed that the relative quantities were different between whole blood samples and DBS, especially for PC, PI, PE, LPC, TG and CE. Additionally, FA presented an unusual high level of detection, which is not typical. The qualitative profiles within each class were checked by controlling the detection of 168 different species. The molecular species profiling was very similar for almost all the classes. The authors ultimately assessed the stability of the lipids in DBS samples after 3 weeks of storage at room temperature in dark finding that the distribution of the main lipid classes within the total were similar (between the initial time and 3 weeks later), which was confirmed regarding the relative quantification of PC, PE, PI, SM, LPE and LPC[37].

Overall, all the studies that compared whole blood with DBS proved that DBS retains the same information in lipid profiling as the analysis of whole blood since the biological matrix is the same. However, one study showed that the lipid profiling in the plasma/serum was different when compared with DBS.

5.4 DBS and lipidomics in clinical settings

Concerning the independent use of DBS method associated with lipidomics analysis in clinical settings, few papers applied the DBS method to create reference intervals, measure diet effects and lipid levels in different pathologies comparing the results with traditional sampling methods (plasma/serum/whole blood samples) and healthy controls (Table 2)[22, 25, 35, 36, 38]. These showed that DBS are not yet established as a conventional sampling method for clinical lipidomic analysis, however, demonstrating quite promising results for example in targeted analysis of acylcarnitines in newborn-screening programs.

The levels of *n*-3 and *n*-6 long chain PUFA of DBS from Zimbabwean healthy children aged 7–9 years old were quantified by GC-FID to determine the reference interval for these

FA[36]. The *n*-3 long chain PUFA (EPA, docosapentaenoic acid *n*-3 and DHA) levels were significantly low while saturated fats, monounsaturated and *n*-6 long chain PUFA (AA) were surprisingly high compared to the already established reference intervals for healthy children. The 7-year-old children had lower EPA and higher AA values[36]. The low EPA and high AA levels lead to very high AA/EPA and total *n*-6 PUFA/total *n*-3 PUFA ratios, which are pro-inflammatory, thus being a health concern matter for those children.

To evaluate the effects of diet, FA esterified to glycerolipids in DBS were profiled by GC-FID and compared with the ones from venous whole blood samples in a fat challenge test[25]. In whole blood, PL are less affected, than the total lipid content, by recent dietary intake, thus are a more stable marker. The study determined that the levels of FA 18:0 esterified to PL were significantly lower in DBS when compared with whole blood. The FA 18:1 *n*-9 esterified to PL showed the opposite behaviour, with a marked increase in DBS samples[25]. In contrast to whole blood total lipids, whole blood glycerophospholipids are less affected by recent dietary intake and thus are a more stable marker.

A method to determine FA ethyl esters, in DBS through LC-MS/MS, was developed and validated by Luginbühl and colleagues[22]. This study shows the capability of the analysis of FA ethyl esters from DBS samples as a short-term confirmation for ethanol ingestion or in the absence of traditional samples (whole blood/plasma/serum). LC-MS/MS approach proved to be advantageous compared to preliminary tests with GC-MS and solid-phase microextraction (SPME) followed by GC-MS due to its higher sensitivity and shorter run-time[22].

In the case of DBS combined with lipidomics for screening diseases, some studies reported its application to different pathologies. DBS were studied to identify markers in disease, either FA[38] or profiling polar lipid species[35]. Using GC-MS approaches, Kimura and partners analysed and compared the free FA levels of DBS with whole blood/serum from healthy controls and children with different fatty acid β-oxidation disorders[38]. Children with very long chain acyl-CoA dehydrogenase deficiency showed a significant increase of FA 14:1. Regarding medium chain acyl-CoA dehydrogenase deficiency, FA 8:0, 10:0 and 10:1 were significantly elevated. In multiple acyl-CoA dehydrogenase deficiency both FA 10:1 and FA

14:1 concentrations were markedly increased. In an infant fed with medium chain triglyceride milk, both FA 8:0 and FA 10:0 were increased. Children with physiological ketosis presented a slight elevation of FA 8:0 and FA 10:0[38].

Lipid levels were also evaluated in DBS from Niemann–Pick disease type B (NPD-B) patients and compared to normal controls using LC-MS[35]. The study determined that DBS lyso-SM levels were considerably elevated in NPD-B patients when compared to normal controls, contrarily with what happens with SM levels (patient values overlapping normal controls)[35]. In this case, lyso-SM has the potential to become a biomarker of this disease, after systematic and longitudinal study of lyso-SM in clinic, evidencing the applicability of DBS sampling method for diagnosis, disease monitoring, therapeutic efficacy, and personalized medicine.

Table 4.1-2. Analysis of the selected studies according with the lipidomic parameters as extraction method, MS approach, identified lipids and considering main goals of each study.

Lipids identified	Goals	Extraction method	MS lipidomic approach	Reference
GC-MS/GC-FID				
Free FA profile (molecular species identified)	✓Comparison between filter paper with whole blood and filter paper with serum	Acetyl chloride + 6% potassium carbonate + hexane	GC-MS with a fused silica DB-5 one	Kimura *et al* (2002)[38]
FA profile (molecular species identified)	✓Stability	Direct transesterification in 14% boron trifluoride in methanol with hexane using a convectional block heater set at 95 °C for 60 minutes	GC-MS with a DB-FFAP capillary column	Metherel *et al* (2013)[21]
FA profile (molecular species identified)	✓Stability ✓Comparison between DBS, plasma, whole blood, and erythrocytes	1% (v/v) H_2SO_4 in anhydrous MeOH, heated at 70 ºC for 3h	GC-FID with a BPX70 capillary column	Liu *et al* (2014)[23]
n-3 and *n*-6 long-chain PUFA profile (molecular species identified)	✓Establishment of reference intervals ✓Comparison between groups by gender and by age	Fingertip Bell method[68]	GLC-FID with a ZB Wax capillary column	Mashavave *et al* (2016)[36]
FA profile (molecular species identified)	✓Lipid identification ✓Stability	MeOH+chloroform/MeOH (1:1, v/v); Modified Folch	GC-FID with a BPX 70 column	Drzymała-Czyz *et al* (2017)[25]
FA profile (molecular species identified)	✓Stability	Hexane + BF_3/MeOH (14%, wt/v)	GC-FID with a SP52-60 capillary column	Marino *et al* (2018)[20]
LC-MS				
Free carnitine and γ-butyrobetaine	✓Comparison between plasma, DBS, and healthy controls	MeOH	LC-ESI-MS/MS (quattro II triple-quadrupole) with a Gilson 231XL autosampler and a Hewlett-Packard HP-1100 HPLC pump	Primassin *et al* (2010)[17]
PL (PC+LPC), Chol, CE, TG	✓Extraction efficiency ✓Ion suppression ✓Matrix ionization effects	MeOH; ACN; IPA; CH_3Cl_2; MTBE; ether; *n*-hexane	HPLC-MS/MS with a Luna Silica analytical column along with a Gemini C18 guard column	Ismaiel *et al* (2012)[15]
TG, PL (PC+PE), SM, CE	✓Comparison between DBS, plasma, and whole blood ✓Lipid identification ✓Stability	H_2O + MeOH + MTBE	DI-MS: Orbitrap using a Triversa Nanomate; LC-MS (LTQ-Orbitrap) with an Hypersil Gold C18 column	Koulman *et al* (2014)[24]

Lyso-SM	✓ Lipid identification	MeOH/ACN/H_2O (80:15:5, v/v/v)	LC-MS/MS (API Qtrap 4000 mass spectrometer System) with a normal-phase silica column	Chuang *et al* (2014)[35]
PL (PC+PE+PS), TG, CE (molecular species identified)	✓Optimization of the extraction protocol ✓Extraction efficiency ✓Comparison between whole blood and DBS	Modified Folch [chloroform/methanol (2:1, v/v) + 0.2 M $NaHPO_4$ in ddH_2O]	UHPLC-MS Q-Orbitrap with a C18 reverse phase column	Henao *et al* (2016)[28]
FA ethyl esters (molecular species identified)	✓Matrix effects ✓Extraction and recovery efficiency ✓Lipid identification	Dried dimethyl sulfoxide + *n*-heptane	LC-MS/MS (Q-Trap) with a coreshell Kinetex C8 column from Phenomenex	Luginbühl *et al* (2016)[22]
PL (PC+LPC, PS), SM, TG, monoacylglycerol	✓Stability ✓Comparison between serum and DBS	Modified Folch [water + chloroform/methanol (2:1, v/v) at -20 °C]	LC-MS/MS (Orbitrap-QTOF) with a Waters HSS T3 column; LC-IMS-MS	Kyle *et al* (2017)[39]
Free PUFA (molecular species identified)	✓Extraction and recovery efficiency ✓Stability ✓Linearity and precision of the method	80% aqueous MeOH; 70% aqueous ACN + 12 mM ammonium formate + 0.02% acetic acid; 80% aqueous ACN; 80% aqueous ACN + 0.02% formic acid; 80% aqueous ACN + 0.05% formic acid	LC–MS/MS (triple quadrupole) with an Eclipse plus C8 column	Hewawasam *et al* (2017)[26]
PC, SM (molecular species identified)	✓Lipid identification ✓Stability ✓Matrix Effect ✓Extraction and recovery efficiency ✓Repeatability	MeOH	UHPLC-ESI-MS (triple quadrupole) with an Agilent ZORBAX Eclipse Plus C18 column; high resolution maXis UHR-TOF	Liao *et al* (2018)[27]
FA, LPC (molecular species identified)	✓Matrix effect ✓Lipid identification ✓Comparison between DBS, the novel wicking device and whole blood	Chloroform:MeOH (2:1, v/v) + BHT + sodium phosphate buffer	GC-FID with a nitroterephathalic acid modified polyethylene glycol capillary column; UHPLC-MS (Quadrupole-Orbitrap) with a C18 Ascentis Express column	Gunash *et al* (2019)[29]
DI-MS				
Acylcarnitine profile	✓ Comparison of the sensitivities and specificities of DBS and serum	MeOH	DI-MS/MS utilizing a Waters Quattro Micro tandem mass spectrometer for MRM data acquisition	Al-Thihli *et al* (2014)[18]
PL, glycerides, glycolipids, SM, acylcarnitines and Cer (molecular species identified)	✓Stability ✓Extraction and recovery efficiency ✓Repeatability ✓Comparison between DBS, plasma, whole blood and serum	Modified Bligh & Dyer [chloroform/methanol (1:1, v/v) + LiCl solution]	QTOF-MS/MS with atmospheric-pressure chemical ionization	Gao *et al* (2017)[13]

PL (PC+LPC), SM, CE, TG, diacylglycerol (molecular species identified)	✓Precision of the method ✓Comparison between DBS	MTBE + H_2O	Orbitrap using a Triversa Nanomate and plasma	Snowden *et al* (2020)[19]
PL, TG	✓Extraction efficiency	INF	Orbitrap using a Triversa Nanomate	Furse *et al* (2020)[16]
		SFC-MS		
CE, Chol, TG, free FA, Cer, SM, PC, PE, PI, PG, LPC, LPE, acylcarnitines (molecular species identified)	✓Method development and optimization ✓Comparison between DBS and whole blood samples	Modified Folch [water + $CHCl_3$:MeOH (50:50; v/v) + internal standard mixture]	UPC^2-QTOF with an ACQUITY UPC^2 Torus diethylamine column	Le Faouder *et al* (2021)[37]

INF: Information not found

6. Concluding remarks and future perspectives

In summary, high-throughput lipidomics proves to be a robust and formidable tool to be applied in the analysis of DBS samples, in particular LC-MS and DI-MS. It has been demonstrated its functionality for investigation of population health and precision medicine in diverse disease states and situations.

Clinical lipidomics is an emerging line of research that focuses on the evaluation of the variation of lipids at a molecular level in several diseases. The development and improvement of MS methods for the detection of lipid molecules has become increasingly important in research field. The molecular profiling of lipids that take part of the mechanisms associated with pathophysiological processes is not yet fully understood[8]. Therefore, the main goals are to comprehend the modulation of the lipid metabolism and its mechanisms, identify new possible therapeutic targets and diagnostic biomarkers and evaluate disease development as well as monitor disease therapeutics[12]. This review gathered information from different types of samples which can be obtained from different extraction methods and MS techniques. Hopefully in a near future DBS can be seen as a promising approach to disease diagnostics/follow-up and therapy monitorization. Thus, the question arises: would it be useful in clinical lipidomic analysis the implementation of the DBS sampling method as a standard procedure? From the studies gathered in this review it may be concluded that DBS are as effective as plasma/serum/whole blood samples, achieving high levels of sensitivity and specificity during MS and MS/MS analysis. The identification of the DBS lipidome through MS/MS lipidomics platforms (GC-MS, LC-MS, DI-MS and SFC-MS) provides useful and important perceptions that empower personalized lipidomics profiling to monitor physiological changes, which could be applied to the diagnosis and follow-up of a disease[13]. However, it is necessary to pay attention to the impact of the aforementioned factors which might influence the results. When analysing lipids extracted via DBS, the possible interaction between the lipidic molecules and DBS card components can lead to ion suppression in the MS source, as well as changes in chromatographic mobility during chromatographic separation and peak sharpness. Hence, when using DBS, it must be taken into consideration the stability of the lipids on the

paper cards during drying and storage, the uniformity of the blood spot, the effect of Hct, and the elution efficiency[8]. If the extraction and analysis method is already optimized, then DBS sampling would be preferable in clinical practice instead of the samples obtained by invasive venous blood collection, since drying of blood biomaterial decreases the risk of contamination with pathological and other infectious agents; and the concentration of lipids in capillary blood may differ from that in venous blood[69]. Additionally, there is a need for more studies showing the applicability of DBS in clinical lipidomics (for instance in diagnostics/follow-up of diseases), where it is independently used the DBS method in clinical settings without comparing the results with traditional samples.

In brief, the studies gathered in this review evidence that attention should be drawn to the storage and lipid extraction methods. Those methods should be made a standard operating procedure and reinforced through quality assessments during and after implementation so that the variability is reduced, and the lipids stability is maximized to promote a successful application of DBS technology and harmonization of clinical lipidomics. Most of the published studies refer to method development and its validation with patients' samples. DBS technology is indeed the most ethical and cost-effective method of collecting, delivering, and storing the biomaterial. The DBS sampling method is a promising candidate to substitute venous blood samples offering several advantages and its application in clinical lipidomics, although still scarce, has been applied in few studies looking for disease lipids biomarkers which seems to be quite promising.

Declarations

Conflict of Interest

The authors declare no conflict of interests.

Acknowledgements & Funding

Thanks are due for the financial support to the University of Aveiro and FCT/MCT for the financial support to research units CESAM (UIDB/50017/2020, UIDP/50017/2020 & LA/P/0094/2020), LAQV-REQUIMTE (UIDB/50006/2020) and CICECO - Aveiro Institute of Materials (UIDB/50011/2020,

UIDP/50011/2020 & LA/P/0006/2020), and to RNEM, Portuguese Mass Spectrometry Network (LISBOA-01-0145-FEDER-402-022125) through national funds and, where applicable, co-financed by the FEDER, within the PT2020. Helena Beatriz Ferreira is grateful to FCT for her PhD Grant (2020.04611.BD). Inês Guerra is grateful to FCT for her PhD Grant (2021.04754.BD). Ana Moreira thanks the contract in the scope of the project "Coccolitho4BioMat" (POCI-01-0145-FEDER-031032). Tânia Melo thanks the Junior Researcher contract in the scope of the Individual Call to Scientific Employment Stimulus 2020 (CEECIND/01578/2020). The authors are thankful to the COST Action EpiLipidNET, CA19105 - Pan-European Network in Lipidomics and EpiLipidomics.

References:

1. Wagner M, Tonoli D, Varesio E, Hopfgartner G (2016) The use of mass spectrometry to analyze dried blood spots. Mass Spectrom Rev 35:361–438. https://doi.org/10.1002/mas.21441
2. Rottinghaus EK, Beard RS, Bile E, Modukanele M, Maruping M, Mine M, Nkengasong J, Yang C (2014) Evaluation of Dried Blood Spots Collected on Filter Papers from Three Manufacturers Stored at Ambient Temperature for Application in HIV-1 Drug Resistance Monitoring. PLoS One 9:e109060. https://doi.org/10.1371/journal.pone.0109060
3. Konig S, Yildiz O, Hermann N, Steurer A, Singrasa M, Dobelin W (2012) A novel concept for sample collection and sample preparation. Int J Pharm Sci Rev Res 15:90–94
4. Rus C-M, Di Bucchianico S, Cozma C, Zimmermann R, Bauer P (2021) Dried Blood Spot (DBS) Methodology Study for Biomarker Discovery in Lysosomal Storage Disease (LSD). Metabolites 11:382. https://doi.org/10.3390/metabo11060382
5. Li K, Naviaux JC, Monk JM, Wang L, Naviaux RK (2020) Improved Dried Blood Spot-Based Metabolomics: A Targeted, Broad-Spectrum, Single-Injection Method. Metabolites 10:82. https://doi.org/10.3390/metabo10030082
6. Nakajima D, Ohara O, Kawashima Y (2021) Toward proteome-wide exploration of proteins in dried blood spots using liquid chromatography-coupled mass spectrometry. Proteomics 21:2100019. https://doi.org/10.1002/pmic.202100019
7. Dhingra N, Diepart M, Dziekan G, Khamassi S, Otaiza F, Wilburn S (2010) WHO guidelines on drawing blood: best practices in phlebotomy. World Health Organization, https://www.euro.who.int/__data/assets/pdf_file/0005/268790/WHO-guidelines-on-drawing-blood-best-practices-in-phlebotomy-Eng.pdf
8. Malsagova K, Kopylov A, Stepanov A, Butkova T, Izotov A, Kaysheva A (2020) Dried Blood Spot in Laboratory: Directions and Prospects. Diagnostics 10:248. https://doi.org/10.3390/diagnostics10040248
9. Lima-Oliveira G, Lippi G, Salvagno GL, Picheth G, Guidi GC (2015) Laboratory Diagnostics and Quality of Blood Collection / Laboratorijska Dijagnostika I Kvalitet Uzimanja Uzoraka Krvi. J Med Biochem 34:288–294. https://doi.org/10.2478/jomb-2014-0043
10. Lim MD (2018) Dried Blood Spots for Global Health Diagnostics and Surveillance: Opportunities and Challenges. Am J Trop Med Hyg 99:256–265. https://doi.org/10.4269/ajtmh.17-0889
11. Burnett JE (2011) Dried blood spot sampling: practical considerations and recommendation for use with preclinical studies. Bioanalysis 3:1099–1107
12. Lv J, Zhang L, Yan F, Wang X (2018) Clinical lipidomics: a new way to diagnose human diseases. Clin Transl Med 7:10–12. https://doi.org/10.1186/s40169-018-0190-9
13. Gao F, McDaniel J, Chen EY, Rockwell HE, Drolet J, Vishnudas VK, Tolstikov V, Sarangarajan R, Narain NR, Kiebish MA (2017) Dynamic and temporal assessment of human dried blood spot MS/MSALL shotgun lipidomics analysis. Nutr Metab (Lond) 14:28. https://doi.org/10.1186/s12986-017-0182-6
14. Wilson I (2011) Global metabolic profiling (metabonomics/metabolomics) using dried blood

spots: advantages and pitfalls. Bioanalysis 3:2255–2257. https://doi.org/10.4155/bio.11.221
15. Ismaiel OA, Jenkins RG, Thomas Karnes H (2013) Investigation of endogenous blood lipids components that contribute to matrix effects in dried blood spot samples by liquid chromatography-tandem mass spectrometry. Drug Test Anal 5:710–715. https://doi.org/10.1002/dta.1421
16. Furse S, Koulman A (2020) Lipid extraction from dried blood spots and dried milk spots for untargeted high throughput lipidomics. Mol Omi 16:563–572. https://doi.org/10.1039/d0mo00102c
17. Primassin S, Spiekerkoetter U (2010) ESI-MS/MS measurement of free carnitine and its precursor γ-butyrobetaine in plasma and dried blood spots from patients with organic acidurias and fatty acid oxidation disorders. Mol Genet Metab 101:141–145. https://doi.org/10.1016/j.ymgme.2010.06.012
18. Al-Thihli K, Sinclair G, Sirrs S, Mezei M, Nelson J, Vallance H (2014) Performance of serum and dried blood spot acylcarnitine profiles for detection of fatty acid β-oxidation disorders in adult patients with rhabdomyolysis. J Inherit Metab Dis 37:207–213. https://doi.org/10.1007/s10545-012-9578-7
19. Snowden SG, Korosi A, de Rooij SR, Koulman A (2020) Combining lipidomics and machine learning to measure clinical lipids in dried blood spots. Metabolomics 16:83. https://doi.org/10.1007/s11306-020-01703-0
20. Di Marino C, De Marco A, Pisanti A, Romanucci V (2018) Effects of Dried Blood Spot Storage on Lipidomic Analysis. Molecules 23:403. https://doi.org/10.3390/molecules23020403
21. Metherel AH, Hogg RC, Buzikievich LM, Stark KD (2013) Butylated hydroxytoluene can protect polyunsaturated fatty acids in dried blood spots from degradation for up to 8 weeks at room temperature. Lipids Health Dis 12:22. https://doi.org/10.1186/1476-511X-12-22
22. Luginbühl M, Schröck A, König S, Schürch S, Weinmann W (2016) Determination of fatty acid ethyl esters in dried blood spots by LC–MS/MS as markers for ethanol intake: application in a drinking study. Anal Bioanal Chem 408:3503–3509. https://doi.org/10.1007/s00216-016-9426-y
23. Liu G, Mühlhäusler BS, Gibson RA (2014) A method for long term stabilisation of long chain polyunsaturated fatty acids in dried blood spots and its clinical application. Prostaglandins, Leukot Essent Fat Acids 91:251–260. https://doi.org/10.1016/j.plefa.2014.09.009
24. Koulman A, Prentice P, Wong MCY, Matthews L, Bond NJ, Eiden M, Griffin JL, Dunger DB (2014) The development and validation of a fast and robust dried blood spot based lipid profiling method to study infant metabolism. Metabolomics 10:1018–1025. https://doi.org/10.1007/s11306-014-0628-z
25. Drzymała-Czyż S, Janich S, Klingler M, Demmelmair J, Walkowiak J, Koletzko B (2017) Whole blood glycerophospholipids in dried blood spots − a reliable marker for the fatty acid status. Chem Phys Lipids 207:1–9. https://doi.org/10.1016/j.chemphyslip.2017.06.003
26. Hewawasam E, Liu G, Jeffery DW, Muhlhausler BS, Gibson RA (2017) A validated method for analyzing polyunsaturated free fatty acids from dried blood spots using LC–MS/MS. Prostaglandins, Leukot Essent Fat Acids 125:1–7. https://doi.org/10.1016/j.plefa.2017.08.010
27. Liao HW, Lin SW, Lin YT, Lee CH, Kuo CH (2018) Identification of potential sphingomyelin markers for the estimation of hematocrit in dried blood spots via a lipidomic strategy. Anal Chim Acta 1003:34–41. https://doi.org/10.1016/j.aca.2017.11.041
28. Aristizabal Henao JJ, Metherel AH, Smith RW, Stark KD (2016) Tailored Extraction Procedure Is Required To Ensure Recovery of the Main Lipid Classes in Whole Blood When Profiling the Lipidome of Dried Blood Spots. Anal Chem 88:9391–9396. https://doi.org/10.1021/acs.analchem.6b03030
29. Gunash J, Aristizabal-Henao JJ, Stark KD (2019) Quantitating fatty acids in dried blood spots on a common collection card versus a novel wicking sampling device. Prostaglandins, Leukot Essent Fat Acids 145:1–6. https://doi.org/10.1016/j.plefa.2019.05.002
30. Li W, Zhang J, Tse FLS (2011) Strategies in quantitative LC-MS/MS analysis of unstable small molecules in biological matrices. Biomed Chromatogr 25:258–277. https://doi.org/10.1002/bmc.1572

31. Grüner N, Stambouli O, Ross RS (2015) Dried Blood Spots - Preparing and Processing for Use in Immunoassays and in Molecular Techniques. J Vis Exp 13:52619. https://doi.org/10.3791/52619
32. Ho NT, Busik J V., Resau JH, Paneth N, Khoo SK (2016) Effect of storage time on gene expression data acquired from unfrozen archived newborn blood spots. Mol Genet Metab 119:207–213. https://doi.org/10.1016/j.ymgme.2016.08.001
33. Pupillo D, Simonato M, Cogo PE, Lapillonne A, Carnielli VP (2016) Short-Term Stability of Whole Blood Polyunsaturated Fatty Acid Content on Filter Paper During Storage at −28 °C. Lipids 51:193–198. https://doi.org/10.1007/s11745-015-4111-z
34. Han J, Higgins R, Lim MD, Lin K, Yang J, Borchers CH (2018) Short-Term Stabilities of 21 Amino Acids in Dried Blood Spots. Clin Chem 64:400–402. https://doi.org/10.1373/clinchem.2017.278457
35. Chuang WL, Pacheco J, Cooper S, McGovern MM, Cox GF, Keutzer J, Zhang XK (2014) Lyso-sphingomyelin is elevated in dried blood spots of Niemann-Pick B patients. Mol Genet Metab 111:209–211. https://doi.org/10.1016/j.ymgme.2013.11.012
36. Mashavave G, Kuona P, Tinago W, Stray-Pedersen B, Munjoma M, Musarurwa C (2016) Dried blood spot omega-3 and omega-6 long chain polyunsaturated fatty acid levels in 7–9 year old Zimbabwean children: a cross sectional study. BMC Clin Pathol 16:14. https://doi.org/10.1186/s12907-016-0035-7
37. Le Faouder P, Soullier J, Tremblay-Franco M, Tournadre A, Martin J-F, Guitton Y, Carlé C, Caspar-Bauguil S, Denechaud P-D, Bertrand-Michel J (2021) Untargeted Lipidomic Profiling of Dry Blood Spots Using SFC-HRMS. Metabolites 11:305. https://doi.org/10.3390/metabo11050305
38. Kimura M, Yoon HR, Wasant P, Takahashi Y, Yamaguchi S (2002) A sensitive and simplified method to analyze free fatty acids in children with mitochondrial beta oxidation disorders using gas chromatography/mass spectrometry and dried blood spots. Clin Chim Acta 316:117–121. https://doi.org/10.1016/S0009-8981(01)00741-0
39. Kyle JE, Casey CP, Stratton KG, Zink EM, Kim Y, Zheng X, Monroe ME, Weitz KK, Bloodsworth KJ, Orton DJ, Ibrahim YM, Moore RJ, Lee CG, Pedersen C, Orwoll E, Smith RD, Burnum-Johnson KE, Baker ES (2017) Comparing identified and statistically significant lipids and polar metabolites in 15-year old serum and dried blood spot samples for longitudinal studies. Rapid Commun Mass Spectrom 31:447–456. https://doi.org/10.1002/rcm.7808
40. Liu G, Patrone L, Snapp HM, Batog A, Valentine J, Cosma G, Tymiak A, Ji QC, Arnold ME (2010) Evaluating and defining sample preparation procedures for DBS LC–MS/MS assays. Bioanalysis 2:1405–1414. https://doi.org/10.4155/bio.10.106
41. Clark GT, Haynes JJ (2011) Utilization of DBS within drug discovery: a simple 2D-LC–MS/MS system to minimize blood- and paper-based matrix effects from FTA elute™ DBS. Bioanalysis 3:1253–1270. https://doi.org/10.4155/bio.11.81
42. Ismaiel OA, Zhang T, Jenkins RG, Karnes HT (2010) Investigation of endogenous blood plasma phospholipids, cholesterol and glycerides that contribute to matrix effects in bioanalysis by liquid chromatography/mass spectrometry. J Chromatogr B 878:3303–3316. https://doi.org/10.1016/j.jchromb.2010.10.012
43. Gurtovenko AA, Mukhamadiarov EI, Kostritskii AY, Karttunen M (2018) Phospholipid–Cellulose Interactions: Insight from Atomistic Computer Simulations for Understanding the Impact of Cellulose-Based Materials on Plasma Membranes. J Phys Chem B 122:9973–9981. https://doi.org/10.1021/acs.jpcb.8b07765
44. Kostritskii AY, Tolmachev DA, Lukasheva N V., Gurtovenko AA (2017) Molecular-Level Insight into the Interaction of Phospholipid Bilayers with Cellulose. Langmuir 33:12793–12803. https://doi.org/10.1021/acs.langmuir.7b02297
45. Skjærvø Ø, Solbakk EJ, Halvorsen TG, Reubsaet L (2019) Paper-based immunocapture for targeted protein analysis. Talanta 195:764–770. https://doi.org/10.1016/j.talanta.2018.12.013
46. McCann L, Benavidez TE, Holtsclaw S, Garcia CD (2017) Addressing the distribution of proteins spotted on μPADs. Analyst 142:3899–3905. https://doi.org/10.1039/C7AN00849J
47. Cobb Z, de Vries R, Spooner N, Williams S, Staelens L, Doig M, Broadhurst R, Barfield M, van

de Merbel N, Schmid B, Siethoff C, Ortiz J, Verheij E, van Baar B, White S, Timmerman P (2013) In-depth study of homogeneity in DBS using two different techniques: results from the EBF DBS-microsampling consortium. Bioanalysis 5:2161–2169. https://doi.org/10.4155/bio.13.171

48. Stickle DF, Rawlinson NJ, Landmark JD (2009) Increased perimeter red cell concentration in filter paper bloodspot samples is consistent with constant-load size exclusion chromatography occurring during application. Clin Chim Acta 401:42–45. https://doi.org/10.1016/j.cca.2008.11.011
49. Kvaskoff D, Ko P, Simila HA, Eyles DW (2012) Distribution of 25-hydroxyvitamin D3 in dried blood spots and implications for its quantitation by tandem mass spectrometry. J Chromatogr B 901:47–52. https://doi.org/10.1016/j.jchromb.2012.05.040
50. Hall E, Flores S, De Jesús V (2015) Influence of Hematocrit and Total-Spot Volume on Performance Characteristics of Dried Blood Spots for Newborn Screening. Int J Neonatal Screen 1:69–78. https://doi.org/10.3390/ijns1020069
51. De Kesel PM, Sadones N, Capiau S, Lambert WE, Stove CP (2013) Hemato-critical issues in quantitative analysis of dried blood spots: challenges and solutions. Bioanalysis 5:2023–2041. https://doi.org/10.4155/bio.13.156
52. Chao TC, Trybala A, Starov V, Das DB (2014) Influence of haematocrit level on the kinetics of blood spreading on thin porous medium during dried blood spot sampling. Colloids Surfaces A Physicochem Eng Asp 451:38–47. https://doi.org/10.1016/j.colsurfa.2014.03.033
53. Youhnovski N, Bergeron A, Furtado M, Garofolo F (2011) Pre-cut dried blood spot (PCDBS): an alternative to dried blood spot (DBS) technique to overcome hematocrit impact. Rapid Commun Mass Spectrom 25:2951–2958. https://doi.org/10.1002/rcm.5182
54. Li F, Ploch S, Fast D, Michael S (2012) Perforated dried blood spot accurate microsampling: the concept and its applications in toxicokinetic sample collection. J Mass Spectrom 47:655–667. https://doi.org/10.1002/jms.3015
55. Ren X, Paehler T, Zimmer M, Guo Z, Zane P, Emmons GT (2010) Impact of various factors on radioactivity distribution in different DBS papers. Bioanalysis 2:1469–1475. https://doi.org/10.4155/bio.10.96
56. Trufelli H, Palma P, Famiglini G, Cappiello A (2011) An overview of matrix effects in liquid chromatography–mass spectrometry. Mass Spectrom Rev 30:491–509. https://doi.org/10.1002/mas.20298
57. Marsh D (2013) Handbook of Lipids Bilayers, 2nd ed. CRC Press, Boca Raton, FL, USA
58. Bligh EG, Dyer WJ (1959) A rapid method of total lipid extraction and purification. Can J Biochem Physiol 37:911–917. https://doi.org/10.1139/o59-099
59. Eggers LF, Schwudke D (2016) Liquid Extraction: Folch. Encycl Lipidomics 1–6. https://doi.org/10.1007/978-94-007-7864-1_89-1
60. Chace DH, Kalas TA, Naylor EW (2003) Use of Tandem Mass Spectrometry for Multianalyte Screening of Dried Blood Specimens from Newborns. Clin Chem 49:1797–1817. https://doi.org/10.1373/clinchem.2003.022178
61. O'Donnell VB, Ekroos K, Liebisch G, Wakelam M (2020) Lipidomics: Current state of the art in a fast moving field. WIREs Syst Biol Med 12:e1466. https://doi.org/10.1002/wsbm.1466
62. Züllig T, Trötzmüller M, Köfeler HC (2020) Lipidomics from sample preparation to data analysis: a primer. Anal Bioanal Chem 412:2191–2209. https://doi.org/10.1007/s00216-019-02241-y
63. Alves MA, Lamichhane S, Dickens A, McGlinchey A, Ribeiro HC, Sen P, Wei F, Hyötyläinen T, Orešič M (2021) Systems biology approaches to study lipidomes in health and disease. Biochim Biophys Acta - Mol Cell Biol Lipids 1866:158857. https://doi.org/10.1016/j.bbalip.2020.158857
64. Domingues P, García A, Skrzydlewska E (2018) Advanced Analytical Chemistry for Life Sciences. AACLifeSci, https://www.umb.edu.pl/photo/pliki/projekty_umb/aac/aaclifesci_-_manual.pdf
65. Li A, Hines KM, Xu L (2020) Lipidomics by HILIC-Ion Mobility-Mass Spectrometry. Methods Mol Biol 2084:119–132. https://doi.org/10.1007/978-1-0716-0030-6_7

66. Laboureur L, Ollero M, Touboul D (2015) Lipidomics by Supercritical Fluid Chromatography. Int J Mol Sci 16:13868–13884. https://doi.org/10.3390/ijms160613868
67. de Sain-van der Velden MGM, Diekman EF, Jans JJ, van der Ham M, Prinsen BHCMT, Visser G, Verhoeven-Duif NM (2013) Differences between acylcarnitine profiles in plasma and bloodspots. Mol Genet Metab 110:116–121. https://doi.org/10.1016/j.ymgme.2013.04.008
68. Gordon Bell J, Mackinlay EE, Dick JR, Younger I, Lands B, Gilhooly T (2011) Using a fingertip whole blood sample for rapid fatty acid measurement: method validation and correlation with erythrocyte polar lipid compositions in UK subjects. Br J Nutr 106:1408–1415. https://doi.org/10.1017/S0007114511001978
69. Mohammed BS, Cameron GA, Cameron L, Hawksworth GH, Helms PJ, McLay JS (2010) Can finger-prick sampling replace venous sampling to determine the pharmacokinetic profile of oral paracetamol? Br J Clin Pharmacol 70:52–56. https://doi.org/10.1111/j.1365-2125.2010.03668.x

4.2 CHAPTER 4.2: LIPIDOMIC ANALYSIS USING DRIED BLOOD SPOTS

This chapter was integrally published as follows.
Reprinted with permission from:

H.B. Ferreira, T. Melo, H. Rocha, A. Paiva, P. Domingues, M.R. Domingues, Lipid profile variability in children at different ages measured in dried blood spots, *Molecular Omics* (2023), 19, 229-237
https://doi.org/10.1039/D2MO00206J

Abstract

Dried blood spot (DBS) is a minimally invasive sampling technique that has several advantages over conventional venipuncture/arterial blood sampling. More recently, DBS has also been applied for lipidomics analysis, but this is an area that requires further research. The few works found in the literature on lipidomics of DBS samples performed the analysis in adult samples, leaving pediatric ages unmapped. The objective of this study was to assess the variability of the lipid profile (identified by high-resolution C18 RP-LC-MS/MS) of DBS at pediatric age (0-10 days, 2-18 months, and 3-13 years) and to identify age-related variations. The results revealed that the lipidomic signature of the three age groups is significantly different, especially for a few species of neutral lipids and phosphatidylcholines. The main contributors to the differentiation of the groups correspond to 3 carnitines (Car), 2 cholesteryl esters (CE), 2 diacylglycerols (DG), 2 triacylglycerols (TG), 3 phosphatidylcholines (PC), 1 ether-linked PC, 1 phosphatidylethanolamine (PE), 1 ether-linked PE and 1 phosphatidylinositol (PI) species, all with statistically significant differences. Additionally, lipid species containing linoleic acid (C18:2) were shown to have significantly lower levels in the 0-10 days group with a gradual increase in the 2-18 month, reaching the highest concentrations in the 3-13 year group. The results of this study highlighted the adaptations of the lipid profile at different pediatric ages. These results may help improve understanding of the evolution of lipid metabolism throughout childhood and should be investigated further.

1. Introduction

Dried blood spot (DBS) is a standardized specimen collection method commonly used in several situations including neonatal screening, diagnosis, treatment monitoring and status assessment of congenital, metabolic, endocrine, haematological and genetic diseases. It can also be used in serodiagnosis for the detection of antibodies as biomarkers of infectious diseases and bacterial infections and for the bioenvironmental monitoring of toxic substances and persistent organic pollutants[1].

DBS is a minimally invasive sampling technique that has several advantages over the conventional collection of whole blood, serum or plasma samples. These include the low blood volume required (less than 25 μL), the relative stability at room temperature, thus facilitating storage, and transportation from the collection site to the laboratory, which reduces the risk of exposure to biohazards during shipment, and the fact that patients or volunteers can collect the sample at home, with minimal training[2,3]. Additionally, the spots remain stable under proper storage conditions for months or years after drying[3]. Thus, DBS is a suitable alternative to venous blood sampling in a home environment, where the patient needs to perform routine tests (e.g., patients in nursing homes or monitoring metabolic diseases), and in rural or underdeveloped areas, where access to good storage conditions or good laboratory facilities are rare[4].

More recently, DBS has also been applied for therapeutic drug monitoring, pharmacokinetics, genomics, proteomics, metabolomics and lipidomics[1,2,5]. Lipids have important biological roles and their monitoring is recognized to be of great value in the assessment of health and disease status. The lipid profile and its variation can be analysed, at the molecular level, using high-throughput lipidomics techniques, allowing to recognize how lipids contribute to the development of the disease and its molecular mechanism. This knowledge is useful and may have a purpose in clinical lipidomics for the study of several diseases[6,7]. Mass spectrometry (MS) methods have been used to analyse DBS, particularly in pharmacokinetic studies and in newborn screening to detect inborn errors of metabolism[8]. In particular, the use of DBS in lipid research is increasing, not only because lipidomic analysis on DBS have has

proven to be as effective as on plasma, but also because lipids in DBS are stable when stored under proper conditions to prevent hydrolysis and oxidation[4,9,10]. Polyunsaturated fatty acids (PUFA) were reported to be stable between 21 days and 2 months at room temperature[11,12] and, in the case of phospholipids (PL), up to 2 weeks at 4 °C or room temperature[2]. However, reducing the storage temperature is not always the solution as it is described for few PUFA (20:4, 20:5, and 22:6) that suffer significant degradation after 10 days of storage at − 28 °C[13]. There is already a substantial body of research using DBS for fatty acid stability and profiling using gas chromatography, however, little is known about the use of DBS for lipidomic profiling using high-performance liquid chromatography (LC-MS) and tandem mass spectrometry (MS/MS)[14].

The few works found in the literature on the association of DBS with lipidomics report the identification in adult samples, leaving pediatric ages unexplored. However, the lipid profile can change with age, at least at the fatty acid level, as shown by different cohort studies that have assessed changes in fatty acid profile at pediatric age[15,16]. The objective of the present study was to assess the lipid profile of DBS samples from pediatric subjects and identify age-related variations. We performed a comprehensive assessment of the variation in the DBS lipid profile in children aged 0-10 days, 2-18 months, and 3-13 years, using an untargeted C18 reverse-phase liquid chromatography high-resolution lipidomics approach.

2. Methods

2.1 Reagents

To extract PL from DBS, methanol (MeOH) and chloroform (CHCl3) were purchased from Fisher Scientific (Leicestershire, UK). To quantify the PL in each sample, dichloromethane was purchased from Fisher Scientific, 70% perchloric acid was obtained from Chem-Lab NV (Zedelgem, Belgium), $NaH_2PO_4 \cdot 2H_2O$ was purchased from Riedell-de Haën (Seelze, Germany), ammonium molybdate ($NaMoO_4 \cdot H_2O$) was acquired from Panreac (Barcelona, Spain) and L(+)-ascorbic acid from VWR Chemicals (Leuven, Belgium). Internal standards of PL 1,2-

dimyristoyl-sn-glycero-3-phosphocholine (dMPC, PC 14:0/14:0), 1,2-dimyristoyl-sn-glycero-3-phosphoethanolamine (dMPE, PE 14:0/14:0), 1,2-dimyristoyl-sn-glycero-3-phospho-(10-rac-)glycerol (dMPG, PG 14:0/14:0), 1,2-dimyristoyl-sn-glycero-3-phospho-L-serine (dMPS, PS 14:0/14:0), tetramyristoylcardiolipin (TMCL, CL 14:0/14:0/14:0/14:0), 1,2-dipalmitoyl-sn-glycero-3-phosphatidylinositol (dPPI, PI 16:0/16:0), N-heptadecanoyl-D-erythro-sphingosylphosphorylcholine (SM d18:1/17:0), 1-nonadecanoyl-2-hydroxy-sn-glycero-3-phosphocholine (LPC 19:0) and 1,2-dimyristoyl-sn-glycero-3-phosphate (dMPA, PA 14:0/14:0) for RP-LC-MS analysis were obtained from Avanti® Polar Lipids, Inc (Alabaster, AI, EUA). Solvents for LC-MS were acetonitrile (ACN), MeOH, isopropanol (Fisher Scientific), Milli-Q water and ammonium acetate (Sigma-Aldrich). Dichloromethane was also purchased from Fisher Scientific. All solvents were high-performance liquid chromatography (HPLC) grade and milli-Q water was used for all experiments (Synergy®, Millipore Corporation, Billerica, MA, USA).

2.2 Blood samples

In this study, whole blood from children 0-13 years of age was collected by heal/fingerprick on multiple 1.3 cm DBS circles of PerkinElmer® 226 filter paper cards and stored at -4 ºC until the extraction of lipids. Storage at -4 ºC was chosen to mimic the household conditions in a refrigerator. Anonymized DBS samples were provided by the National Institute of Health Doutor Ricardo Jorge. A total of 24 DBS samples from healthy children without any inborn errors of metabolism were analysed by LC-MS. The samples were divided into three different pediatric age groups and labelled as DBS_0-10 days (subjects with 0-10 days old, 12 samples, 33% females), DBS_2-18 months (subjects with 2-18 months old, 6 samples, 67% females) and DBS_3-13 years (subjects with 3-13 years old, 6 samples, 33% females).

2.3 Extraction of lipids and measurement of phosphorus

Lipids were extracted from DBS using the method of Bligh & Dyer[17]. For this, 5 circles of 3.2 mm were punched out from the DBS circles and placed in extraction tubes (Pyrex tube). To each tube was added 1 mL of milli-Q water, 3.75 mL of a mixture of CH_2Cl_2: MeOH in the ratio

of 1: 2 (v/v) and vortexed for 1 min. Then, the tubes were left on ice for 30 min to promote the separation of the organic and aqueous phases. After 30 min, the tubes were again vortexed for 30 seconds. Subsequently, 1.25 mL of CH_2Cl_2 and 1.25 mL of milli-Q water were added to each tube, vortexing for 1 min between each addition. The tubes were placed in the centrifuge (Mixtasel, 540 P Selecta model) for 5 min at 112 g to separate the two phases. The organic phase from each tube was collected for a new tube. To the aqueous phase, 1.88 mL of CH_2Cl_2 was added, and the tubes were vortexed for 1 min, which were then re-centrifuged under the same conditions to separate the aqueous phase from the remaining organic phase. The organic phase was collected to a new tube, dried under a stream of nitrogen and stored at -80 ºC.

The quantification of the total PL recovered after extraction was carried out according to the method of Bartlett & Lewis[18]. The detailed experimental procedures have been previously described by Ferreira et al[19]. Briefly, the PL extracts were dissolved in 100 µL of dichloromethane, and a volume of 10 µL was transferred, in duplicate, to a glass tube, previously washed with 5% nitric acid. The solvent was dried under a stream of nitrogen and 125 µL of 70 % perchloric acid was added to each tube. Samples were incubated in a heating block (Stuart, U.K.) for 1h at 180 °C. After cooling to room temperature, a volume of 825 µL of milli-Q water, 125 µL of 2.5% ammonium molybdate (2.5 g/ 100 mL of milli-Q water) and 125 µL of 10% ascorbic acid (0.1 g/1 mL milli-Q water) was added to each sample, with vortexing between each addition. The samples were then incubated in a water bath at 100 °C for 10 minutes. Then the samples were immediately cooled in a cold-water bath. Phosphate standards of 0.1 to 2 µg phosphorus (P) were prepared from sodium dihydrogen phosphate dihydrate (NaH2PO4·2H2O, 100 µg/mL P). The standards underwent the same experimental procedure as the samples without the heat block step. Absorbance was measured at 797 nm in a Multiskan GO 1.00.38 Microplate Spectrophotometer (Thermo Scientific, Hudson, NH, USA) controlled by SkanIT version 3.2 software (Thermo Scientific™). Samples were stored in vials at -80 ºC. The amount of P present in each sample was calculated by linear regression. For each lipid extract, the amount of total PL was calculated by multiplying the amount of phosphorus by 25.

2.4 Reverse phase liquid chromatography-mass spectrometry (RP-LC-MS)

2.4.1 Sample preparation

The PL extracts obtained from DBS were resuspended in dichloromethane to have a PL concentration of 1 μg PL/μL. Subsequently, in a vial with a micro-insert, 10 μL of each sample, 8 μL of a mixture of internal standards and 82 μL of isopropanol:MeOH (1:1) were added. The internal standard mixture contained 0.04 μg of phosphatidylcholine (PC, 14:0/14:0), 0.04 μg of phosphatidylethanolamine (PE, 14:0/14:0), 0.024 μg of phosphatidylglycerol (PG, 14:0/14:0), 0.04 μg of phosphatidylinositol (PI, 16:0/16:0), 0.08 μg of phosphatidylserine (PS, 14:0/14:0), 0.16 μg of phosphatidic acid (PA, 14:0/14:0), 0.04 μg of lyso-PC (LPC, 19:0), 0.04 μg of sphingomyelin (SM, d18:1/17:0), 0.08 μg of ceramide (d18:1/17:0) and 0.16 μg of cardiolipin (CL, 14:0/14:0/14:0/14:0). The initial chromatographic phase consisted of two mobile phases at a proportion of 68% of eluent A (60% acetonitrile, 40% methanol, 10 mM ammonium formate and 0.1% formic acid) and 32% of eluent B (90% isopropanol, 10% acetonitrile, 10 mM ammonium formate and 0.1% formic acid).

2.4.2 Data and statistical analysis

Lipids were separated by a C18 reverse phase column, using an Ascentis® Express 90 Å C18 HPLC column (15 cm x 2.1 mm; 2.7 μm, Supelco®) inserted into an HPLC system (Ultimate 3000 Dionex, Thermo Fisher Scientific, Bremen, Germany) with an autosampler coupled online to a Q-Exactive™ Hybrid Quadrupole-Orbitrap™ Mass Spectrometer (Thermo Fisher Scientific, Bremen, Germany). A volume of 5 μL of each sample mixture was injected into the HPLC column, at a flow rate of 260 μL/min. The temperature of the column oven was maintained at 50 °C. Elution started with 32% of mobile phase B, and the gradient used was: 45% B (1.5 min), 52% B (4 min), 58% B (5 min), 68% B (8 min), 70% B (11 min), 85% B (14 min), 97% B (18 min, maintained for 7 min), and 32% B (25.01 min, followed by a re-equilibration period of 8 min prior next injection).

The Q-Exactive™ orbitrap mass spectrometer with a heated electrospray ionization source was operated in the positive mode (electrospray voltage of 3.0 kV) and negative modes

(electrospray voltage of −2.7 kV). The sheath gas flow was 35 U, the auxiliary gas was 3 U, the capillary temperature was 320 °C, the S-lenses RF was 50 U and the probe`s temperature was 300 °C. Full scans MS spectra were acquired both in positive and negative ionisation modes in an m/z range of 300-1600, with a resolution of 70.000, automatic gain control (AGC) target of $1x10^6$ and maximum injection time of 100 ms. For tandem MS (MS/MS) experiments, a top-10 data-dependent method was used. The top 10 most abundant precursor ions in full MS were selected to be fragmented in the collision cell HCD. A stepped normalized collision energy™ scheme was used and ranged between 25 and 30 eV for positive ion mode and between 20, 24 and 28 for the negative ion mode. The MS/MS spectra were obtained by combining different collision energies applied to each ionization mode. The MS/MS spectra were obtained with a resolution of 17,500; an AGC target of $1x10^5$; an isolation window of 1 m/z; and a maximum injection time of 100 ms. The cycles consisted of one full scan mass spectrum and ten data-dependent MS/MS scans, which were repeated continuously throughout the experiments, with the dynamic exclusion of 30 s and an intensity threshold of $8x10^4$. Data acquisition was carried out using the Xcalibur data system (V3.3, Thermo Fisher Scientific, USA).

LC-MS data were identified using MS-DIAL v4.7[20] and integrated using MZmine v2.42 software[21]. Identification of the PL species was performed as previously described[19,22]. Briefly, to correctly identify the PL species, all peaks with raw intensity less than $1x10^4$ and mass error greater than 5 ppm were excluded. The assignment of each PL species was confirmed by analysis and interpretation of the MS/MS spectra with the aid of MS-DIAL. PC, LPC and SM were analysed in the LC-MS spectra in the positive ion mode, as $[M+H]^+$ ions. The presence of the fragment ion at m/z 184, corresponding to the phosphocholine polar head group, in the MS/MS of $[M+H]^+$ ions allows identifying PL molecular species belonging to the PC, LPC and SM classes, which were further differentiated by the characteristic retention times (Supplementary Figure S1). The identification of PC, LPC and SM classes was confirmed in the LC-MS spectra in the negative ion mode, as formate adducts ($[M+HCOO]^-$ ions). MS/MS spectra of $[M+HCOO]^-$ ions of these three PL classes should display the typical fragment ion at m/z 168 (phosphocholine polar head group minus a methyl moiety). Carboxylate anions of fatty

acyl chains can also be seen for PC and LPC. PE and LPE classes were analysed in negative ion mode ($[M-H]^-$ ions). The fragment ion at m/z 140 (phosphoethanolamine polar head group) and the carboxylate anions of fatty acyl chains can be found in the MS/MS data from negative ion mode (Supplementary Figure S2). PI and PS species were analysed in negative ion mode, as $[M-H]^-$ ions. The presence of the fragment ion at m/z 241, corresponding to the phosphoinositol polar head group, in the MS/MS of $[M-H]^-$ ions, allows the identification of PI molecular species (Supplementary Figure S3). PS species were identified in the MS/MS of $[M-H]^-$ ions by the neutral loss of -87Da from the molecular ion. The identification of the remaining lipid species belonging to the classes of carnitines (CAR), cholesteryl esters (CE, fragment ion at m/z 369) and triacylglycerols (TG), was made in LC-MS spectra in the positive ion mode, as $[M+H]^+$ ions (CAR), $[M+NH_4]^+$ ions (CE) and $[M+NH_4]^+$ ions (TG) respectively. Diacylglycerols (DG) were identified by both $[M+Na]^+$ and $[M+NH_4]^+$ ions.

Relative quantification was performed by exporting the peak area values to a computer spreadsheet. For data normalization, the peak areas of the extracted ion chromatograms (XIC) of the lipid precursors of each class were divided by the peak areas of the internal standards selected for the class. Missing values were replaced by 1/5 of the minimum positive values detected in the data set. The data sets composed of the XIC areas obtained by the RP-LC-MS analysis were normalized to the internal standard, generalized log2 and normalized with EigenMS[23]. Principal component analysis (PCA) was performed using the R libraries FactoMineR[24] and factoextra[25], and ellipses were drawn with a level of 0.90. Univariate statistical analysis was performed using the ANOVA test following Tukey`s post hoc test, after testing for normality (Shapiro–Wilk test) and homogeneity of variance (Levene test). If normality was rejected, Kruskal-Wallis followed by Dunn tests were applied. P values were adjusted for multiple comparisons by the false discovery rate (FDR) correction (q-value). Heatmaps were created using the R package pheatmap using “Euclidean” as the clustering distance and “ward.D” as the clustering method[26]. Univariate and multivariate statistical analyses were performed using R version 3.5.1 in Rstudio version 1.1.4. All graphics and boxplots were created using the R package ggplot2[27].

3. Results

The lipid profile of the DBS samples was analysed by a high-resolution RP-LC-MS and MS/MS platform. This lipidomic analysis allowed the identification of 156 different lipid species (m/z values of molecular ions) belonging to 11 different classes, namely 30 phosphatidylcholines (PC) including diacyl, alkyl-acyl and alkenyl-acyl species, 12 lyso PC (LPC), 21 phosphatidylethanolamines (PE) including diacyl, alkyl-acyl and alkenyl-acyl species, 7 lyso PE (LPE), 3 phosphatidylinositols (PI), 3 phosphatidylserines (PS), 3 sphingomyelins (SM), 6 carnitines (CAR), 5 cholesteryl esters (CE), 19 diacylglycerols (DG) and 47 triacylglycerols (TG) (Supplementary Table S1).

The differences between the lipid profile of DBS_0-10 days (12 samples), DBS_2-18 months (6 samples) and DBS_3-13 years (6 samples), were assessed using multivariate statistical analysis. The principal component analysis (PCA) plot showed that the three groups were separated into three different clusters (90% confidence interval), in a two-dimensional score plot that represented the analysis describing 44.6% of the total variance, including dimension 1 (27.6%) and dimension 2 (17%) (Figure 1). The samples from the group DBS_0-10 days were scattered in the left region of the PCA plot while the group of DBS_3-13 years were scattered in the right region. DBS_2-18 months samples are clustered in the middle scattering to the right region of the PCA plot.

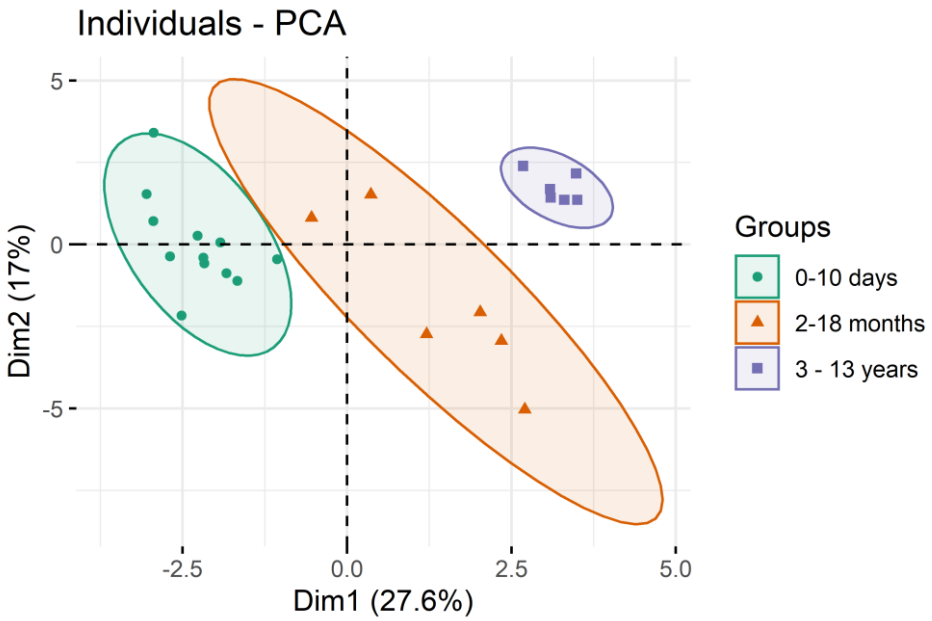

Figure 4.2-1. Principal component analysis (PCA) in a two-dimensional score scatter plot of lipid profiles of the 0-10 days, 2-18 months and 3-13 years groups.

Univariate analysis of the RP-LC-MS data from the three groups was performed to test for significant differences between the three groups (Supplementary Table S2). The 16 major contributors with the lowest q-value ($q<0.05$) (Figure 2) correspond to 3 CAR, 2 CE, 2 DG, 2 TG, 3 PC, 1 ether-linked PC, 1 PE, 1 ether-linked PE and 1 PI species, all with statistically significant differences. These include 6 neutral lipids (CE, DG and TG) and 7 PL. Of these, all PL and neutral lipids showed progressively higher levels with age. In the opposite trend, CAR showed higher levels in the first group (0-10 days), followed by the third group (3-13 years), while the middle age group (2-18 months) showed the lowest levels.

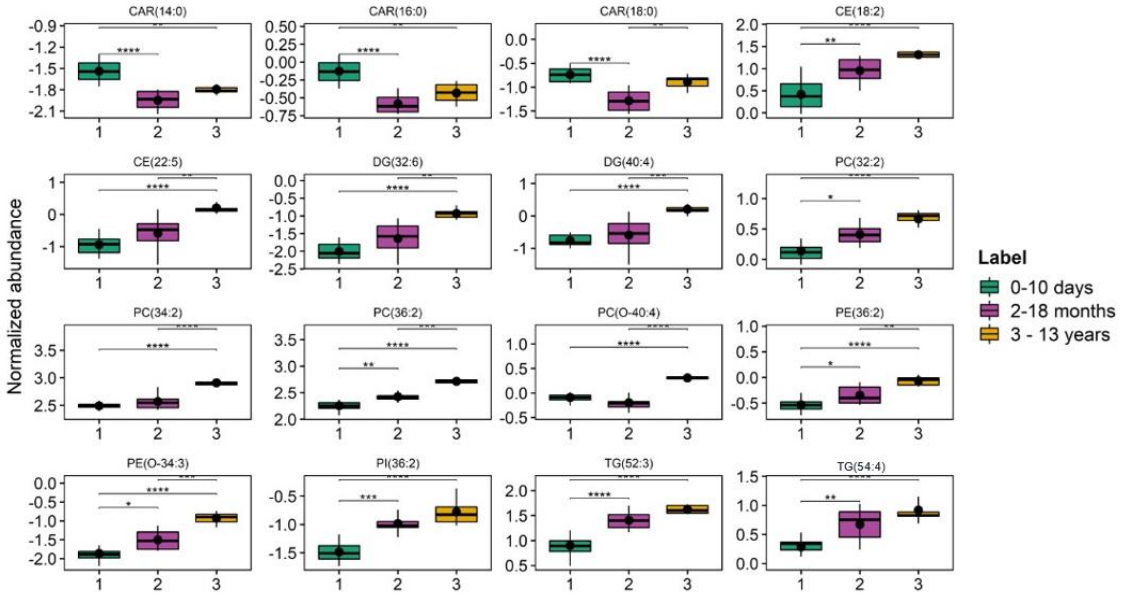

Figure 4.2-2. Box plots of the 16 most discriminating lipid species with the lowest q-values were obtained from a univariate analysis of the 0-10 days (1), 2-18 months (2) and 3-13 years (3) groups. *q < 0.05, ** q<0.01; ***q<0.001, ****q<0.0001.

Additionally, we performed a hierarchical clustering analysis (HCA) on the lipid data sets of the three groups (Figure 3). The results were used to create a heatmap of the top 25 lipid species with the lowest q-values in the ANOVA test, and a dendrogram with a two-dimensional hierarchical clustering of the age and variables that reflect the most important lipid species contributing to differentiating DBS samples of the different age groups. The resulting HCA dendrogram (Figure 3) showed a noticeable separation of the three data in the first dimension (upper hierarchical dendrogram) where samples are independently clustered into three groups, DBS_0-10 days (green), DBS_2-18 months (purple) and DBS_3-13 years (orange). Moreover, the second dimension shows two principal clusters: the first group includes 18 lipid species, namely 3 PE, 3 PC, 2 CE, 3 DG, 1 PI and 6 TG, which are lower in the DBS_0-10 days group; while the second group has 7 different lipid species which are less abundant in the group DBS_2-18 months, and include 3 CAR, 2 PC plasmalogens, 1 PC specie and 1 SM species.

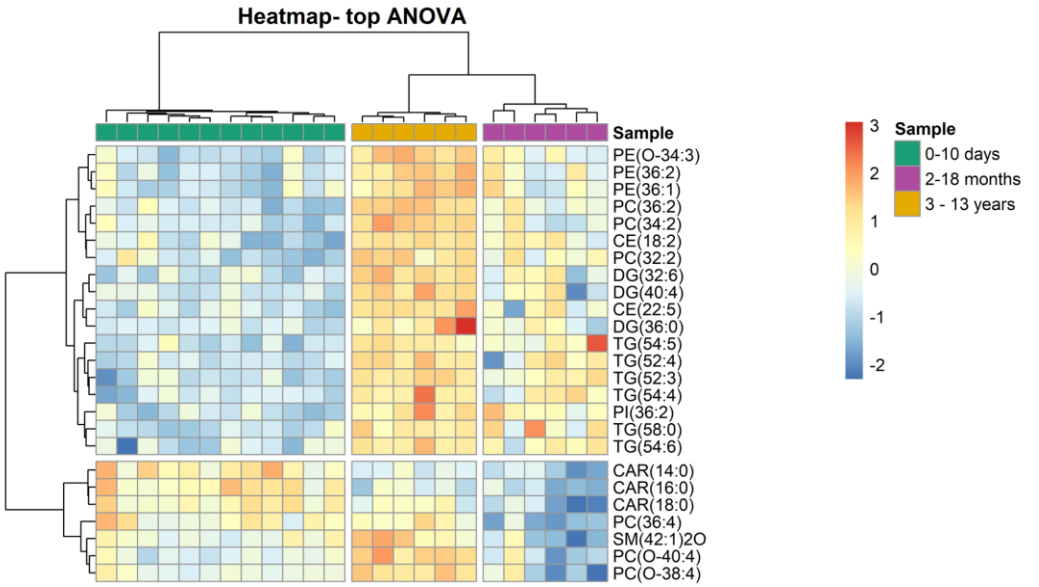

Figure 4.2-3. Two-dimensional hierarchical clustering heatmap of the 25 most discriminating lipid molecular species of DBS groups. Relative abundance levels are shown on the colour scale, with numbers indicating the fold difference from the overall mean. The clustering of the groups 0-10 days (green), 2-18 months (purple) and 3-13 years (orange) groups are represented by the dendrogram at the top. The clustering of individual lipid molecular species is represented by the dendrogram on the left.

4. Discussion

DBS cards are important for monitoring the health status of children and adults with metabolic diseases. They have been used to identify inborn errors of metabolism in newborns, through newborn screening programs, and to monitor disease throughout the patient's life[28]. But more recently, DBS is being evaluated for lipidomics studies[10] as a promising tool for disease monitoring, diagnosis and prognosis.

Lipids are essential molecules in the body, so regulation of lipid metabolism is important to maintain homeostasis. Lipidomics approaches provide new insights into how the lipidome adapts in different circumstances allowing the understanding of multiple pathologies[29]. Previous studies have shown that the results of lipidomic analysis of DBS samples did not differ significantly from those obtained for whole blood samples[10]. Additionally, the vast majority of reported results have been obtained using samples from adult subjects, and very few from

pediatric subjects. However, as mentioned earlier, the lipid profile, especially at the fatty acid level, changes with age, as shown by different studies that have detected fatty acid alterations at different childhood ages[15,16]. Thus, in paediatric studies it is important to stratify the samples into different agesets because there are significant alterations of the lipid species. This study evaluated the lipid profile of DBS cards from individuals of different pediatric ages to possibly shed light on the variability with the age of the lipidome (not only fatty acids as in the majority of the studies) of blood obtained using DBS. All samples included in this study belonged to healthy children who were classified into three age groups, 0-10 days, 2-18 months and 3-13 years (demographic information in Table 1). Lipidomics data were analyzed by multivariate principal component analysis (PCA) and hierarchical cluster analysis (HCA) as well as univariate analysis.

A comparison between the three age groups was performed to assess differences between paediatric ages. Analysis of the PCA score plot (Figure 1) indicated that the DBS lipid profile of the three age groups was significantly different, most likely because the adaptation of lipid metabolism throughout the paediatric ages leads to variation in the abundance of lipid species.

TGs are the body´s main store of energy[30] and, in this study, six species were among the 25 most different species (Figure 3). These TG species, namely TG(54:5); TG(52:4); TG (52:3); TG (54:4); TG (58:0); TG (54:6), were all significantly reduced in the 0-10 days group, compared to the other groups. The relative abundance of these TG species increased with age which agrees with the fact that TG represent 98% of the lipid fraction of the breast milk, thus, its consumption during child development leads to an increase of TG in the blood lipidome[31]. Also, the species that increased are those bearing PUFA residues, namely 18:2 and 22:6. The low levels of these species in the first days of life, and the subsequent and gradual rise in the other two age groups, may be attributed to the lack of fatty acid accumulation in newborns. TG(54:5) was identified as TG(18:1_18:2_18:2), thus bearing two linoleic acids (18:2). Linoleic acid is an essential fatty acid which must be obtained by consumption in the diet once it is not synthesized *in vivo*. Breast milk is rich in linoleic acid and α-linolenic acid which are the precursors of long-chain PUFA ω-6 and ω-3. These PUFA are essential for brain development,

including docosahexaenoic acid (22:6, DHA). As brain growth continues during the child's first weeks of life, this intake of DHA is essential[32]. Therefore, reduced levels of 18:2 and 22:6 in newborns (0-10 days) and high levels in children 3-13 years old were expected. Indeed, the positively age-associated increase in C18:2 n-6 with age has been previously reported, in the whole blood[15], serum[33] and red blood cells[34] from paediatric patients.

Our results also showed that some PC species also adapt to the age of children. PC is the most abundant class of PL in cell membranes and plasma[35]. In our study, few PC species discriminated the 0-10 days group from the 2-18 months and 3-13 years groups. Different PC species contributed to this differentiation such as the diacyl species PC(36:2); PC(34:2); PC(32:2) and PC(36:4), and the alkyl-acyl PC(O-40:4) and PC(O-38:4). The species PC(36:2); PC(34:2) and PC(32:2) show significantly lower abundances in the 0-10 days group compared to significantly higher abundances in the 3-13 years group. The remaining PC species [PC(36:4); PC(O-40:4) and PC(O-38:4)] showed a different trend, being significantly reduced in the 2-18 month group compared to the 0-10 days and 3-13 years groups which showed similar abundances (Figure 2). PC(36:2) was identified as PC(18:0_18:2), thus bearing a linoleic acid (18:2). This trend of increasing lipid species esterified with linoleic acid with age is consistent with the trend observed previously for TG, reinforcing the fact that C18:2 is low at birth due to the lack of its consumption (breast milk content on linoleic acid changes with the mother`s diet and the maturity of the milk[36]), and is consistent with the literature for fatty acids[15,33,34]. Throughout the 0-10 days, 2-18 months, and 3-13 years age groups, there was a gradual increase in the levels of linoleic acid residues in PL, which is consistent with increased consumption of this fatty acid in the diet. A C18:2 increase in PL in erythrocytes was also reported by Jakobik *et al* who assessed erythrocyte membrane PC fatty acyl residues` levels. This study found that the values of linoleic acid residue (C18:2 n-6) increased significantly between birth and infancy and increased further in young adulthood, supporting our findings[34]. Koulman *et al*[8] also found significant differences in PC(34:2), with linoleic acid increased in the 12-month-old infants and PC(36:2), also identified with linoleic acid increased in the 3-month-old infants. These results are consistent with the variability reported in the 2-18 month group in

our study, and with a differentiated lipidome signature dependent on the paediatric age, which needs to be further exploited. Additionally, the other PC species that showed an increase were PC(O-40:4) and PC(O-38:4), which are ether-linked species. These species had significantly higher levels in the 0-10 days and 3-13 year age group compared to the 2-18 months group. Alkyl-acyl species, namely plasmalogens are considered important players in cellular antioxidant defence. Also, a major function attributed to this type of lipids, particularly in the central nervous system, is the storage of PUFA[37]. Thus, we hypothesise that the increase in PC alkyl acyl in the group 0-10 days could be explained by the influence of the mother's metabolism through breast feeding, since the blood lipidome of children exclusively breastfed is very different than receiving an infant formula, with differences on the levels of PC, TG and sphingomyelins[38]. In the 2-18 month group, the mother`s metabolism (through the umbilical cord) no longer influences infant development, so the baby must begin to produce endogenous antioxidant defences on its own (besides the ones that receives through the breast milk), hence the decrease in plasmalogen levels. At the age of 3-13 years, the organism has already established the production of these species, explaining the subsequent increase in this age group. Although little is known about the role of this alkyl-PC in children, it is known that changes in its plasma levels have been reported in metabolic diseases such as Sjögren-Larsson syndrome[39] and phenylketonuria[40]. Knowledge of its plasma levels is therefore important and can be valuable for the diagnosis of metabolic diseases.

PE is the second most abundant class of PL in cells and biofluids. The results gathered in the present work showed that PE species contributed to the differentiation between different age groups. PE species PE(O-34:3); PE(36:2) and PE(36:1) had significantly reduced concentrations in the 0-10 days group (Figure 3). PE(O-34:3) and PE(36:2) were also found to be significantly different when comparing the three age groups with each other (Figure 2). As described in PC, PE(36:2) is a PE esterified with a linoleic acid residue, supporting the results reported for other lipid classes. In our study, PE(36:1), bearing an oleic acid residue, followed a similar trend with age. It has been reported that the PE profile is maintained in homeostasis with a specific pattern

and that all diacyl PE and alkyl acyl PE are essential for maintaining both cell membrane structure and function and cell homeostasis[37].

DGs result from the hydrolysis of one fatty acid from the TG molecule and have several biological roles, being key intermediates in the biosynthesis of PL and a plethora of other metabolic pathways[41,42]. In this study, the DG species, in particular, DG(32:6); DG(40:4); DG(36:0); showed the same behaviour as their precursor molecules and were found with significantly lower levels in the newborn group and higher levels in the 3-13 year group. These results are similar to those obtained for the TG class.

CAR is a very important class of lipids that is analysed in newborn screening programs[43]. In our work, we found that CAR(14:0); CAR(16:0) and CAR(18:0) were significantly lower in the 2-18 months group. These results can be explained as described in the PC class, they have higher levels in the newborn group, lower in the 2-18 month group and increased in the 3-13 year group due to better lipid metabolism. The establishment of age-related reference values for CAR, measured by MS/MS, would be important for the optimal investigation and management of inborn errors of the metabolism as they are currently not available[44]. Beken *et al*[45] and Gucciardi *et al*[46] previously determined the CAR profile of neonates but not in older children. Primassin *et al*[47] analysed the concentrations of free carnitine and γ-butyrobetaine in plasma and DBS, but only in children with fatty acid oxidation disorders and organic acidurias. Cavedon *et al*[44] determined age-related variations in CAR and free carnitine concentrations and found that free carnitines were significantly higher in children of older agesets than in newborns. On the other side, CAR concentrations tended to be significantly lower in groups of older children than in the newborns group[44]. This highlights the need for more lipidomic studies regarding the lipid profile of different paediatric ages to ascertain reference values.

CE species were also detected in this study. CE(18:2) and CE(22:5) had significantly lower abundances in the 0-10 day group compared to the 2-18 months and 3-13 years groups. CEs are important for neuronal development and constitute a reserve pool of cholesterol and fatty acyl residues which are used for the formation of myelin sheaths and synaptic contacts[48]. Therefore, a gradual increase in its concentrations from 0-10 days (significantly reduced) to 3-13 years

(significantly increased) is expected. This increase with age may not only be explained by the high content of the breast milk in cholesterol (precursor of hormones and involved in brain development)[32], but also by the key role of CE in brain development, and the need for PUFA throughout the different age groups[48]. The results for CE-bearing fatty acyl residue 18:2 are in agreement with the reduced levels of this fatty acid obtained for the other lipid classes (PI(36:2), PC(36:2) and PE(36:2)).

The increase with age of lipid species with esterified PUFAs was also detected in our work, which is in agreement with Jakobik *et al*[34] who showed a positive correlation with age of C20:5n-3, C22:6n-3, n-3 PUFAs and n-3 long-chain PUFAs, whereas C20:4n-6, n-6 PUFA and n-6 long-chain PUFAs showed a negative trend. However, these results are in contrast to Wolters *et al*[15], revealing the need for more studies to reach value standardization.

5. Conclusions

The DBS sampling method is widely applied to newborn screening programs (typically for inborn errors of the metabolism associated with metabolic diseases) and has recently been associated with lipidomics as a tool for the diagnosis of diseases. However, most studies have used adult samples and the majority of them concern the optimization of the method. Very few studies in children focus primarily on the fatty acid profile. Our study is the first to assess changes in multiple classes of lipids using RP-LC-MS/MS in three different pediatric age groups. Our results showed that the lipidomic signature of the three age groups is significantly different. Lipid species containing linoleic acid residue (C18:2) were shown to have significantly lower levels in the 0-10 day group with a gradual increase in the 2-18 months, reaching the highest concentrations in the last 3-13 years group.

The results of this work provide new insights into the lipid profile variability in children at different ages that may help improve our knowledge of the evolution of lipid metabolism throughout childhood and should be further explored in cohort studies. It also shows that DBS and lipidomics can be explored together for clinical lipidomics, which is one of the best

approaches to better understand these changes and find suitable biomarkers for precision medicine.

Data Availability Statement

The datasets supporting this article have been uploaded as part of the supplementary material. Data for this paper, including mzML data files are available at Science Data Bank, 2022 [2022-08-16] at http://doi.org/10.57760/sciencedb.02267. DOI:10.57760/sciencedb.02267

Private link: https://www.scidb.cn/s/nMnUji

Conflicts of interest

There are no conflicts to declare.

Acknowledgements

Thanks are due for the financial support to the University of Aveiro and FCT/MCT for the financial support to research units CESAM (UIDB/50017/2020+UIDP/50017/2020+LA/P/0094/2020), LAQV-REQUIMTE (UIDB/50006/2020) and CICECO (UIDB/50011/2020+UIDP/50011/2020), and to RNEM, Portuguese Mass Spectrometry Network (LISBOA-01-0145-FEDER-402-022125) through national funds and, where applicable, co-financed by the FEDER, within the PT2020. Helena Beatriz Ferreira is grateful to FCT for her PhD Grant (2020.04611.BD). Tânia Melo thanks the Junior Researcher contract in the scope of the Individual Call to Scientific Employment Stimulus 2020 (CEECIND/01578/2020). The authors are thankful to the COST Action EpiLipidNET, CA19105 - Pan-European Network in Lipidomics and EpiLipidomics.

References

1 K. Malsagova, A. Kopylov, A. Stepanov, T. Butkova, A. Izotov and A. Kaysheva, Diagnostics, 2020, 10, 248.
2 F. Gao, J. McDaniel, E. Y. Chen, H. E. Rockwell, J. Drolet, V. K. Vishnudas, V. Tolstikov, R. Sarangarajan, N. R. Narain and M. A. Kiebish, Nutr. Metab. (Lond)., 2017, 14, 28.
3 H. W. Liao, S. W. Lin, Y. T. Lin, C. H. Lee and C. H. Kuo, Anal. Chim. Acta, 2018, 1003, 34–41.
4 S. G. Snowden, A. Korosi, S. R. de Rooij and A. Koulman, Metabolomics, 2020, 16, 83.
5 P. Le Faouder, J. Soullier, M. Tremblay-Franco, A. Tournadre, J.-F. Martin, Y. Guitton, C. Carlé, S. Caspar-Bauguil, P.-D. Denechaud and J. Bertrand-Michel, Metabolites, 2021, 11, 305.
6 Y. Y. Zhao, X. long Cheng and R. C. Lin, Int. Rev. Cell Mol. Biol., 2014, 313, 1–26.
7 J. Lv, L. Zhang, F. Yan and X. Wang, Clin. Transl. Med., 2018, 7, 10–12.

8 A. Koulman, P. Prentice, M. C. Y. Wong, L. Matthews, N. J. Bond, M. Eiden, J. L. Griffin and D. B. Dunger, Metabolomics, 2014, 10, 1018–1025.
9 S. Furse and A. Koulman, Mol. Omi., 2020, 16, 563–572.
10 H. B. Ferreira, I. M. S. Guerra, T. Melo, H. Rocha, A. S. P. Moreira, A. Paiva and M. R. Domingues, Anal. Bioanal. Chem., 2022, 414, 7085–7101.
11 G. Liu, B. S. Mühlhäusler and R. A. Gibson, Prostaglandins Leukot. Essent. Fat. Acids, 2014, 91, 251–260.
12 A. H. Metherel, R. C. Hogg, L. M. Buzikievich and K. D. Stark, Lipids Health Dis., 2013, 12, 22.
13 D. Pupillo, M. Simonato, P. E. Cogo, A. Lapillonne and V. P. Carnielli, Lipids, 2016, 51, 193–198.
14 J. J. Aristizabal Henao, A. H. Metherel, R. W. Smith and K. D. Stark, Anal. Chem., 2016, 88, 9391–9396.
15 M. Wolters, H. Schlenz, R. Foraita, C. Galli, P. Risé, L. A. Moreno, D. Molnár, P. Russo, T. Veidebaum, M. Tornaritis, K. Vyncke, G. Eiben, L. Iacoviello and W. Ahrens, Int. J. Obes., 2014, 38, S86–S98.
16 J. Nikkilä, M. Sysi-Aho, A. Ermolov, T. Seppänen-Laakso, O. Simell, S. Kaski and M. Orešič, Mol. Syst. Biol., 2008, 4, 197.
17 E. G. Bligh and W. J. Dyer, Can. J. Biochem. Physiol., 1959, 37, 911–917.
18 E. M. Bartlett and D. H. Lewis, Anal. Biochem., 1970, 36, 159–167.
19 H. B. Ferreira, T. Melo, A. Monteiro, A. Paiva, P. Domingues and M. R. Domingues, Arch. Biochem. Biophys., 2021, 697, 108672.
20 Mass Spectrometry-Data Independent Analysis (MS-DIAL), http://prime.psc.riken.jp/compms/msdial/main.html.
21 T. Pluskal, S. Castillo, A. Villar-Briones and M. Oresˇic, BMC Bioinf, 2010, 11, 395.
22 S. Colombo, T. Melo, M. Martínez-López, M. J. Carrasco, M. R. Domingues, D. Pérez-Sala and P. Domingues, Sci. Rep., 2018, 8, 1–13.
23 Y. V. Karpievitch, S. B. Nikolic, R. Wilson, J. E. Sharman and L. M. Edwards, PLoS One, 2014, 9, 1–10.
24 S. Le, J. Josse and F. Husson, J. Stat. Softw., 2008, 25, 1–18.
25 A. Kassambara and F. Mundt, factoextra: Extract and Visualize the Results of Multivariate Data Analyses. R package version 1.0.7., 2020.
26 R. Kolde, pheatmap Pretty Heatmaps. R Packag., 2019, CRAN. R-pr, version 1.0.12.
27 H. Wickham, ggplot2 – Elegant Graphics for Data Analysis., Springer Nature, 2nd Editio., 2016.
28 M. D. Lim, Am. J. Trop. Med. Hyg., 2018, 99, 256–265.
29 M. A. Alves, S. Lamichhane, A. Dickens, A. McGlinchey, H. C. Ribeiro, P. Sen, F. Wei, T. Hyötyläinen and M. Orešič, Biochim. Biophys. Acta - Mol. Cell Biol. Lipids, 2021, 1866, 158857.
30 J. G. Robinson, in Goldman-Cecil Medicine, Elsevier, 26th Editi., 2020, vol. 2-volume S, pp. 1355-1365.e2.
31 N. J. Andreas, B. Kampmann and K. Mehring Le-Doare, Early Hum. Dev., 2015, 91, 629–635.
32 C. Y. Boquien, Front. Pediatr., 2018, 6, 1–9.
33 C. Glaser, H. Demmelmair, S. Sausenthaler, O. Herbarth, J. Heinrich and B. Koletzko, J. Pediatr., 2010, 157, 826-831.e1.
34 V. Jakobik, I. Burus and T. Decsi, Eur. J. Pediatr., 2009, 168, 141–147.
35 P. Risé, S. Eligini, S. Ghezzi, S. Colli and C. Galli, Prostaglandins Leukot. Essent. Fat. Acids, 2007, 76, 363–369.
36 B. Koletzko, Ann. Nutr. Metab., 2017, 69, 28–40.
37 F. Dorninger, A. Brodde, N. E. Braverman, A. B. Moser, W. W. Just, S. Forss-Petter, B. Brügger and J. Berger, Biochim. Biophys. Acta - Mol. Cell Biol. Lipids, 2015, 1851, 117–128.
38 P. Prentice, A. Koulman, L. Matthews, C. L. Acerini, K. K. Ong and D. B. Dunger, J. Pediatr., 2015, 166, 276-281.e6.
39 P. Staps, W. B. Rizzo, F. M. Vaz, M. Bugiani, M. Giera, B. Heijs, A. H. C. Kampen, M. L. Pras-Raves, M. Breur, A. Groen, S. Ferdinandusse, M. Graaf, G. Van Goethem, M. Lammens, R. A. Wevers and M. A. A. P. Willemsen, J. Inherit. Metab. Dis., 2020, 43, 1265–1278.

40 I. M. S. Guerra, L. Diogo, M. Pinho, T. Melo, P. Domingues, M. R. Domingues and A. S. P. Moreira, J. Proteome Res., 2021, 20, 2651–2661.
41 T. O. Eichmann and A. Lass, Cell. Mol. Life Sci., 2015, 72, 3931–3952.
42 M. Schuhmacher, A. T. Grasskamp, P. Barahtjan, N. Wagner, B. Lombardot, J. S. Schuhmacher, P. Sala, A. Lohmann, I. Henry, A. Shevchenko, Ü. Coskun, A. M. Walter and A. Nadler, Proc. Natl. Acad. Sci., 2020, 117, 7729–7738.
43 H.-R. Yoon, Ann. Pediatr. Endocrinol. Metab., 2015, 20, 119.
44 C. T. Cavedon, P. Bourdoux, K. Mertens, H. V. Van Thi, N. Herremans, C. De Laet and P. Goyens, Clin. Chem., 2005, 51, 745–752.
45 S. Beken, S. Abali, N. Yildirim Saral, B. Guner, T. Dinc, E. Albayrak, M. Ersoy, M. Kilercik, M. Halici, E. Bulbul, D. Kaya, M. Karabay, Z. A. Ay, G. Z. Eksi, F. Benli Aksungar, A. Korkmaz and M. Serteser, Front. Pediatr., 2021, 9, 646860.
46 A. Gucciardi, P. Zaramella, I. Costa, P. Pirillo, D. Nardo, M. Naturale, L. Chiandetti and G. Giordano, Pediatr. Res., 2015, 77, 36–47.
47 S. Primassin and U. Spiekerkoetter, Mol. Genet. Metab., 2010, 101, 141–145.
48 A. M. Petrov, M. R. Kasimov and A. L. Zefirov, Acta Naturae, 2016, 8, 58–73.

5. CHAPTER 5: CONCLUDING REMARKS AND FUTURE PERSPECTIVES

Concluding remarks and future perspectives

AID are a major health concerning issue of the modern society because they affect a large number of people and their pathogenesis still remains unclear. The difficulty of the diagnosis, the lack of specific biomarkers for each disease, and the poor therapy outcomes are challenges that need to be overcome. Lipids have important biological functions, like their key role in many signalling pathways that are related with the maintenance of cell and tissue homeostasis. They are also being considered as important players in several diseases. Changes in lipid metabolism, lipid profile and individual lipid molecular species are fundamental parameters of several pathologies, including MSs, SLE, SS and RA. However, the plasticity and molecular profiling of lipids associated with pathophysiological processes is not yet fully understood. In this sense, clinical lipidomics is nowadays the best methodological approach to reveal the modulation of lipid metabolism in health and disease, expand the knowledge on disease pathology and pinpoint promising disease biomarkers. Thus, the present Thesis aimed to contribute to personalised medicine by means of exploring the lipidic signatures of the most common AID, by applying modern MS-based lipidomic approaches under the scope of clinical lipidomics. The results gathered in this Thesis allowed the enrichment of our knowledge, not only on lipid alterations of AID, but also on a possible new less invasive sampling method for lipidomic analysis.

Alteration in lipids seems to be a common issue in MSs, one of most common AID, showing the importance of lipid (de)regulation in MSs pathogenesis, however, it is far from being completely elucidated due to controversial results reported in the literature so far. A systematic review on MS-based lipidomic studies on different MSs diseases and based on the analysis of different matrices was detailed in chapter 2.1. This review allowed to pinpoint that major published works focused on fatty acid analysis, showing the decrease of FA 18:2, FA 20:4 and total PUFA, with compensatory increases of saturated FA with shorter carbon chains. Oxidized PL were also reported in few studies about MSs revealing that the oxidative imbalance is a key feature of this disease. It was concluded that the screening methodologies to address the changes in the lipid profile of MSs patients must be improved in a timely manner as lipids are promising biomarkers for the diagnosis of this disease. Additionally, an untargeted lipidomic approach to analyse the MSs lipidome on the same type of matrix to identify the MSs lipid profile should be considered.

In chapter 2.2, to advance the lipid adaptation in MSs disease, the lipid profile of serum from MSs patients was evaluated. From this study, we can conclude that the phospholipidomic signature of MSs is significantly different from that of healthy controls. The pathogenesis of MSs is associated with changes in the lipid profile, namely for the diacyl PE, PC, LPE and ether-linked PE and PC species. Additionally, the lipid profile of MSs patients in relapse was

different from the one of MSs patients in remission, mainly in PC species, particularly PC(38:1). The significant variations of PE(40:10) and PC(38:1) in patients with MSs make these species possible serum biomarkers of this disease and may be suitable for clinical applications. These findings shed light on lipidomic changes in MSs and may help improve our understanding of the characteristics of MSs pathogenesis.

Regarding the evaluation of lipid contribution to SLE and SS pathology, in chapter 2.3 a comprehensively assessment of the blood and plasma lipid profile alterations were performed by the analysis of samples from patients diagnosed with one of these diseases. The results gathered evidence that there are marked changes in the lipid profile of SLE and SS patients, mainly in SM, Cer and PUFA species. The study showed that SM and Cer molecular species are very important to differentiate SS disease from other pathologies because these species are significantly increased in plasma samples of SS, namely SM(d36:2), SM(d36:3), SM(d42:2), SM(d42:3), and SM(d44:2) and Cer(d38:1), Cer(d40:0), and Cer(d44:2). PC(38:1) might be seen as a possible plasma biomarker of AID due to their significant variations in the patients with SLE, SS and MSs as previously seen in the study of chapter 2.2. TG levels were also found to be increased in plasma of SLE, corroborating previous findings of dyslipoproteinemia in SLE patients. Blood and plasma analysis showed comparable and consonant results. The analysis of blood samples instead of plasma/serum should be carefully addressed in future investigations because it reveals the lipid alterations that may happen at a cellular level or even in the surrounding tissues. Moreover, the analysis of blood samples gives new possibilities to analyse the lipidome of AID patients by using less invasive sampling, like the dried blood spot method, easily self-collected at home. This study gives new insights on the metabolic alterations in SLE and SS patients, which may help improve our understanding of AID pathological consequences.

The importance of lipids in inflammation, autoimmunity and in the onset (pre-clinical RA) and development of RA was considered in chapter 3.1 with a systematic review of the published scientific literature. RA pathogenesis induces alterations of the lipid metabolism however these changes are not fully understood. From the evidence gathered in this review, lipid alterations in RA can be observed even before disease manifestations, suggesting a close link between lipid molecular species and the metabolic changes caused by inflammation. The metabolism of FA, PE and PC is primarily affected in this disease, with presence of oxidized PL species. Nevertheless, the results of different studies are not consistent thus an effort for harmonization of lipidomic workflows in the future studies of RA are needed for the identification of reliable biomarkers for early diagnosis of this disease is highly needed.

Interestingly, the review manuscript of RA pointed out for a major contribution of oxidative stress in this disease and few OxPL were identified, however, no studies pointed out for oxidized cholesterol, usually a target of ROS and oxidative stress. This lack of knowledge on this subject could be due to the lack of knowledge on the specific fragmentation

fingerprinting of oxidized cholesterol in high resolution instruments. The fragmentation of oxCE was determined for the first time by high-resolution LC−MS/MS and the reported findings were presented in chapter 3.2. CE species, including CE 18:1, CE 18:2 and CE 20:4, were oxidized, by the hydroxyl radical generated under a Fenton-like reaction, in a mimetic model system of free-radical induced oxidation, and the specific fragmentation fingerprinting of their [M+NH4]+ adducts was identified by C18 reversed phase (RP) LC−MS/MS. The fragmentation of CE precursor ions originates a typical cholestenyl product ion, which is key to consistently assign the oxCE species for their structural characterization in lipidomic analysis. In this study, the RPLC−MS analysis allowed also to discriminate oxCE species structural isomers, eluting at different retention times. The isomeric species were identified by the typical fragmentation patterns obtained from tandem MS analysis, namely the hydroxy/hydroperoxy group can be either in the fatty acyl moiety or in the cholesterol ring, leading to the formation of characteristic ions such as cholestenyl with or without oxygen. This fragmentation allowed the identification of the oxidation in the cholesterol ring (cholestenyl with oxygen) or in the fatty acyl chain (cholestenyl without oxygen). Additionally, CE short-chain products resulting from oxidative cleavage of the fatty acyl chain in the vicinity of the oxidative modification were also identified and showed a clear fragmentation pattern confirming the modification in the fatty acyl chain. Overall, this study revealed the characteristic fragmentation patterns of several oxCE species. This knowledge should be applied in the detection of these species in biological samples of disease conditions, contributing for the detection of these oxidized lipids and to unravel the biological role of oxCE.

Nowadays there has been an increasing interest in improving blood collection methods possible to be less invasive and able to be performed at home by the patient, particularly relevant in chronic diseases that requires an effective and continuous disease management and in elderly people. This tendency aroused our interest in exploring DBS as a pre-analytical step, prior to lipidomic analysis. Thus, to advance the possibility of DBS method being applied in (clinical) lipidomic analysis, we performed a systematic review of the scientific literature, in chapter 4.1, about the use of DBS for the analysis of lipids. In this review, we have analysed the parameters that can impact the lipid profiling from DBS samples, including type of DBS card, homogeneity of the blood drop, extraction efficiency of different extraction methods, matrix effects on lipid recovery, lipid stability, and lipidomic profiling of DBS samples. Based on the literature it seems that DBS is as effective as plasma/serum/whole blood samples for lipidomic analysis, with results achieving high levels of sensitivity and specificity (comparing with the conventional samples) during MS and MS/MS analysis. However, it is necessary to pay attention to the impact certain factors like storage conditions or the lipid extraction method, which might influence the results. In summary, it was demonstrated the functionality and applicability of DBS in the investigation of population health and precision medicine in diverse

disease states and situations. Hopefully in a near future, DBS can be seen as a promising sampling method and approach to disease diagnostics/follow-up and therapy monitorization instead of using the conventional pre-analytical sampling that have concerns related with the puncture site cleansing, storage, transportation, and potential loss or contamination of the blood samples during its collection.

With the intention of testing the efficiency of DBS method in lipidomic investigations, the method was applied in the study of the typical lipid profile in three different pediatric age using RP-LC-MS/MS. The results gathered were detailed in chapter 4.2 and showed that the lipid species containing linoleic acid residue (C18:2) had significantly lower levels in the 0–10-days-old group with a gradual increase in the 2–18 months, reaching the highest concentrations in the last 3–13-years-old group. This work sheds light on the evolution of the lipid metabolism throughout childhood by showing the variability of the lipid profile in children at different ages. It was also demonstrated that DBS and lipidomics can be explored together in clinical lipidomics for the purpose of finding suitable biomarkers for precision medicine and better understand disease-induced changes on the lipid metabolism.

Overall, the work developed in this Thesis contributes to the development of new tools for clinical lipidomics and AID to meet with the 3rd goal of the Sustainable development of ONU - Good health and wellbeing. It also contributes to personalized medicine through the identification of new lipid biomarkers of AID and validation of a potential new sampling method (DBS), all tailored for the best therapeutic response and highest safety to ensure better patient care. Future investigations must continue to advance in this field of research and focus on: (1) lipidomics of blood/plasma/lipoproteins of patients with AID to characterize their typical lipidomic signature, (2) lipidomic analysis in the different stages of the disease to unveil biomarker discovery; and (3) lipidomics of immune cells from healthy and AID patients for detailed characterization of the modifications in their lipid profile to understand how they can correlate with the dysfunction of these cells and the development of AID pathogenesis.

6. CHAPTER 6: SUPPLEMENTARY DATA

6.1 LIPIDOMIC ANALYSIS IN MULTIPLE SCLEROSIS (Chapter 2.2)

PC

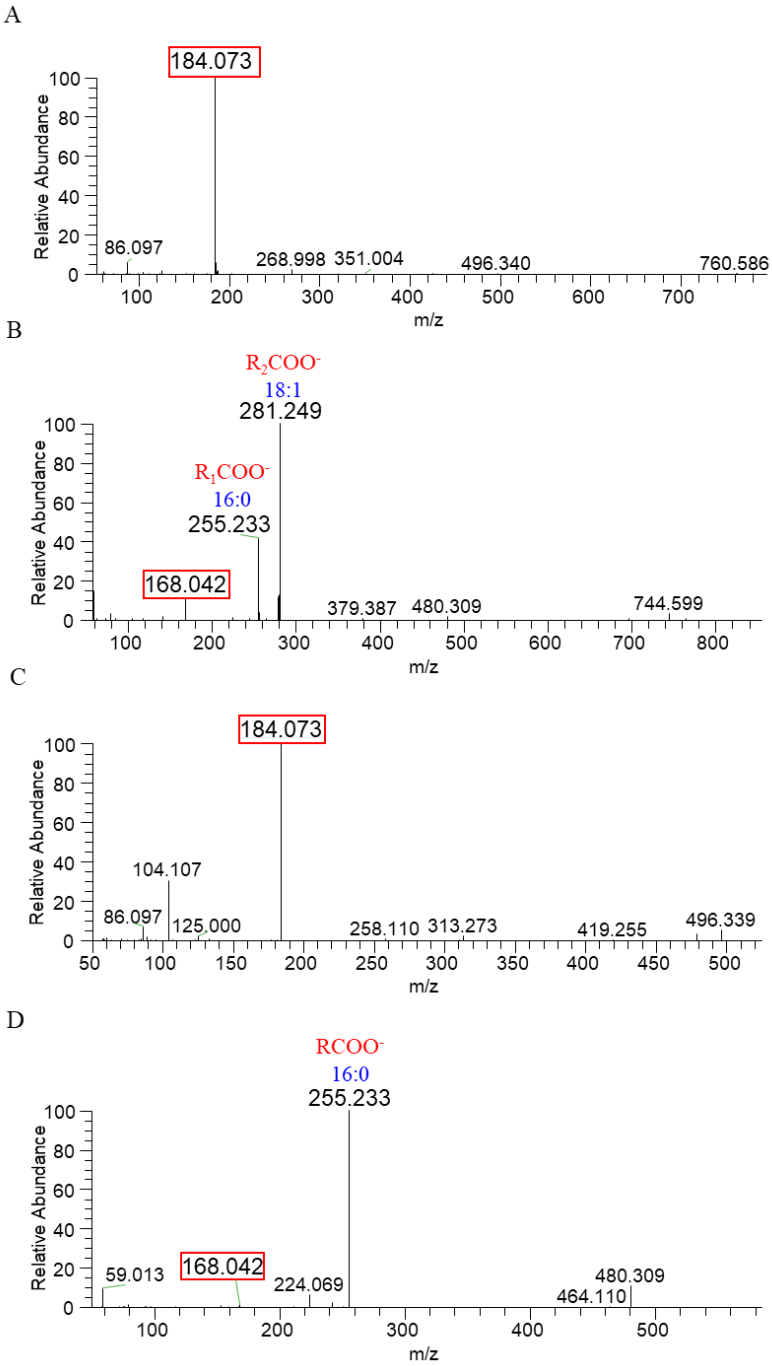

Supplementary Figure S6.1-1. PC and LPC identification. A: LC-MS/MS spectrum of the $[M+H]^+$ ion of PC(34:1) at m/z 760.586. B: LC-MS/MS spectrum of the $[M+CH_3COO]^-$ ion of PC(34:1) at m/z 818.645. C: LC-MS/MS spectrum of the $[M+H]^+$ ion of LPC(16:0) at m/z 496.339. D: LC-MS/MS spectrum of the $[M+CH_3COO]^-$ ion of LPC(16:0) at m/z 554.347. Fragment ions characteristic of PC and LPC classes are highlighted in a red box, namely the typical product ions at m/z 184.07 in the LC-MS/MS spectrum of $[M+H]^+$ ions of PC that correspond to the phosphocholine polar head group, and the product ions at m/z 168.04 in the LC-MS/MS spectrum of $[M+CH_3COO]^-$ ions of PC that correspond to phosphocholine polar head group minus a methyl group (CH_3). The carboxylate anions of the fatty acyl chains were also identified at m/z 255.23 (R_1COO^-) and m/z 281.25 (R_2COO^-) corresponding to C16:0 and C18:1, respectively, forming the PC(16:0/18:1) species.

PE

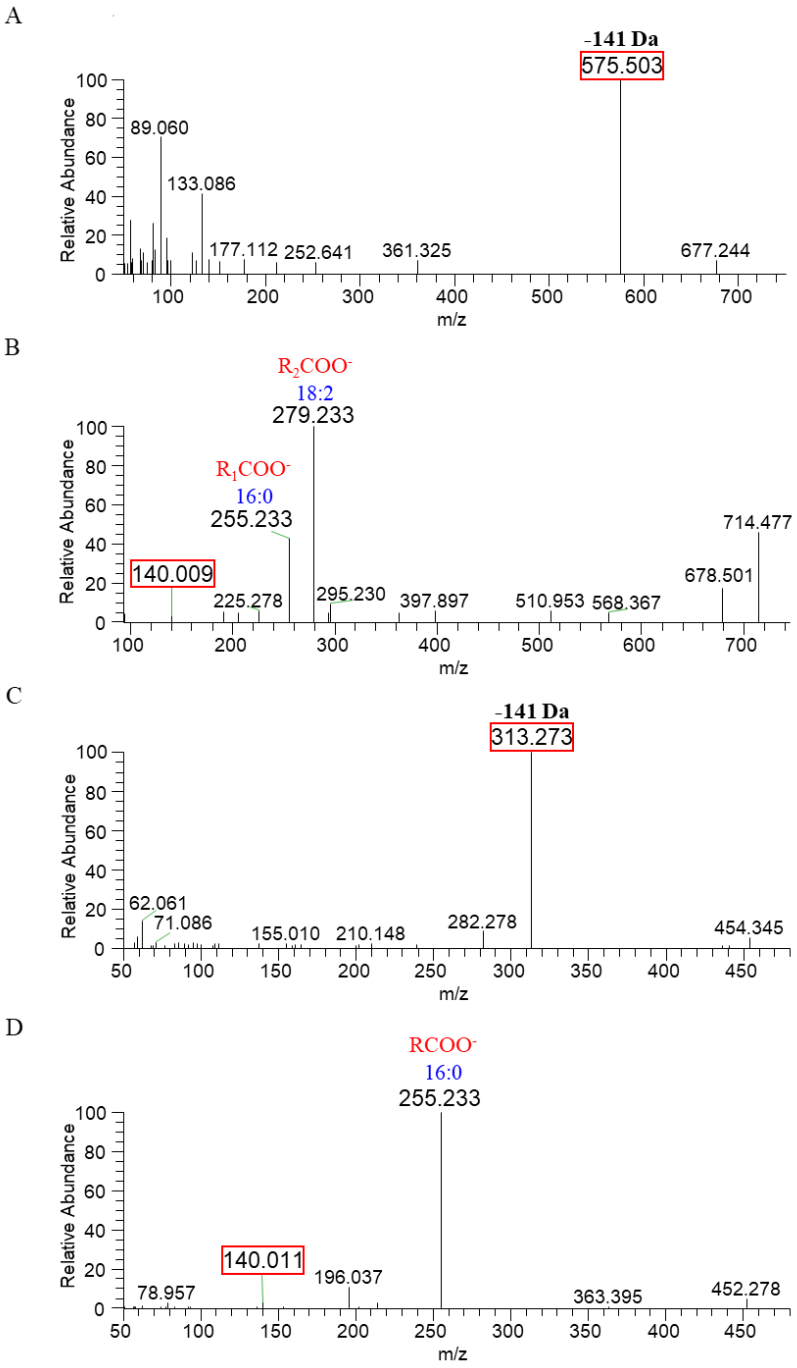

Supplementary Figure S6.1-2. PE and LPE identification. A: LC-MS/M spectrum of the $[M+H]^+$ ion of PE(34:2) at m/z 716.503. B: LC-MS/MS spectrum of the $[M-H]^-$ ion of PE(34:2) at m/z 714.477. C: LC-MS/MS spectrum of the $[M+H]^+$ ion of LPE(16:0) at m/z 454.345. D: LC-MS/MS spectrum of the $[M-H]^-$ ion of LPE(16:0) at m/z 452.278. Fragment ions characteristic of PE and LPE classes are highlighted in a red box, namely the typical neutral loss of 141 Da in the LC-MS/MS spectrum of $[M+H]^+$ ions of PE and the typical product ions at m/z 140.0 in the LC-MS/MS spectrum of $[M-H]^-$ ions of PE, which correspond to phosphethanolamine polar head group. The carboxylate anions of the fatty acyl chains were also identified at m/z 255.233 (R_1COO^-) and m/z 279.233 (R_2COO^-) corresponding to C16:0 and C18:2, respectively, forming the PE(16:0/18:2) species.

SM

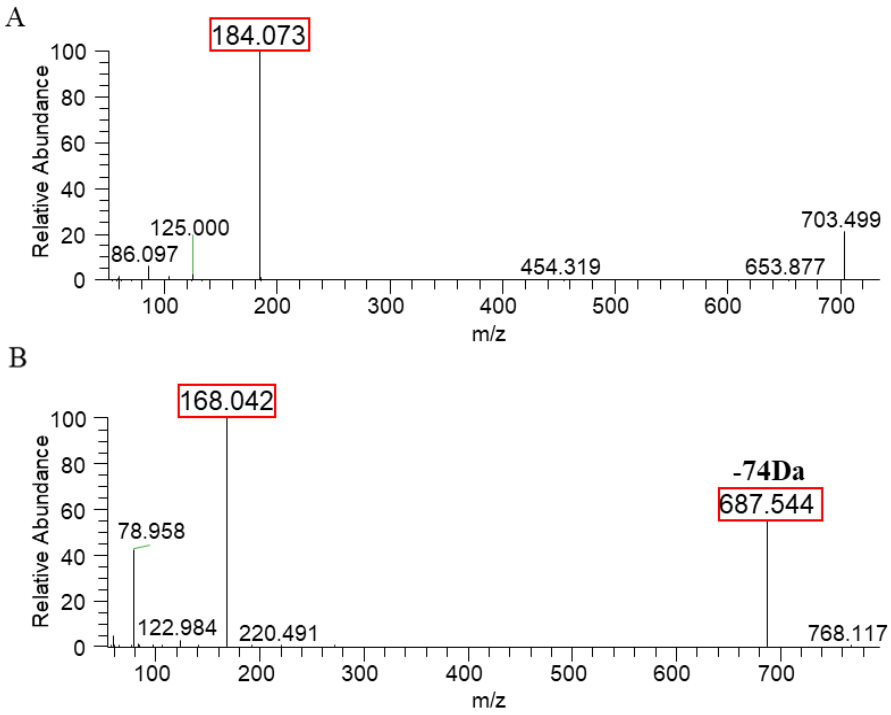

Supplementary Figure S6.1-3. SM identification. A: LC-MS/MS spectrum of the $[M+H]^+$ ion of SM(d34:1) (m/z 703.530). B: MS/MS spectrum of the $[M+CH_3COO]^-$ ions of SM(d34:1) (m/z 761.536). Fragment ions characteristic for the SM class are highlighted in a red box. The carboxylate anions of the fatty acyl chains could not be identified.

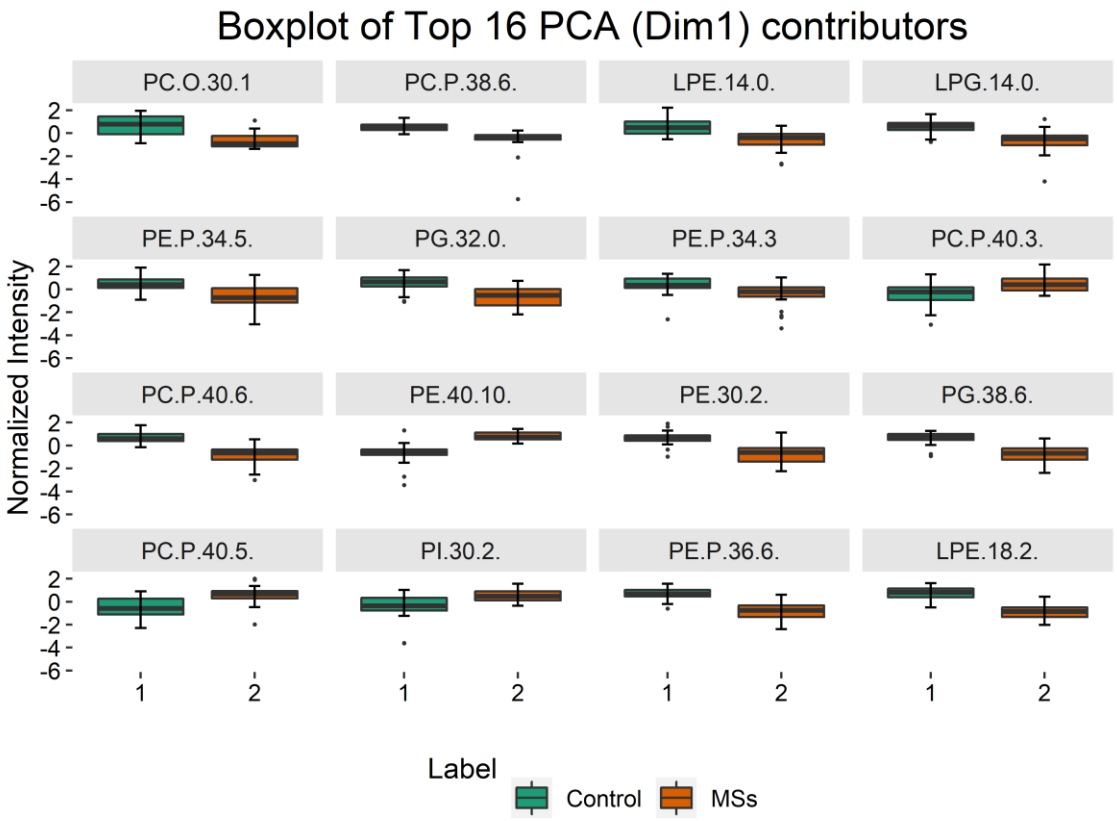

Supplementary Figure S6.1-4. Box plots of the 16 most discriminant PL molecular species (VIP list) obtained from PCA analysis of HC (Control) and MuS patients (MSs). The box plots of these PL species, which reports the PL normalized intensities, shows that the majority of the PL species with higher discriminant potential are ether-linked (akyl-acyl and alkenyl-acyl) PC, PE and LPE species, which are generally decreased in MSs.

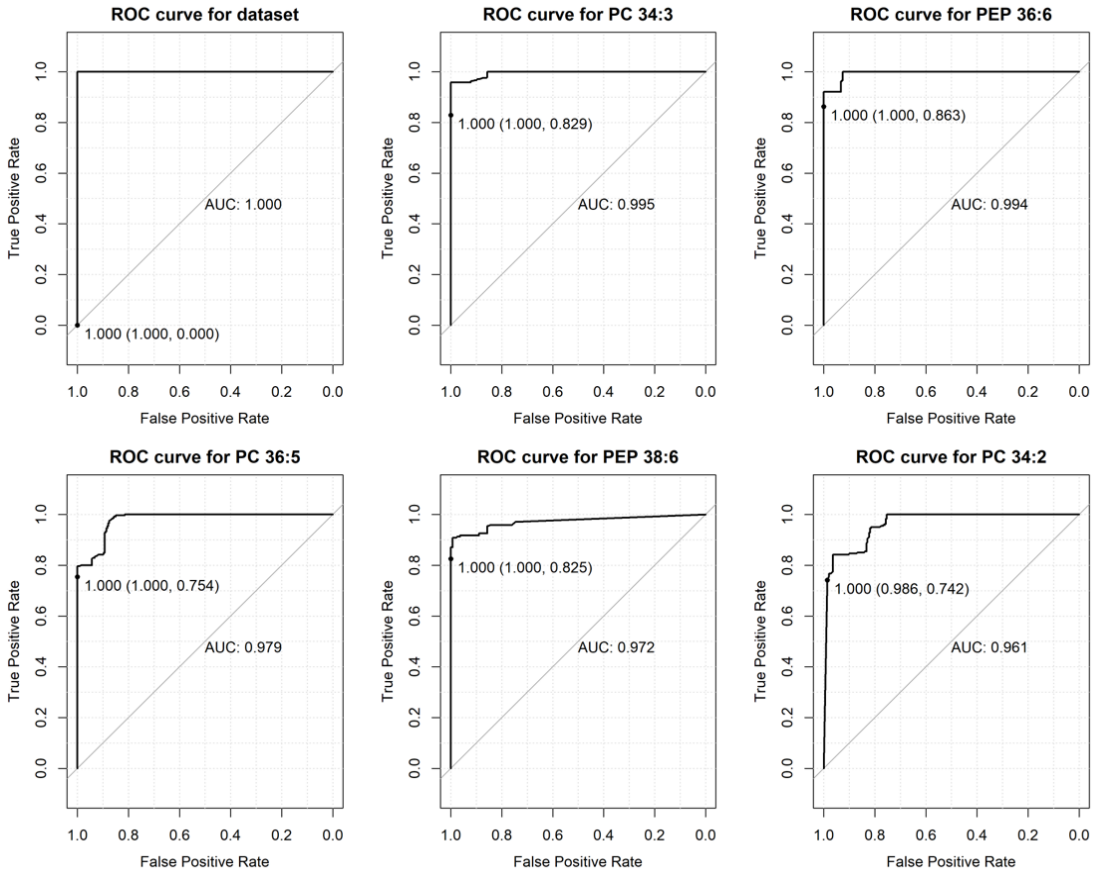

Supplementary Figure S6.1-5. Receiver operator characteristic analysis of the dataset and the 5 phospholipids with lowest with the lowest q-values in the Wilcoxon test.

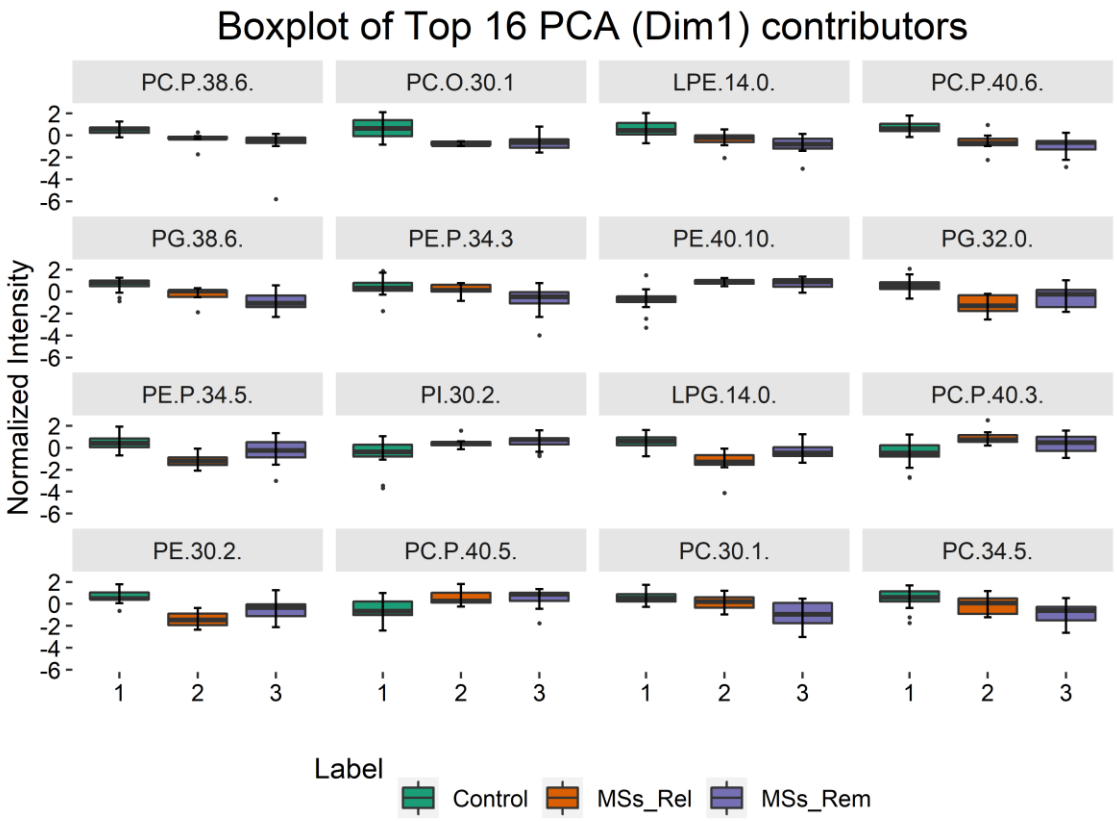

Supplementary Figure S6.1-6. Box plots of the 16 most discriminant PL molecular species (VIP list) obtained from PCA analysis of HC (Control), MSs_Rel and MSs_Rem.

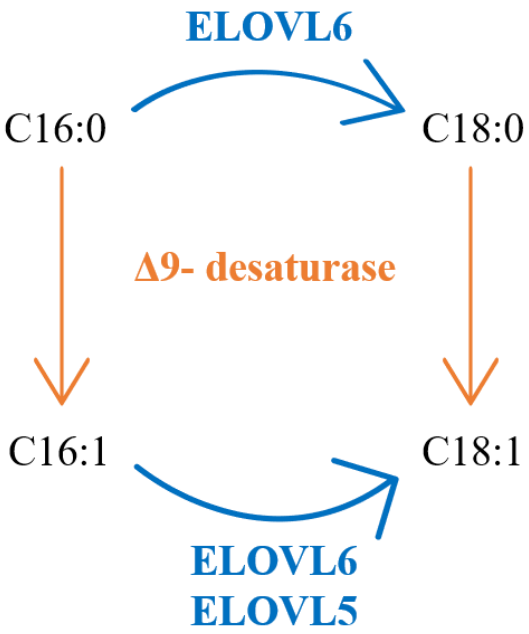

Supplementary Figure S6.1-7. Fatty acid biosynthesis pathway. Orange arrows represent the desaturation process of FA 16:0 and FA 18:0 by 9-desaturase. Blue arrows represent the elongation process by ELOVL6 and ELOVL5 elongases of FA 16:0 and FA 16:1.

Table 6.1-1. PL molecular species identified in MSs and HC samples by HILIC-MS.

Lipid specie (C:N)	Theoretical *m/z*	Observed *m/z*	Error (ppm)	Fatty acyl chains (C:N)	Formula
PC identified as $[M+H]^+$					
PC(30:0)	706.5387	706.5398	-1.5569	14:0/16:0	C38H77NO8P
PC(30:1)	704.5230	704.5245	-2.1291	14:0/16:1	C38H75NO8P
PC(32:0)	734.5700	734.5707	-0.9529	**	C40H81NO8P
PC(32:1)	732.5543	732.5551	-1.0921	14:0/18:1 and 16:0/16:1	C40H79NO8P
PC(32:2)	730.5387	730.5404	-2.3270	14:0/18:2 and 16:1/16:1	C40H77NO8P
PC(34:1)	760.5856	760.5844	1.5777	16:0/18:1	C42H83NO8P
PC(34:2)	758.5700	758.5715	-1.9774	16:0/18:2 and 16:1/18:1	C42H81NO8P
PC(34:3)	756.5543	756.5559	-2.1149	16:0/18:3 and 16:1/18:2	C42H79NO8P
PC(34:4)	754.5387	754.5386	0.1325	**	C42H77NO8P
PC(34:5)	752.5230	752.5225	0.6644	**	C42H75NO8P
PC(36:1)	788.6169	788.6135	4.3113	16:0/20:1 and 18:0/18:1	C44H87NO8P
PC(36:2)	786.6013	786.6018	-0.6356	16:0/20:2 and 18:0/18:2 and 18:1/18:1	C44H85NO8P
PC(36:3)	784.5856	784.5863	-0.8922	16:0/20:3 and 18:1/18:2	C44H83NO8P
PC(36:4)	782.5700	782.5709	-1.1501	16:0/20:4 and 16:1/20:3 and 18:1/18:3 and 18:2/18:2	C44H81NO8P
PC(36:5)	780.5543	780.5543	0.0000	16:0/20:5 and 16:1/20:4 and 18:2/18:3	C44H79NO8P
PC(36:6)	778.5387	778.5377	1.2845	*	C44H77NO8P
PC(38:1)	816.6482	816.6457	3.0613	16:0/22:1 and 18:0/20:1 and 18:1/20:0	C46H91NO8P
PC(38:2)	814.6326	814.6317	1.1048	16:0/22:2 and 18:0/20:2 and 18:1/20:1 and 18:2/20:0	C46H89NO8P
PC(38:3)	812.6169	812.6191	-2.7073	16:0/22:3 and 18:0/20:3 and 18:1/20:2 and 18:2/20:1	C46H87NO8P
PC(38:4)	810.6013	810.6019	-0.7402	16:0/22:4 and 18:0/20:4 and 18:1/20:3 and 18:2/20:2	C46H85NO8P
PC(38:5)	808.5856	808.5848	0.9894	16:0/22:5	C46H83NO8P
PC(38:6)	806.5700	806.5697	0.3719	16:0/22:6 and 18:1/20:5 and 18:2/20:4	C46H81NO8P
PC(38:7)	804.5543	804.5528	1.8644	16:1/22:6	C46H79NO8P
PC(38:8)	802.5387	802.5354	4.1120	*	C46H77NO8P
PC(40:4)	838.6326	838.6329	-0.3577	18:0/22:4	C48H89NO8P
PC(40:5)	836.6169	836.6151	2.1515	18:0/22:5 and 18:1/22:4 and 20:1/20:4	C48H87NO8P
PC(40:6)	834.6013	834.6009	0.4793	18:0/22:6 and 18:1/22:5	C48H85NO8P
PC(40:7)	832.5856	832.5849	0.8408	18:1/22:6	C48H83NO8P
PC(40:8)	830.5699	830.5680	2.2876	*	C48H81NO8P

PC(40:9)	828.5543	828.5513	3.6208	20:4/20:5	C48H79NO8P
PC(42:6)	862.6326	862.6313	1.5070	**	C50H89NO8P
PC(42:7)	860.6169	860.6148	2.4401	**	C50H87NO8P
PC(42:9)	856.5856	856.5827	3.3855	**	C50H83NO8P
PC(44:5)	892.6795	892.6799	-0.4481	**	C52H95NO8P
PC(O-30:0)	692.5594	692.5602	-1.1551	**	C38H79NO7P
PC(P-30:0)/PC(O-30:1)	690.5438	690.5454	-2.3170	**	C38H77NO7P
PC(O-32:0)	720.5907	720.5915	-1.1102	*	C40H83NO7P
PC(P-32:0)/PC(O-32:1)	718.5751	718.5755	-0.5567	*	C40H81NO7P
PC(P-34:0)/PC(O-34:1)	746.6064	746.6067	-0.4018	P-18:0/16:0 or O-16:0/18:1 or O-18:1/16:0	C42H85NO7P
PC(P-34:1)/PC(O-34:2)	744.5907	744.5897	1.3430	O-16:0/18:2 or O-18:2/16:0 or O-16:1/18:1 or O-18:1/16:1	C42H83NO7P
PC(P-34:2)/PC(O-34:3)	742.5751	742.5764	-1.7507	*	C42H81NO7P
PC(P-36:1)/PC(O-36:2)	772.6220	772.6225	-0.6471	P-20:1/16:0 or P-20:0/16:1 or P-18:0/18:1 or O-18:1/18:1	C44H87NO7P
PC(P-36:2)/PC(O-36:3)	770.6064	770.6052	1.5572	*	C44H85NO7P
PC(P-36:3)/PC(O-36:4)	768.5907	768.5911	-0.5204	O-18:2/18:2	C44H83NO7P
PC(P-36:4)/PC(O-36:5)	766.5751	766.5759	-1.0436	*	C44H81NO7P
PC(P-38:3)/PC(O-38:4)	796.6220	796.6211	1.1298	P-16:0/22:3 or P-16:1/22:2 or P-20:1/18:2 or O-16:0/22:4 or O-18:2/20:2	C46H87NO7P
PC(P-38:4)/PC(O-38:5)	794.6064	794.6072	-1.0068	*	C46H85NO7P
PC(P-38:5)/PC(O-38:6)	792.5907	792.5905	0.2523	O-16:0/22:6	C46H83NO7P
PC(P-40:3)/PC(O-40:4)	824.6533	824.6536	-0.3638	P-18:022:3 or P-18:1/22:2 or O-18:1/22:3	C48H91NO7P
PC(P-40:4)/PC(O-40:5)	822.6377	822.6386	-1.0940	P-18:1/22:3 or P-20:0/20:4	C48H89NO7P
PC(P-40:5)/PC(O-40:6)	820.6220	820.6213	0.8530	**	C48H87NO7P
PC(P-32:1)/(O-32:2)	716.5594	716.5589	0.6978	**	C40H79NO7P
PC(P-36:5)	764.5594	764.5591	0.3924	**	C44H79NO7P
PC(P-38:6)	790.5751	790.5738	1.6444	P-16:0/22:6	C46H81NO7P
PC(P-40:6)	818.6064	818.6056	0.9773	*	C48H85NO7P
LPC identified as $[M+H]^+$					
LPC(14:0)	468.3090	468.3098	-1.7083	14:0	C22H47NO7P
LPC(16:0)	496.3403	496.3411	-1.6118	16:0	C24H51NO7P
LPC(16:1)	494.3247	494.3258	-2.2253	16:1	C24H49NO7P
LPC(18:0)	524.3716	524.3723	-1.3349	18:0	C26H55NO7P
LPC(18:2)	520.3403	520.3412	-1.7296	18:2	C26H51NO7P
LPC(18:3)	518.3247	518.3231	3.0869	18:3	C26H49NO7P
LPC(20:0)	552.4029	552.4038	-1.6292	20:0	C28H59NO7P
LPC(20:1)	550.3873	550.3883	-1.8169	20:1	C28H57NO7P
LPC(20:2)	548.3716	548.3711	0.9118	*	C28H55NO7P

LPC(20:3)	546.3560	546.3553	1.2812	*	C28H53NO7P
LPC(20:4)	544.3403	544.3406	-0.5511	20:4	C28H51NO7P
LPC(20:5)	542.3247	542.3234	2.3971	20:5	C28H49NO7P
LPC(22:0)	580.4342	580.4332	1.7228	*	C30H63NO7P
LPC(22:1)	578.4186	578.4179	1.2102	*	C30H61NO7P
LPC(22:4)	572.3716	572.3723	-1.2230	22:4	C30H55NO7P
LPC(22:5)	570.3560	570.3570	-1.7533	*	C30H53NO7P
LPC(22:6)	568.3403	568.3401	0.3519	22:6	C30H51NO7P
LPC(24:0)	608.4655	608.4669	-2.3009	*	C32H67NO7P
LPC(O-14:0)	454.3298	454.3313	-3.3016	*	C22H49NO6P
LPC(O-16:0)	482.3611	482.3621	-2.0731	16:0	C24H53NO6P
LPC(P-16:0)/LPC(O-16:1)	480.3454	480.3467	-2.7064	P-16:0	C24H51NO6P
LPC(O-18:0)	510.3924	510.3942	-3.5267	18:0	C26H57NO6P
LPC(P-18:0)/LPC(O-18:1)	508.3767	508.3777	-1.9670	P-18:0 or O-18:1	C26H55NO6P
LPC(O-20:0)	538.4237	538.4242	-0.9286	*	C28H61NO6P
LPC(P-18:1)	506.3611	506.3616	-0.9874	*	C26H53NO6P
LPC(P-20:0)	536.4080	536.4091	-2.0507	P-20:0	C28H59NO6P
PE identified as $[M+H]^+$					
PE(30:2)	660.4604	660.4606	-0.3028	*	C35H67NO8P
PE(30:3)	658.4448	658.4438	1.5187	*	C35H65NO8P
PE(34:1)	718.5387	718.5384	0.4175	16:0/18:1	C39H77NO8P
PE(34:2)	716.5230	716.5246	-2.2330	16:0/18:2	C39H75NO8P
PE(34:3)	714.5074	714.5095	-2.9391	*	C39H73O8NP
PE(36:4)	740.5230	740.5244	-1.8906	18:2/18:2	C41H75NO8P
PE(36:5)	738.5074	738.5077	-0.4062	16:0/20:5	C41H73O8NP
PE(38:4)	768.5543	768.5554	-1.4313	18:0/20:4	C43H79O8NP
PE(38:5)	766.5387	766.5386	0.1305	*	C43H77NO8P
PE(38:6)	764.5230	764.5241	-1.4388	16:0/22:6 and 18:1/20:5	C43H75O8NP
PE(38:8)	760.4917	760.4904	1.7094	*	C43H71NO8P
PE(40:5)	794.5700	794.5666	4.2790	*	C45H81O8NP
PE(40:6)	792.5543	792.5557	-1.7664	*	C45H79O8NP
PE(40:7)	790.5387	790.5402	-1.8974	*	C45H77NO8P
PE(40:8)	788.5230	788.5207	2.9168	*	C45H75O8NP
PE(40:9)	786.5074	786.5049	3.1786	*	C45H73O8NP
PE(40:10)	784.4917	784.4920	-0.3824	*	C45H71NO8P
PE(42:8)	816.5543	816.5526	2.0819	*	C47H79NO8P
PE(42:9)	814.5387	814.5368	2.3326	*	C47H77O8NP
PE(46:9)	870.6013	870.6020	-0.8040	*	C51H85O8NP
PE(48:5)	906.6952	906.6917	3.8602	*	C53H97O8NP
PE(48:12)	892.5856	892.5879	-2.5768	*	C53H83O8NP
PE(P-34:1)/PE(O-34:2)	702.5438	702.5422	2.2774	**	C39H77NO7P
PE(P-34:2)/PE(O-34:3)	700.5281	700.5307	-3.7115	**	C39H75NO7P
PE(P-34:3)/PE(O-34:4)	698.5125	698.5149	-3.4359	**	C39H73NO7P

PE(P-34:5)	694.4812	694.4835	-3.3118	*	C39H69O7NP
PE(P-36:1)/PE(O-36:2)	730.5751	730.5730	2.8744	**	C41H81NO7P
PE(P-36:2)/PE(O-36:3)	728.5594	728.5601	-0.9608	O-18:1/18:2 or O-18:2/18:1	C41H79NO7P
PE(P-36:3)/PE(O-36:4)	726.5438	726.5446	-1.1011	**	C41H77NO7P
PE(P-36:4)/PE(O-36:5)	724.5281	724.5297	-2.2083	*	C41H75O7NP
PE(P-36:6)	720.4968	720.4974	-0.8328	**	C41H71O7NP
PE(P-38:3)/PE(O-38:4)	754.5751	754.5716	4.6384	**	C43H81O7NP
PE(P-38:4)/PE(O-38:5)	752.5594	752.5610	-2.1261	**	C43H79NO7P
PE(P-38:5)/PE(O-38:6)	750.5438	750.5451	-1.7321	**	C43H77NO7P
PE(P-38:6)	748.5281	748.5297	-2.1375	**	C43H75O7NP
PE(P-38:7)	746.5125	746.5132	-0.9377	*	C43H73O7NP
PE(P-40:4)/PE(O-40:5)	780.5907	780.5906	0.1281	**	C45H83NO7P
PE(P-40:5)/PE(O-40:6)	778.5751	778.5761	-1.2844	**	C45H81NO7P
PE(P-40:6)	776.5594	776.5613	-2.4467	**	C45H79O7NP
PE(P-40:7)	774.5438	774.5449	-1.4202	**	C45H77O7NP
LPE identified as $[M+H]^+$					
LPE(14:0)	426.2621	426.2620	0.2346	**	C19H41NO7P
LPE(16:0)	454.2934	454.2941	-1.5409	16:0	C21H45NO7P
LPE(16:1)	452.2777	452.2778	-0.2211	16:1	C21H43NO7P
LPE(18:0)	482.3247	482.3258	-2.2806	18:0	C23H49NO7P
LPE(18:1)	480.3090	480.3102	-2.4984	**	C23H47NO7P
LPE(18:2)	478.2934	478.2942	-1.6726	18:2	C23H45NO7P
LPE(20:3)	504.3090	504.3067	4.5607	**	C25H47NO7P
LPE(20:4)	502.2934	502.2940	-1.1945	20:4	C25H45NO7P
LPE(20:5)	500.2777	500.2769	1.5991	**	C25H43NO7P
LPE(22:5)	528.3090	528.3085	0.9464	**	C27H47NO7P
LPE(22:6)	526.2934	526.2939	-0.9500	22:6	C27H45NO7P
LPE(O-16:0)	440.3141	440.3150	-2.0440	**	C21H47NO6P
LPE(O-18:0)	468.3454	468.3467	-2.7757	**	C23H51NO6P
LPE(P-16:0)	438.2985	438.2992	-1.5971	P-16:0	C21H45NO6P
LPE(P-18:0)/LPE(O-18:1)	466.3298	466.3309	-2.3588	P-18:0	C23H49NO6P
PG identified as $[M-H]^-$					
PG(32:0)	721.5020	721.5025	-0.6930	**	C38H74O10P
PG(34:1)	747.5176	747.5176	0.0000	**	C40H76O10P
PG(36:0)	777.5646	777.5650	-0.5144	**	C42H82O10P
PG(38:5)	795.5176	795.5148	3.5197	**	C44H76O10P
PG(38:6)	793.5020	793.5000	2.5205	**	C44H74O10P
LPG identified as $[M-H]^-$					
LPG(14:0)	455.2410	455.2432	-4.8326	**	C20H40O9P
PI identified as $[M-H]^-$					
PI(30:2)	777.4554	777.4557	-0.3859	**	C39H70O13P
PI(36:5)	855.5024	855.4993	3.6236	**	C45H76O13P
LPI identified as $[M-H]^-$					

LPI(16:0)	571.2883	571.2905	-3.8509	**	C25H48O12P
SM identified as $[M+H]^+$					
SM(d30:1)	647.5128	647.5143	-2.3166	*	C35H72N2O6P
SM(d32:0)	677.5598	677.5589	1.3283	**	C37H78N2O6P
SM(d32:1)	675.5441	675.5456	-2.2204	**	C37H76N2O6P
SM(d32:2)	673.5285	673.5296	-1.6332	*	C37H74N2O6P
SM(d34:1)	703.5754	703.5766	-1.7056	*	C39H80N2O6P
SM(d34:2)	701.5598	701.5609	-1.5679	*	C39H78N2O6P
SM(d36:1)	731.6067	731.6080	-1.7769	*	C41H84N2O6P
SM(d36:2)	729.5911	729.5921	-1.3706	*	C41H82N2O6P
SM(d36:3)	727.5754	727.5770	-2.1991	*	C41H80N2O6P
SM(d38:1)	759.6380	759.6389	-1.1848	*	C43H88N2O6P
SM(d38:2)	757.6224	757.6237	-1.7159	*	C43H86N2O6P
SM(d38:3)	755.6067	755.6091	-3.1763	**	C43H84N2O6P
SM(d40:1)	787.6693	787.6683	1.2696	*	C45H92N2O6P
SM(d40:2)	785.6537	785.6551	-1.7820	*	C45H90N2O6P
SM(d40:3)	783.6380	783.6392	-1.5313	*	C45H88N2O6P
SM(d42:2)	813.6850	813.6859	-1.1061	*	C47H94N2O6P
SM(d42:3)	811.6693	811.6707	-1.7248	*	C47H92N2O6P

The identification of the PL species in the negative mode was based only on the exact mass measurements and retention time since those species have lower abundance. Even though these species did not have MS/MS spectra, they were still considered to this study due to the fact that, besides having already been described in the literature [25,36,37], they eluted in the correct RT and the exact mass was under 5 ppm. On the other side, the identification of PL species in the positive mode was more efficient due to the higher abundance of these species in human serum, which allowed the identification of the loss of the polar head group and FA composition. C – total of carbon atoms in fatty acids; N – number of double bonds; *identified based on exact mass measurements, retention time and loss of the polar head group, no FA acyl-chain fragments observed; **identified based on exact mass measurements and retention time, no loss of the polar head group and FA acyl-chain fragments observed

Table 6.1-2. Univariate analysis of HILIC-MS data. Wilcoxon test of controls and MSs samples showing the 16 major contributors with the lowest p-value.

Lipid specie	F.value	p-value	FDR
PC(34:3)	672	4.69E-15	7.55E-13
PC(36:6)	671	9.38E-15	7.55E-13
PC(38:1)	669	3.28E-14	1.76E-12
PE(P-38:6)/PE(O-38:7)	667	8.91E-14	3.59E-12
PC(36:5)	664	3.14E-13	1.01E-11
PC(34:2)	663	4.55E-13	1.22E-11
PC(34:4)	662	6.52E-13	1.31E-11
PE(P-38:7)/PE(O-38:8)	662	6.52E-13	1.31E-11
PE(P-38:5)/PE(O-38:6)	660	1.28E-12	2.28E-11
LPE(20:5)	659	1.75E-12	2.82E-11
PC(P-38:6)	658	2.38E-12	3.49E-11
LPE(20:4)	655	5.69E-12	7.04E-11
PC(P-34:2)/PC(O-34:3)	655	5.69E-12	7.04E-11
PC(32:2)	654	7.49E-12	8.61E-11
PC(P-36:4)/PC(O-36:5)	653	9.79E-12	1.05E-10
LPE(18:2)	652	1.27E-11	1.28E-10

Table 6.1-3. Univariate analysis of HILIC-MS data. Kruskal−Wallis test followed by Dunn's multiple comparison post-hoc test of controls, MSs_Rem and MSs_Rel samples showing the 16 major contributors with the lowest p-value.

Lipid specie	K.W.	p-value	FDR
PC(34:3)	40.02403	2.04E-09	2.28E-07
PC(36:6)	38.56083	4.23E-09	2.28E-07
PC(34:2)	37.97525	5.67E-09	2.28E-07
PC(36:5)	37.76815	6.29E-09	2.28E-07
PE(P-38:6)/ PE(O-38:7)	37.4387	7.42E-09	2.28E-07
PC(38:1)	37.16406	8.51E-09	2.28E-07
PE(P-38:5) /PE(O-38:6)	36.06024	1.48E-08	2.37E-07
PC(P-36:2)/PC(O-36:3)	36.01207	1.51E-08	2.37E-07
PE(P-36:3)/PE(O-36:4)	35.94952	1.56E-08	2.37E-07
PC(34:4)	35.93334	1.57E-08	2.37E-07
LPE(20:5)	35.87722	1.62E-08	2.37E-07
PE(P-38:7)	35.69386	1.77E-08	2.38E-07
PC(32:2)	35.21823	2.25E-08	2.48E-07
PE(P-38:3)/PE(O-38:4)	35.21787	2.25E-08	2.48E-07
LPE(20:4)	35.16841	2.31E-08	2.48E-07
PC(P-38:6)	34.77273	2.81E-08	2.83E-07

6.2 LOOKING IN DEPTH AT OXIDIZED CHOLESTERYL ESTERS (Chapter 3.2)

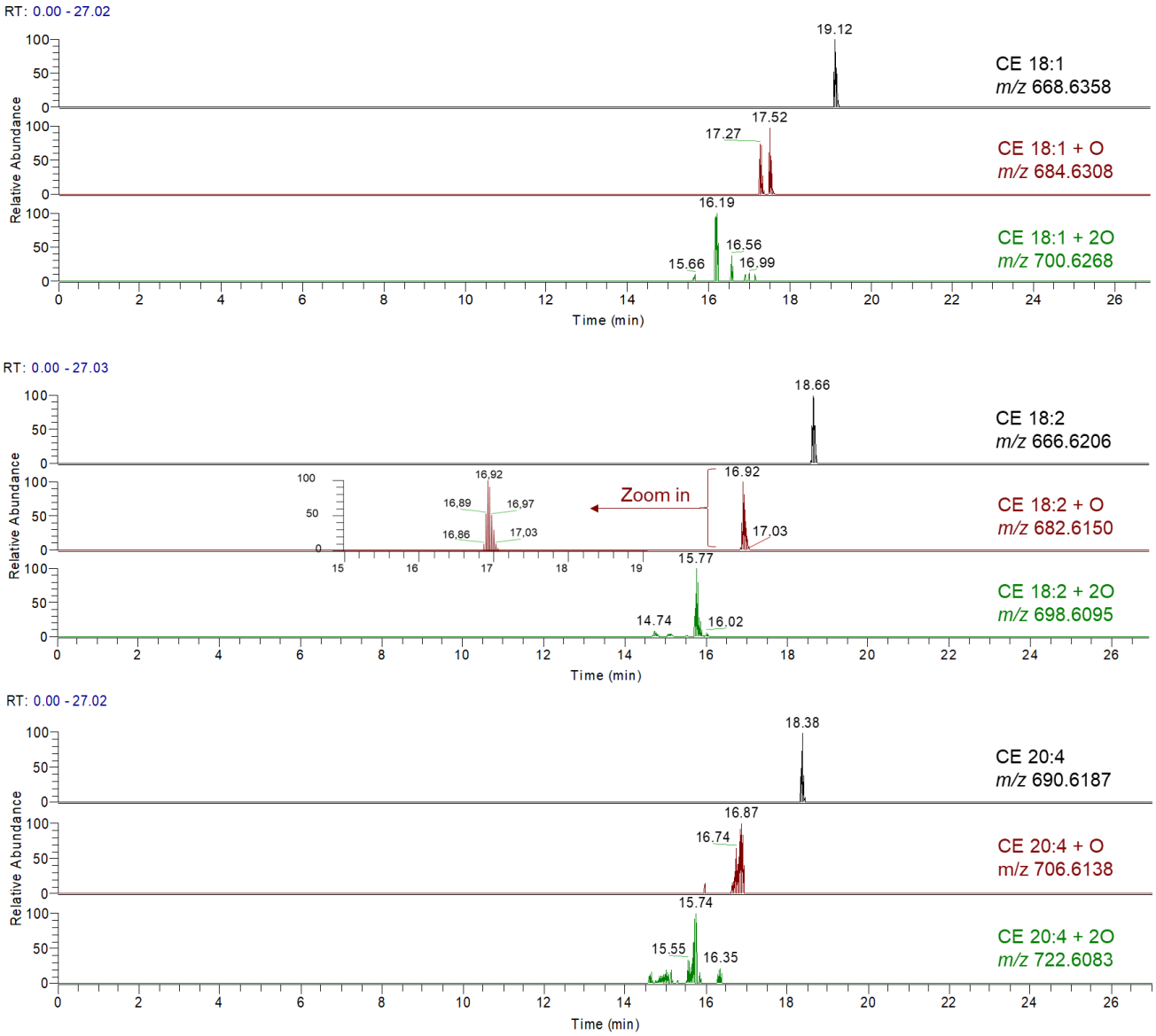

Supporting Figure 6.2-1. RIC of long-chain oxCE derivatives formed by radical oxidation induced by the hydroxyl radical generated under Fenton reaction in a biomimetic system. The presence of structural isomers is seen by the different peaks eluting with different RT indicated in the chromatogram.

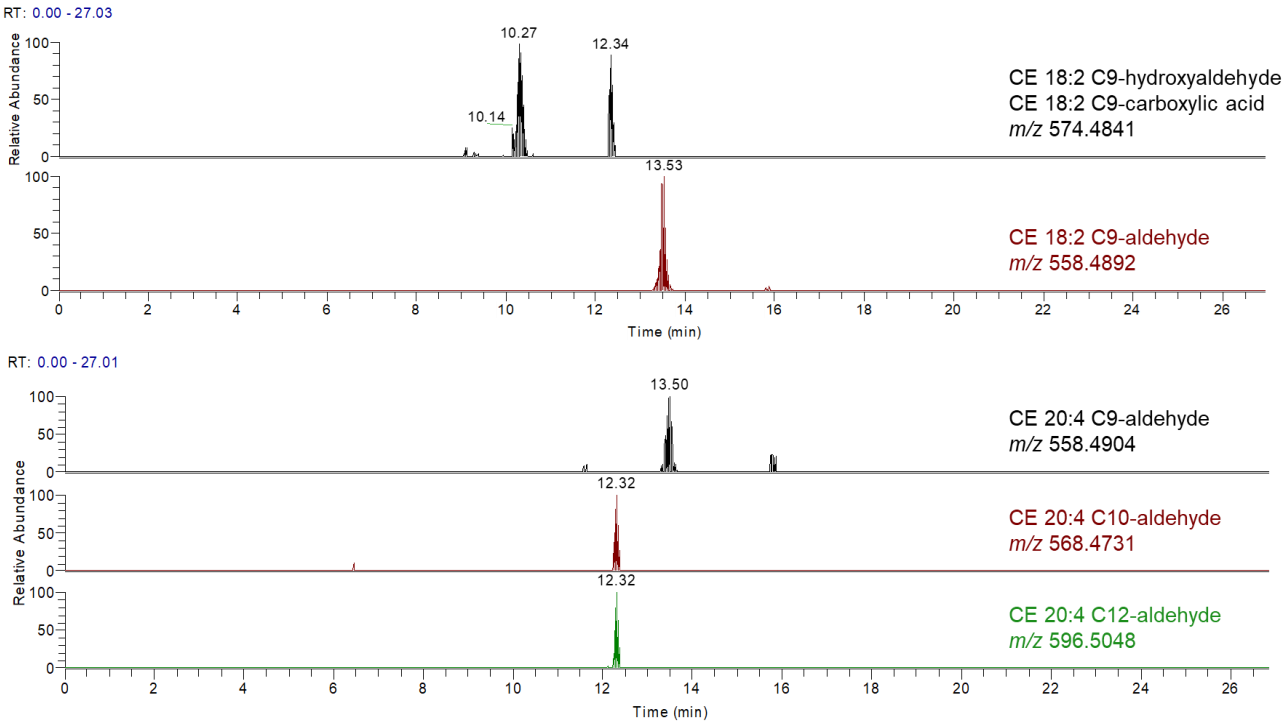

Supporting Figure 6.2-2. RIC of short-chain oxCE derivatives formed by radical oxidation induced by the hydroxyl radical generated under Fenton reaction in a biomimetic system. The presence of structural isomers is seen by the different peaks eluting with different RT indicated in the chromatogram. In the RIC of CE 18:2 short-chain products, the top black panel refers to two structural isomers for CE 18:2 truncated in C9. At RT 10.27 min elutes the CE 18:2 C9-hydroxyaldehyde and at RT 12.34 min elutes the CE 18:2 C9-carboxylic acid.

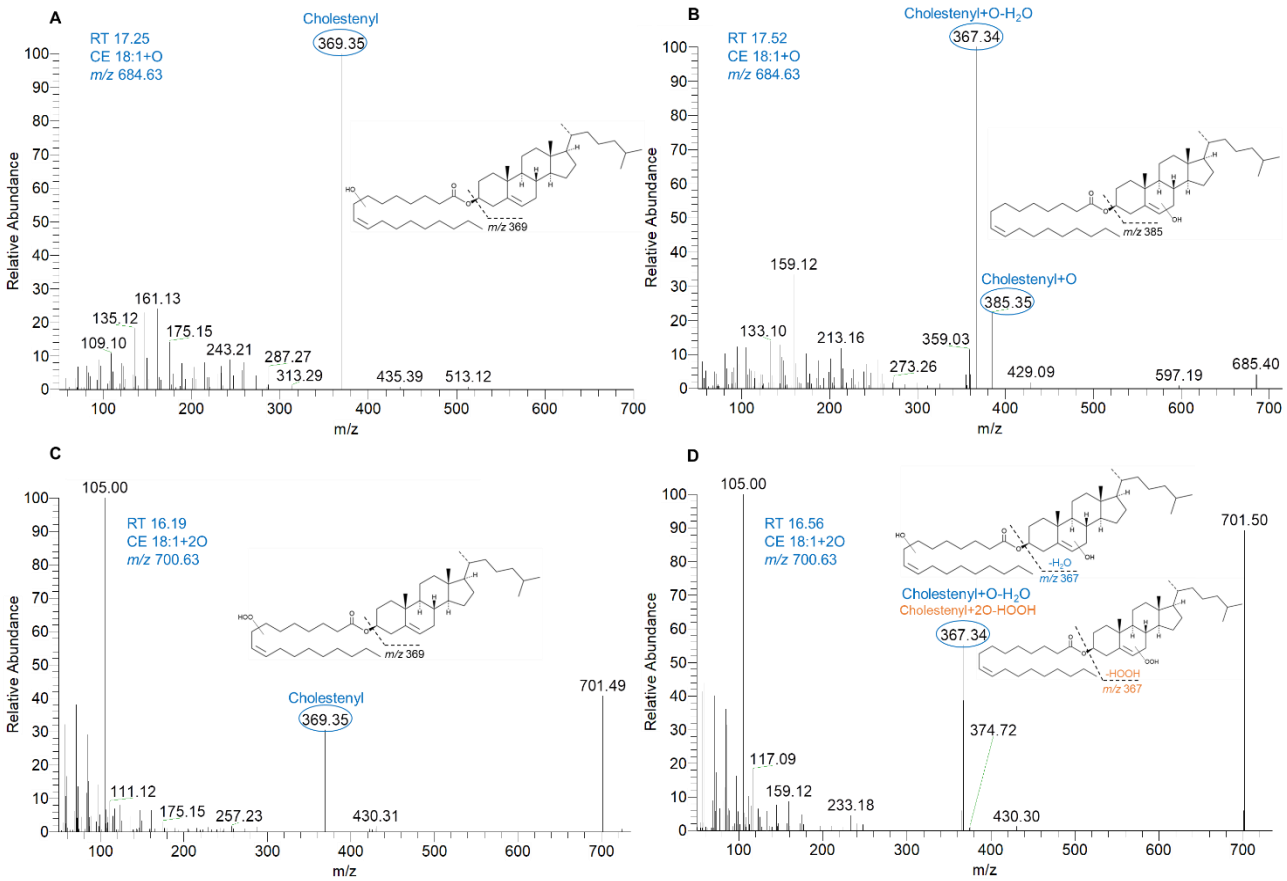

Supporting Figure 6.2-3. LC-MS/MS spectra of CE 18:1 oxidation products. Diagnostic product ions are circled in blue. A: CE 18:1 hydroxy isomer ($[M+NH_4]^+$ at *m/z* 684.63) with the hydroxy group on the fatty acyl chain confirmed by the presence of the ion at *m/z* 369.35. B: CE 18:1 hydroxy isomer ($[M+NH_4]^+$ at *m/z* 684.63) with the hydroxy group on the cholesterol ring, confirmed by the ions at *m/z* 385.35 $[Cholestenyl+O]^+$ and at *m/z* 367.34 $[Cholestenyl+O-H_2O]^+$. C: CE 18:1 hydroperoxy isomer ($[M+NH_4]^+$ at *m/z* 700.63) with the hydroperoxy group on the fatty acyl chain confirmed by the presence of the ion at *m/z* 369.35. D: CE 18:1 di-hydroxy isomer (a hydroperoxy isomer structure (in orange) is also considered) ($[M+NH_4]^+$ at *m/z* 700.63) with a hydroxy group on the cholesterol ring and the other in the fatty acyl chain, confirmed by the ion at *m/z* 367.34 $[Cholestenyl+O-H_2O]^+$ (or $[Cholestenyl+2O-HOOH]^+$ highlighted in orange).

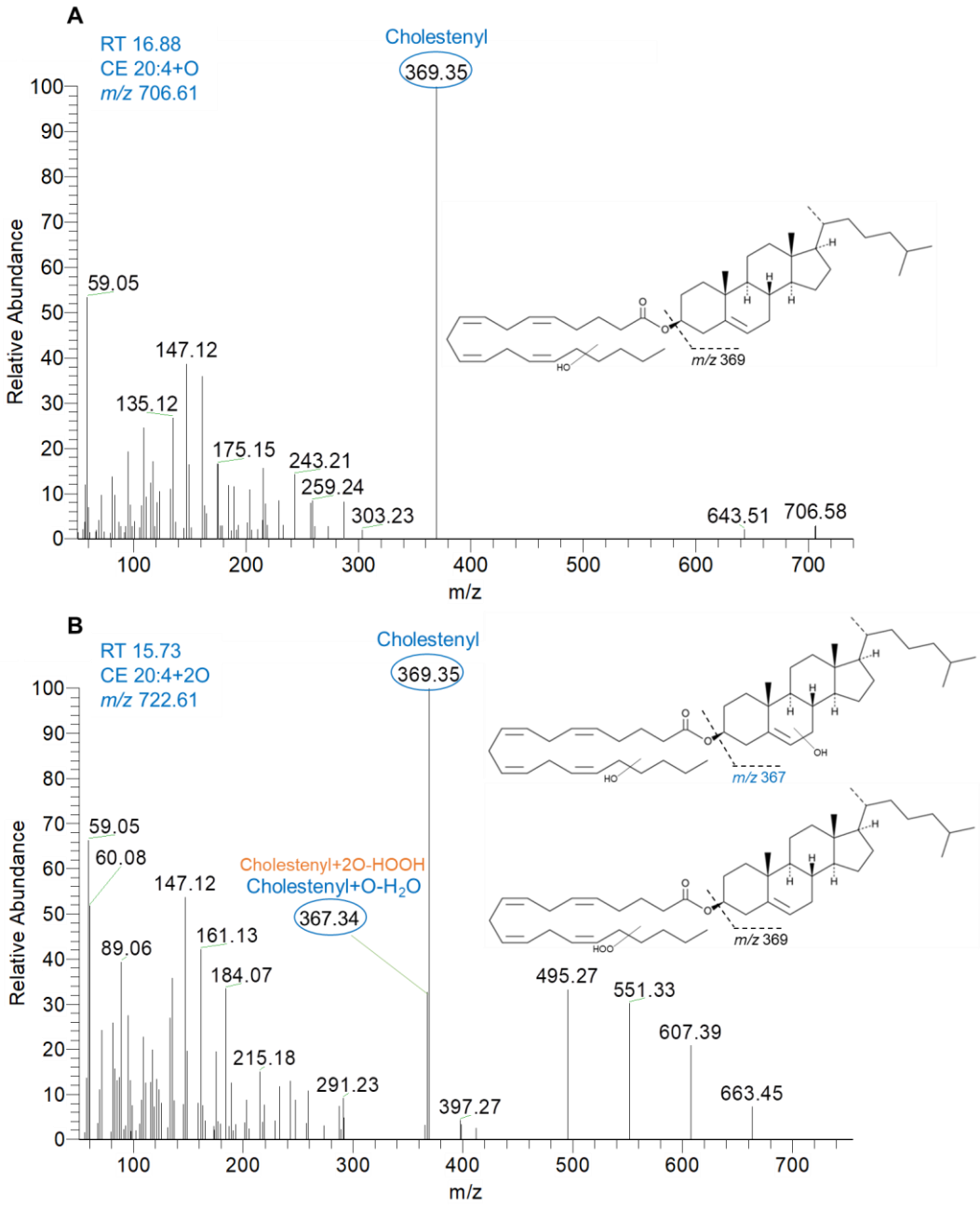

Supporting Figure 6.2-4. LC-MS/MS spectra of CE 20:4 long-chain oxidation products. Diagnostic ions are circled in blue. A: CE 20:4 hydroxy isomer ($[M+NH_4]^+$ at *m/z* 706.61) with the hydroxy group on the fatty acyl chain confirmed by the presence of the ion at *m/z* 369.35. B: CE 20:4 di-hydroxy or hydroperoxy isomers ($[M+NH_4]^+$ at *m/z* 722.61). Identification of the isomer with the hydroperoxy group on the fatty acyl chain confirmed by the presence of the ion at *m/z* 369.35, which is the most abundant isomer. The MS/MS spectrum also revealed the ion at *m/z* 367.34 corresponding to the di-hydroxy isomer with an hydroxy group on the cholesterol ring and another on the fatty acyl chain (the hypothesis of this being a hydroperoxy isomer (in orange) with 2 oxygens linked to the cholestenyl ion cannot be discarded).

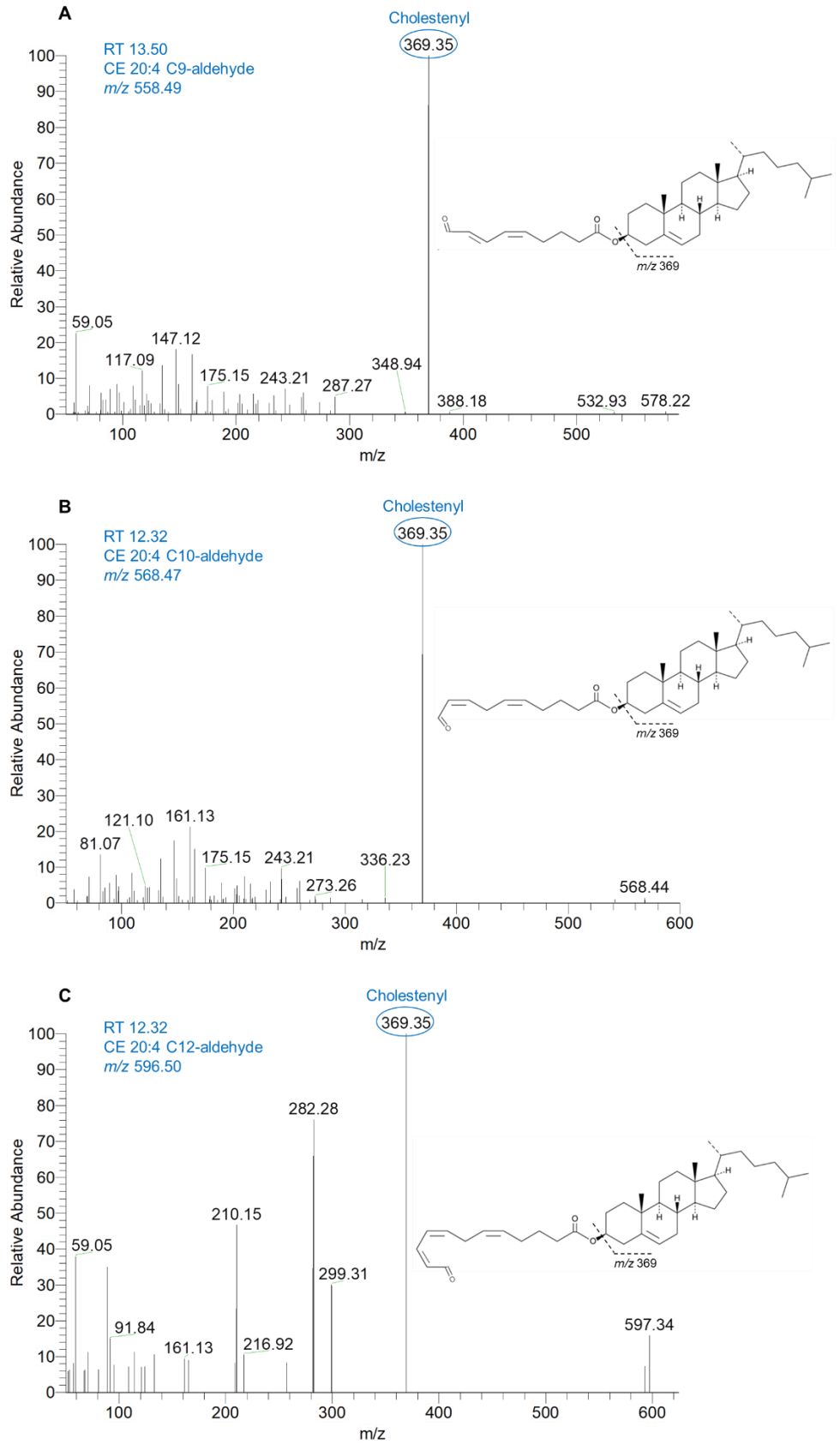

Supporting Figure 6.2-5. Short-chain products of oxCE 20:4. Diagnostic ions are circled in blue. A: CE 20:4 C9-aldehyde ($[M+NH_4]^+$ at *m/z* 558.49) with oxidation on the fatty acyl chain (*m/z* 369.35). B: CE 20:4 C10-aldehyde ($[M+NH_4]^+$ at *m/z* 568.47) with oxidation on the fatty acyl chain (*m/z* 369.35). C: CE 20:4 C12-aldehyde ($[M+NH_4]^+$ at *m/z* 596.50) with oxidation on the fatty acyl chain (*m/z* 369.35).

6.3 LIPIDOMIC ANALYSIS USING DRIED BLOOD SPOTS (Chapter 4.2)

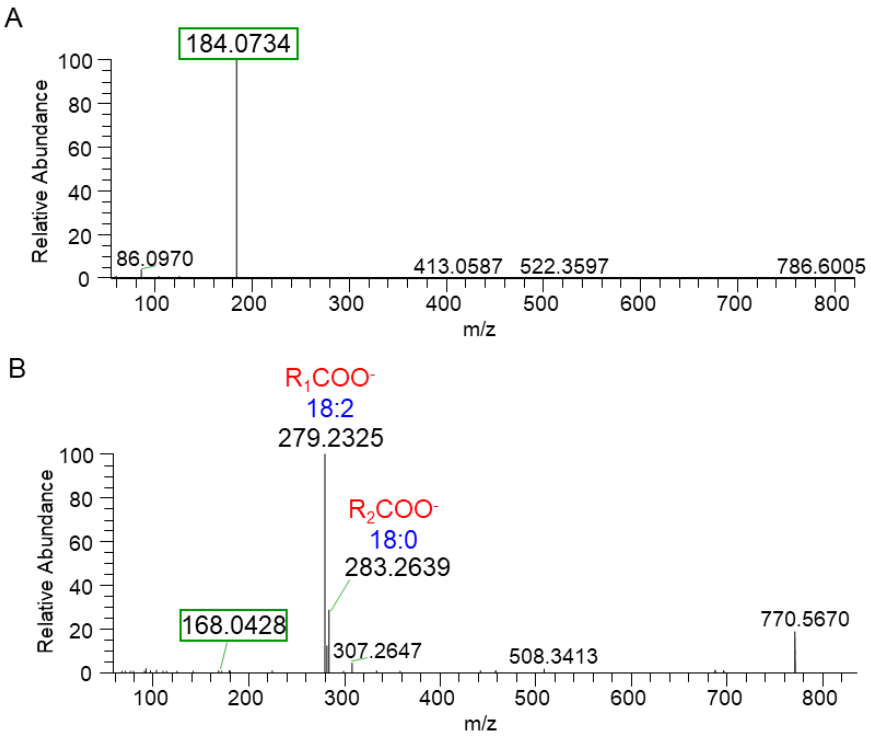

Supplementary Figure 6.3-1. PC identification. A: LC-MS/MS spectrum of the $[M+H]^+$ ion of PC(36:2) at *m/z* 786.6007. B: LC-MS/MS spectrum of the $[M+HCOO]^-$ ion of PC(36:2) at *m/z* 830.5914. Fragment ions characteristic of the polar head group of PC class (and thus also of LPC class) are highlighted in a green box, namely the typical product ions at *m/z* 184.07 in the LC-MS/MS spectrum of $[M+H]^+$ ions of PC that correspond to the phosphocholine polar head group, and the product ions at *m/z* 168.04 in the LC-MS/MS spectrum of $[M+HCOO]^-$ ions of PC that correspond to phosphocholine polar head group minus a methyl group (CH_3). The carboxylate anions of the fatty acyl residues were also identified at *m/z* 279.23 (R_1COO^-) and *m/z* 283.26 (R_2COO^-) corresponding to C18:2 and C18:0, respectively, forming the PC(18:0_18:2) species.

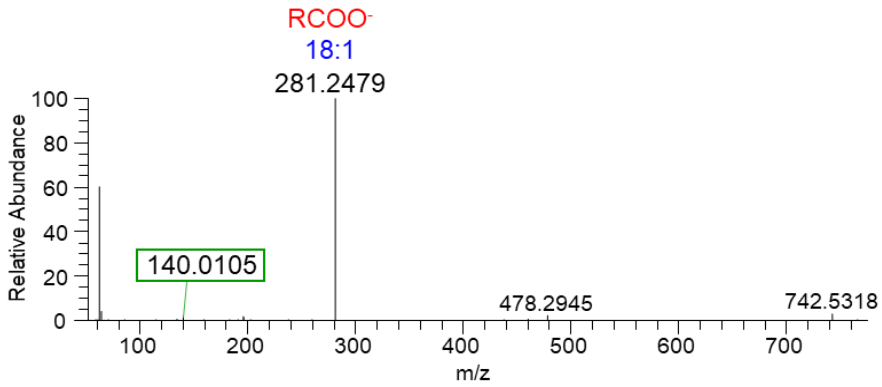

Supplementary Figure 6.3-2. PE identification. LC-MS/MS spectrum of the $[M-H]^-$ ion of PE(36:2) at *m/z* 742.5350. Fragment ion characteristic of the polar head group of PE class (and thus also of LPE class) is highlighted in a green box, namely the typical product ion at *m/z* 140.01 in the LC-MS/MS spectrum of $[M-H]^-$ ions of PE, which corresponds to the phosphoethanolamine polar head group. The carboxylate anions of the fatty acyl residues were also identified at *m/z* 281.2479 ($RCOO^-$) corresponding to C18:1, forming the PE(18:1_18:1) species.

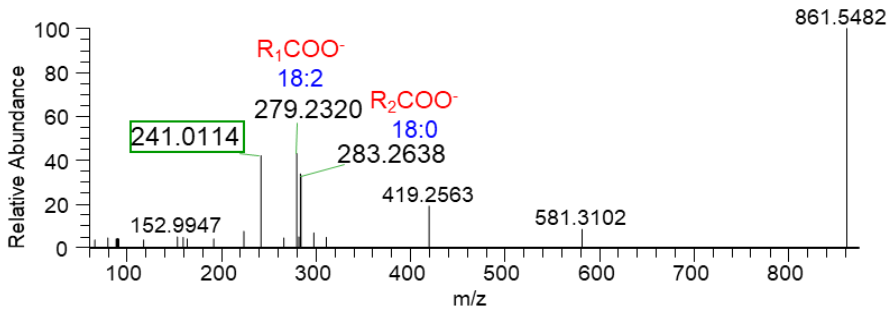

Supplementary Figure 6.3-3. PI identification. LC-MS/MS spectrum of the $[M-H]^-$ ion of PI(36:2) at *m/z* 861.5468. Fragment ion characteristic of PI class is highlighted in a green box, namely the typical product ion at *m/z* 241.01, which correspond to the phosphoinositol polar head group. The carboxylate anions of the fatty acyl residues were also identified at *m/z* 279.23 ($R1COO^-$) and *m/z* 283.26 ($R2COO^-$) corresponding to C18:2 and C18:0, respectively, forming the PI(18:0_18:2) species.

Table 6.3-1. Lipid species identified in DBS samples of all age groups.

Lipid specie (C:N)	Theoretical *m/z*	Observed *m/z*	Error (ppm)	Fatty acyl chains (C:N)	Formula
PC identified as $[M+H]^+$					
PC 30:0	706.5386	706.5374	1.6984	14:0_16:0	C38H76NO8P
PC 32:0	734.5671	734.5696	-3.4034	16:0_16:0	C40H80NO8P
PC 32:1	732.5511	732.5534	-3.1397	14:0_18:1 16:0_16:1	C40H78NO8P
PC 32:2	730.5367	730.5370	-0.4107	14:0_18:2 16:1_16:1	C40H76NO8P
PC 34:0	762.5991	762.6004	-1.7047	16:0_18:0	C42H84NO8P
PC 34:1	760.5852	760.5850	0.2630	16:0_18:1	C42H82NO8P
PC 34:2	758.5699	758.5697	0.2637	16:0_18:2	C42H80NO8P
PC 36:1	788.6162	788.6146	2.0289	16:0_20:1 18:0_18:1	C44H86NO8P
PC 36:2	786.6035	786.6007	3.5596	18:0_18:2 18:1_18:1	C44H84NO8P
PC 36:3	784.5834	784.5826	1.0196	16:0_20:3 18:0_18:3 18:1_18:2	C44H82NO8P
PC 36:4	782.5704	782.5679	3.1946	18:2_18:2	C44H80NO8P
PC 38:3	812.6162	812.6143	2.3381	18:0_20:3	C46H86NO8P
PC 38:4	810.5988	810.6005	-2.0972	16:0_22:4 18:0_20:4 18:1_20:3	C46H84NO8P
PC 38:5	808.5835	808.5844	-1.1131	16:0_22:5 18:0_20:5	C46H82NO8P
PC 40:4	838.6323	838.6353	-3.5773	*	C48H88NO8P
PC 40:5	836.6148	836.6146	0.2391	18:0_22:5 20:1_20:4	C48H86NO8P
PC 40:6	856.5817	856.5844	-3.1521	*	C48H84NO8P
PC 42:2	870.6940	870.6927	1.4931	*	C50H96NO8P
PC O-30:0	692.5577	692.5590	-1.8771	O-14:0_16:0	C38H78NO7P
PC O-30:2	688.5229	688.5206	3.3405	*	C38H74NO7P
PC O-32:0	720.5902	720.5902	0.0000	O-16:0_16:0	C40H82NO7P
PC O-32:1	718.5759	718.5743	2.2266	*	C40H80NO7P
PC O-34:0	748.6229	748.6206	3.0723	*	C42H86NO7P
PC O-34:1	746.6070	746.6055	2.0091	O-16:0_18:1	C42H84NO7P
PC O-38:4	796.6205	796.6206	-0.1255	*	C46H86NO7P
PC O-38:5	794.6041	794.6058	-2.1394	*	C46H84NO7P
PC O-40:4	824.6499	824.6513	-1.6977	*	C48H90NO7P
PC O-40:5	822.6377	822.6351	3.1606	*	C48H88NO7P

PC O-40:7	818.6079	818.6048	3.7869	*	C48H84NO7P
PC O-42:5	850.6687	850.6706	-2.2335	*	C50H92NO7P
LPC identified as $[M+H]^+$					
LPC 14:0	468.3081	468.3079	0.4271	14:0	C22H46NO7P
LPC 16:0	496.3397	496.3397	0.0000	16:0	C24H50NO7P
LPC 16:1	494.3243	494.3242	0.2023	16:1	C24H48NO7P
LPC 18:0	524.3709	524.3715	-1.1442	18:0	C26H54NO7P
LPC 18:1	522.3554	522.3557	-0.5743	18:1	C26H52NO7P
LPC 18:2	520.3400	520.3399	0.1922	18:2	C26H50NO7P
LPC 20:1	550.3867	550.3865	0.3634	20:1	C28H56NO7P
LPC 20:3	546.3551	546.3556	-0.9152	20:3	C28H52NO7P
LPC 20:4	544.3409	544.3392	3.1230	20:4	C28H50NO7P
LPC 20:5	542.3251	542.3231	3.6878	20:5	C28H48NO7P
LPC 22:5	570.3564	570.3561	0.5260	22:5	C30H52NO7P
LPC 22:6	568.3397	568.3398	-0.1760	22:6	C30H50NO7P
CAR identified as $[M+H]^+$					
CAR 14:0	372.3109	372.3101	2.1487	14:0	C21H41NO4
CAR 16:0	400.3414	400.3419	-1.2489	16:0	C23H45NO4
CAR 16:1	398.3263	398.3255	2.0084	16:1	C23H43NO4
CAR 18:0	428.3729	428.3731	-0.4669	18:0	C25H49NO4
CAR 18:1	426.3576	426.3574	0.4691	18:1	C25H47NO4
CAR 18:2	424.3415	424.3420	-1.1783	18:2	C25H45NO4
CE identified as $[M+NH_4]^+$					
CE 16:0	642.6179	642.6182	-0.4668	16:0	C43H76O2
CE 18:1	668.6343	668.6350	-1.0469	18:1	C45H78O2
CE 18:2	666.6180	666.6190	-1.5001	18:2	C45H76O2
CE 20:4	690.6179	690.6175	0.5792	20:4	C47H76O2
CE 22:5	716.6201	716.6173	3.9072	22:5	C49H78O2
DG identified as $[M+Na]^+$					
DG 24:3	473.3172	473.3186	-2.9578	*	C27H46O5
DG 26:1	505.3913	505.3898	2.9680	*	C29H54O5
DG 28:2	531.4072	531.4078	-1.1291	*	C31H56O5
DG 30:0	563.4688	563.4671	3.0170	*	C33H64O5
DG 30:3	557.4136	557.4132	0.7176	*	C33H58O5
DG 30:5	553.3914	553.3898	2.8913	*	C33H54O5
DG 32:0	591.4963	591.4971	-1.3525	*	C35H68O5
DG 32:1	589.4813	589.4827	-2.3750	*	C35H66O5
DG 32:6	579.4017	579.4019	-0.3452	*	C35H56O5
DG 34:0	619.5263	619.5268	-0.8071	*	C37H72O5
DG 36:0	647.5584	647.5585	-0.1544	*	C39H76O5
DG 36:5	637.4695	637.4684	1.7256	*	C39H66O5
DG 38:5	665.5015	665.5006	1.3524	*	C41H70O5
DG 40:4	695.5757	695.5728	4.1692	*	C43H76O5

DG 44:6	747.5947	747.5920	3.6116	*	C47H80O5
DG identified as $[M+NH_4]^+$					
DG 34:1	612.5552	612.5559	-1.1428	16:0_18:1	C37H70O5
DG 34:2	610.5425	610.5412	2.1293	16:0_18:2	C37H68O5
DG 36:2	638.5736	638.5721	2.3490	18:1_18:1	C39H72O5
DG 36:3	636.5549	636.5565	-2.5135	18:1_18:2	C39H70O5
TG identified as $[M+NH_4]^+$					
TG 44:0	768.7070	768.7072	-0.2602	12:0_14:0_18:0	C47H90O6
TG 44:1	766.6896	766.6915	-2.4782	12:0_18:0_14:1	C47H88O6
TG 44:2	764.6750	764.6765	-1.9616	12:0_14:0_18:2	C47H86O6
TG 46:0	796.7385	796.7385	0.0000	14:0_16:0_16:0	C49H94O6
TG 46:1	794.7216	794.7228	-1.5100	14:0_16:0_16:1	C49H92O6
TG 46:2	792.7069	792.7073	-0.5046	12:0_16:0_18:2	C49H90O6
TG 46:3	790.6943	790.6920	2.9088	10:0_18:1_18:2	C49H88O6
TG 48:0	824.7697	824.7689	0.9700	16:0_16:0_16:0	C51H98O6
TG 48:1	822.7558	822.7543	1.8231	14:0_16:0_18:1	C51H96O6
TG 48:2	820.7396	820.7384	1.4621	14:0_16:0_18:2	C51H94O6
TG 48:3	818.7252	818.7228	2.9314	12:0_18:1_18:2	C51H92O6
TG 50:0	852.8033	852.8008	2.9315	16:0_16:0_18:0	C53H102O6
TG 50:1	850.7875	850.7860	1.7631	16:0_16:0_18:1	C53H100O6
TG 50:2	848.7715	848.7701	1.6494	16:0_16:1_18:1	C53H98O6
TG 50:3	846.7523	846.7542	-2.2439	16:0_16:1_18:2	C53H96O6
TG 50:4	844.7401	844.7377	2.8733	16:0_16:1_18:3	C53H94O6
TG 52:2	876.8036	876.8015	2.3951	16:0_18:1_18:1	C55H102O6
TG 52:3	874.7879	874.7858	2.4006	16:0_18:1_18:2	C55H100O6
TG 52:4	872.7733	872.7699	3.8956	16:0_18:1_18:3	C55H98O6
TG 52:5	870.7531	870.7536	-0.5742	16:1_18:2_18:2	C55H96O6
TG 52:7	866.7220	866.7205	1.7307	16:1_16:1_20:5	C55H92O6
TG 54:1	906.8496	906.8476	2.2054	16:0_20:0_18:1	C57H108O6
TG 54:2	904.8330	904.8307	2.5419	16:0_18:1_20:1	C57H106O6
TG 54:3	902.8165	902.8160	0.5538	18:0_18:1_18:2	C57H104O6
TG 54:4	900.8003	900.8005	-0.2220	16:0_18:1_20:3	C57H102O6
TG 54:5	898.7847	898.7849	-0.2225	16:0_18:2_20:3	C57H100O6
TG 54:6	896.7692	896.7694	-0.2230	16:0_16:0_22:6	C57H98O6
TG 54:7	894.7540	894.7539	0.1118	18:2_18:2_18:3	C57H96O6
TG 54:8	892.7393	892.7390	0.3360	16:1_18:2_20:5	C57H94O6
TG 56:0	936.8945	936.8929	1.7078	14:0_20:0_22:0	C59H114O6
TG 56:1	934.8783	934.8790	-0.7488	16:0_22:0_18:1	C59H112O6
TG 56:2	932.8622	932.8624	-0.2144	16:0_18:1_22:1	C59H110O6
TG 56:3	930.8470	930.8464	0.6446	20:0_18:1_18:2	C59H108O6
TG 56:4	928.8303	928.8319	-1.7226	18:0_18:1_20:3	C59H106O6
TG 56:5	926.8196	926.8155	4.4237	18:1_18:2_20:2	C59H104O6
TG 56:6	924.8012	924.8011	0.1081	16:0_18:1_22:5	C59H102O6

TG 56:7	922.7842	922.7849	-0.7586	16:0_18:1_22:6	C59H100O6
TG 56:8	920.7673	920.7698	-2.7151	16:1_18:2_22:5	C59H98O6
TG 58:0	964.9253	964.9246	0.7254	16:0_18:0_24:0	C61H118O6
TG 58:2	960.8922	960.8943	-2.1855	16:0_20:1_22:1	C61H114O6
TG 58:3	958.8773	958.8787	-1.4600	22:0_18:1_18:2	C61H112O6
TG 58:4	956.8652	956.8638	1.4631	18:1_22:1_18:2	C61H110O6
TG 58:7	950.8168	950.8157	1.1569	18:1_18:1_22:5	C61H104O6
TG 58:8	948.8037	948.8006	3.2673	18:1_18:2_22:5	C61H102O6
TG 58:10	944.7697	944.7702	-0.5292	18:2_18:2_22:6	C61H98O6
TG 60:2	988.9277	988.9254	2.3258	24:0_18:1_18:1	C63H118O6
TG 60:3	986.9122	986.9095	2.7358	18:1_18:1_24:1	C63H116O6
PE identified as $[M-H]^-$					
PE 32:0	690.5078	690.5075	0.4345	16:0_16:0	C37H74NO8P
PE 32:1	688.4918	688.4900	2.6144	16:0_16:1	C37H72NO8P
PE 34:1	716.5214	716.5204	1.3956	16:0_18:1	C39H76NO8P
PE 36:1	744.5551	744.5531	2.6862	*	C41H80NO8P
PE 36:2	742.5366	742.5350	2.1548	18:1_18:1	C41H78NO8P
PE 36:4	738.5059	738.5064	-0.6770	16:0_20:4	C41H74NO8P
PE 38:4	766.5391	766.5381	1.3046	16:0_22:4 18:0_20:4	C43H78NO8P
PE 38:5	764.5241	764.519	6.1607	*	C43H76NO8P
PE 40:4	794.5704	794.5711	-0.8810	18:0_22:4	C45H82NO8P
PE O-34:2	700.5283	700.5283	0.0000	O-16:1_18:1	C39H76NO7P
PE O-34:3	698.5137	698.5125	1.7179	O-16:1_18:2	C39H74NO7P
PE O-36:2	728.5580	728.5580	0.0000	O-18:1_18:1	C41H80NO7P
PE O-36:3	726.5431	726.5417	1.9269	O-18:2_18:1	C41H78NO7P
PE O-36:5	722.5100	722.5114	-1.9377	O-16:1_20:4	C41H74NO7P
PE O-36:6	720.4973	720.4961	1.6655	O-16:1_20:5	C41H72NO7P
PE O-38:5	750.5411	750.5419	-1.0659	*	C43H78NO7P
PE O-38:6	748.5255	748.5275	-2.6719	O-18:1_20:5 O-18:2_20:4	C43H76NO7P
PE O-38:7	746.5115	746.5117	-0.2679	O-16:1_22:6	C43H74NO7P
PE O-40:5	778.5741	778.5746	-0.6422	O-18:1_22:4	C45H82NO7P
PE O-40:7	774.5447	774.5430	2.1948	O-18:1_22:6	C45H78NO7P
PE O-40:8	772.5298	772.5268	3.8833	O-18:2_22:6	C45H76NO7P
LPE identified as $[M-H]^-$					
LPE 16:0	452.2783	452.2774	1.9899	16:0	C21H44NO7P
LPE 18:0	480.3095	480.3086	1.8738	18:0	C23H48NO7P
LPE 18:1	478.2928	478.2931	-0.6272	18:1	C23H46NO7P
LPE 18:2	476.2771	476.2775	-0.8398	18:2	C23H44NO7P
LPE 20:4	500.2782	500.2777	0.9994	20:4	C25H44NO7P
LPE 22:4	528.3080	528.3091	-2.0821	22:4	C27H48NO7P
LPE 22:6	524.2776	524.2777	-0.1907	22:6	C27H44NO7P

PI identified as $[M-H]^-$					
PI 34:1	835.5337	835.5320	2.0346	16:0_18:1	C43H81O13P
PI 36:2	861.5496	861.5468	3.2500	18:0_18:2	C45H83O13P
PI 38:4	885.5489	885.5472	1.9197	18:0_20:4	C47H83O13P
PS identified as $[M-H]^-$					
PS 36:1	788.5413	788.5442	-3.6777	18:0_18:1	C42H80NO10P
PS 38:4	810.5254	810.5273	-2.3442	18:0_20:4	C44H78NO10P
PS 40:6	834.5284	834.5260	2.8759	18:0_22:6	C46H78NO10P
SM identified as $[M+HCOO]^-$					
SM 34:2;2O	745.5487	745.5488	-0.1341	12:2;2O/22:0	C39H77N2O6P
SM 38:1;2O	803.6270	803.6277	-0.8711	*	C43H87N2O6P
SM 42:2;2O	859.6882	859.6890	-0.9306	18:1;2O/24:0	C47H95N2O6P

C – total of carbon atoms in fatty acids; N – number of double bonds; *identified based on exact mass measurements and retention time, no loss of the polar head group and FA acyl-chain fragments observed.

Table 6.3-2. Univariate analysis of the RP-LC-MS data from of the three groups. Homogeneity of variances was tested using the Levine test. Normality was assessed using Shapiro-Wilk normality test. P-values were calculated using the ANOVA test (in green). In cases where non-normality was suspected, p-values were calculated using the Kruskal-Wallis test (in orange). P-values were adjusted using Benjamin-Hochberg correction (p.adj). Adjusted p-value significance symbols (p.adj.signif): **** p<0.0001, *** p<0.001, ** p<0.01, *p<0.05.

Variable	p.adj	p.adj.signif
PC.36.2	1.20E-05	****
PE.O.34.3	1.37E-05	****
TG.52.3	1.37E-05	****
PC.34.2	1.37E-05	****
PC.O.40.4	6.16E-05	****
PI.36.2	9.42E-05	****
DG.32.6	0.000133	***
PE.36.2	0.000139	***
CE.18.2	0.000176	***
CAR.16.0	0.000205	***
CAR.14.0	0.000234	***
CAR.18.0	0.000299	***
DG.40.4	0.000299	***
PC.32.2	0.000354	***
PC.36.4	0.000366	***
TG.58.0	0.000424	***
PC.O.38.4	0.000425	***
TG.54.6.TG.16.0_16.0_22.6	0.000425	***
PE.36.1	0.000448	***
TG.52.4	0.000452	***
TG.54.5.TG.18.1_18.2_18.2	0.000537	***
DG.36.0	0.000537	***
TG.54.4.TG.18.0_18.2_18.2	0.0006	***
SM.42.1.2O	0.0006	***
PC.38.5	0.000668	***
PC.O.38.5	0.000669	***
CAR.16.1	0.000778	***
TG.50.3.TG.16.1_16.1_18.1	0.000793	***
TG.52.2	0.000948	***
TG.52.5.TG.16.1_18.2_18.2	0.001061	**
TG.54.3.TG.18.0_18.1_18.2	0.001132	**
PE.O.36.5	0.001285	**
SM.34.2.2O	0.001298	**
PE.O.38.6.PE.O.18.1_20.5	0.001405	**
LPC.18.2	0.001561	**
DG.36.3	0.001903	**
PC.32.1	0.001903	**
LPE.18.2	0.002	**
TG.52.5.TG.16.0_16.0_20.5	0.002063	**

PC.34.0	0.00216	**
TG.44.1.TG.12.0_18.0_14.1	0.002714	**
CE.18.1	0.003125	**
PE.O.38.6.PE.O.18.2_20.4	0.003125	**
PE.32.0	0.003125	**
TG.50.2	0.003125	**
PE.O.38.5	0.003125	**
CAR.18.2	0.003125	**
PC.O.30.2	0.003125	**
TG.56.7	0.005833	**
LPE.22.4	0.005833	**
PC.O.34.0	0.007648	**
TG.46.2	0.007648	**
TG.56.4	0.007955	**
TG.54.1.TG.16.0_20.0_18.1	0.007955	**
PC.O.32.0	0.007955	**
LPC.18.0	0.007955	**
PC.O.32.1	0.007955	**
CE.22.5	0.008413	**
TG.54.4.TG.16.0_18.1_20.3	0.008468	**
PC.O.34.1	0.008468	**
PE.38.5	0.008468	**
TG.56.2	0.009859	**
DG.44.6	0.009859	**
TG.56.5.TG.18.0_18.1_20.4	0.009859	**
DG.36.5	0.009859	**
PE.O.36.3	0.009859	**
TG.54.5.TG.16.0_18.2_20.3	0.01088	*
PC.O.42.5	0.010929	*
PC.O.40.7	0.011513	*
CAR.18.1	0.011513	*
DG.30.3	0.011513	*
TG.44.2.TG.10.0_16.0_18.2	0.011513	*
PC.38.4	0.012547	*
DG.30.0	0.013291	*
PC.32.0	0.013291	*
LPE.16.0	0.015123	*
TG.51.0	0.015901	*
PC.O.40.5	0.016042	*
PE.32.1	0.016471	*
CE.20.4	0.016471	*
LPC.20.4	0.016471	*
TG.54.6.TG.16.1_18.1_20.4	0.017787	*
LPC.20.1	0.017898	*
LPE.20.4	0.017898	*
PC.40.6	0.017898	*

PE.38.4.PE.16.0_22.4	0.019444	*
TG.56.5.TG.18.1_18.2_20.2	0.019961	*
PE.O.36.6	0.020924	*
PE.O.38.7	0.021209	*
LPC.20.3	0.022581	*
PE.40.4	0.023425	*
SM.38.1.2O	0.024623	*
TG.56.6	0.025789	*
TG.58.2.TG.16.0_20.1_22.1	0.026014	*
PE.36.4	0.027344	*
LPC.22.5	0.028866	*
PS.40.6	0.030357	*
PC.42.2	0.031205	*
PS.38.4	0.031818	*
TG.50.3.TG.16.0_16.1_18.2	0.031912	*
DG.24.3	0.031912	*
PC.40.4	0.032053	*
CE.16.0	0.032083	*
LPC.20.5	0.035	*
TG.56.8	0.035693	*
DG.30.5	0.036386	*
TG.52.0	0.039078	*
PE.38.4.PE.18.0_20.4	0.040385	*
TG.44.0.TG.14.0_14.0_16.0	0.043333	*
TG.56.1	0.04743	*
PC.36.3	0.048449	*
PI.34.1	0.055093	ns
PE.34.1	0.055093	ns
TG.46.1	0.065826	ns
PE.O.34.2	0.071591	ns
DG.28.2	0.078829	ns
TG.52.7	0.079688	ns
TG.58.7	0.080531	ns
TG.44.1.TG.10.0_16.0_18.1	0.08136	ns
TG.56.3.TG.20.0_18.1_18.2	0.085217	ns
TG.58.4	0.0875	ns
DG.32.0	0.088235	ns
DG.26.1	0.088235	ns
TG.48.2.TG.16.0_16.1_16.1	0.094792	ns
DG.38.5	0.095455	ns
TG.46.0	0.115244	ns
PE.O.40.8	0.117137	ns
TG.48.2.TG.14.0_16.0_18.2	0.122638	ns
DG.36.2	0.128516	ns
PC.O.30.0	0.130233	ns
TG.56.3.TG.18.1_18.1_20.1	0.130577	ns

TG.54.1.TG.18.0_18.0_18.1	0.133588	ns
TG.54.3.TG.18.1_18.1_18.1	0.151136	ns
TG.48.1	0.161842	ns
TG.58.10	0.173694	ns
PI.38.4	0.177574	ns
TG.58.2.TG.22.0_18.1_18.1	0.177574	ns
PE.O.36.2	0.180109	ns
TG.54.8	0.188949	ns
LPC.16.0	0.22536	ns
LPE.18.1	0.23	ns
LPC.16.1	0.230851	ns
LPE.18.0	0.232923	ns
TG.48.3	0.250874	ns
TG.44.0.TG.12.0_14.0_18.0	0.260069	ns
TG.54.2	0.26431	ns
TG.52.1	0.306849	ns
TG.44.2.TG.12.0_14.0_18.2	0.351174	ns
TG.46.3	0.351174	ns
TG.48.0	0.355833	ns
TG.50.4	0.410265	ns
TG.56.0	0.423684	ns
DG.34.1	0.435784	ns
TG.50.1	0.476136	ns
PS.36.1	0.483226	ns
LPC.14.0	0.528365	ns
LPC.22.6	0.534968	ns
PC.34.1	0.534968	ns
PC.30.0	0.537107	ns
DG.34.2	0.552344	ns
PE.O.40.5	0.56087	ns
TG.60.3	0.589815	ns
DG.32.1	0.613037	ns
LPC.18.1	0.621037	ns
TG.54.7	0.668182	ns
LPE.22.6	0.691566	ns
TG.58.8	0.748204	ns
PE.O.40.7	0.76875	ns
PC.36.1	0.783876	ns
TG.60.2	0.788529	ns
PC.40.5	0.819737	ns
DG.34.0	0.842442	ns
TG.58.3	0.906358	ns
PC.38.3	0.92227	ns
TG.50.0	0.927	ns

Species underlined in green show the result of the Anova test; species underlined in orange show the result of the Kruskal-wallis test

6.4 LIPIDOMIC ANALYSIS IN SYSTEMIC LUPUS ERYTHEMATOSUS AND SYSTEMIC SCLEROSIS (Chapter 2.3)

Table 6.4-1. Lipid species identified in whole blood/plasma samples of SLE and SS patients.

Lipid specie (C:N)	Theoretical *m/z*	Observed *m/z*	Error (ppm)	Fatty acyl chains (C:N)	Formula
PC identified as $[M+H]^+$					
PC 30:0	706.5386	706.5384	0.2831	14:0_16:0	C38H76NO8P
PC 30:1	704.5230	704.5220	1.4194	14:0_16:1	C38H74NO8P
PC 32:0	734.5700	734.5711	-1.4975	16:0_16:0	C40H80NO8P
PC 32:1	732.5511	732.5508	0.4095	14:0_18:1 16:0_16:1	C40H78NO8P
PC 32:2	730.5367	730.5384	-2.3271	14:0_18:2 16:1_16:1	C40H76NO8P
PC 34:0	762.5991	762.6005	-1.8358	16:0_18:0	C42H84NO8P
PC 34:1	760.5852	760.5854	-0.2630	16:0_18:1	C42H82NO8P
PC 34:2	758.5699	758.5701	-0.2637	16:0_18:2	C42H80NO8P
PC 34:3	756.5543	756.5540	0.3965	16:1_18:2	C42H78NO8P
PC 34:4	754.5387	754.5386	0.1325	16:1_18:3	C42H76NO8P
PC 36:0	790.6326	790.6316	1.2648	16:0_20:0 18:0_18:0	C44H88NO8P
PC 36:1	788.6162	788.6160	0.2536	16:0_20:1 18:0_18:1	C44H86NO8P
PC 36:2	786.6035	786.6011	3.0511	16:0_20:2 18:0_18:2 18:1_18:1	C44H84NO8P
PC 36:3	784.5834	784.5841	-0.8922	16:0_20:3 18:1_18:2	C44H82NO8P
PC 36:4	782.5704	782.5695	1.1501	16:0_20:4 18:2_18:2	C44H80NO8P
PC 36:5	780.5543	780.5543	0.0000	16:0_20:5 16:1_20:4	C44H78NO8P
PC 36:6	778.5387	778.5386	0.1284	16:1_20:5 18:3_18:3	C44H76NO8P
PC 38:1	816.6482	816.6478	0.4898	16:0_22:1 18:0_20:1	C46H90NO8P
PC 38:2	814.6326	814.6316	1.2275	16:0_22:2 18:0_20:2	C46H88NO8P
PC 38:3	812.6162	812.6160	0.2461	18:0_20:3	C46H86NO8P
PC 38:4	810.5988	810.6006	-2.2206	18:0_20:4 18:1_20:3	C46H84NO8P
PC 38:5	808.5835	808.5834	0.1237	16:0_22:5 18:1_20:4	C46H82NO8P
PC 38:6	806.5700	806.5692	0.9919	16:0_22:6	C46H80NO8P
PC 38:7	804.5543	804.5542	0.1243	16:1_22:6 18:2_20:5	C46H78NO8P

				18:3_20:4	
PC 40:1	844.6795	844.6785	1.1839	16:0_24:1 18:0_22:1 18:1_22:0	C48H94NO8P
PC 40:4	838.6323	838.6327	-0.4770	18:0_22:4 18:2_22:2	C48H88NO8P
PC 40:5	836.6148	836.6155	-0.8367	18:0_22:5 20:1_20:4	C48H86NO8P
PC 40:6	834.6013	834.5991	2.6360	18:0_22:6	C48H84NO8P
PC 40:7	832.5856	832.5838	2.1619	18:1_22:6 18:2_22:5 18:3_22:4 20:2_20:5 20:3_20:4	C48H82NO8P
PC 40:8	830.5699	830.5693	0.7224	18:2_22:6 20:4_20:4	C48H80NO8P
PC 40:9	828.5543	828.5514	3.5001	18:3_22:6 20:4_20:5	C48H78NO8P
PC 40:10	826.5387	826.5358	3.5086	20:5_20:5	C48H76NO8P
PC 42:1	872.7108	872.7102	0.6875	18:0_24:1 18:1_24:0 20:0_22:1	C50H98NO8P
PC 42:2	870.6940	870.6949	-1.0337	18:1_24:1 18:2_24:0 20:0_22:2	C50H96NO8P
PC 42:5	864.6482	864.6494	-1.3878	20:0_22:5 20:1_22:4 20:3_22:2	C50H90NO8P
PC 42:7	860.6169	860.6173	-0.4648	20:1_22:6 20:3_22:4	C50H86NO8P
PC 42:8	858.6013	858.6006	0.8153	20:2_22:6 20:4_22:4	C50H84NO8P
PC 42:10	854.5700	854.5695	0.5851	20:4_22:6	C50H80NO8P
PC 44:5	892.6795	892.6805	-1.1202	22:1_22:4	C52H94NO8P
PC O-30:0	692.5577	692.5590	-1.8771	O-14:0_16:0 O-16:0_14:0	C38H78NO7P
PC O-32:0	720.5902	720.5893	1.2490	O-16:0_16:0	C40H82NO7P
PC O-32:1	718.5759	718.5752	0.9741	O-14:0_18:1 O-16:0_16:1	C40H80NO7P
PC O-34:0	748.6229	748.6216	1.7365	O-16:0_18:0 O-18:0_16:0	C42H86NO7P
PC O-34:1	746.6070	746.6054	2.1430	O-16:0_18:1	C42H84NO7P
PC O-34:2	744.5907	744.5905	0.2686	O-16:0_18:2	C42H82NO7P

PC O-34:3	742.5751	742.5747	0.5387	O-16:0_18:3 O-16:1_18:2	C42H80NO7P
PC O-36:1	774.6377	774.6370	0.9036	O-16:0/20:1	C44H88NO7P
PC O-36:2	772.6220	772.6218	0.2589	O-16:0/20:2 O-18:0_18:2 O-18:1_18:2	C44H86NO7P
PC O-36:3	770.6064	770.6062	0.2595	O-16:0/20:3	C44H84NO7P
PC O-36:4	768.5907	768.5886	2.7323	O-16:0/20:4	C44H82NO7P
PC O-36:5	766.5751	766.5748	0.3914	O-16:0/20:5 O-16:1/20:4	C44H80NO7P
PC O-38:2	800.6533	800.6523	1.2490	O-16:0/22:2 O-18:0/20:2	C46H90NO7P
PC O-38:3	798.6377	798.6358	2.3791	O-18:0/20:3	C46H88NO7P
PC O-38:4	796.6205	796.6212	-0.8787	O-16:0/22:4	C46H86NO7P
PC O-38:5	794.6041	794.6060	-2.3911	O-16:0/22:5 O-18:0/20:5 O-18:1/20:4	C46H84NO7P
PC O-38:6	792.5907	792.5903	0.5047	O-16:0/22:6	C46H82NO7P
PC O-40:4	824.6499	824.6522	-2.7891	O-18:0/22:4	C48H90NO7P
PC O-40:5	822.6377	822.6372	0.6078	O-18:0/22:5	C48H88NO7P
PC O-40:6	820.6220	820.6222	-0.2437	O-18:0/22:6	C48H86NO7P
PC O-42:2	856.7159	856.7153	0.7003	O-18:2/24:0 O-20:0/22:2	C50H98NO7P
PC O-42:3	854.7003	854.6989	1.6380	O-24:0/18:3	C50H96NO7P
PC O-42:4	852.6846	852.6845	0.1173	O-20:0/22:4	C50H94NO7P
PC O-42:6	848.6533	848.6546	-1.5318	O-20:0/22:6	C50H90NO7P
PC O-44:4	880.7159	880.7141	2.0438	O-22:1/22:3 O-22:2/22:2 O-24:0/20:4	C52H98NO7P
PC O-44:5	878.7003	878.6998	0.5690	O-22:2/22:3	C52H96NO7P
PC P-36:5	764.5594	764.5584	1.3079	P-16:0_20:5	C44H78NO7P
PC P-38:6	790.5751	790.5763	-1.5179	P-16:0_22:6	C46H80NO7P
PC P-40:6	818.6064	818.6049	1.8324	P-18:0_22:6	C48H84NO7P
PC P-42:4	850.6690	850.6689	0.1176	P-20:0_22:4	C50H92NO7P
PC P-42:6	846.6377	846.6373	0.4725	P-20:0_22:6	C50H88NO7P
LPC identified as $[M+H]^+$					
LPC 14:0	468.3081	468.3087	-1.2812	14:0	C22H46NO7P
LPC 16:0	496.3397	496.3400	-0.6044	16:0	C24H50NO7P
LPC 16:1	494.3243	494.3245	-0.4046	16:1	C24H48NO7P
LPC 18:0	524.3709	524.3719	-1.9070	18:0	C26H54NO7P
LPC 18:1	522.3554	522.3559	-0.9572	18:1	C26H52NO7P
LPC 18:2	520.3400	520.3400	0.0000	18:2	C26H50NO7P
LPC 18:3	518.3247	518.3229	3.4727	18:3	C26H48NO7P

LPC 20:1	550.3867	550.3872	-0.9085	20:1	C28H56NO7P
LPC 20:2	548.3716	548.3715	0.1824	20:2	C28H54NO7P
LPC 20:3	546.3551	546.3560	-1.6473	20:3	C28H52NO7P
LPC 20:4	544.3409	544.3403	1.1023	20:4	C28H50NO7P
LPC 20:5	542.3251	542.3247	0.7376	20:5	C28H48NO7P
LPC 22:5	570.3564	570.3559	0.8766	22:5	C30H52NO7P
LPC 22:6	568.3397	568.3403	-1.0557	22:6	C30H50NO7P
LPC O-16:0	482.3611	482.3606	1.0366	O-16:0	C24H52NO7P
LPC O-16:1	480.3454	480.3451	0.6246	O-16:1	C24H50NO7P
LPC O-18:1	508.3767	508.3765	0.3934	O-18:1	C26H54NO7P
CAR identified as $[M+H]^+$					
CAR 10:0	316.2482	316.2482	0.0000	10:0	C17H33NO4
CAR 12:0	344.2795	344.2793	0.5809	12:0	C19H37NO4
CAR 14:1	370.2952	370.2950	0.5401	14:1	C21H39NO4
CAR 14:2	368.2795	368.2794	0.2715	14:2	C21H37NO4
CAR 16:0	400.3414	400.3423	-2.2481	16:0	C23H45NO4
CAR 16:1	398.3263	398.3262	0.2511	16:1	C23H43NO4
CAR 18:0	428.3729	428.3733	-0.9338	18:0	C25H49NO4
CAR 18:1	426.3576	426.3578	-0.4691	18:1	C25H47NO4
CE identified as $[M+NH_4]^+$					
CE 16:0	642.6179	642.6189	-1.5561	16:0	C43H76O2
CE 18:0	670.6496	670.6504	-1.1929	18:0	C45H80O2
CE 18:1	668.6343	668.6347	-0.5982	18:1	C45H78O2
CE 18:2	666.6180	666.6188	-1.2001	18:2	C45H76O2
CE 20:2	694.6496	694.6500	-0.5758	20:2	C47H80O2
CE 20:3	692.6340	692.6343	-0.4331	20:3	C47H78O2
CE 20:4	690.6179	690.6186	-1.0136	20:4	C47H76O2
CE 20:5	688.6027	688.6026	0.1452	20:5	C47H74O2
CE 22:6	714.6184	714.6185	-0.1399	22:6	C49H76O2
Cer and GalCer identified as $[M+H]^+$					
Cer d(34:1)	538.5199	538.5197	0.3714	d18:1_16:0 d16:1_18:0	C34H67NO3
Cer d(36:1)	566.5512	566.5514	-0.3530	d18:1_18:0 d16:1_20:0	C36H71NO3
Cer d(38:1)	594.5825	594.5825	0.0000	d16:1_22:0 d18:1_20:0	C38H75NO3
Cer d(40:0)	624.6289	624.6286	0.4803	d18:0_22:0 d16:0_24:0 d20:0_20:0	C40H81NO3
Cer d(40:1)	622.6138	622.6137	0.1606	d18:1_22:0 d16:1_24:0	C40H79NO3
Cer d(40:2)	620.5982	620.5986	-0.6445	d18:2_22:0	C40H77NO3
Cer d(42:0)	652.6602	652.6605	-0.4597	d18:0_24:0	C42H85NO3

Cer d(42:1)	650.6451	650.6449	0.3074	d18:1_24:0	C42H83NO3
Cer d(42:2)	648.6295	648.6296	-0.1542	d18:2_24:0	C42H81NO3
Cer d(43:1)	664.6602	664.6608	-0.9027	d18:1_25:0	C43H85NO3
Cer d(44:1)	678.6764	678.6762	0.2947	d18:1_26:0	C44H87NO3
Cer d(44:2)	676.6608	676.6607	0.1478	d18:2_26:0	C44H85NO3
GalCer d18:1_16:0	700.5722	700.5735	-1.8556	d18:1_16:0	C40H77NO8
GalCer d18:1_22:0	784.6661	784.6667	-0.7647	d18:1_22:0	C46H89NO8
GalCer d18:1_24:0	812.6974	812.6983	-1.1074	d18:1_24:0	C48H93NO8
GalCer d18:1_24:1	810.6817	810.6834	-2.0970	d18:1_24:1	C48H91NO8
		DG identified as $[M+NH_4]^+$			
DG 36:2	638.5736	638.5723	2.0358	18:1_18:1	C39H72O5
DG 36:3	636.5549	636.5567	-2.8277	18:1_18:2	C39H70O5
		TG identified as $[M+NH_4]^+$			
TG 42:0	740.6763	740.6766	-0.4050	14:0_14:0_14:0	C45H86O6
TG 44:0	768.7070	768.7076	-0.7805	14:0_14:0_16:0	C47H90O6
TG 44:1	766.6896	766.6922	-3.3912	14:0_14:0_16:1	C47H88O6
TG 44:2	764.6750	764.6767	-2.2232	14:1_14:1_16:0	C47H86O6
TG 46:0	796.7385	796.7387	-0.2510	14:0_16:0_16:0	C49H94O6
TG 46:1	794.7216	794.7229	-1.6358	14:0_16:0_16:1	C49H92O6
TG 46:2	792.7069	792.7077	-1.0092	14:0_14:0_18:2	C49H90O6
TG 46:3	790.6943	790.6923	2.5294	14:0_14:1_18:2	C49H88O6
TG 46:4	788.6763	788.6770	-0.8876	14:1_14:1_18:2	C49H86O6
TG 48:0	824.7697	824.7699	-0.2425	16:0_16:0_16:0	C51H98O6
TG 48:1	822.7558	822.7543	1.8231	14:0_16:0_18:1 16:0_16:0_16:1	C51H96O6
TG 48:2	820.7396	820.7386	1.2184	14:0_16:0_18:2 14:0_16:1_18:1	C51H94O6
TG 48:3	818.7252	818.7235	2.0764	14:0_16:0_18:3	C51H92O6
TG 48:4	816.7076	816.7078	-0.2449	14:0_16:1_18:3	C51H90O6
TG 48:5	814.6919	814.6923	-0.4910	14:1_16:1_18:3	C51H88O6
TG 50:1	850.7875	850.7855	2.3508	16:0_16:0_18:1	C53H100O6
TG 50:2	848.7715	848.7705	1.1782	16:0_16:0_18:2 16:0_16:1_18:1	C53H98O6
TG 50:3	846.7523	846.7550	-3.1887	16:0_16:1_18:2	C53H96O6
TG 50:4	844.7401	844.7382	2.2492	14:0_18:2_18:2 16:1_16:1_18:2	C53H94O6
TG 50:5	842.7232	842.7236	-0.4747	14:0_18:2_18:3	C53H92O6
TG 50:6	840.7076	840.7083	-0.8326	14:0_18:3_18:3	C53H90O6
TG 52:0	880.8328	880.8325	0.3406	16:0_18:0_18:0	C55H106O6
TG 52:1	878.8171	878.8151	2.2758	16:0_16:0_20:1 16:0_18:0_18:1	C55H104O6
TG 52:2	876.8036	876.8010	2.9653	16:0_18:1_18:1	C55H102O6
TG 52:3	874.7879	874.7852	3.0865	16:0_18:1_18:2	C55H100O6

TG 52:4	872.7733	872.7707	2.9790	16:0_18:1_18:3 16:0_18:2_18:2 16:1_18:1_18:2	C55H98O6
TG 52:5	870.7531	870.7535	-0.4594	16:0_18:2_18:3 16:1_18:2_18:2	C55H96O6
TG 52:6	868.7389	868.7390	-0.1151	14:0_16:0_22:6	C55H94O6
TG 52:7	866.7220	866.7243	-2.6537	14:0_16:1_22:6	C55H92O6
TG 54:0	908.8641	908.8648	-0.7702	16:0_18:0_20:0 18:0_18:0_18:0	C57H110O6
TG 54:1	906.8496	906.8486	1.1027	16:0_18:0_20:1 16:0_18:1_20:0 18:0_18:0_18:1	C57H108O6
TG 54:2	904.8330	904.8321	0.9947	16:0_18:1_20:1 18:0_18:1_18:1	C57H106O6
TG 54:3	902.8165	902.8163	0.2215	18:0_18:1_18:2 18:1_18:1_18:1	C57H104O6
TG 54:4	900.8003	900.8001	0.2220	16:0_18:1_20:3 16:0_18:0_20:4 18:1_18:1_18:2	C57H102O6
TG 54:5	898.7847	898.7834	1.4464	16:0_18:1_20:4 16:0_18:2_20:3 18:1_18:2_18:2	C57H100O6
TG 54:6	896.7692	896.7704	-1.3381	16:0_18:2_20:4 18:1_18:2_18:3 18:2_18:2_18:2	C57H98O6
TG 54:7	894.7540	894.7547	-0.7823	16:0_18:2_20:5 18:2_18:2_18:3	C57H96O6
TG 54:8	892.7393	892.7400	-0.7841	18:2_18:3_18:3 16:1_18:3_20:4	C57H94O6
TG 56:0	936.8945	936.8963	-1.9212	16:0_18:0_22:0 16:0_20:0_20:0 18:0_18:0_20:0	C59H114O6
TG 56:1	934.8783	934.8805	-2.3532	16:0_18:1_22:0 16:0_18:0_22:1	C59H112O6
TG 56:2	932.8622	932.8646	-2.5727	16:0_18:1_22:1 18:1_18:1_20:0	C59H110O6
TG 56:3	930.8470	930.8474	-0.4297	18:0_18:1_20:2 18:1_18:1_20:1 18:0_18:2_20:0	C59H108O6
TG 56:4	928.8303	928.8319	-1.7226	18:0_18:1_20:3	C59H106O6
TG 56:5	926.8196	926.8166	3.2369	16:0_20:1_20:4 18:0_18:1_20:4	C59H104O6
TG 56:6	924.8012	924.8005	0.7569	16:0_18:1_22:5	C59H102O6
TG 56:7	922.7842	922.7841	0.1084	16:0_18:1_22:6	C59H100O6

TG 56:8	920.7673	920.7691	-1.9549	16:1_18:1_22:6	C59H98O6
TG 56:9	918.7545	918.7558	-1.4150	16:0_18:3_22:6 16:1_18:2_22:6	C59H96O6
TG 58:1	962.9110	962.9120	-1.0385	16:0_20:1_22:0 18:0_18:1_22:0	C61H116O6
TG 58:2	960.8922	960.8964	-4.3709	16:0_20:1_22:1 18:1_18:1_22:0 18:0_18:1_22:1	C61H114O6
TG 58:3	958.8773	958.8805	-3.3372	18:1_18:2_22:0	C61H112O6
TG 58:4	956.8652	956.8629	2.4037	18:1_18:2_22:1	C61H110O6
TG 58:5	954.8484	954.8487	-0.3142	18:1_18:2_22:2 18:1_18:1_22:3 18:2_18:2_22:1	C61H108O6
TG 58:6	952.8328	952.8307	2.2040	18:0_18:1_22:5 18:1_18:1_22:4 18:1_20:1_20:4	C61H106O6
TG 58:7	950.8168	950.8175	-0.7362	18:0_18:1_22:6 18:1_18:1_22:5	C61H104O6
TG 58:8	948.8037	948.8016	2.2133	18:1_18:1_22:6 18:1_18:2_22:5 18:1_20:3_20:4	C61H102O6
TG 58:9	946.7858	946.7849	0.9506	16:0_20:3_22:6 18:1_18:2_22:6	C61H100O6
TG 60:1	990.9423	990.9431	-0.8073	18:1_20:0_22:0	C63H120O6
TG 60:2	988.9277	988.9279	-0.2022	18:1_20:1_22:0 18:1_20:0_22:1	C63H118O6
TG 60:3	986.9122	986.9122	0.0000	18:1_20:0_22:2 18:1_20:1_22:1	C63H116O6
TG 60:4	984.8954	984.8962	-0.8123	18:1_20:1_22:2 18:2_20:1_22:1	C63H114O6
TG 60:7	978.8484	978.8469	1.5324	18:1_20:2_22:4 18:1_20:0_22:6	C63H108O6
TG 60:8	976.8328	976.8340	-1.2285	18:1_20:1_22:6 18:0_20:2_22:6	C63H106O6
TG 60:10	972.8015	972.8014	0.1028	18:0_20:4_22:6	C63H102O6
TG 62:13	994.7858	994.7864	-0.6031	18:1_22:6_22:6 18:2_22:5_22:6 18:3_22:4_22:6	C65H100O6
PE identified as $[M-H]^-$					
PE 34:1	716.5214	716.5229	-2.0934	16:0_18:1	C39H76NO8P
PE 34:2	714.5070	714.5056	1.9594	16:0_18:2	C39H74NO8P
PE 36:1	744.5551	744.5552	-0.1343	18:0_18:1	C41H80NO8P
PE 36:2	742.5366	742.5394	-3.7709	18:1_18:1	C41H78NO8P
PE 36:4	738.5059	738.5077	-2.4374	16:0_20:4	C41H74NO8P

PE 38:4	766.5391	766.5400	-1.1741	18:0_20:4	C43H78NO8P
PE 38:6	762.5070	762.5086	-2.0983	16:0_22:6	C43H74NO8P
PE 38:5	764.5241	764.5216	3.2700	18:1_20:4	C43H76NO8P
PE O-34:2	700.5283	700.5295	-1.7130	O-16:1_18:1	C39H76NO7P
PE O-36:2	728.5580	728.5581	-0.1373	O-18:1_18:1	C41H80NO7P
PE O-36:5	722.5130	722.5136	-0.8304	O-16:1_20:4	C41H74NO7P
PE O-38:5	750.5411	750.5421	-1.3324	O-16:1_22:4	C43H78NO7P
PE O-38:7	746.5115	746.5139	-3.2150	O-16:1_22:6	C43H74NO7P
PE O-40:5	778.5741	778.5766	-3.2110	O-18:1_22:4	C45H82NO7P
PE O-40:7	774.5447	774.5445	0.2582	O-18:1_22:6	C45H78NO7P
PE identified as $[M+H]^+$					
PE 32:0	692.5230	692.5223	1.0108	16:0_16:0	C37H74NO8P
PE 32:1	690.5074	690.5045	4.1998	16:0_16:1	C37H72NO8P
PE(36:3)	742.5387	742.5388	-0.1347	18:1_18:2	C41H76NO8P
PE(36:5)	738.5074	738.5062	1.6249	16:0_20:5 16:1_20:4 18:2_18:3	C41H72NO8P
PE(38:2)	772.5856	772.5852	0.5177	18:1_20:1 16:1_22:1	C43H82NO8P
PE(38:7)	762.5074	762.5048	3.4098	16:1_22:6 18:2_20:5 18:3_20:4	C43H72NO8P
PE(40:4)	796.5856	796.5848	1.0043	18:0_22:4 18:2_22:2	C45H82NO8P
PE(40:6)	792.5543	792.5541	0.2523	18:0_22:6 18:2_22:4	C45H78NO8P
PE(40:7)	790.5387	790.5380	0.8855	18:1_22:6 18:3_22:4	C45H76NO8P
PE(40:8)	788.5230	788.5221	1.1414	18:2_22:6 20:4_20:4	C45H74NO8P
PE(40:9)	786.5074	786.5044	3.8143	18:3_22:6 20:4_20:5	C45H72NO8P
PE O-34:3	700.5281	700.5274	0.9992	O-16:1_18:2	C39H74NO7P
PE O-36:4	726.5438	726.5433	0.6882	O-16:0_20:4	C41H76NO7P
PE O-36:5	724.5281	724.5281	0.0000	O-16:1_20:4	C41H74NO7P
PE O-36:6	722.5125	722.5124	0.1384	O-16:1_20:5	C41H72NO7P
PE O-38:4	754.5751	754.5749	0.2650	O-16:0_22:4 O-18:0_20:4	C43H80NO7P
PE O-38:5	752.5594	752.5597	-0.3986	O-16:0_22:5 O-18:0_20:5	C43H78NO7P
PE P-36:1	730.5751	730.5742	1.2319	P-18:0_18:1 P-16:0_20:1	C41H80NO7P
PE P-38:5	750.5438	750.5435	0.3997	P-18:0_20:5	C43H76NO7P
PE P-38:6	748.5281	748.5281	0.0000	P-16:0_22:6	C43H74NO7P

PE P-40:4	780.5907	780.5905	0.2562	P-20:0_20:4	C45H82NO7P
PE P-40:7	774.5438	774.5440	-0.2582	P-18:1_22:6	C45H76NO7P
LPE identified as $[M-H]^-$					
LPE 18:0	480.3090	480.3093	-0.6246	18:0	C23H48NO7P
LPE 18:2	476.2777	476.2781	-0.8398	18:2	C23H44NO7P
LPE 20:4	500.2777	500.2782	-0.9994	20:4	C25H44NO7P
PI identified as $[M-H]^-$					
PI 32:0	809.5186	809.5168	2.2235	16:0_16:0	C45H83O13P
PI 38:4	885.5499	885.5482	1.9197	18:0_20:4	C47H83O13P
PS identified as $[M-H]^-$					
PS 38:4	810.5291	810.5285	0.7403	18:0_20:4	C44H78NO10P
PS 40:6	834.5291	834.5269	2.6362	18:0_22:6	C46H78NO10P
PS identified as $[M+H]^+$					
PS 36:1	790.5593	790.5590	0.3795	18:0_18:1 16:0_20:1	C42H80NO10P
PS 40:4	840.5749	840.5746	0.3569	18:0_22:4 20:0_20:4	C46H81NO10P
PS 40:5	838.5593	838.5580	1.5503	18:1_22:4 18:3_22:2 20:1_20:4	C46H79NO10P
SM identified as $[M+HCOO]^-$					
SM d(32:1)	719.5363	719.5345	2.5016	d16:1_16:0	C37H75N2O6P
SM d(34:1)	747.5676	747.5653	3.0766	d16:1_18:0	C39H79N2O6P
SM d(34:2)	745.5519	745.5495	3.2191	d16:1_18:1	C39H77N2O6P
SM d(36:1)	775.5989	775.5970	2.4497	d16:1_20:0	C41H83N2O6P
SM d(36:2)	773.5832	773.5808	3.1024	d16:1_20:1	C41H81N2O6P
SM d(38:1)	803.6302	803.6285	2.1154	d16:1_22:0	C43H87N2O6P
SM d(40:1)	831.6615	831.6609	0.7214	d16:1_24:0	C45H91N2O6P
SM d(40:2)	829.6458	829.6449	1.0848	d16:1_24:1	C45H89N2O6P
SM d(42:1)	859.6928	859.6916	1.3958	d18:0_24:1	C47H95N2O6P
SM d(42:2)	857.6771	857.6755	1.8655	d18:1_24:1	C47H93N2O6P
SM d(42:3)	855.6615	855.6595	2.3374	d18:2_24:1	C47H91N2O6P
SM identified as $[M+H]^+$					
SM d(32:2)	673.5285	673.5296	-1.6332	d18:2_14:0	C37H74N2O6P
SM d(34:0)	705.5911	705.5892	2.6928	d16:0_18:0 d18:0_16:0	C39H82N2O6P
SM d(36:0)	733.6224	733.6220	0.5452	d16:0_20:0 d18:0_18:0	C41H86N2O6P
SM d(36:3)	727.5754	727.5749	0.6872	d18:2_18:1	C41H80N2O6P
SM d(38:0)	761.6537	761.6536	0.1313	d16:0_22:0 d18:0_20:0	C43H90N2O6P
SM d(38:2)	757.6224	757.6231	-0.9239	d16:1_22:1 d18:1_20:1	C43H86N2O6P

				d18:2_20:0	
SM d(38:3)	755.6067	755.6075	-1.0588	d18:2_20:1	C43H84N2O6P
SM d(40:3)	783.6380	783.6377	0.3828	d18:2_22:1	C45H88N2O6P
SM d(44:1)	843.7319	843.7315	0.4741	d18:0_26:1	C49H100N2O6P
SM d(44:2)	841.7163	841.7160	0.3564	d18:1_26:1	C49H98N2O6P

C – total of carbon atoms in fatty acids; N – number of double bonds.